Cyclic sulfoximine mimics of ribosides and 2-deoxyribosides as enzyme inhibitors

Kwong, Joey Sum Wing

Award date:
2007

Awarding institution:
University of Bath

Cyclic Sulfoximine Mimics of Ribosides and 2-Deoxyribosides as Enzyme Inhibitors

submitted by

Joey Sum Wing Kwong

for the degree of PhD

of the University of Bath

2007

The research work in this thesis has been carried out in the Department of Pharmacy and Pharmacology, under the supervision of Dr Michael D. Threadgill and Dr Matthew D. Lloyd.

Signed : 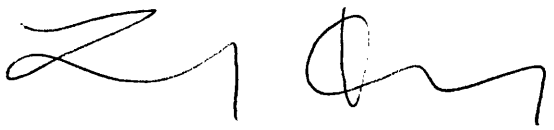

17th April 2007

ProQuest LLC
789 East Eisenhower Parkway
P.O. Box 1346
Ann Arbor, MI 48106-1346

Abstract

Thymidine phosphorylase (TP) cleaves thymidine, giving 2-deoxy-*D*-ribose-1α-phosphate and hence the angiogenic mediator 2-deoxy-*D*-ribose. Poly(ADP-ribose) polymerase-1 (PARP-1) is responsible for controlling cellular DNA repair and inhibitors have potential as chemosensitisers and radiosensitisers in cancer therapy. Inosine-5'-monophosphate dehydrogenase (IMPDH) is a key enzyme in the *de novo* biosynthesis of guanine nucleotides and inhibitors, such as tiazofurin, are cytotoxic. The substrates for all three enzymes are ribosides or 2-deoxyribosides. In this thesis, mimics of the substrates are designed with the tetrahedral sulfoximine group replacing the anomeric carbon.

Synthetic approaches to 1*R*,3*R*,4*R*-1-aryl-4-hydroxy-3-hydroxymethyl-1λ^4-isothiazole-1-oxides were studied. Several routes were investigated to produce sulfoximines; the most effective was rhodium-catalysed oxidative imination of sulfoxides with trifluoroacetamide and iodosobenzene diacetate. However, reaction of anions derived from S-methylsulfoximines to aldehydes gave only low yields of the required secondary alcohols. Alternatively, diastereomeric 4*S*,5*R*-4-(benzyloxymethyl)-2,2-dimethyl-5-(3-arylsulfonimidoylmethyl)-1,3-dioxolanes were synthesised by thio-Mitsunobu coupling of thiophenols with 4*S*,5*S*-4-(benzyloxymethyl)-2,2-dimethyl-5-hydroxymethyl-1,3-dioxolane, followed by sulfoxidation and imination. The separated diastereoisomers were identified by X-ray crystallography. Deprotection gave the vicinal diol, which was subjected to cyclisation studies.

The second series of targets, 1*S*,3*R*,4*R*-1-arylimino-3-hydroxy-4-hydroxymethyltetrahydro-1λ^6-thiophene-1-oxides, were approached initially through 1,3-dipolar cycloadditions of chiral (*E*)-3-benzyloxypropenoates with the $H_2C{=}S^+{-}CH_2^-$ but technical difficulties frustrated this route. Following an alternative strategy, a Dieckmann cyclisation furnished racemic 3-oxotetrahydrothiophene-4-carbonitrile. Reduction of the ketone and hydration of the nitrile gave *trans* 3-hydroxytetrahydrothiophene-4-carboxamide, as shown by NMR and X-ray crystallography. The secondary alcohol was protected and the sulfur was oxidised to the sulfoxide. In this sequence, it only remains to develop methods for imination at the sulfoxide and conversion of the carboxamide to a CH_2OH group.

Thus the major hurdles in the synthetic routes to both types of sulfoximine-based riboside mimics have been overcome, providing late intermediates with appropriate configurations for future elaboration to the targets.

Acknowledgements

I have had the assistance and kindness from many people during this PhD:

Firstly, I would like to sincerely thank my supervisors, Dr Mike Threadgill and Dr Matthew Lloyd, for their guidance, patience and trust. I am forever thankful to have the opportunity to work with such enthusiastic and dedicated scientists, and together we have overcome many hurdles and shed light on this challenging project.

Thank you to Dr Steve Black and Dr Tim Woodman for their NMR services, Mr Chris Cryer and Mr James Amato for the provision of Mass Spectra, Dr Mary Mahon for X-ray crystallography and also to all the PhDs and post-docs in labs 3.11 and 3.14 for their help and friendship.

Special thanks go to Dr Andy Westwell (University of Cardiff), Dr Steve Husbands and Dr James Dowden for their valuable discussions at the PhD and transfer vivas.

I thank the University of Bath for a departmental studentship and the Royal Society of Chemistry, the British Association of Cancer Research and the Society of Chemical Industry for travel bursaries.

Thank you to everybody I have worked with over the years in 3.5/7 (a severely female-dominated lab): Anna, Annika, Archana, Christian, Claire, Dan, Esther, Ghadeer, Maria, Mervat, Pete, Sabela, Vanja and Victoria, for all your advice, friendship and for making me laugh in the lab.

Thank you to all my friends for standing by me and cheering me on.

This thesis is dedicated to my parents: without your love and support, I would've given up a long time ago. Only you would know just how difficult these past few years have been. Thank you, for letting me follow my dreams and for always believing in them. For having faith in me when I didn't have any myself. For being there at the darkest and the brightest hours. Most of all, for your help, patience and understanding during the writing/re-writing stage, when I thought this day would never come. Thank you, for everything.

Contents

List of Figures, Schemes and Tables

Figures

Schemes

Tables

Abbreviations

δ	Chemical shift
AA	Amino acid
Ac	Acetyl
acac	Acetylacetonate (ligand)
AcOH	Acetic acid
ADDP	1,1'-(Azodicarbonyl)dipiperidine
ADP	Adenosine 5'-diphosphate
AGT	O^6-Alkylguanine-DNA alkyltransferase
Ala	Alanine
AMP	Adenosine 5'-monophosphate
Aq	Aqueous
Ar	Aryl
Arg	Arginine
Asn	Asparagine
Asp	Aspartic acid
ATP	Adenosine 5'-triphosphate
BAD	Benzamide adenine dinucleotide
BER	Base excision repair
BINAP	2,2'-Bis(diphenylphosphino)-1,1'-binaphthyl
BINOL	1,1'-Bi-2-napthol
Bn	Benzyl
Boc	*tert*-Butoxycarbonyl
BRCT	Breast cancer susceptibility protein, BRCA1, C-terminus
BSO	Buthionine sulfoximine
(*t*-)BuLi	(*tert*-)Butyllithium
***t*-BuOK**	Potassium *tert*-butoxide
Bu	Butyl
Bz	Benzoyl
Calcd	Calculated
C_q	Quaternary carbon
COSY	Correlation spectroscopy
CSA	10-Camphorsulfonic acid
Cys	Cysteine
d	Day(s)
Da	Dalton

dba	Dibenzylideneacetone
DCC	*N,N'*-Dicyclohexylcarbodiimide
DCM	Dichloromethane
DDQ	2,3-Dichloro-5,6-dicyano-1,4-benzoquinone
DEAD	Diethyl azodicarboxylate
DEPT	Distortionless enhancement by polarisation transfer
DET	Diethyl tartrate
DEVD	Asp-Glu-Val-Asp
DIAD	Diisopropyl azodicarboxylate
DIBAL-H	Diisobutylaluminium hydride
DMA	*N,N*-Dimethylacetamide
DMAP	4-(Dimethylamino)pyridine
DMF	*N,N*-dimethylformamide
DMP	2,2-Dimethoxypropane
DNA	Deoxyribonucleic acid
DPPE	1,2-Bis(diphenylphosphino)ethane
EC	Endothelial cells
ee	Enantiomeric excess
EI	Electron ionisation
Equiv	Equivalent(s)
ES	Electrospray
Et	Ethyl
Et_3N	Triethylamine
Et_2O	Diethyl ether
EtOAc	Ethyl acetate
EtOH	Ethanol
FAB	Fast atom bombardment
FGF	Fibroblast growth factor
FGI	Functional group interconversion
Fmoc	Fluoren-9-ylmethoxy carbonyl
5-FU	5-Fluorouracil
g	Gram(s)
γ-GCS	γ-Glutamylcysteine synthetase
GDP	Guanine 5'-diphosphate
Gln	Glutamine
Gly	Glycine
GMP	Guanine 5'-monophosphate

GS	Glutamine synthetase
GSH	Glutathione
GSSG	Glutathione disulfide
GTP	Guanine 5'-triphosphate
h	Hour(s)
Hz	Hertz
HIF	Hypoxia-inducible factor
His	Histidine
HMBC	Heteronuclear multiple bond correlation
HMQC	Heteronuclear multiple quantum coherence
HRMS	High-resolution mass spectroscopy
HSP	Heat shock proteins
IC_{50}	Concentration required for 50% inhibition of activity
IF	Interferon
IL	Interleukin
Ile	Isoleucine
IMP	Inosine 5'-monophosphate
IMPDH	Inosine 5'-monophosphate dehydrogenase
***i*Pr**	Isopropyl
IR	Infrared
J	Coupling constant
K_I	Inhibition constant
LAH	Lithium aluminium hydride
Leu	Leucine
LHMDS	Lithium hexamethyldisilazide
Lit.	Literature
Lys	Lysine
M	Molar
M^+	Parent molecular ion
m/z	Mass-to-charge ratio
MCP	Macrophage chemoattractant protein
***m*CPBA**	*meta*-Chloroperoxybenzoic acid
Me	Methyl
MeCN	Acetonitrile
MeOH	Methanol
Met	Methionine
MGMT	O^6-methylguanine-DNA methyltransferase

MHz	Megahertz
min	Minute(s)
mL	Millilitre(s)
MM2	Molecular mechanics 2
MMF	Mycophenolate mofetil
mmol	Millimole(s)
MMP	Matrix metalloprotease
MMR	Mismatch repair
mol	Mole(s)
mp	Melting point
MPA	Mycophenolic acid
Ms	Methanesulfonyl (mesyl)
MS	Mass spectrum
MSH	*O*-Mesitylenesulfonylhydroxylamine
MSO	Methionine sulfoximine
NAD^+	Nicotinamide adenine dinucleotide
NADH	Reduced nicotinamide adenine dinucleotide
NADPH	Reduced nicotinamide adenine dinucleotide phosphate
NER	Nucleotide excision repair
NF	Nuclear factor
NLS	Nuclear localisation signal
NMR	Nuclear magnetic resonance
NOE	Nuclear Overhauser effect
NOESY	Nuclear Overhauser enhancement spectroscopy
NOS	Nitric oxide synthase
Ns	*para*-Nitrophenylsulfonyl (nosyl)
OPFP	Pentafluorophenoxy
PAG	Phosphate-activated glutaminase
PARG	Poly(ADP-ribose) glycohydrolase
PARP	Poly(ADP-ribose) polymerase
PD-ECGF	Platelet-derived endothelial cell growth factor
Pet. ether	Petroleum ether
PFPOH	Pentafluorophenol
Ph	Phenyl
Phe	Phenylalanine
PMB	*para*-Methoxybenzyl
p.p.m.	Parts per million

PRPP	5-Phosphoribosyl-1-pyrophosphate
Redox	Reduction-oxidation
R_f	Retention factor
RNA	Ribonucleic acid
ROS	Reactive oxygen species
RT	Room temperature
SAD	Selenazole-4-carboxamide adenine dinucleotide
SAR	Structure-activity relationship
Sat.	Saturated
Ses	Trimethylsilylethylsulfonyl
Ser	Serine
S_N2	Bimolecular nucleophilic substitution
TAD	Thiazole-4-carboxamide adenine dinucleotide
TANK	Tankyrase
TBAF	Tetrabutylammonium fluoride
TBHP	*tert*-Butyl hydroperoxide
TBP	Tributylphosphine
Tert	Tertiary
Tf	Trifluoromethanesulfonyl (triflate)
TF	Tiazofurin
TFA	Trifluoroacetic acid / trifluoroacetyl
TFMP	Tiazofurin 5'-monophosphate
TGF	Transforming growth factor
THF	Tetrahydrofuran
Thr	Threonine
TLC	Thin-layer chromatography
TMSi	Trimethylsilyl
TMZ	Temozolomide
TNF	Tumour necrosis factor
Tolyl	*para*-methylphenyl
TP	Thymidine phosphorylase
TPP	Triphenylphosphine
Ts	*para*-Toluenesulfonyl (tosyl)
TSP	Thrombospondin

Tyr	Tyrosine
Val	Valine
VEGF	Vascular endothelial growth factor
XMP	Xanthosine 5'-monophosphate
XRCC	X-ray cross-complementing

Chapter 1 Introduction

1.1 Anti-cancer drug discovery – the call for target-driven strategy

Despite continuous research effort and breakthrough, cancer maintains its position as one of the biggest causes of death in the world. There is a great need for better treatment options to decrease mortality rates and increase the quality of life for cancer patients. Traditional medical intervention centres on chemotherapy, radiotherapy and surgery. However, most available techniques lack selectivity and result in undesirable adverse effects and treatment failure. Current research aims to identify and investigate tumour-specific enzymes and markers as potential drug targets, with the recent discovery of agents such as Gleevec® and Herceptin® providing examples of this approach in the treatment of chronic myelogenous leukaemia and metastatic breast cancer, respectively.[1,2] The positive outcomes of these agents further reinforce the necessity of understanding tumour biology and the importance of targetted agents in anti-cancer drug discovery.

Cancer cells possess elaborate systems that enable them to grow and spread rapidly, with a protective mechanism against conventional cancer treatment. For the purpose of this thesis, the following tumour cellular processes as potential drug targets will be discussed:

- Tumour angiogenesis (Section 1.2)
- Mis-regulated cell proliferation and differentiation (Section 1.3)
- DNA repair and resistance to anti-cancer therapy (Section 1.4)

1.2 Tumour angiogenesis

1.2.1 Introduction

Angiogenesis, the formation of new blood vessels from existing vasculature, occurs in a number of physiological processes, such as wound healing, regrowth of the uterine lining after menstruation, pregnancy and foetal development.[3] It is a complex, multi-step process that begins with the activation of endothelial cells (ECs) by an angiogenic stimulus (*vide infra*, Figure 1). Injured or diseased tissues synthesise and release angiogenic factors which bind to the EC receptors. The activated ECs release proteases to break down the basement membrane surrounding the vessels; matrix metalloproteases (MMPs) are also released to break down extracellular matrix and allow for invasion, migration and proliferation through the disrupted basement membrane, creating a capillary sprout. Adhesion molecules (integrins $\alpha_v\beta_3$ and $\alpha_v\beta_5$)

are employed to pull the sprouting vessel forward, forming a blood vessel tubule. Finally, new basement membrane and muscle layer are created to form a new capillary network.[4]

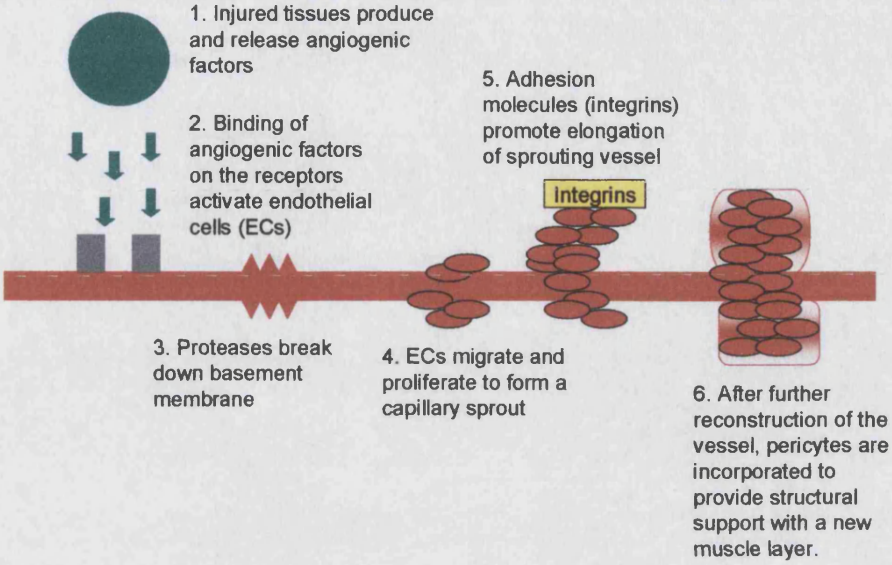

Figure 1. The angiogenic process, highlighting the steps involved in developing a new capillary network.[4]

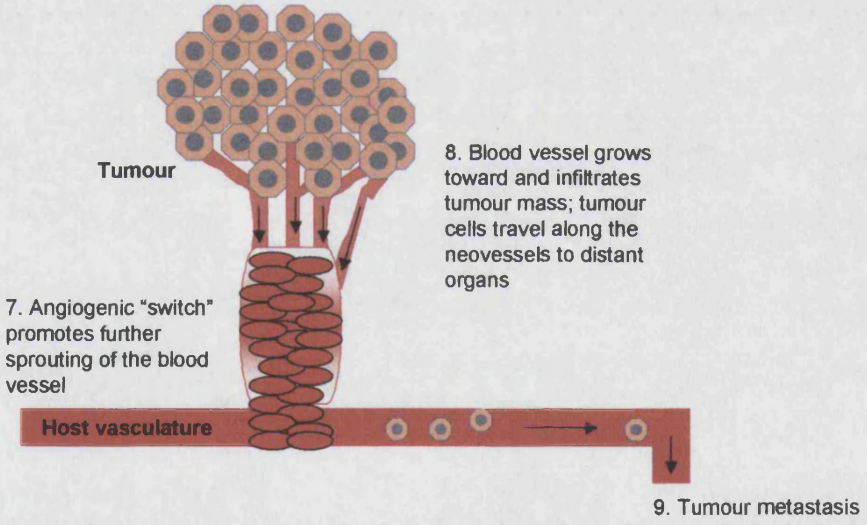

Figure 2. Tumour angiogenesis and subsequent metastasis *via* the newly developed neovascular network.[4]

Tumour cells acquire oxygen and nutrients for their growth and metastasis from nearby host neovasculature by simple passive diffusion. However, once tumours grow up to the size of 1-3 mm^3, this blood supply is no longer sufficient for further growth and the angiogenic "switch" is turned on to accommodate the increasingly high metabolic demand.[5] This may be a result of genetic changes, hypoxia or oxidative stress. The "on-switch" triggers the recruitment of host vasculature to encourage further sprouting

of blood vessels, which subsequently grow toward and infiltrate the tumour mass, providing the required circulation of oxygen and nutrients (*vide supra*, Figure 2).

In metastasis, the tumour cells are able to travel to distant organs through this newly developed capillary network and form secondary tumours. Furthermore, a disrupted vessel remodelling mechanism is known to be responsible for the twisted chaotic tumour neovasculature, which ultimately leads to hypoxia, and the tumour angiogenesis process is repeated.[6]

1.2.2 Regulation of angiogenesis

In normal conditions, angiogenesis is tightly controlled by a balanced activity of angiogenic stimulators and inhibitors (Table 1 and Table 2).[7] In cancer, increased levels of angiogenic factors, along with reduced levels of angiogenic inhibitors, disturb the balance and lead to excessive angiogenesis. Triggered by the tumour angiogenic switch, activating factors are released by tumour cells, by the surrounding tissue or by infiltrating macrophages and fibroblasts to activate endothelial cells and thereby initiate the angiogenic process.

Pro-angiogenic factors	
VEGF	IL-6, 8
Basic FGF	Angiopoietin-1
Acidic FGF	Angiopoietin-2 (in the presence of VEGF)
TGF-α, β	Angiogenin
TP (PD-ECGF)	MCP-1
MMPs	Leptin
NOS	TNF-α

Table 1. Angiogenesis stimulators.[3,7] (Abbreviations: VEGF – vascular endothelial growth factor; IL – interleukin; FGF – fibroblast growth factor; TGF – transforming growth factor; TP – thymidine phosphorylase; PD-ECGF – platelet-derived endothelial cell growth factor; MCP – macrophage chemoattractant protein; MMP – matrix metalloprotease; NOS – nitric oxide synthase; TNF – tumour necrosis factor.)

The most active angiogenic factors belong to the VEGF family (VEGF-A, -B, -C, -D and -E).[8] They regulate vascular permeability, ECs proliferation and apoptosis in many tumour types. VEGF-A, particularly, is highly expressed in many tumours, including those in the lung, brain and gastrointestinal tract.

Among the numerous naturally occurring angiogenesis inhibitors, angiostatin is the most well known. It is a product of proteolysis of plasminogen and it inhibits ECs proliferation.[9]

The mechanisms of initiating the angiogenic switch are complex and only partly known. The angiogenic stimulators and inhibitors play different roles under different circumstances. Certain oncogenes and tumour-suppressor genes also regulate angiogenesis. Ras, myc, raf, HER-2/neu, src and c-Jun upregulate VEGF or down-regulate thrombospondin-1 (TSP-1);[7,10] mutant p53 upregulates VEGF, whereas wild-type p53 upregulates TSP-1 and downregulates VEGF.[11] The angiogenic pathway is linked to apoptosis, with certain naturally occurring angiogenic inhibitors (angiostatin, endostatin, IL and TSP-1) inducing apoptosis in both EC and tumour cells.[8]

Naturally occurring angiogenic inhibitors	
Angiostatin	Endostatin (collagen XIII fragment)
Antithrombin-III fragment	TSP-1
IF-α, β	IL-4, 12, 18
Plasminogen activator inhibitor	Canstatin
Fibronectin fragment	Heparinases
Prolactin	Retinoids

Table 2. Angiogenesis inhibitors.[3,7,8] (Abbreviations: TSP – thrombospondin; IL – interleukin; IF – interferon)

1.2.3 Thymidine phosphorylase (TP) in angiogenesis

1.2.3.1 Background

Thymidine phosphorylase (TP, EC 2.4.2.4) catalyses the phosphorolysis of thymidine **1**, with inorganic phosphate to give thymine **2** and 2-deoxy-*D*-ribose-1α-phosphate **3**. Dephosphorylation of the latter generates 2-deoxy-*D*-ribose **4** (*vide infra*, Scheme 1). The enzyme also catalyses 2-deoxyribosyl transfer from one deoxynucleoside to another nucleobase.[12] TP forms part of the catabolic / salvage pathway of pyrimidine nucleic acids, recycling thymidine to thymine for DNA repair and replication.

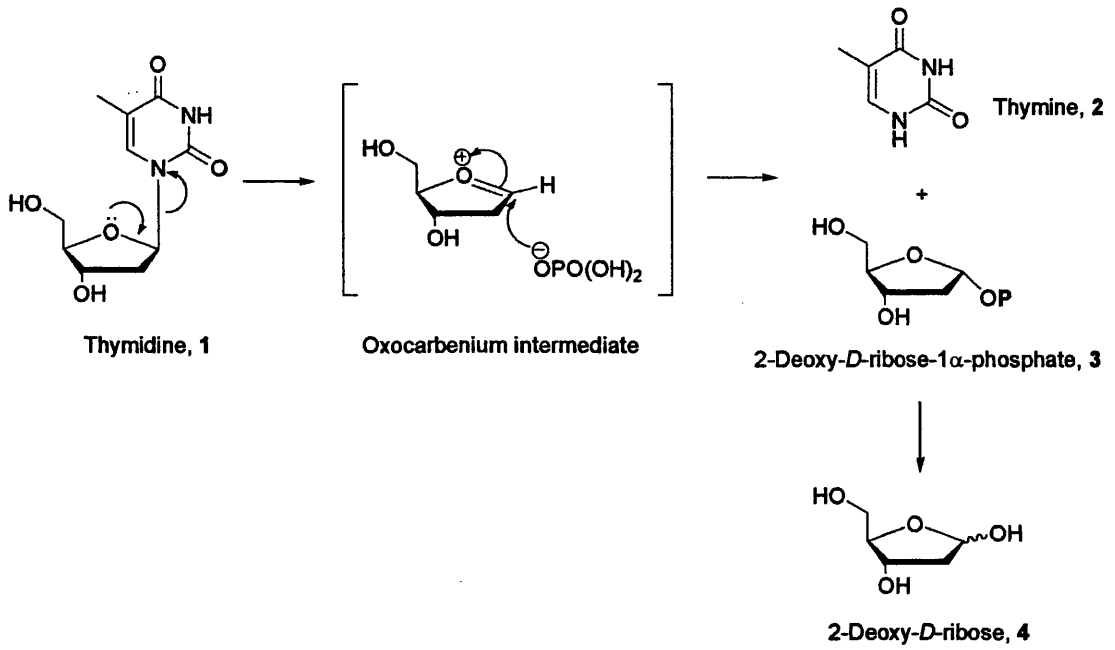

Scheme 1. TP-catalysed phosphorolysis of thymidine **1**.[12]

1.2.3.2 Structure of TP

TP was first described in 1954 by Friedkin and Roberts as a nucleoside metabolism enzyme.[13] Purification of the enzyme from both *Escherichia coli* and *Salmonella typhimurium* in the mid-1970s provided the first glimpse at the structure of TP.[14] *E. coli* TP is a homodimer of 45 KDa subunits, whilst human TP is a homodimer of 55 KDa subunits.[15] The expressed *E. coli* protein contains 441 amino acids and shows 34% homology to human TP. In the 1980s, an angiogenic protein extracted from human platelet lysate was named platelet-derived endothelial cell growth factor (PD-ECGF) and was later found to be identical to TP.[16]

A crystal structure of thymine **2** bound to *E. coli* TP reveals the structure of the active site (*vide infra*, Figure 3). Thymine interacts with a cavity at the top of the active-site cleft *via* hydrogen bonds to the heterocyclic ring (Arg 202, Tyr 199, Ser 217) and hydrophobic interactions with the methyl group (Val 208, Ile 214).[17,18]

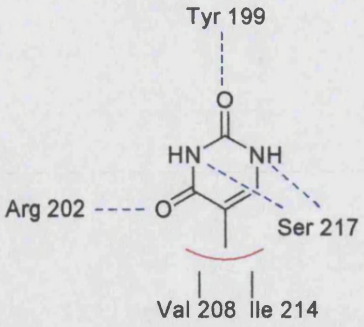

Figure 3. Interactions of thymine **2** within the active site of TP.[17,18] (Hydrophobic interactions – red; hydrogen bonds – blue)

1.2.3.3 Functions of TP

Upregulation of TP is stimulated by hypoxia, hypoglycaemia and cytokines (TNF-α, IL-1, IF-γ) within the tumour microenvironment. Radiotherapy and chemotherapeutic agents such as taxanes and cyclophosphamide are also known inducers of TP.[12]

TP has been implicated in tumour growth and metastasis and high levels of the enzyme have been found in many solid tumours, including those of colon, stomach, lung, bladder, pancreas, cervix, uterus, ovary, kidney, thyroid, oesophagus and breast.[16] An increase in TP expression as high as 260-fold was found in invasive bladder tumours compared to the level in normal tissue.[19] A separate investigation found that human KB epidermoid carcinoma cells transfected with TP had a higher angiogenic activity and apoptotic index than non-transfected cells.[20] Additionally, the growth rate of KB/TP cells was significantly higher than that of normal cells under hypoxic conditions.[21]

TP stimulates chemotaxis of endothelial cells *in vitro* and angiogenic activity *in vivo*.[22] The exact mechanism is unclear but it was hypothesised that the angiogenic activity involves either the reduction of extracellular thymidine levels, which is inhibitory to angiogenesis, or the activity of 2-deoxy-*D*-ribose as an angiogenic mediator.[16] The latter also displays chemotactic properties *in vitro* and angiogenic activity *in vivo*; it stimulates cell migration in the endothelium *via* its concentration gradient. A hypothesis supporting this activity is that 2-deoxy-*D*-ribose could be intracellularly phosphorylated to 2-deoxy-*D*-ribose-5-phosphate, which is then cleaved to acetaldehyde and glyceraldehyde 3-phosphate. These molecules can enter the glycolytic pathway and generate ATP, therefore serving as an cellular energy source.[22] 2-Deoxy-*D*-ribose has also been shown as an anti-apoptotic factor in hypoxia.[23] Studies suggested that this is

achieved by the ability of 2-deoxy-*D*-ribose to suppress the effects of several apoptotic factors such as caspase 3 and HIF-1α (hypoxia-inducible factor), although more experimental data are required for a better understanding.[24,25]

Brown *et al.* described the role of 2-deoxy-*D*-ribose-1α-phosphate in TP-induced oxidative stress and subsequent secretion of angiogenic factors.[26] The group revealed that 2-deoxy-*D*-ribose-1α-phosphate is a strong reducing sugar that is capable of generating oxygen radicals during protein glycation. The putative mechanism involves transition metal-catalysed auto-oxidation of 2-deoxy-*D*-ribose-1α-phosphate. The latter is converted to 2-deoxy-*D*-ribose-5α-phosphate by phosphopentomutase; the open-chain ribosyl group of the product is coupled to an amino residue of an intra-cellular protein and this condensation product (Schiff base) rearranges to give an α-hydroxyketone which reacts with oxygen and, in the presence of oxidised redox-active transition metal ions (Cu^{2+}, Fe^{3+}), give a superoxide anion that is further converted to hydrogen peroxide and hydroxyl radicals.[25,26]

It is interesting to note that, while 2-deoxy-*D*-ribose is a recognised angiogenic mediator, 2-deoxy-*L*-ribose, the enantiomer, has been found to have activity opposite to those of both TP and 2-deoxy-*D*-ribose. 2-Deoxy-*L*-ribose was shown to inhibit EC migration and endothelial tube formation; it suppressed TP-induced angiogenesis, tumour growth and metastasis, and increased the proportion of apoptotic cells by suppressing TP-stimulated production of angiogenic factors (VEGF and IL-8).[27,28] Further study is required to explore the potential of 2-deoxy-*L*-ribose as a useful therapeutic agent in angiogenesis.

1.2.3.4 Therapeutic potentials of TP inhibition

Scheme 2 (*vide infra*) summarises the diverse activities of TP in tumour development. Targetting this enzyme is of great pharmacological interest because inhibition of TP could promote apoptosis and suppress tumour angiogenesis and metastasis.

Whilst TP inhibition is of great value, few TP inhibitors are currently known. Most are mono-cyclic derivatives of uracil, with TPI (5-chloro-6-[1-(2-iminopyrrolidinylmethyl)]-uracil hydrochloride, **5**), with a reported IC_{50} of 35 nM (*vide infra*, Figure 4), being the most potent inhibitor.[29] An increase in both the rate of growth of the KB cells and the density of blood vessels in the tumours were observed when the cells were subjected to high TP concentrations. In addition, the proportion of apoptotic cells was also raised,

supporting the role of TP in apoptosis and angiogenesis. TPI caused a substantial reduction in tumour growth of human KB epidermoid carcinoma cells with high TP activity. Prior to the discovery of TPI, the strongest inhibitor was 6-amino-5-bromouracil **6** (*vide infra*, Figure 4) with an IC_{50} of 30 μM.[30]

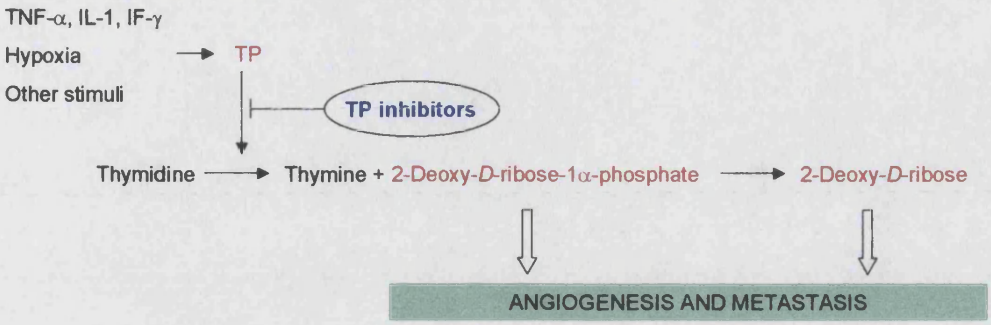

Scheme 2. Schematic overview of the roles of TP and the clinical application of TP inhibitors.

The 2-iminopyrrolidine cation in TPI **5** was designed to mimick the intermediate oxonium in TP-catalysed phosphorolysis of thymidine **1** (*vide supra*, Scheme 1). Recently, the structure-activity relationship (SAR) of TPI was established with a crystal structure of human TP in complex with the inhibitor, thereby giving information on the structure of human TP active site. It consists of two components, one interacting with the uracil ring and the other with the 2-iminopyrrolidinyl moiety, with a network of water molecules occupying the phosphate-binding site. A number of hydrogen bonds to the uracil ring and the 2-iminopyrrolidinyl moiety are present within the active site (*vide infra*, Figure 4); the chlorine atom is responsible for several hydrophobic interactions. The SAR and improved inhibitory profile of TPI provides opportunities for future *in silico* screening and drug design.[31]

1.2.3.5 TP: The two-face Janus

Interestingly, the early focus on TP in anti-cancer drug discovery was associated with the relationship between the enzyme activity and sensitivity to chemotherapy. Besides all the roles discussed above, TP also catalyses the conversion of the antimetabolite 5-fluorouracil (5-FU) to 5-fluoro-2'-deoxyuridine, the first step in its metabolism to the anti-cancer compound, 5-fluoro-2'-deoxyuridine triphosphate, a thymidine synthetase inhibitor. Doxifluridine (5'-deoxy-5-fluorouridine), cepecitabine (N-4-pentyloxy-carbonyl-5'-deoxy-5-fluorocytidine) and tegafur [1-(tetrahydro-2-furanyl)-5-fluorouracil] are prodrugs of 5-FU that are established anti-cancer agents. Furthermore, as discussed before, certain chemotherapeutic agents (taxanes, cyclophosphamide)

increase TP levels and co-administration with prodrugs of 5-FU would provide a synergistic effect. For these TP-target agents, high enzyme levels in tumours are required for their activities thus deeming TP inhibition in combination with 5-FU or its prodrugs inappropriate.[32]

To circumvent this problem, a potential solution is to inhibit specifically the downstream mediators of the TP catalysis pathway rather than to inhibit TP activity directly.

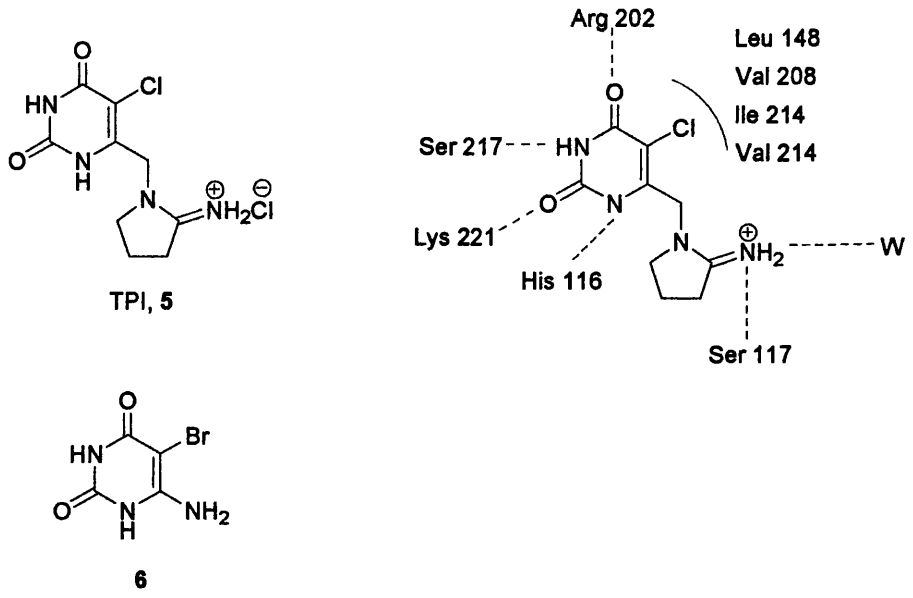

Figure 4. TP inhibitors. Recent crystallography of TPI **5** with human TP provides valuable information on the structure of active site and aids future drug screening. TPI was found to possess a 1000-fold higher inhibitory activity than 6-amino-5-bromouracil **6**, one of the most potent TP inhibitors previously synthesised.[29-31] (W – water molecule; hydrogen bonds – blue; hydrophobic interactions – red)

1.3 Mis-regulated cell proliferation and differentiation in cancer

1.3.1 Tumour cell proliferation – an imbalanced biosynthesis of nucleotides

The relationship between malignancy and cell differentiation has long been a target for anti-cancer drug design. An increase in the rate of cell proliferation and growth is essential for rapidly dividing cells and an accumulation of mutations of oncogenes and tumour suppressor genes allows tumour cells to escape the normally controlled nature of the cell cycle.

In normal cells, enzymes in the anabolic (synthetic) pathways and the catabolic (degradation) pathways act as the rate-limiting factors in DNA and RNA biosynthesis

and their activities are balanced. Tumour cells have a reprogrammed metabolic and enzymatic imbalance, resulting in an elevation of the activity of anabolic enzymes with decreased activity of opposing enzymes. This altered nucleotide metabolism contributes to rapid tumour growth and the identification of the enzyme targets offers opportunities for targetted drug therapy.[33]

1.3.1.1 Purine nucleotide metabolism

Nucleotides are synthesised from simple building blocks in a step-wise manner (*de novo* pathway, *vide infra*, Scheme 3) or by the recycling of preformed bases (salvage pathway). The former starts with the synthesis of purine ring from amino acids (aspartate, glycine, glutamine), tetrahydrofolate derivatives and CO_2. The sugar phosphate moiety comes from 5-phosphoribosyl-1-pyrophosphate (PRPP), a product of ribose-5-phosphate and ATP. This is the central precursor of purine nucleotide metabolism and a series of reactions gives rise to the branch-point purine nucleotide, inosine 5'-monophosphate (IMP, **7**, *vide infra*, Scheme 3). Adenine 5'-monophosphate (AMP, **8**, *vide infra*, Scheme 3) is synthesised from IMP by substitution of an amino group for the carbonyl oxygen atom at C-6, with aspartate and GTP contributing for the amino group and phosphate group, respectively. Oxidation of IMP gives xanthosine 5'-monophosphate (XMP, **9**, *vide infra*, Scheme 3) with nicotinamide adenine dinucleotide (NAD^+) as the hydrogen acceptor; subsequent conversion of XMP produces guanine 5'-monophosphate (GMP, **10**, *vide infra*, Scheme 3) by the insertion of an amino group at C-2 with glutamine as the amine donor and ATP as the phosphate donor.[34]

Free purine bases formed by the hydrolytic degradations of nucleic acids and nucleotides can be recycled by the salvage pathway *via* the utilisation of PRPP. The ribose phosphate moiety of PRPP is transferred to a free purine ring, forming the corresponding ribonucleotide. Two salvage enzymes operate to recover purine bases; adenine phosphoribosyl transferase catalyses the formation of AMP and hypoxanthine-guanine phosphoribosyl transferase catalyses the formation of IMP and GMP.[34]

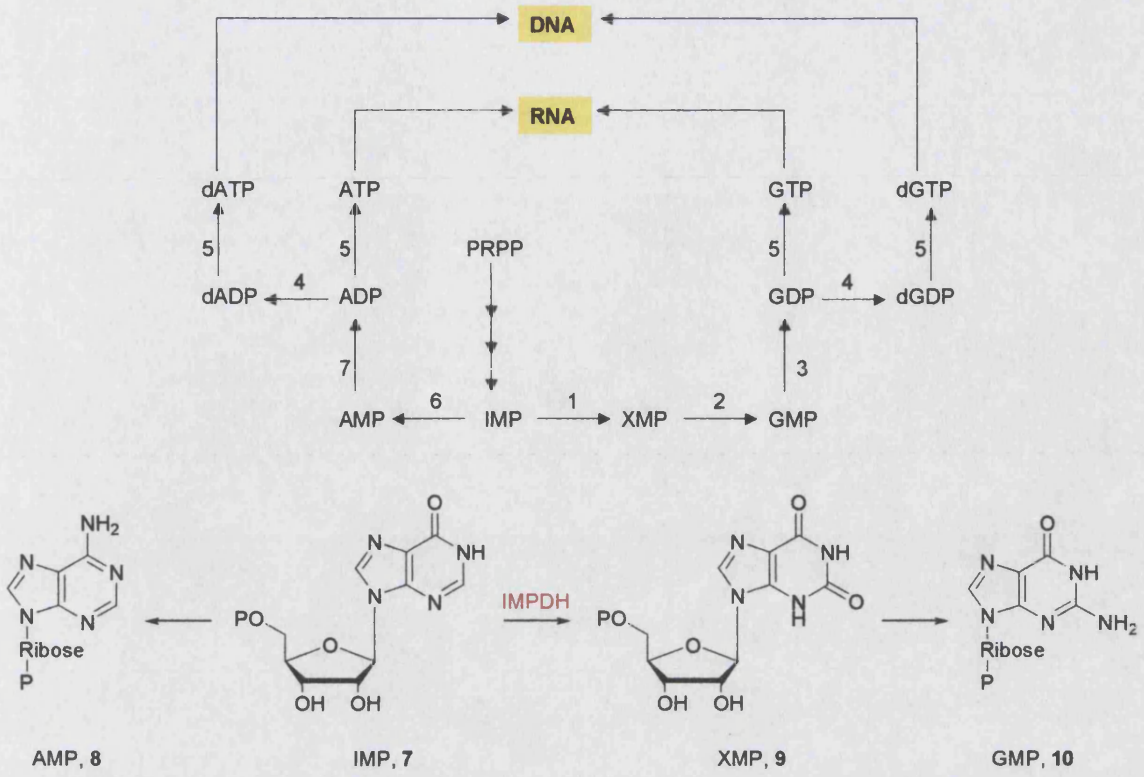

AMP, **8** IMP, **7** XMP, **9** GMP, **10**

Scheme 3. Schematic representation of the *de novo* biosynthesis of purine ribo- and 2'-deoxy-ribonucleotides; IMPDH catalyses the key step in the biosynthesis of guanine nucleotides, coverting IMP **7** to XMP **9**.[34] [Enzymes: 1 = inosine 5'-monophosphate dehydrogenase (IMPDH); 2 – GMP synthase; 3 – GMP kinase; 4 – ribonucleotide reductase; 5 – nucleoside diphosphate kinase; 6 (i) adenylsuccinate synthetase; (ii) AMP lyase; 7 – AMP kinase]

1.3.1.2 Control of purine biosynthesis

A feedback mechanism and other regulatory mechanisms operate in the regulation of purine synthesis. The reactions leading from IMP, the branch point in synthesis, are main sites of feedback inhibition. AMP inhibits the conversion of IMP to adenylo-succinate, its immediate precursor; GMP inhibits the oxidation of IMP to XMP in a similar fashion. These two feedback inhibitors also act at the site of PRPP conversion to IMP.

1.3.2 Inosine-5'-monophosphase dehydrogenase (IMPDH) in guanine nucleotide biosynthesis

1.3.2.1 Background

As shown above, IMPDH (EC 1.1.1.205) is the key enzyme involved in the *de novo* biosynthesis of guanine nucleotides. It catalyses the irreversible oxidative conversion of

IMP **7** to XMP **9** using NAD^+ as a reagent (Scheme 3 and Scheme 4). The reaction involves a nucleophilic addition of a cysteine residue to C-2 of the purine ring, followed by hydride transfer to NAD^+. Upon the release of the reduced NAD^+, NADH, the C–S covalent bond of E~XMP **13** is hydrolysed to release XMP from E•XMP **14** (Scheme 4).[35] It is noteworthy that this reaction follows an ordered Bi-Bi sequence, where IMP binds to the active site before NAD^+, and NADH is released prior to XMP.[36] This mechanism is different from most NAD^+-dependent dehydrogenases, in which there is either a random order of binding or they require NAD^+ binding before the substrates.

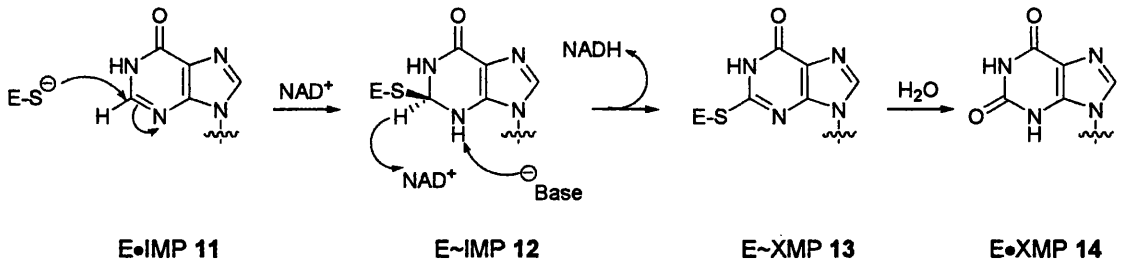

E•IMP **11** E~IMP **12** E~XMP **13** E•XMP **14**

Scheme 4. Proposed mechanism of IMPDH reaction. After IMP binding to the enzyme active site (E•) and subsequent binding of NAD^+, a covalent bond (~) is formed between C-2 and a cysteine residue. Hydride transfer at this E~IMP intermediate **12** releases NADH, giving the thioimidate intermediate E~XMP **13**. This is hydrolysed to E•XMP **14** and XMP is released from the active site, completing the enzymatic reaction.[35]

Given the central position of IMPDH in guanine nucleotide biosynthesis, targetting this enzyme is of great pharmacological interest. The enzyme is upregulated in rapidly proliferating tumour cells and investigations have demonstrated that lymphocytes, in particular, are dependent on the *de novo* pathway of nucleotide biosynthesis, thus making IMPDH a potential immunosuppressive target.[36]

1.3.2.2 Structure of IMPDH

The active enzyme has a molecular weight of 56-58 KDa per subunit and is a tetramer comprised of identical subunits. Two isoforms of the enzyme are known to exist: type I and type II. In human IMPDH, each of the two genes encodes a protein of 514 amino acids with high levels of sequence homology between the two isoforms (84% amino acid identity).[37] Type I isoform is constitutively expressed in normal cells, while type II is predominantly upregulated in neoplastic and rapidly proliferating cells,[38] including human leukaemic cell lines,[39] human ovarian tumours and leukaemic cells from patients with chronic myeloid leukaemia.[39,40]

Each IMPDH monomer consists of two domains. The 394-residue catalytic domain, with attached N- and C-terminals, contains the active site. Catalysis occurs through binding at two sites – a substrate-binding region (IMP) and a co-factor-binding region (NAD^+). The smaller domain (residues 110-244) lies adjacent to the catalytic domain. The function of this domain is unknown; it is not required for activity but may act as a regulatory region.[41]

The structure of IMPDH in complex with an XMP reaction intermediate provides information on the active site (Figure 5). This reaction intermediate (E~XMP, **13**, *vide supra*, Scheme 4) is generated after both the hydride transfer and NADH release but before the production of XMP.[36] A covalent bond between C-2 of XMP and the sulfur atom of Cys 331 is formed, along with numerous hydrogen bonds from the substrate to the enzyme.

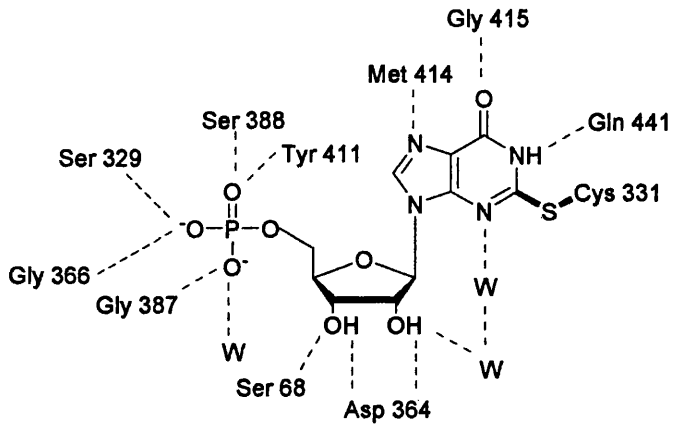

Figure 5. XMP reaction intermediate (E~XMP, **13**) in complex with IMPDH.[36] (W – water molecule; hydrogen bonds – blue)

1.3.2.3 Therapeutic potentials of IMPDH inhibition

Depletion of the pool of guanine nucleotides and consequent reduction in tumour DNA and RNA biosynthesis are the primary effects of IMPDH inhibition. Together with the marked increase of enzyme activity in tumour cells as a drug target, several IMPDH inhibitors have been widely described in the literature.

Tiazofurin (TF, **15**, *vide infra*, Figure 6), 2-(β-*D*-ribofuranosyl)thiazole-4-carboxamide, is a C-nucleoside NAD^+ analogue that has been used to investigate effects of IMPDH inhibition.[42] It requires metabolic activation: TF penetrates cell membranes and is phosphorylated by adenosine kinase to tiazofurin 5'-monophosphate (TFMP), which is coupled with AMP by NAD^+-pyrophosphorylase to give thiazole-4-carboxamide adenine

dinucleotide (TAD). The latter is an NAD^+ analogue where the nicotinamide ring is replaced by thiazole-4-carboxamide and is more potent than TFMP or TF itself, with a K_i of $\approx$ 0.2 μM against IMPDH Type II. Kinetic studies suggest that TAD inhibits IMPDH by binding at the NAD^+ site.[41] TF showed significant anti-tumour activity in phase II trials for patients with end-stage acute non-lymphocytic leukaemia or myeloblastic crisis of chronic myeloid leukaemia.[41] However, the adverse effect profile (severe neuro- and cardiovascular toxicities) is a limiting factor for treatment with TF. Analogues of TF have since been synthesised with modification of the ribose moiety or the thiazole ring with the aim of providing better pharmacological profiles.[43] In fact, an analogue containing selenium instead of sulfur was synthesised and its corresponding dinucleotide was found to be more potent (by 5- to 10-fold) than TF.[44] Selenazofurin (**16**, *vide infra*, Figure 6) is converted to selenazole-4-carboxamide adenine dinucleotide (SAD, **17**, *vide infra*, Figure 6) in the same fashion as TAD and the crystal structures of both dinucleotides in complex with IMPDH provided SAR-related information.

In the crystal structure of SAD bound to human type II IMPDH, an interaction is observed between the carboxamide group and Asn 303 (*vide infra*, Figure 6). The selenazole ring binds in an *anti*-conformation with the selenium atom adjacent to the furanose oxygen, suggesting an intramolecular Se–O interaction. In addition, the electrophilic Se atom makes contact with Gln 334. The adenosine ring is stacked between four residues (Phe 282, His 253, Thr 45 and Thr 252) together with hydrogen bonds from the amino group and N-3. Additional interactions with the adenine ribose and the two phosphates are also observed.[41] The crystal structure of TAD bound to horse liver alcohol dehydrogenase revealed that, in addition to the intramolecular interaction between the sulfur atom and the furanose oxygen similar to that seen with selenium in SAD, the thiazole-4-carboxamide group fitted in the NAD^+-nicotinamide pocket *via* three hydrogen bonds from the amide and the carboxamide NH_2 group is *cis* to the thiazole ring nitrogen.[45]

To conclude, interactions are observed from the carboxamide group and this is consistent with the requirement of a 4-carboxamide in the thiazole or selenazole ring for activity. The thiazole or selenazole ring binds in an *anti*-conformation with the positively charged sulfur or selenium atom adjacent to the furanose oxygen. This intramolecular electrostatic interaction limits rotation around the glycosidic bond which fixes the conformation.[46-48] The *anti*-conformation is in accord with NMR studies suggesting that this conformation is adopted by NADH bound to IMPDH. In the case of

TAD, the *cis* conformation of the thiazole-4-carboxamide is also consistent with the NMR data.[49]

Another synthetic nucleoside designed as an NAD^+ analogue in IMPDH inhibition is 3-β-*D*-ribofuranosylbenzamide (benzamide riboside, **18**, Figure 6), where the nicotinamide group is replaced by a benzamide.[50] In addition to promising toxicity against IMPDH (K_i = 0.118 μM), benzamide riboside was found to be more potent (3-fold, IC_{50} = 2.5 μM) than TF (IC_{50} = 7.5 μM) against human myelogenous leukaemia K562 cells in culture.[50,51] Furthermore, a study using K562 cells incubated with isotope-labelled adenosine and benzamide riboside or TF revealed that the corresponding active metabolite of benzamide riboside, benzamide adenine dinucleotide (BAD), was produced in 2-3 fold higher quantities than TAD.[50,51] Similar to TF and selenazofurin, benzamide riboside requires anabolism to BAD.[50,51]

Despite their promising inhibitory profiles, these adenine dinucleotides are not ideal IMPDH inhibitors because of their metabolic instability. They are quickly degraded by cellular phosphodiesterases to the corresponding nucleosides and resistance to TF is associated with both the decreased anabolic activity of NAD^+-pyrophosphorylase (the converting enzyme) with increased degradation of TAD by phosphodiesterase.[52]

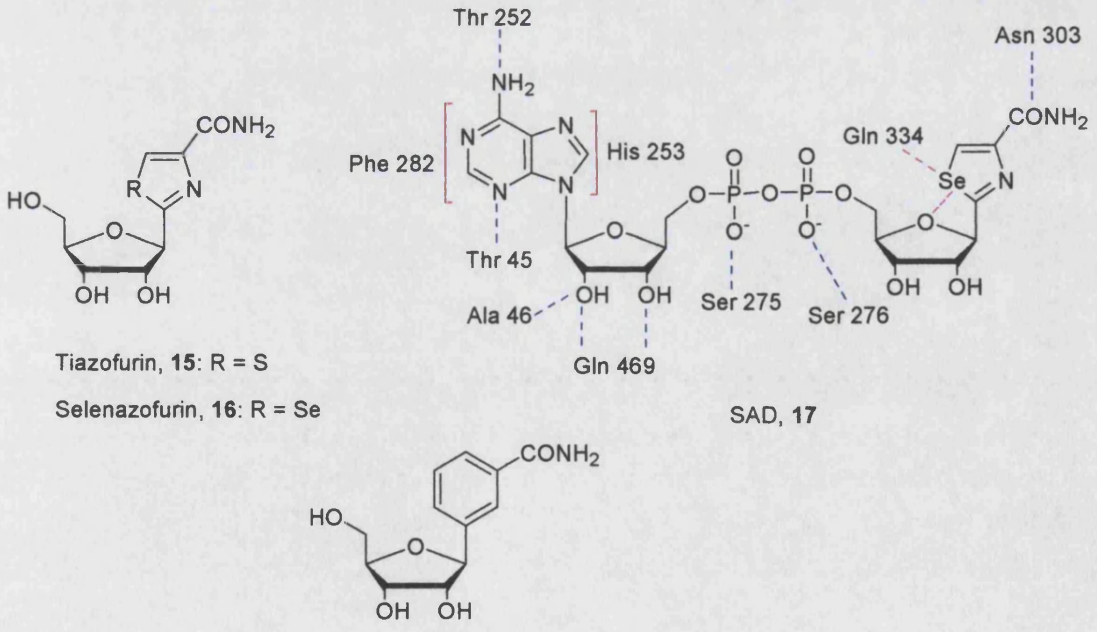

Figure 6. IMPDH inhibitors tiazofurin (TF, **15**), selenazofurin **16** and benzamide riboside **18**, with interactions of SAD **17** to the active site of IMPDH.[41,42,44,50,51] (Electrostatic interactions – purple; hydrogen bonds – blue; ring stackings – red brackets)

Mycophenolate mofetil (MMF, CellCept®, **19**, Figure 7), an ester prodrug of the natural product mycophenolic acid (MPA, **20**, Figure 7), is an uncompetitive IMPDH inhibitor and was approved for the prevention of acute kidney and heart transplantation rejection in combination with steroids and cyclosporin A.[53] MPA was preferred to TF because the latter must be activated by phosphorylation. The efficacy of cell phosphorylation varies in different cell types. In addition, the toxicity profile of TF prompted a new candidate with reduced side effects and enhanced anti-tumour activity. MPA (K_i = 11 nM) displays a 5-fold preference towards type II IMPDH than type I.[54] In additional to the role in depleting guanine nucleotides pool, it induces apoptosis of activated T-lymphocytes, thereby eliminates cells responding to antigenic stimulation and suppresses the recruitment of lymphocytes into sites of graft injection and inflammation.[37]

Interactions between MPA and IMPDH reveal that one face of the bicyclic ring system is stacked on the XMP hypoxanthine ring, while the other makes contact with the active site (Figure 7).[55] Van der Waals interactions are seen from the hexenoic acid chain, methyl and methoxy substituents of the benzofuranone core with Asp 274, Arg 322, Asn 303, Gly 415 and Met 414, together with several hydrogen bonds.

The gastrointestinal toxicity associated with CellCept® highlights the importance in selectively inhibiting type II over type I IMPDH. Further research in developing isoforms-specific compounds as chemotherapeutic agents continues.

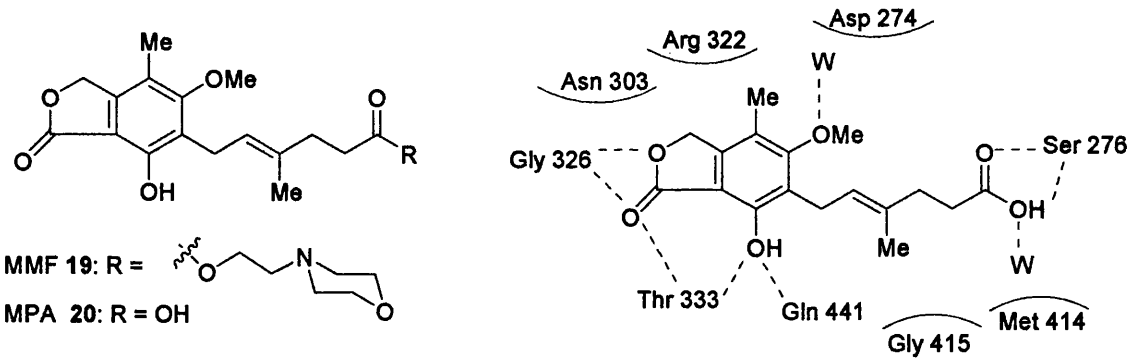

Figure 7. IMPDH inhibitor MMF **19**, a prodrug of the natural product MPA **20**; MPA interactions with the active site reveal numerous hydrophobic contacts.[53-55] (Hydrophobic interactions – red; hydrogen bonds – blue)

1.4 Tumour DNA repair and resistance to chemotherapy and radiotherapy

1.4.1 DNA repair

The survival and integrity of a cell relies fundamentally on genome stability. DNA is frequently damaged by many agents such as oxygen radicals, UV light, ionising radiation, and DNA-damaging chemotherapy, and it is estimated that the average rate of damage is about 10^4 events per cell per day.[56] Highly conserved DNA damage sensor mechanisms are employed to respond to potential cytotoxic effects. There are four complex systems:[57]

1. DNA repair
2. Cell cycle checkpoint control
3. Apoptosis
4. Damage tolerance

DNA repair is the most effective defence system by directly removing the lesions from DNA and comprises five mechanisms:

1. Base excision repair (BER)
2. Nucleotide excision repair (NER)
3. Mismatch repair (MMR)
4. Recombinational repair
5. Direct reversal of damage

Endogenous DNA damage (base damage and single strand breaks) is mainly repaired by BER, whereas NER is an important mechanism for removing a variety of damages, especially lesions of bulky DNA adducts. MMR corrects mismatched bases (insertion/deletion). Recombinational repair is required for double strand breaks and is important for damages induced by radiation. Direct reversal of damage is highly specialised; O^6-methylguanine-DNA methyltransferase (MGMT) is responsible for the irreversible and stoichiometric transfer of a methyl group directly from O^6-methyl-guanine from within the DNA.

Cell cycle checkpoint control involves prolongation of the G1 and G2 phases of the cell cycle to permit more effective DNA repair and avoids DNA synthesis in the presence of excessive DNA damage. Induction of apoptosis eliminates heavily damaged cells, thus protecting the genomic stability and integrity.

Some DNA lesions with high levels of damage or poorly repaired lesions often escape the above systems and persist through replication of DNA, in which case cells adapt the damage tolerance system to allow replication in the presence of DNA damage by lesion bypass and template switching. Lesion bypass directly utilises the damaged template by a) incorporating nucleotide opposite the lesion, followed by b) extension of DNA synthesis. Template switching involves synthesis of DNA on the undamaged template only.

Most anti-tumour agents and radiotherapy target cancer cells by damaging cellular DNA; alkylating agents directly damage DNA, whereas topoisomerase inhibitors inhibit DNA strand repair. Radiotherapy employs ionising radiation (X-ray, γ-ray) that induces damage either by attacking the DNA sugar backbone or producing free radicals. In the less aggressive tumour tissues, sufficient damage can be sustained to achieve cytotoxicity and treatment success. However, the increasing problem of drug resistance and remission indicates that tumour cells employ a highly efficient surveillance system that senses and repairs such damages; another common disadvantage of the conventional treatment is dose-related toxicity to the surrounding healthy tissues. Therefore, it is clear that inhibiting the specific DNA repair proteins are beneficial for tumour selectivity and increased treatment response.

1.4.2 Poly(ADP-ribose) polymerase-1 (PARP-1): the "guardian angel" of the genome

1.4.2.1 Background

BER is involved in the repair of single-strand breaks, leading to the resistance of ionising radiation and alkylating chemotherapeutic agents. This pathway is divided into short-patch and long-patch repair. Short-patch repair (major pathway) removes one base only, whereas long-patch repair can remove 2-15 nucleotides. Short-patch BER removes the incorrect or damaged base by a DNA glycosylase; this generates an apurinic/apyrimidinic site which is cleaved by an AP endonuclease/3'-phosphodiesterase, leaving a single-strand break.[58] Replacement of the damaged base and religation of the DNA involves the binding of poly(ADP-ribose) polymerase-1 (PARP-1) and/or PARP-2, members of the PARP superfamily, then recruitment of a repair complex including DNA polymerase β, DNA ligase I or III and XRCC I (X-ray cross-complementing).[56,59] Long-patch repair is thought to contribute to the repair of oxidised or reduced apurinic/apyrimidinic sites as a minor sub-pathway.

1.4.2.2 PARP-1 and other members of the PARP family

PARP-1 (EC 2.4.2.30) is the founding member of the PARP enzyme family. It is a abundant nuclear protein (about 10^6 molecules / cell).[60] The number of PARP-family members has recently been increased to 17 and the main members are categorised into the following groups:[61]

- DNA-damage-dependent PARPs (PARP-1 and PARP-2)
- Tankyrases (tankyrase-1 and tankyrase-2)
- Other PARPs (PARP-3, PARP-4/vPARP, PARP-6, PARP-8, PARP-10 and PARP-11)

In addition to PARP-1, five members of the PARP superfamily are well characterised:[62] PARP-2 is most similar to PARP-1; it is a 64.8-KDa DNA-binding protein with a similar activity to PARP-1 and includes a nuclear localisation signal (NLS) and a severely modified DNA-binding domain (*vide infra*, Figure 9). PARP-3 is a 60-KDa protein that is thought to interfere with the progression of cell cycle through G1-S phase. Both PARP-2 and PARP-3 lack an automodification domain. PARP-4/vPARP is the largest PARP member (193 KDa) and is the catalytic domain of vault particles, which are barrel-shaped ribonucleoprotein complexes that are involved in multidrug resistance of human tumours. Tankyrase-1 (PARP-5a) is a 142-KDa protein and a positive regulator of telomere length. Telomeres are proteins situated at the end of eukaryotic chromosomes and are essential for chromosomal stability. Tankyrase-2 (PARP-5b) shows 85% amino-acid homology to tankyrase-1 but its role has not been determined.

1.4.2.3 Mechanism of action of PARP-1: poly(ADP-ribosyl)ation

Poly(ADP-ribosyl)ation occurs in almost all nucleated cells of mammals, plants and lower eukaryotes but is absent from yeast.[63] It consists of the synthesis of ADP-ribose polymer on target proteins and both PARP-1 activation and poly(ADP-ribosyl)ation represent an immediate cellular response to DNA damage.[64]

PARP-1 functions as a DNA-nick sensor; it binds to and is activated by DNA strand breaks and concomitantly cleaves NAD^+ **21** into nicotinamide **23** (*vide infra*, Scheme 5).[65] Cleavage of the nicotinamide–ribose bond proceeds *via* a transition state **22** and the pyridinium–N-glycosidic bond breaking gives rise to the intermediate oxocarbenium ion (**24**, *vide infra*, Scheme 5).[66] This is followed by the transfer of the resulting ADP-ribosyl unit onto acceptor proteins (initiation).

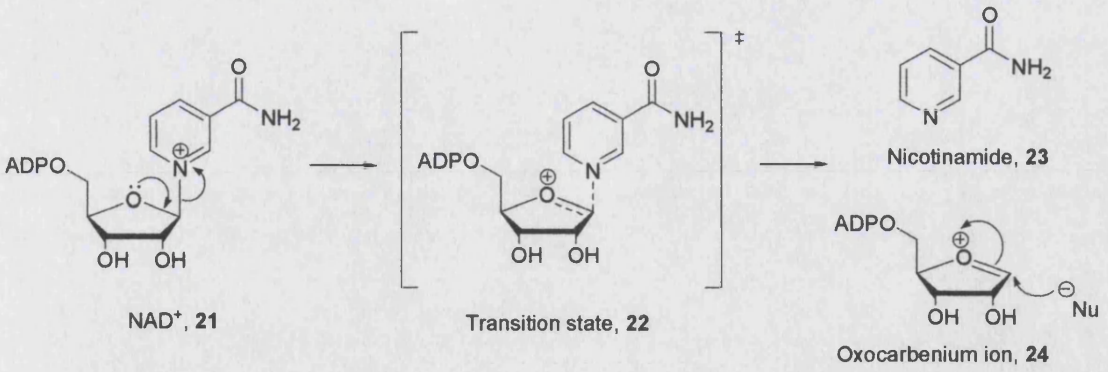

Scheme 5. The proposed mechanism of NAD^+ cleavage of PARP-1.[66]

Subsequent polymerisation of ADP-ribose units occurs on the 2'-hydroxyl group of the adenine ribose (chain elongation), with an α(1'' → 2') glycosidic bond linking the C-1 of the nicotinamide ribose; polymerisation also occurs on the 2''-OH of the nicotinamide ribose, with a (1''' → 2'') glycosidic bond linking the C-1 of the nicotinamide ribose (branching). The size of the branched polymer can be up to 200 ADP-ribose units (Figure 8).[67] Mostly, the target acceptor protein of poly(ADP-ribosyl)ation is PARP-1 itself (automodification), but many other proteins have been described including p53, NF-κB (nuclear factor-κB), histones, DNA ligases, DNA polymerases, topoisomerases I and II and DNA-dependent protein kinase.[68] The net effect of linking a long, negatively charged polymer to a protein is altered protein activity.[69] As discussed above, most substrates of PARP-1 are proteins involved in DNA replication, transcription and repair. Therefore, modification of their properties may have a profound effect on their DNA binding abilities.

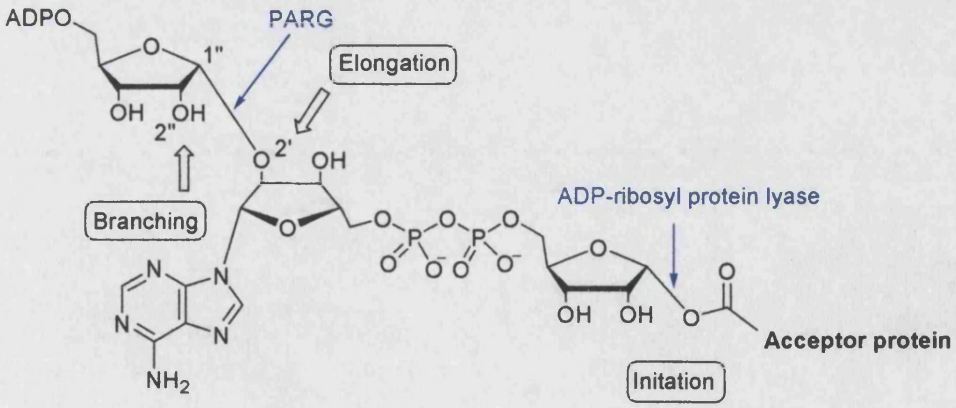

Figure 8. Poly(ADP-ribosyl)ation: initiation, elongation and branching.[67]

Poly(ADP-ribosyl)ation is a dynamic process with a short (< 1 min) half-life of the polymer *in vivo*.[67] Upon automodification of PARP-1 on the DNA lesion site, the enzyme departs under the effects of electrostatic repulsion between the negatively charged ADP-ribose chains and the negatively charged DNA. Local relaxation of the chromatin allows access of DNA-repair enzymes and poly(ADP-ribose) glycohydrolase (PARG, EC 3.2.1.143) is recruited to hydrolyse ADP-ribose polymers rapidly (Scheme 6).[70,71] ADP-ribosyl protein lyase is another enzyme responsible for PARP-1 catabolism. While PARG cleaves ribose-ribose bonds of both linear and branched poly(ADP-ribose) polymers, ADP-ribosyl protein lyase removes the protein-proximal ADP-ribosyl group from the acceptor protein (*vide supra*, Figure 8).[71]

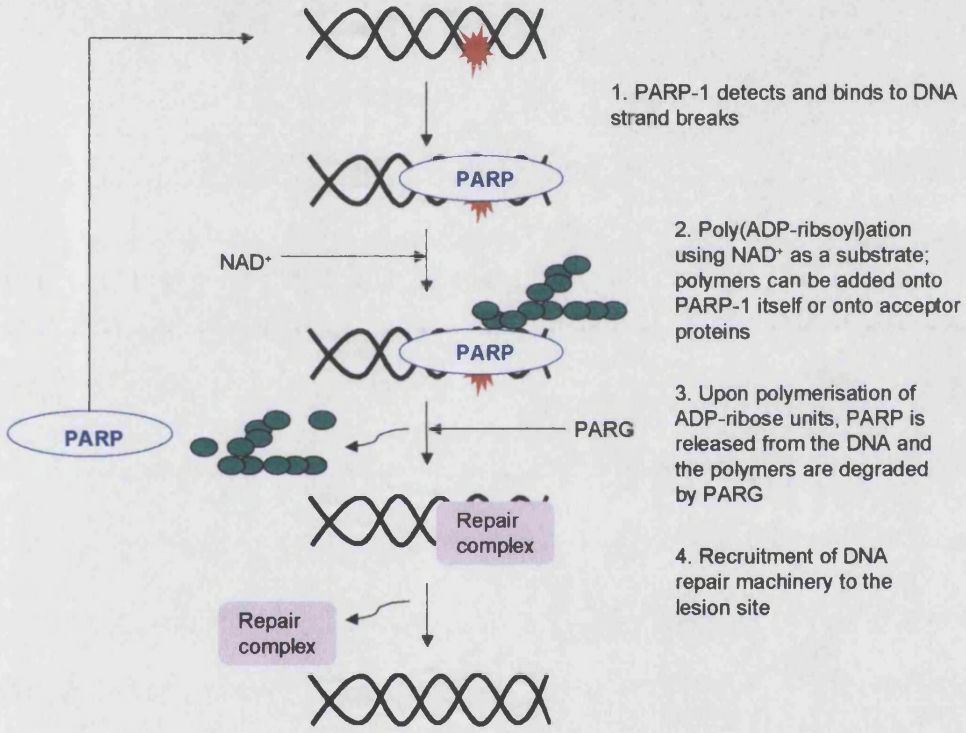

Scheme 6. Mechanism of action of PARP-1.[70,71]

1.4.2.4 Structure of PARP-1

The human PARP-1 is a 113-KDa protein composed of 1014 amino acid residues.[72] The gene coding for this protein is at the q41 – q42 position of the chromosome.[72] Under normal conditions, inactive PARP-1 resides in the nucleoplasm and in the mitochondria.[73] There are three functional domains (*vide infra*, Figure 9):[73]

- The N-terminal DNA-binding domain with a molecular weight of 46 KDa. It contains two zinc fingers which are responsible for DNA binding and some

protein-protein interactions. The first zinc finger is essential for PARP-1 activation upon DNA damage, whereas the second is essential for recognition of DNA single-strand breaks but not double-strand breaks. A DNA nick sensor, nuclear localisation signal (NLS) is also present within a caspase-cleavage site (DEVD).

- The 22-KDa central automodification domain is rich in glutamic acid residues, which is consistent with the fact that poly(ADP-ribosyl)ation occurs on such residues. It contains a BRCT motif (breast cancer susceptibility protein, BRCA1, C-terminus), which is common in many DNA repair and cell cycle checkpoint proteins. Through BRCT, PARP-1 participates in protein-protein interactions.

- The C-terminal catalytic domain (54 KDa); it is highly conserved in eukaryocytes. The active site consists of a 50-amino acid sequence known as the "PARP-1 signature" that shows 100% homology among vertebrates. It is essential for NAD^+ binding, ADP-ribosyl transfer, elongation and branching reactions.

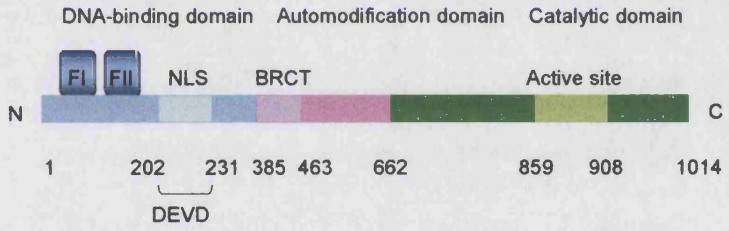

Figure 9. Schematic representation of the structure of hPARP-1, showing the three functional domains.[73]

1.4.2.5 Therapeutic potentials of inhibition of PARP-1

In addition to its role in DNA repair, PARP-1 activation also regulates both apoptosis and necrosis and the extent of DNA damage directly affects the mode of cell death.[74] Moderate DNA damage induces apoptosis, and caspases recognise the DEVD motif in the NLS and cleave PARP-1 into two fragments: p89 and p24. The enzyme cleavage separates the DNA-binding domain from the catalytic domain and inactivates the enzyme. The fragments further suppress the activity of PARP-1 by inhibiting dimerisation and further binding of intact PARP-1 to DNA.[75,76]

In cases of severe DNA damage, PARP-1 is overactivated and excessive utilisation of the intracellular storage of NAD^+ depletes ATP. This prevents cells from initiating

apoptosis because many stages in the apoptotic pathway rely on ATP and cells are subjected to necrosis.[77] It is confirmed that necrosis is a more severe mode of cell death compared to apoptosis. Necrosis is associated with the disintegration of plasma membrane; leakage of cellular contents from necrotic cells into the surrounding tissue may contribute to organ injury and inflammation. In comparison, apoptotic cells remain intact and are rapidly cleared from the tissues by macrophages. Therefore, PARP-1 serves as a determinant in the survival of cells and can shift the mode from necrosis to apoptosis (Scheme 7).[78]

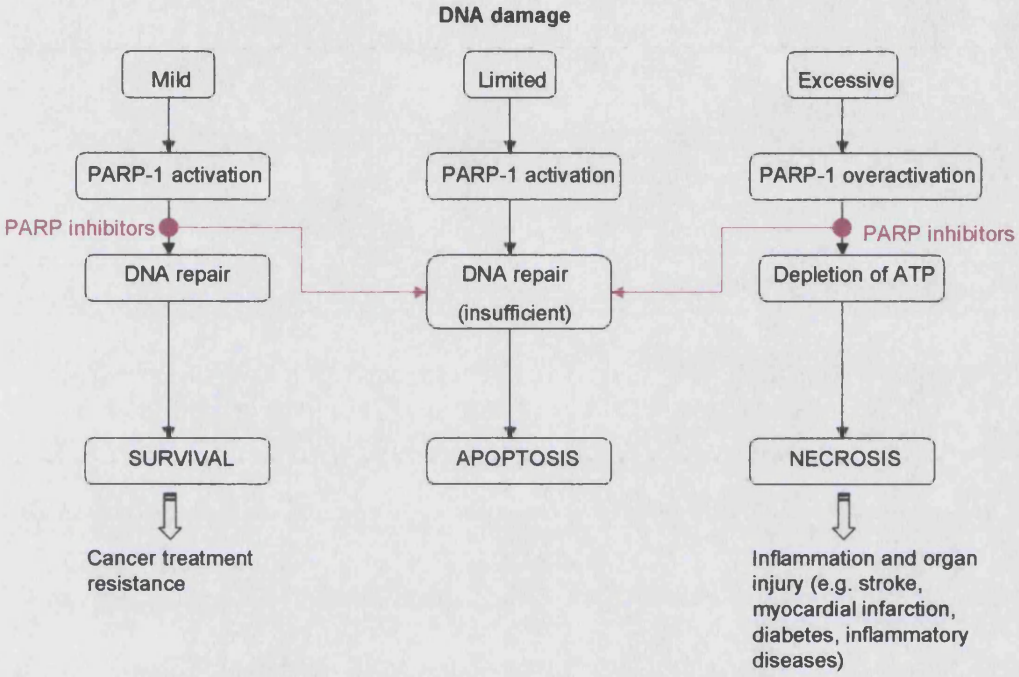

Scheme 7. PARP-1 inhibition in cell survival and death. Degree of DNA damage determines the outcome of cell survival and death. In the case of mild DNA damage, PARP-1 inhibitors suppress repair mechanism, leading to cell apoptosis; if the damage is severe, PARP-1 inhibition protects energy pools thus shifting necrosis to apoptosis.[78]

The design of PARP-1 inhibitors is based on the interaction of NAD^+ with the enzyme active site. The carboxamide group on the nicotinamide ring, adenine ribose phosphate and the adenine ring all form hydrogen bonds with the DNA-binding domain. In addition, there are π-π interactions between the nicotinamide ring and the active site (*vide infra*, Figure 10). Early structure-based drug design used nicotinamide as a NAD^+ mimic. However, nicotinamide was found to be a poor candidate for PARP-1 inhibition due to weak inhibitory activity and lack of specificity. It is a target for NAD^+-metabolising enzymes such as nicotinamide-N-methyltransferase and phospho-ribosyl transferase.[66]

Benzamide, a close analogue of nicotinamide, was shown to be an effective inhibitor because it lacks a ring nitrogen and therefore cannot be metabolised by NAD^+-metabolising enzymes. Unfortunately, the poor solubility of this hydrophobic compound prompted search for related compounds with better solubility.[66]

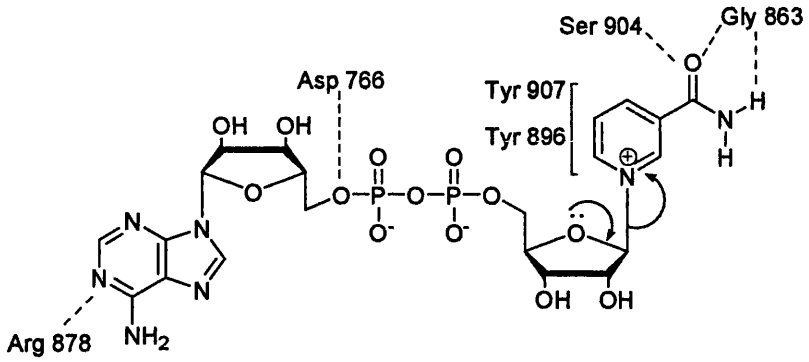

NAD^+, **21**

Figure 10. Interactions of NAD^+ **21** with PARP-1 active site.[66] (Hydrogen bonds – blue; π–π interactions – red brackets)

A systemic investigation of benzamide derivatives in the 1980's revealed that substitution at the 3-position with polar groups improved solubility in water while retaining inhibitory activity (*vide infra*, Figure 11).[79] This position mimics the ring nitrogen of nicotinamide and these 3-substituted benzamides occupy the nicotinamide-binding site with the 3-substituent binding to the ribose nucleoside-binding domain. These compounds lack a cleavable C–N bond and are incapable of undergoing analogous C–N bond cleavage, thus serving as competitive inhibitors. The carbonyl oxygen interacts with the active site as an electron donor and the ability to form hydrogen bonds is further enhanced by conjugation to an electron-rich aromatic ring. In addition, there is also non-polar interaction between the aromatic ring and the active site. A free amido hydrogen is also necessary for hydrogen bond interaction with the active site. The preferred *anti*-conformation of the carboxamide group mimics the biologically active conformation adopted by enzyme-bound NAD^+. 3-Aminobenzamide and 3-methoxybenzamide became the "benchmark" PARP-1 inhibitors with excellent water solubility and K_i values of less than 2 μM.[66] Thereafter, a large number of PARP-1 inhibitors have been synthesised with attention to increased potency and improved pharmacokinetics profile. Bi-, tri- and tetracyclic derivatives and the more recent nucleic-acid and nucleoside derivatives showed promising results.[80-84]

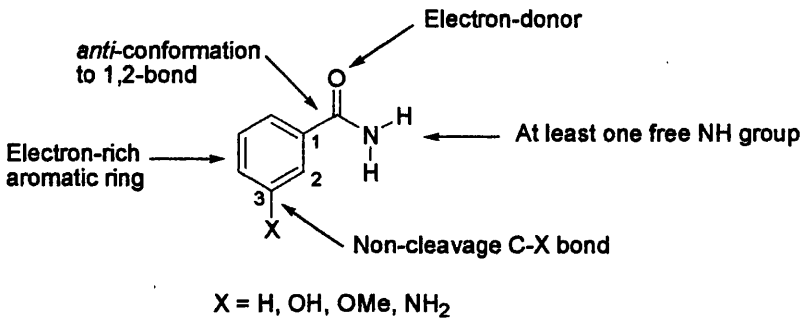

Figure 11. SAR properties for benzamide inhibitors of PARP-1.[66,79]

1.4.2.6 PARP-1 inhibitors in cancer

Inhibition of PARP-1 has been extensively studied with the theory that by suppressing PARP-1 activity, cytotoxicity induced by chemotherapy or radiotherapy is enhanced by impairing the DNA repair system and promoting cell apoptosis in response to sustained damage. Furthermore, its role in cell necrosis may also assist in protection against chemotherapy-induced toxicity. Several lines of investigations have supported the significant clinical indications of PARP-1 inhibitors as chemosensitisers, radio-sensitisers and as protective agents in treatment-induced toxicities.[85,86]

A number of studies have evaluated the potential role of PARP-1 inhibitors as chemosensitisers; co-administration of a PARP-1 inhibitor with cytotoxic drugs that cause single- and double-strand DNA breaks potentiates their effects and causes persistent DNA damage.

Temozolomide (TMZ) is a methylating agent for treatment of primary brain tumours and metastases, including malignant melanoma. However, frequent drug resistance presents a problem for its clinical response. One of the modified bases is O^6-methylguanine (O^6-MeG) and resistance to TMZ is the result of efficient repair of methyl adducts from O^6-MeG by high levels of O^6-alkylguanine-DNA alkyltransferase (AGT) and tolerance to O^6-MeG toxicity due to functional defects of the mismatch repair (MR) system. In AGT-proficient or MR-deficient tumour cells, inhibition of PARP-1 restored susceptibility to TMZ by disrupting the function of PARP-1 in the BER process. Treatment with PARP-1 inhibitors prior to exposure to TMZ results in increased DNA strand breaks, apoptosis and tumour growth inhibition.[87-89]

PARP-1 inhibitors have been shown to enhance the cytotoxicity of DNA topoisomerase I inhibitors camptothecin and irinotecan. Topoisomerase I cleaves a single strand of

DNA and relaxes DNA supercoiling, favouring DNA replication and RNA transcription. Topoisomerase I inhibitors act by binding non-covalently to topoisomerase I-DNA thus stabilising the cleaved complex and preventing DNA re-ligation. PARP-1 interacts with and promotes the activity of topoisomerase I and poly(ADP-ribosyl)ated PARP-1 facilitates resealing of strand breaks.[87-90]

Similar lines of research also identified potential chemopotentiating effects of PARP-1 inhibitors in combination with a number of anti-cancer agents such as bleomycin, doxorubicin, cisplatin and the DNA minor-groove binder $MeOSO_2(CH_2)_2$-lexitropsin (Me-Lex).[87-89]

Another potential application of PARP-1 inhibitors is radiopotentiation. Ionising radiation generates single- and double-strand breaks and induces apoptosis. While single-strand breaks are repaired by BER and activated PARP-1, double-strand breaks are mostly repaired by the recombinational pathway that recruits DNA-dependent protein kinase (DNA-PK). PARP-1 inhibitors have been shown to increase single- and double-strand breaks and potentiate cytotoxicity of γ-radiation. Although PARP-1 is mainly associated with single-strand breaks, evidence suggests that it also stimulates DNA-PK activity, thus facilitating repair of double-strand breaks.[87-89]

The use of PARP-1 inhibitors as adjuvant therapies to counteract toxicity induced by anti-cancer drugs has also been considered. As shown before, PARP-1 is actively involved in the regulation of cell necrosis and inhibition of the enzyme protects normal tissues from oxidative stress generated by chemotherapy that can cause serious side effects. Clinical uses of doxorubicin and cisplatin are limited by their serious, often irreversible, dose-dependent cardiotoxicity (cardiac myopathy and heart failure) and nephrotoxicity (kidney damage), respectively. Both agents cause oxidative stress by the production of reactive oxygen species, which leads to single-strand breaks and PARP-1 activation. Studies have shown that co-administration of PARP-1 inhibitors with doxorubicin or cisplatin significantly reduced the level of drug-induced toxicities.[89]

1.4.2.7 PARP-1 inhibitors in other clinical indications

The cellular protective effect of PARP-1, due to its role as a determinant in cell death mode, makes the enzyme inhibitors useful agents in the treatment of a range of pathophysiological diseases including stroke,[91] myocardial infarction,[92] diabetes,[93] shock,[94] glaucoma,[85] neurodenegerative diseases and several other inflammatory

diseases.[85,87,94-96] PARP-1 inhibition prevents the decrease in intracellular NAD^+ and ATP levels, thereby shifting the necrotic cell death to apoptosis and preventing cell dysfunction and organ injury.

1.5 Use of sulfoximines in drug design

1.5.1 Discovery of sulfoximines

Between the years 1946 and 1950, several publications described a toxic agent in processed flour.[97] Flour made from freshly milled wheat is unsuitable for baking and it requires aging with treatment agents, including nitrogen trichloride, "agene". However, agenised flour, used traditionally as part of a diet for dogs, gave rise to epileptic seizures and death. In 1949, a highly active crystalline material was isolated from agenised gluten and zein as a sulfur-containing compound with a formula of $C_5H_{12}N_2O_3S$.[97] It was concluded that "a molecule $C_5H_{12}N_2O_3S$ can be regarded formally as being derived from methionine sulfoxide by the addition of =NH, or from methionine sulfone by the replacement of O by =NH. In such a molecule there is clearly the possibility that the sulfur atom is asymmetric". This new class of compounds was called sulfoximines and the toxic agent was named methionine sulfoximine (MSO, **25**, Figure 12).[98]

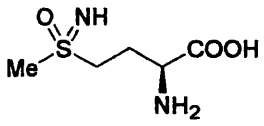

MSO, **25**

Figure 12. Structure of methionine sulfoximine (MSO, **25**), the first sulfoximine discovered.[98]

1.5.2 Structure and properties of sulfoximines

Sulfoximines are chemically and configurationally stable compounds. They possess extremely versatile chemistry and are tetrahedral in shape (*vide infra*, Figure 13). The sulfur atom carries both a nitrogen and oxygen function, with the nitrogen being weakly basic. If the two carbon substituents are different, the sulfur atom is chiral. The whole unit is electron-withdrawing. The sulfoximine group also contains acidic hydrogens on the α-carbon and the nitrogen.[98]

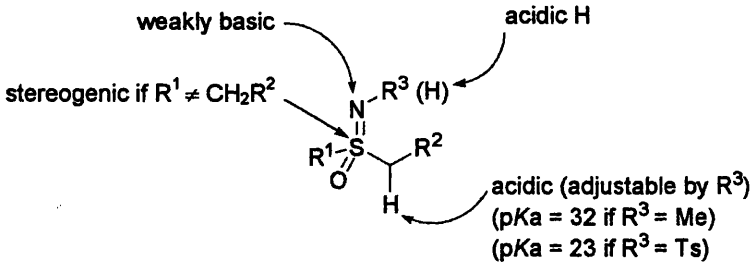

Figure 13. The versatile sulfoximine group, with a stereogenic sulfur atom, basic nitrogen and acidic α-hydrogens.[98]

The IR spectra of sulfoximines exhibit absorption bands for O=S=N (ν 1100-1200 cm^{-1}) and for the NH stretch (free sulfoximines) at 3100-3400 cm^{-1}.[98] The chemical shifts of the α-methylene protons in the NMR spectra are similar to those for the corresponding sulfone, with a small downfield shift because sulfoximines are more acidic. The whole unit is slightly more electron-withdrawing than the sulfone (if R^3 is electron-withdrawing) and more so than the sulfoxide. The chemical shift of the α-protons resonates in the range of δ 3.0-3.5 depending on the nature of the N-substituents.[98]

Due to the chirality at both the sulfur atom and carbon atom, MSO has four isomers. The absolute configuration of the biologically active isomer was found to be *S,S* (Figure 14).[97]

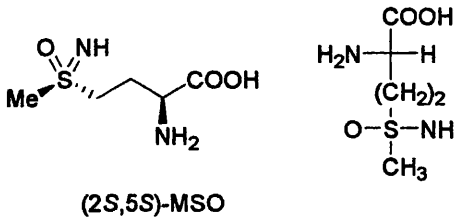

Figure 14. The biologically active MSO has the absolute configuration of *S,S*.[97]

1.5.3 Biological activities of sulfoximines

1.5.3.1 Methionine sulfoximine (MSO)

MSO was identified as a convulsant and an irreversible inhibitor of glutamine synthetase (GS, EC 6.3.1.2).[99] Glutamine (Gln) is a major nitrogen source in amino-acid biosynthesis and GS catalyses the formation of Gln from glutamate and ammonium ion (*vide infra*, Scheme 8):[34]

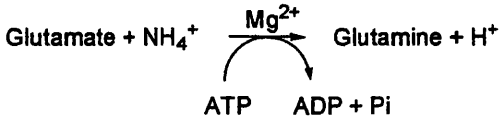

Scheme 8. Glutamine synthetase-catalysed conversion of glutamate to glutamine.[34]

Ronzio and Meister first investigated the mechanism of inhibition of GS by MSO in 1968 and revealed that the irreversible inhibition of GS by MSO is associated with its phosphorylation by ATP at the sulfoximine nitrogen and the tight binding of this phosphorylated derivative.[99] They confirmed that MSO adopts a conformation similar to that proposed for *L*-glutamate and thus can bind to both the glutamate- and ammonia-binding sites as a bifunctional reagent. Subsequent data by Ronzio and Meister identified the following properties of MSO:[100-103]

i. Only one of the four isomers, (*S*,*S*)-MSO, is phosphorylated by GS and produces irreversible inhibition. Furthermore, the tetrahedral nature of (*S*,*S*)-MSO is closely related to the tetrahedral intermediate formed in GS-catalysed Gln synthesis;
ii. The same isomer that inhibits GS is also responsible for the convulsant effect; administered MSO was found to cause swelling of nerve endings and loss of synaptic vesicles especially of the noncholinergic types.

Following on this body of evidence, Richman *et al.* documented another activity of MSO.[104] A different enzyme is also involved in the utilisation of glutamate: γ-glutamyl-cysteine synthetase (γ-GCS, EC 6.3.2.2), which catalyses the first step in the synthesis of glutathione (γ-GluCysGly, GSH), a highly important tripeptide (*vide infra*, Section 1.5.4.2). An amide linkage is formed between the γ-carboxyl group of glutamate and the amino group of cysteine in the presence of ATP. Subsequent condensation with glycine, catalysed by the enzyme glutathione synthetase, gives rise to glutathione (Scheme 9).[34]

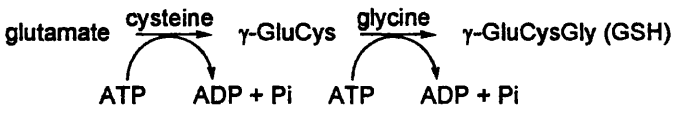

Scheme 9. γ-Glutamylcysteine synthetase (γ-GCS) catalyses the first step of the synthesis of glutathione.[34]

Both of these reactions involve a γ-glutamyl intermediate **26** (*vide infra*, Figure 15) and it was this consideration that led Richman *et al.* to examine the effect of MSO on

γ-GCS.[104] They found that MSO inhibits γ-GCS in a similar fashion, *i.e.* it involves the formation of a phosphorylated derivative (ATP) at the sulfoximine nitrogen (**29**, Figure 15). However, MSO phosphate **29** binds more tightly to the active site of GS than γ-GCS, and the same isomer, *i.e.* (*S*,*S*)-MSO that inhibits GS, also inhibits γ-GCS. It is interesting to note that MSO-induced convulsions were shown to associate with inhibition of GS, not of γ-GCS.

Subsequent structural studies by Griffith and Meister revealed that, by replacing the methyl group of MSO with other alkyl groups (ethyl or propyl), the inhibition of GS decreases but not that of γ-GCS.[105] Computer mapping of the active site of GS indicated that the methyl group of MSO binds to the ammonia-binding site **28** in the enzyme, which is relatively smaller in capacity than the cysteine-binding site **27** in γ-GCS (Figure 15).[106]

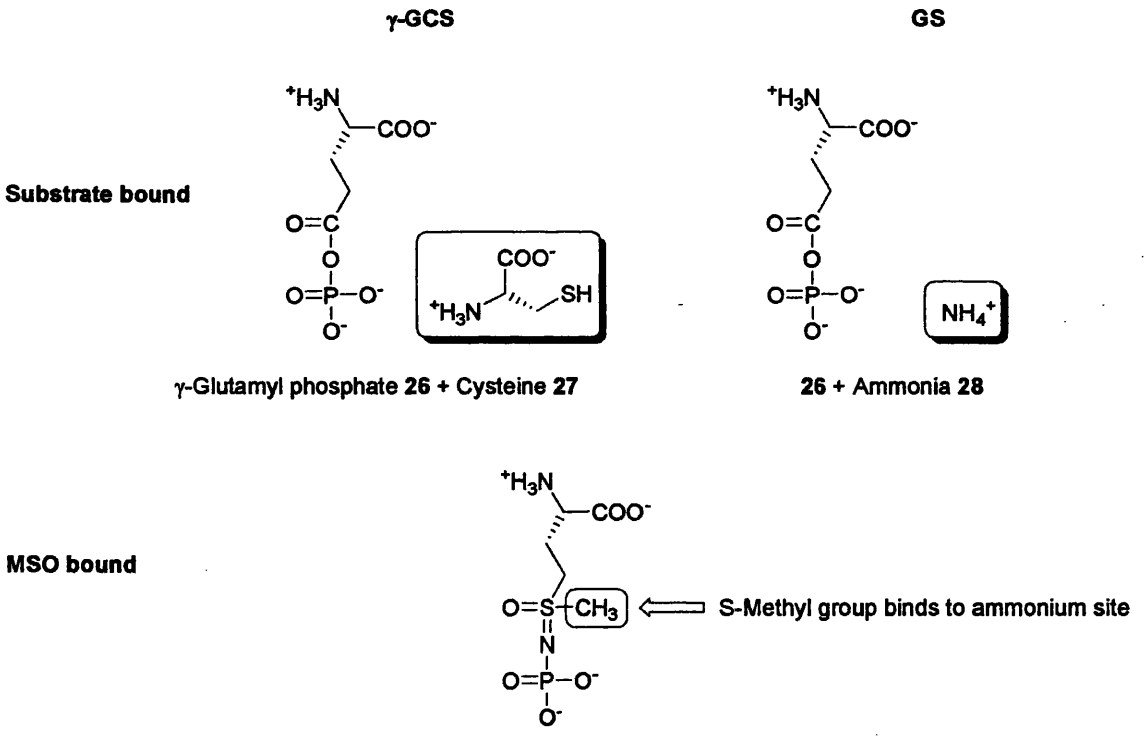

Figure 15. Diagrammatic representation of substrate- and inhibitor-bound active sites of γ-GCS and GS. S-methyl of MSO occupies the ammoium ion site **28**.[106] Therefore, substituting the methyl group with bulkier alkyls diminishes the affinity for GS (smaller binding site) but not for γ-GCS (large binding site for cysteine **27**).

1.5.3.2 Buthionine sulfoximine (BSO)

A series of MSO analogues were studied for their inhibitory activity of γ-GCS based on the structural information above.[107] The most potent is the butyl derivative, buthionine sulfoximine (BSO, **30**, *vide infra*, Figure 16). The active isomer, (*S*,*S*)-BSO, inhibited γ-GCS 20 times more effectively than the propyl derivative, prothionine sulfoximine, and at least 100 times more effectively than MSO. Hence, it was confirmed that bulky substituents at the sulfoximine sulfur affect the selectivity and affinity for GS and γ-GCS.[107,108]

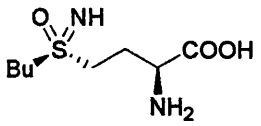

(2*S*,5*S*)-BSO, **30**

Figure 16. 2*S*,5*S*-Buthionine sulfoximine (BSO, **30**), the most potent inhibitor of γ-GCS.[107,108]

More recent evidence suggested that both MSO and BSO inhibit γ-GCS by serving as a tetrahedral intermediate or transition-state analogue formed in the reaction of enzyme-bound γ-glutamyl phosphate with cysteine (Scheme 10).[109]

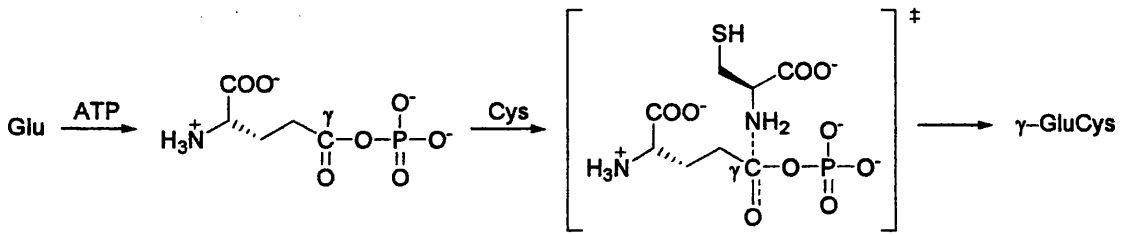

26 transition state, **31**

Scheme 10. Proposed mechanisms of the γ-GCS-catalysed reaction, with the initial formation of γ-glutamylphosphate **26**, followed by nucleophilic attack of cysteine *via* a tetrahedral intermediate **31**.[109]

1.5.4 Pharmaceutical applications of sulfoximines

1.5.4.1 Glutamine (Gln)

Gln is the most abundant amino acid in the body, with its primary source in the skeletal muscle, from where it is released into the bloodstream and transported to various target organs and cells such as kidney, intestine, liver, heart, neurons, lymphocytes, macrophages, neutrophils, pancreatic β-cells and white adipocytes.[110] Gln stimulates a

large variety of cellular reactions and it is an important fuel in cell functions. A high rate of glutamine uptake is characteristic of rapidly dividing cells and in the absence of Gln, tissues cells cannot grow.[111] Many studies have been performed to study the various functions of Gln and the main features are summarised in Table 3.[110,111]

Activity	Mechanism of action
Cell metabolism and proliferation	• Cellular fuel: precursor of glucose; nitrogen source for urea synthesis; carbon source for lipid synthesis • Induces cell swelling in hepatocytes • Precursor of amino acids, peptides, proteins, purines and pyrimidines, and thus of nucleic acids and nucleotides – regulates DNA and protein synthesis
Cell defence and repair	• Enhancer of heat shock proteins (HSP), which are important in cellular survival and endurance of physiological stresses. • Inhibits nitric oxide synthesis *in vivo* in rats; protects cells from stress response and prevents organ injury • Glutamate source for glutathione (GSH) synthesis *via* the γ-glutamyl cycle (*vide infra*, Scheme 11) – GSH is a major determinant in redox status and a key cellular antioxidant (*vide infra*, Section 1.5.4.2). • Protects leukocytes against apoptosis by upregulating Bcl-2 (anti-apoptotic) and downregulating Bax and Bcl-X_s (pro-apoptotic) expression; prevents activation of caspases-3 and -8 in enterocytes
Immune function	• Source for cytokine production (e.g. TNF-α, IL-1β and IL-6) • Oxidative response – increases production of superoxide anion (O_2^-) by NADPH oxidase in neutrophils

Table 3. Main functions of the multifaceted amino-acid, glutamine (Gln).[110,111]

GS catalyses the ATP-dependent synthesis of Gln from glutamate and ammonia. It is found in all organisms and contributes to ammonia detoxification and, in neural tissues, the recycling of the neurotransmitter glutamate *via* localisation of the enzyme to the cytoplasm of glial cells. There are three types of GS: GS-I is found mostly in prokaryotes, GS-II is located mostly in eukaryotes and GS-III, also found in prokaryotes.[112] GS-I is the most characterised and the structure is determined to be a dodecamer, with each monomer containing ~470 residues. There are two domains within a monomer, the smaller N-terminal domain and the larger C-terminal domain, with the latter holding most of the active site residues. Two metal ions (Mg^{2+} or Mn^{2+}) present in each active site are crucial to the enzymatic activity.[112] The structure of the

smaller eukaryotic GS-II (~370 residues) has just been studied from the plant *Phaseolus vulgaris* and found to be an octamer with four active sites. It binds to eight ATP molecules but only four molecules of MSO.[112]

1.5.4.2 Glutathione (GSH)

GSH is present in most mammalian and many prokaryotic cells and is the most abundant intracellular thiol (0.1-10 mM).[113] It can be present as a reduced form (GSH) and an oxidised form, glutathione disulfide (GSSG). GSH is kept in its reduced form by the NADPH-dependent GSSG reductase intracellularly, and, under physiological conditions, the concentration of the reduced form is 10-100 fold higher than the oxidised form.[114] When cells are subjected to oxidative stress, the ratio of GSH/GSSG is decreased with a raised concentration of GSSG or depleted GSH levels and this ratio is important in relation to cell death.[111]

The first step in the synthesis of GSH is catalysed by γ-GCS in the γ-glutamyl cycle (Scheme 11).[113] The *E. coli* γ-GCS has been cloned and sequenced and found to be a single polypeptide chain; the rat kidney enzyme was the first mammalian form to be purified and investigated and was found to be highly homologous to the human enzyme.[113] It is a heterodimer with two subunits. The heavy 73-KDa subunit is catalytically active and contains the site of GSH feedback inhibition. The lighter 31-KDa subunit has no catalytic activity but exhibits a regulatory effect on the heavier subunit when they are co-expressed.[115]

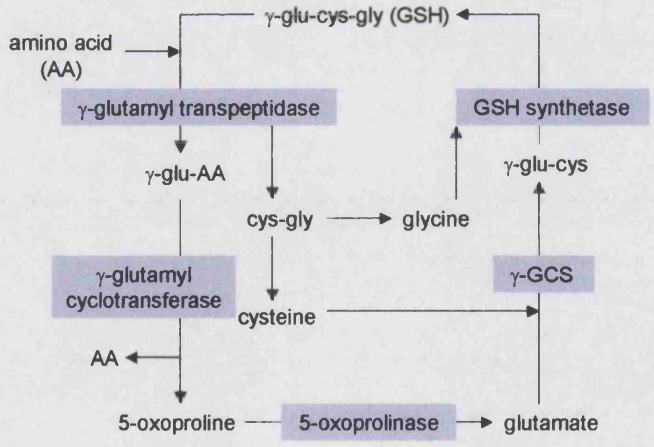

Scheme 11. Glutathione (GSH) synthesis – the γ-glutamyl cycle.[113]

Besides its role as a redox buffer, GSH is involved in the metabolism and maintenance of the thiol moieties of proteins and low molecular weight compounds such as cysteine. GSH is a cellular antioxidant, and detoxification is achieved by reacting with toxic exogenous or endogenous compounds and forming GSH conjugates.[114]

1.5.4.3 Clinical aspects in cancer

It is clear that both Gln and GSH play important roles in cell proliferation, function and death. Gln mainly contributes to tumour growth and cell proliferation, being a precursor in nucleotide and nucleic acid synthesis and a fuel source for cells, along with its role in apoptosis. However, the most striking feature among the many functions of Gln is its relation to GSH biosynthesis, the latter being a valuable redox factor in oxidative stress and tumour growth. GSH is essential in protecting cells from oxidative damage and the detoxifying activity has been implicated in resistance of tumours against effects of chemotherapeutic agents that act by producing oxygen radicals and/or by causing oxidative stress and eventual apoptosis. The role of GSH has been studied extensively, and many data demonstrate that it is a good target for cancer and that inhibition by BSO may be beneficial (*vide infra*, Scheme 12).

Levels of GSH were found to increase in many drug-resistant tumours and tumour cell lines.[116] Intracellular inactivation of cisplatin has been proposed as a mechanism of cisplatin resistance. Rudin *et al.* investigated this hypothesis in MCF-7 breast cancer cell lines transfected with the apoptotic inhibitor Bcl-2.[117] Overexpression of Bcl-2 has been shown to increase cisplatin resistance by antagonising the apoptotic-induced production of reactive oxygen species (ROS). The investigators found that the Bcl-2/MCF-7 cells had a nearly 3-fold increase in cellular GSH levels and an increased cisplatin resistance. Treatment with BSO reduced glutathione levels and prevented Bcl-2-mediated cisplatin resistance without affecting Bcl-2 expression. Therefore, inhibition of glutathione in Bcl-2-positive tumours that may prove to be a potential anti-cancer target.

Calvert *et al.* reported that L1210 murine leukaemia cells with melphalan resistance had higher GSH levels than normal cells and that drug sensitivity was restored completely by decreasing GSH concentrations.[116] Anderson and Reynolds observed a similar synergistic cytotoxicity of BSO and melphalan in neuroblastoma cell lines.[118] Phase I clinical trials at a later stage by Bailey documented an increase in myelo-supression with BSO and melphalan.[119]

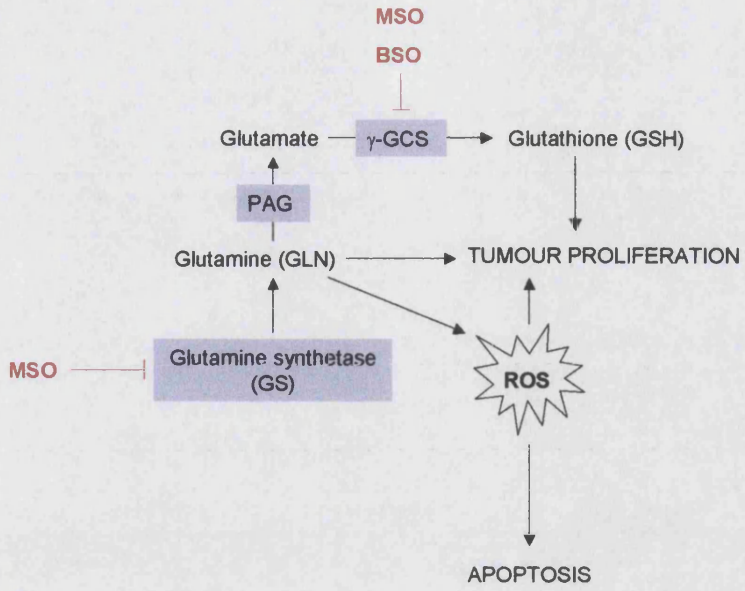

Scheme 12. Roles of MSO and BSO in Gln and GSH synthesis and metabolism. (PAG – phosphate-activated glutaminase)

Subsequent investigations of the effect of GSH with other chemotherapeutic agents, such as the bioreductive agent tirapazamine, mitomycin C and doxorubicin all demonstrated the relation of drug resistance and treatment failure to GSH levels, reinforcing the role of BSO and other glutathione inhibitors in anti-cancer therapy.[120-122] A recent publication by Chew *et al.* highlighted the role of GSH in modulating apoptosis induced by a novel series of heteroaromatic-substituted hydroxycyclohexadienones (quinols) synthesised in their laboratory.[123] These compounds exhibited *in vitro* anti-tumour activity by apoptosis against a variety of cancer cell lines and *in vivo* anti-tumour activity in different tumour xenografts. Increased GSH levels were observed upon treatment with the anti-tumour quinols, indicating the recruitment of GSH in response to protect cells from oxidative damage caused by the quinols. Furthermore, the cells were found to be 6-10 times more sensitive to the compounds when GSH levels were depleted by administration of BSO.

Recent studies also pointed to the inhibition of GS being clinically relevant in the treatment of *Mycobacterium tuberculosis* infections.[124] GS released by mycobacteria is involved in the formation of the pathogen's cell wall and GS inhibitors may be useful antibacterials.

Interestingly, the sulfoximine moiety has itself been applied in the design of transition-state analogue inhibitors of *E. coli* γ-GCS. The compound synthesised by Hiratake *et al.* (**32**, *vide infra*, Figure 17) has a carboxyl function at the β-carbon to the

tetrahedral central heteroatom mimicking the carboxyl group of cysteine in the transition state (**31**, Figure 17).[125]

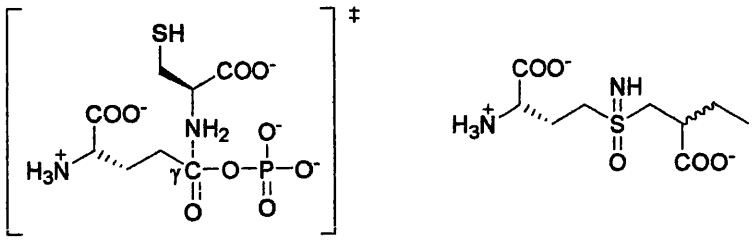

Transition state, **31** **32**

Figure 17. Sulfoximine transition-state analogue of γ-GCS, **32**.[125]

The sulfoximine analogue **32** (Figure 17) was found to be a potent ATP-dependent inactivator of γ-GCS with an overall affinity (K_i = 99 nM) of a thousand times greater than that of BSO (K_i = 49 μM). The *E. coli* enzyme was inactivated only by the (*R*)-sulfoximine, not (*S*)-sulfoximine. The latter demonstrated a reversible inhibitory effect with a K_i of 12 μM. It was concluded that the two diastereoisomers may be interesting species-selective drug targets based on the geometry of individual enzyme active sites and the required stereochemistry.[125]

1.5.4.4 Sulfoximine pseudopeptides

The use of peptides in pharmaceutical applications can be affected by their poor bioavailability and rapid degradation by peptidases. In recent years, pseudopeptides have been extensively studied in order to overcome these problems. However, it is important to bear in mind that these modified peptides must possess the same specific activity of the original peptides. Several publications by Bolm *et al.* reported the synthesis of a variety of pseudopeptides bearing a sulfoximine group as chiral backbone-modifying element; the stability of these peptidomimetics towards proteinase K was investigated and they displayed enhanced bond stability (bond A) and reduced reactivity (bond B) towards enzymatic hydrolysis (Figure 18).[126-128]

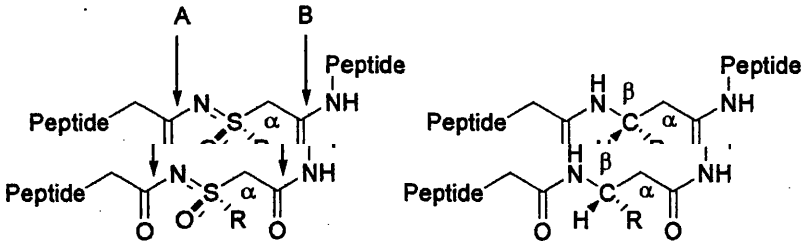

Figure 18. Comparison of sulfoximine pseudopeptides **33** and a β-amino acid **34**.[126-128]

1.5.4.5 Miscellaneous applications

Apart from the targets discussed above, the chemically stable sulfoximines have been candidates for the design of transition state or intermediate analogues. Back in the 1990's Mock *et al.* had designed sulfoximine transition-state-analogue inhibitors for carboxypeptidase A.[129,130] The sulfoximine nitrogen atom coordinates strongly with a Zn^{2+} ion, mimicking the transition-state carbonyl oxygen atom. The stable tetrahedral configuration correlates to the preferred geometry of active site binding and it replaces the enzymatically-unstable amide linkage. The same structural features also prompted Levenson and Meyer to design transition-state analogues as potential dihydroorotase inhibitors, with the sulfoximine group mimicking the presumed tetrahedral transition state in the enzymatic reaction.[131]

1.5.5 Drug molecules containing chiral sulfur atoms

Drug enantiomers often have different physiological actions and pharmaceutical properties. A good example of pharmaceutical agents containing chiral sulfur atoms is the successful sulfoxide drug, omeprazole (Losec®, **35**, Figure 19), a proton-pump inhibitor used for the treatment of gastrointestinal diseases such as peptic ulcers and gastro-oesophageal reflux disease.[132] It is formulated as a racemate and both isomers undergo biotransformation to the active metabolite.[132] However, omeprazole has variable pharmacokinetics and patients with a cytochrome P450 deficiency require higher doses.[132] A drug with improved bioavailability was sought and the *S*-enantiomer of omeprazole was synthesised, with enhanced bioavailability and potency. Esomeprazole (Nexium®, **36**, Figure 19) has replaced omeprazole as the "golden" drug for gastro-oesophageal reflux disease.

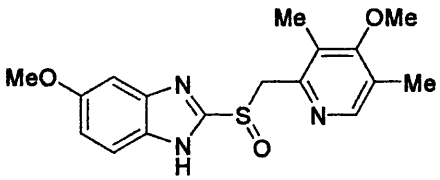

Omeprazole, **35**

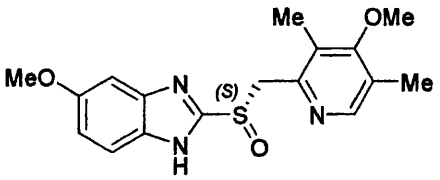

Esomeprazole, **36**

Figure 19. The best-selling sulfoxide drug, omeprazole **35**, and its chiral successor esomeprazole **36**.[132]

Despite the versatile chemistry and the many successful sulfoxide and sulfonamide drugs, relatively little information is available on the use of sulfoximines in medicinal

applications, with BSO being the only candidate in clinical trials. Therefore, the utilisation of sulfoximines in drug design is innovative.

Chapter 2 Aims and Objectives

2.1 Aim

The principal aim of this project is to develop a new approach to inhibition of enzymes, which use ribonucleosides and 2-deoxyribosides as substrates and which are important in cancer.

2.2 Research proposal

The specific objectives are:

1. To identify innovative analogues of 2-deoxyribonucleosides and 2-deoxyribose in the design and development of novel enzyme inhibitors and anti-angiogenic agents.
2. To synthesise mimics of nucleosides and 2-deoxynucleosides in which the anomeric carbon has been replaced by the tetrahedral sulfoximine.
3. To synthesise mimics of 2-deoxyribose containing sulfoximines in this position as anti-angiogenic agents.

There is a relatively small amount of research on the application of sulfoximines in drug design and their application in the design of ribose mimics has not been previously reported. Most published inhibitors of TP, PARP-1 and IMPDH have a pharmacophore based on the relevant bases of nucleosides and 2-deoxynucleosides. For example, uracil analogues have been studied for their inhibitory activity to TP; tiazofurin and selenazofurin are good IMPDH inhibitors where the nicotinamide of NAD^+ is replaced by thiazole-4-carboxamide and selenazole-4-carboxamide, respectively; a great deal of attention has been focussed on the benzamide analogues as PARP-1 inhibitors. There is very little known, to date, on the direct modification of the substrate ribosyl moiety for these enzyme targets.

Structures of the proposed target compounds are shown in Figure 20 (*vide infra*). Compounds **37** and **38** are designed as inhibitors of TP. Target **37** is a 2-deoxy-*D*-ribose-1α-phosphate analogue with a carboxylate anion located in the phosphate site. The anomeric carbon is replaced by the sulfoximine sulfor atom and with the basic nitrogen mimicking the ribosyl oxygen. In **38**, the anomeric carbon is also replaced by the tetrahedral sulfoximine group; since it is not known which of the interconverting anomers of 2-deoxyribose binds to its receptor, both diastereoisomers **38a** and **38b** would be synthesised.

Compounds **39** and **40** are mimics of nicotinamide riboside. As the parent compound, these are designed as PARP-1 inhibitors and, after conversion to the corresponding dinucleotide with adenosine, are expected to also be IMPDH inhibitors. This conversion may be metabolic in a similar fashion as seen with tiazofurin and selenazofurin, or, for the purpose of biological evaluation for enzyme inhibition, synthetic. Target **39** is a strict analogue of benzamide 2-deoxyriboside with the sulfoximine replacing the anomeric carbon. Target **40** is designed as a transition-state nucleoside mimic for PARP-1 inhibition. The first step in the mechanism of PARP-1 is stretching of the C–N bond between the anomeric carbon of the ribose and the nicotinamide. This stretched bond of the transition state is mimicked by the S=N–C bonds of the sulfoximine.

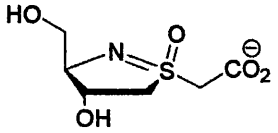

37

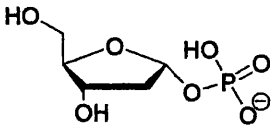

2-Deoxy-*D*-ribose-1α-phosphate

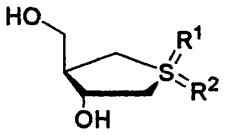

38a: R^1 = NH, R^2 = O
38b: R^1 = O, R^2 = NH

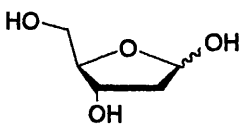

2-Deoxy-*D*-ribose

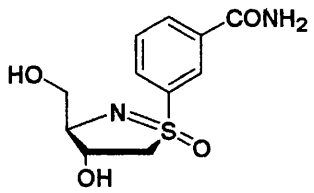

39

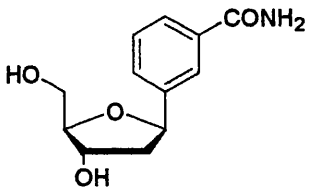

Benzamide 2-deoxyriboside

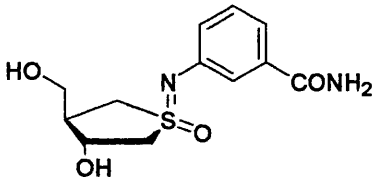

40

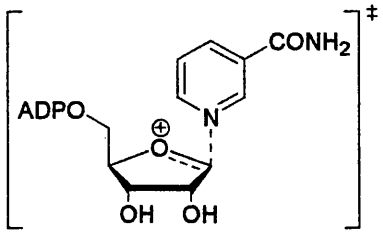

PARP-1 transition state

Figure 20. Structures of target molecules.

Chapter 3 Results and Discussion I

Synthesis of a benzamide 2-deoxyriboside analogue

3.1 Route I: addition of a three-carbon unit to a one-carbon unit

3.1.1 Retrosynthesis

The first target compound investigated was the benzamide 2-deoxyriboside analogue **39**, designed as a potential PARP-1 inhibitor and, after conversion to the corresponding dinucleotide with adenosine, as an IMPDH inhibitor. The tetrahedral sulfoximine group replaces the anomeric carbon, with the nitrogen mimicking ribosyl oxygen. The configuration of the sulfur atom would be established independently to the other two chiral centres of the five-membered ring. In the design of synthetic routes, efficiency and utilisation of reliable reaction types that will allow good stereocontrol are key issues.

The retrosynthetic analysis for target **39** is illustrated in Scheme 13 (*vide infra*). Disconnection at the C–N bond of the ribose ring, *i.e.* the ring-opening, focuses on the formation of an intramolecular cyclisation between the amine and the secondary alcohol. The convergent Mitsunobu reaction is reasonable, as it is a well-documented procedure; the conditions are mild and the ring-closure will proceed with inversion of configuration at the electrophilic centre. Synthesis of **39** from parent compound **41** requires removal of the hydroxy protecting groups and a functional group interconversion (FGI). A nitrile group is a potential starting functional group for an amide since nitriles are relatively stable and can be hydrated to amides.

Some fine adjustment of protecting groups of both nitrogen and oxygen centres led to the intermediate **43**. Disconnection at the C–C bond of this aldol-like product led to two starting materials: a *meta*-substituted aromatic sulfoximine bearing a nitrogen protecting group and chirality at the sulfur atom **45** (one-carbon unit) and *S*-2,2-dimethyl-1,3-dioxolane-4-carboxaldehyde **44** (three-carbon unit). The synthesis of **44** is well-reported, highly efficient and reliable (*vide infra*, Scheme 26). Strong base (*e.g.* butyl lithium) will form a nucleophilic S-methyl anion of **45** and addition to the aldehyde **44** should proceed with diastereoselectivity, since stereocontrol is governed by the chirality of **44**. Therefore, the four-carbon addition product **43** would have all three chiral centres with the required configuration. The N-protecting group may play a role in diastereoselectivity, thus two protecting groups (Boc, $SiMe_3$) will be investigated to test the hypothesis.

Therefore, this synthetic sequence is convergent: two of the chiral centres are provided by separate compounds (chiral sulfoximine and chiral aldehyde), while the third is generated in a diastereoselective addition to a chiral aldehyde (C–C bond formation).

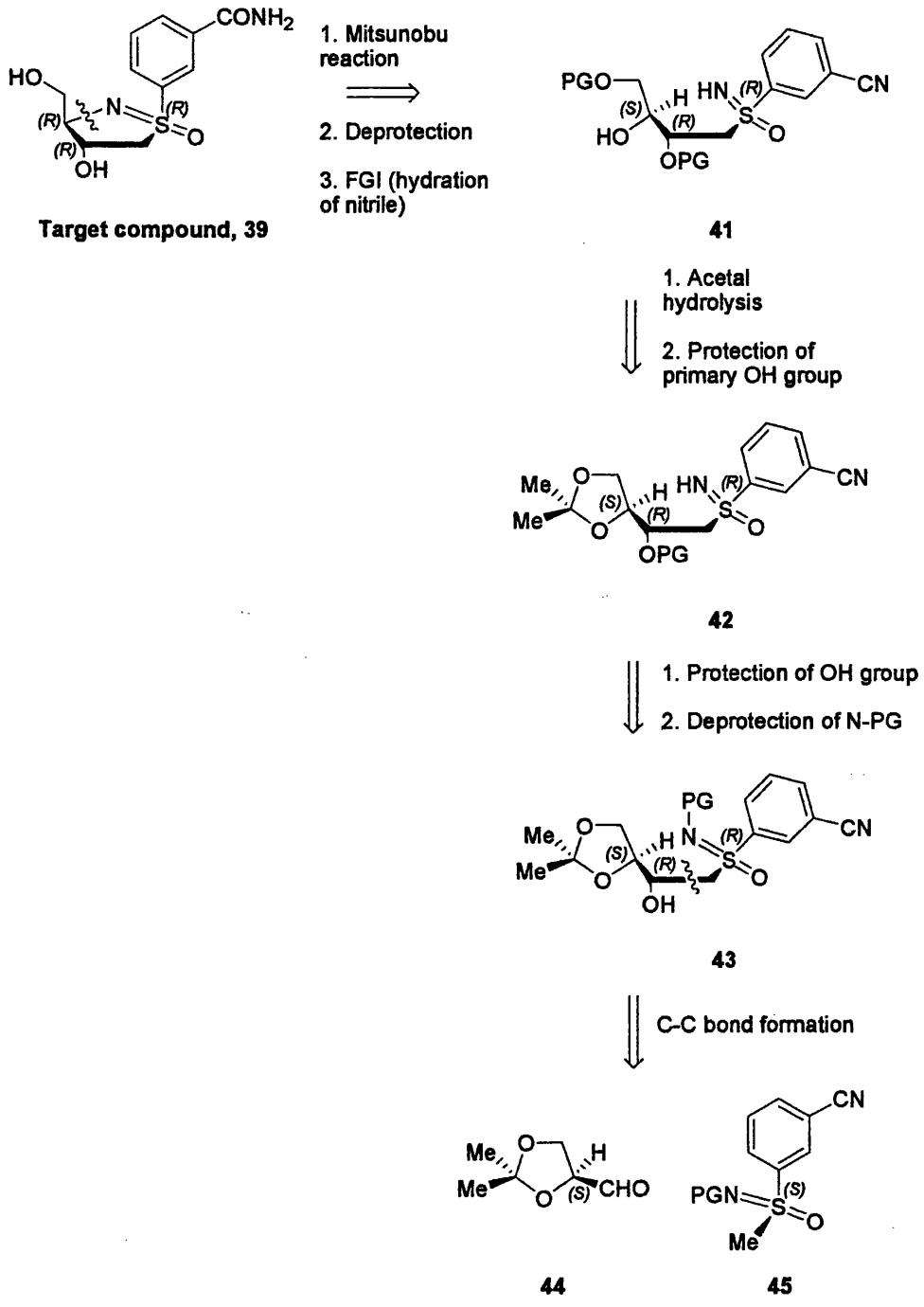

Scheme 13. Retrosynthesis of target compound **39**, an analogue of benzamide 2-deoxyriboside. (PG = protecting group)

It was decided that a model reaction with racemic S-methyl-S-phenylsulfoximine would first be explored to clarify any synthetic difficulties. An aromatic aldehyde would be

used to probe the stereocontrol of different N-protecting groups in the critical C–C bond-forming step. Ultimately, enantioselective synthesis of the required configuration at the sulfur of a 3-substituted S-methyl-S-phenylsulfoximine would be pursued either *via* a chiral sulfoxidation or resolution of a racemate using (+)-10-camphorsulfonic acid (CSA).[133,134]

3.1.2 Synthesis of S-methyl-S-phenylsulfoximine

In general, sulfoximines can be prepared by three strategies: nucleophilic substitution of sulfonimidoyl halides, oxidation of sulfilimines and imination of sulfoxides (Scheme 14). The latter is the most widely reported and utilised method.[135]

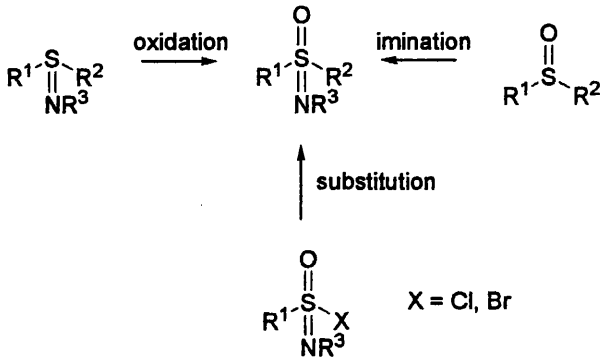

Scheme 14. Routes of synthesis of sulfoximines.

Armed with this knowledge, the first step of the model reaction would be to synthesise (±)-S-methyl-S-phenylsulfoxide **47** (*vide infra*, Scheme 15). This is followed by imination to give the corresponding sulfoximine (**50**, *vide infra*, Scheme 15). Although both compounds, including the individual enantiomers, are commercially available, it was decided that the literature methods on their syntheses would be studied in order to determine the most efficient synthetic route. The acidic NH proton of **50** can then be easily deprotonated and a suitable protecting group will be introduced to form the model sulfoximine.

3.1.2.1 Sulfoxidation

The most common reagents for the oxidation of sulfides to sulfoxides are *meta*-chloro-peroxybenzoic acid (*m*CPBA),[136] sodium periodate and hydrogen peroxide.[137,138] However, their use is often complicated with over-oxidation of sulfoxides to sulfones. Despite careful monitoring of reaction time, temperature and amount of oxidants, it

remains a common problem in almost all oxidation conditions and column chromatography is often required for separating sulfoxides from the corresponding sulfones.

The first step of the model reaction involved an investigation into the efficiency and reliability of the above three oxidants for comparative purposes. Thioanisole (**46**, *vide infra*, Scheme 15), which is commercially available and cheap, was treated with *m*CPBA in dichloromethane (DCM), sodium periodate in MeOH/water, and the recently-reported system using 35% aq. hydrogen peroxide and phenol.[138] The use of phenol as a solvent with hydrogen peroxide is particularly interesting because the system is thought to minimise the formation of sulfones from sulfoxides. Xu *et al.* proposed that an interaction between phenol and H_2O_2 increases the electrophilicity of peroxy oxygen atom and assists the leaving group (H_2O) in departing.[138] Moreover, the strong hydrogen bond formed between the OH of phenol and H_2O_2 decreases the nucleophilicity of the sulfur atom in the sulfoxide, thus reducing the likelihood of over-oxidation to sulfones.

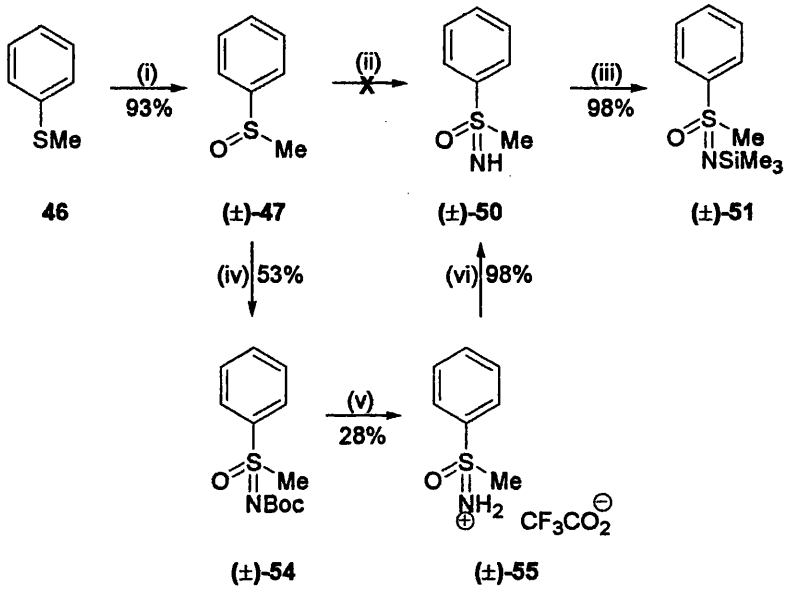

Scheme 15. Synthesis of the model racemic N-protected S-methyl-S-phenylsulfoximine. Both the N-Boc and N-$SiMe_3$ compounds would be investigated in the subsequent aldehyde addition reaction. *Reagents and conditions: (i) $NaIO_4$, MeOH, H_2O; (ii) MSH* ***49****, DCM; (iii) Et_2NSiMe_3, MeCN, 65°C; (iv) $BocN_3$* ***53****, $FeCl_2$, DCM, 0°C; (v) TFA, DCM, 0°C; (vi) Na_2CO_3, MeOH.*

This comparative study found that $NaIO_4$ is superior to *m*CPBA and H_2O_2 in oxidising **46** to the corresponding sulfoxide **(±)-47** in terms of yield, lack of over-oxidation and ease of handling (*vide infra*, Table 4). The use of the H_2O_2/phenol system is limited to

small-scale reactions, due to the relatively large amount of phenol required and its subsequent neutralisation using NaOH. Hence $NaIO_4$ was the preferred reagent.

Oxidant	Reaction conditions	Work-up	Over-oxidation	Yield (%)
*m*CPBA[136]	1 mol equiv., DCM, 0°C	Wash with $NaHCO_3$	Yes	92
$NaIO_4$[137]	1 mol equiv., MeOH, RT	Filtration	No	93
H_2O_2[138]	2 mol equiv., 12 mol equiv. phenol, RT	Excess H_2O_2 quenched with Na_2SO_3; phenol neutralised with NaOH.	No	92

Table 4. Oxidative conditions applied for the conversation of thioanisole **46** to racemic S-methyl-S-phenyl-sulfoxide **(±)-47**.

3.1.2.2 Non-catalytic imination

With racemic S-methyl-S-phenylsulfoxide [**(±)-47**, *vide infra*, Scheme 15] in hand, attention was turned to explore the various imination strategies available. A large pool of data on the imination of sulfoxides has been reported, the oldest method being the hydrazoic acid (HN_3) route.[139] Sulfoxides are treated with NaN_3 and concentrated H_2SO_4, then basified to give the free N–H sulfoximine. However, concerns over the toxic and explosive nature of HN_3 has diminished its utilisation since being discovered in the 1950's. Besides the hazardous properties of HN_3, another disadvantage is that, under such acidic conditions, racemisation may occur at the sulfur centre of chiral sulfoxides and thus it is not applicable in synthesising enantiomerically pure sulfoximines.

The explosive *O*-mesitylenesulfonylhydroxylamine (MSH, **49**, *vide infra*, Scheme 16) was discovered to be a useful electrophilic sulfoxide-iminating agent by Tamura *et al.* in 1972.[140] Johnson *et al.* subsequently reported the synthesis of chiral sulfoximines from chiral sulfoxides using MSH and retention of configuration at the sulfur atom was observed.[141] MSH **49** is normally prepared by acid-hydrolysis of ethyl *O*-(mesitylene-sulfonyl)acetohydroxamate **48** with 70% aq. perchloric acid in dioxane at 0°C (*vide infra*, Scheme 16).[142] A more recent example used 50% aq. H_2SO_4 in Et_2O and tri-fluoroacetic acid has also been used.[143] However, in the present work, hydrolysis of **48** could not be achieved in numerous attempts using different acids at various temperatures. The reason for encountering such difficulty in synthesising this widely-reported compound remains unknown.

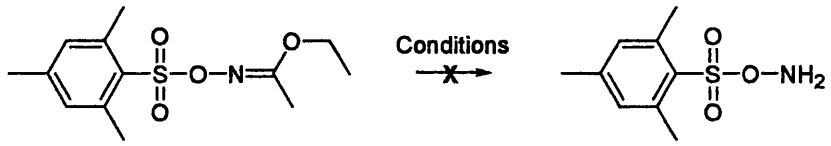

48 49

Scheme 16. Attempted synthesis of MSH **49**. *Reagents and conditions: (i) $HClO_4$, 1,4-dioxane, 0℃; (ii) $HClO_4$, THF, 0℃; (iii) TFA, THF, 0℃; (iv) TFA, THF, 45℃; (v) 50% aq. H_2SO_4, Et_2O.*

To avoid the use of toxic and potentially explosive traditional imination agents such as HN_3 and MSH, efforts have been concentrated on the search for alternative methods. An interesting electrochemical imination was recently developed by Siu *et al.* using N-aminophthalimide as a nitrene source.[144] The reaction proceeds with retention of configuration and no racemisation occurred during the nitrene transfer. Furthermore, the group solved the "chemically impossible" removal of the N-phthalimido group by an electrochemical reductive N–N bond cleavage.

Krasnova *et al.* also studied the use of N-aminophthalimide in imination of sulfoxides.[145] Iodosobenzene diacetate [$PhI(OAc)_2$] was found to promote nitrene formation by forming a reactive iminoiodane (*vide infra*, Figure 21) and a number of sulfoxides were converted to the corresponding sulfoximines in good yields.

3.1.2.3 Metal-catalysed imination

Recent interest focuses on metal-catalysed nitrene-transfer reactions to sulfoxides and these are summarised in Table 5 (*vide infra*). They often proceed under relatively mild conditions with retention of configuration at sulfur.

Muller *et al.* first reported the use of the iminoiodane [N-(*p*-toluenesulfonyl)imino]-phenyliodinane (PhI=NTs) as a reagent for imination of racemic and chiral sulfoxides in 1998 (*vide infra*, entry 1, Table 5).[146] Copper(I) triflate was used as a catalyst and a range of N-tosylsulfoximines were afforded in high yield, with retention of configuration at the sulfur atom.

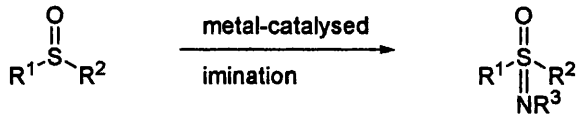

Entry	Metal catalyst	Nitrene source	R^1	R^2	R^3	Yield (%)
1	CuOTf (5 mol %)[146]	PhI=NTs	Ph	Me	Ts	84
2	$CuPF_6$ (5 mol %)[147]	PhI=N-X X = Ts, Ns, Ses	Ph	Me	Ts, Ns, Ses	59-69
3	$Cu(OTf)_2$ (10 mol %)[148]	PhI=NTs	Et	*p*-tolyl	Ts	96
4	$AgNO_3$ (8 mol %)[149]	$X\text{-}NH_2$, $PhI(OAc)_2$ X = Ns, Ts, Ses	Ph	Me	Ns, Ts, Ses	79-83
5	$Fe(acac)_3$ (5 mol %)[150]	$X\text{-}NH_2$, PhI=O X = Ns, Ts, Ses	Ph	Me	Ns, Ts, Ses	66-96
6	$Rh_2(OAc)_4$ (2.5 mol %)[151]	PhI=NNs	Ph	Me	Ns	93
		$X\text{-}NH_2$, $PhI(OAc)_2$ X = $COCF_3$, Ns, Ms	Ph	Me	$COCF_3$, Ns, Ms	79-86
7	$FeCl_2$ (50 mol %)[152,153]	$BocN_3$	Ph	Me	Boc	74

Table 5. Metal-catalysed imination methods of sulfoxides (Abbreviations: Tf = trifluoromethanesulfonyl; Ts = *p*-toluenesulfonyl; Ns = *p*-nitrophenylsulfonyl; Ses = trimethylsilylethylsulfonyl; *p*-tolyl = *p*-methylphenyl; Ms = methanesulfonyl; acac = acetylacetonate).

Other copper catalysts such as $CuPF_6$ and $Cu(OTf)_2$ were investigated (Table 5, entries 2 and 3).[147,148] Furthermore, since most N-Ts sulfoximines are difficult to convert to the free amines, iminoiodanes with other protecting groups such as nosyl- (Ns, *p*-nitrophenylsulfonyl) and Ses- (trimethylsilylethylsulfonyl) protected sulfoximines were studied. Cren *et al.* found that MSH-resistant sulfoxide substrates could be successfully iminated to the corresponding N-protected sulfoximines in good yield and the group reported, for the first time, the efficient deprotection of N-Ns and N-Ses sulfoximines.[147] The Ns group could be removed using thiophenol and Cs_2CO_3 in acetonitrile in 59% yield; removal of the Ses group proceeded smoothly with TBAF in THF at 50°C in 86% yield.

Iminoiodanes are hypervalent iodine (III) reagents first described about thirty years ago and have since been recognised as useful nitrene precursors (*vide infra*, Figure 21).[154]

However, their preparations are often tedious and irreproducible (usually synthesised from the corresponding amide and iodosobenzene diacetate with potassium hydroxide in methanol). Recent advances in the preparation *in situ* allow more convenient one-pot procedures (*vide infra*, Scheme 24).

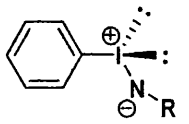

Figure 21. Types of N-substituted iminoiodanes.

Several independent reports by the Bolm Group described the use of silver ($AgNO_3$),[149] iron [$Fe(acac)_3$] and rhodium [$Rh_2(OAc)_4$] salts with *in-situ*-formed iminoiodanes [X-NH_2, $PhI(OAc)_2$/PhI=O] in nitrene transfer reactions and this provides additional information on the type of metal catalysts compatible with the system (*vide supra*, entries 4-6, Table 5).[150,151] The group synthesised a range of sulfoximines bearing new protecting groups such as N-mesyl and N-trifluoroacetyl groups. It is noteworthy that the same group also described, in a subsequent publication, a metal-free imination method during investigation of silver catalysts.[155] They found that imination also proceeds without $AgNO_3$ and that the nitrogen-transfer agent is formed *in situ* from $NsNH_2$ and $PhI(OAc)_2$. However, the high temperature (reflux in acetonitrile over a period of 16 h) required for this metal-free imination contributes to partial racemisation of enantiomerically pure (*S*)-S-methyl-S-phenylsulfoxide, making this method unsuitable for asymmetric synthesis.

However, despite the positive results described above, the use of Ns or Ses in sulfoximination is not without limitations. A simpler process involving a nitrene source that is easy to synthesise, with the introduction of a versatile N-protecting group, is essential to reduce the number of synthetic steps.

Bach *et al.* investigated the role of *tert*-butoxycarbonyl azide ($BocN_3$, **53**) as a nitrene-transfer reagent with the aid of $FeCl_2$ as a catalyst (*vide supra*, entry 7, Table 5).[152,153] The Boc group is a universally known protecting group and the deprotection procedure is well documented.[152,153] N-Boc-protected sulfoxides were synthesised; enantiomerically pure (*R*)-(+)-S-methyl-S-phenylsulfoxide was converted to (*R*)-(−)-S-methyl-S-phenylsulfoximine with good stereoselectivity (85% ee).

With this procedure in mind, $BocN_3$ **53** was synthesised by diazotisation of *tert*-butyl carbazate **52** with sodium nitrite in acetic acid and water (*vide infra*, Scheme 17).[156] Since $BocN_3$ is explosive, it was treated immediately, as a concentrated solution in DCM, with sulfoxide **47**. N-Boc sulfoximine [(±)-**54**, *vide supra*, Scheme 15] was synthesised in moderate yield (53%).

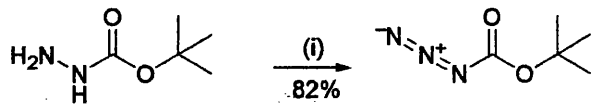

52 **53**

Scheme 17. Synthesis of $BocN_3$ **53**. *Reagents and conditions: (i) $NaNO_2$, H_2O, AcOH, DCM, 0 °C.*

It was postulated that an intermediate Fe(IV)-nitrene complex (Scheme 18), formed once $FeCl_2$ reacts with $BocN_3$ **53**, acts as the nitrene-transfer reagent. Upon nucleophilic attack by a sulfoxide, the corresponding N-Boc sulfoximine is formed.[157]

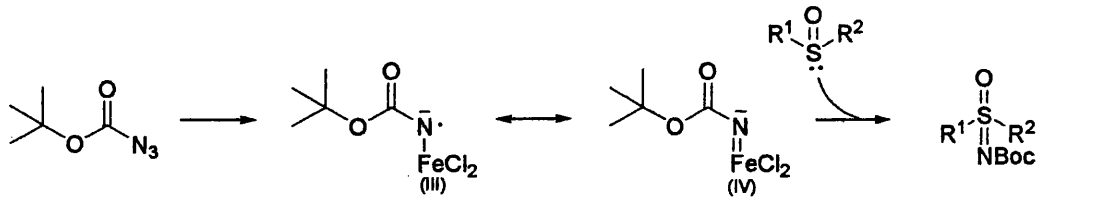

$BocN_3$ Fe(IV)-nitrene complex N-Boc sulfoximine

Scheme 18. Proposed mechanism of $BocN_3/FeCl_2$ nitrene transfer reaction by Bach *et al.*[157]

3.1.3 Addition of model methylthio carbanions to aldehydes

Having obtained the N-Boc sulfoximine (±)-**54**, attention was turned to study the influence of N-protecting groups on the diastereoselective addition of sulfoximine carbanions to achiral aldehydes. N-protecting groups are required to prevent anion formation at the nitrogen instead of the S-methyl carbon atom. Hwang *et al.* reported that,[158] with the trimethylsilyl (TMSi) group, this type of sulfoximine anion adds to aldehydes with some diastereoselectivity, which was thought to be caused by the size of the N-protecting group, with the use of larger N-silyl groups enhancing diastereoselectivity. Therefore, this diastereoselectivity is driven by the configuration at the sulfur of the sulfoximines. Hwang *et al.* reasoned that TMSi groups are sterically bulky and lack metal-coordinating properties.[158] However, the electron-withdrawing Boc group stabilises the carbanion formed with possible metal-coordinating activities.

The use of a Boc group was initially explored by treating **(±)-54** with benzaldehyde and n-BuLi. However, after a series of attempts the reaction failed to proceed, leading only to the discovery of starting materials. Therefore, the more potent *tert*-BuLi was used instead and the reaction gave a mixture of three products (Scheme 19). The least polar product was separated chromatographically and was characterised as the alkene **(±)-56**. This condensation product was confirmed as the *E* isomer by the ^{1}H NMR spectrum which showed a coupling constant J = 15.3 Hz between the alkene protons. The other two products (formed in 62% total yield) were inseparable. ^{1}H NMR showed that these were the diastereomeric alcohols **(±)-57a/b**, formed in the ratio 7:1. Since they were afforded as a colourless oil, X-ray analysis was not possible. Therefore, a tentative assignment of the relative configuration was made on the basis of a NOESY spectrum of the mixture in $CDCl_3$. The conformation of both diastereoisomers appears to contain an intramolecular hydrogen bond from the OH, giving six-membered rings in approximate chair conformations (*vide infra*, Figure 22a/b). In both **(±)-57a/b**, the C-Ph group is equatorial, as shown by the ^3J = 9.9 Hz coupling between H_x and H_{ax}. The H_{eq}-H_x coupling is as expected for the major isomer (^3J = 2.0 Hz) but is slightly smaller in the minor isomer (^3J = 1.2 Hz). Interestingly, the couplings between OH and H_x follow the same pattern, with ^3J = 2.0 Hz for the major isomer and ^3J = 1.2 Hz for the minor isomer. These data point to a full chair for the major isomer and a slightly flattened chair for the minor.

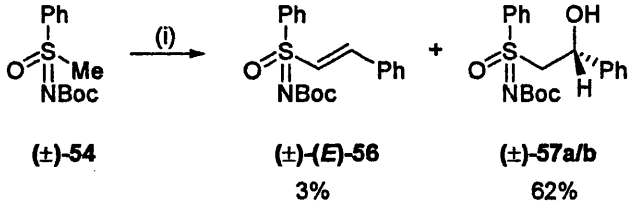

(±)-54 **(±)-(*E*)-56** 3% **(±)-57a/b** 62%

Scheme 19. Diastereoselective addition of N-Boc S-methyl-S-phenylsulfoximine **(±)-54** to benzaldehyde. *Reagents and conditions: (i) t-BuLi, PhCHO, THF, –78°C.*

Attention was then turned to study if the OH is hydrogen-bonded to the sulfoximine oxygen or to the sulfoximine nitrogen. Hwang *et al.* suggested that, in the corresponding molecule lacking the Boc group, the intramolecular hydrogen bonding occurs from OH to the basic nitrogen.[158] Similarly, Hainz *et al.* showed hydrogen bonding from OH to sulfoximine nitrogen in a related structure in which the nitrogen carried a methyl group.[159] In both cases, the basicity of the nitrogen is claimed to play a role. For the present diastereoisomers, it could be argued that the carbamate nitrogen is not basic and should not be capable of being a hydrogen-bond acceptor. Hence, two

structures are possible for the major isomer, one with the nitrogen in-ring and one with the sulfoximine oxygen in-ring. The NOE connectivities from the S-Ph to H_{eq} and H_x shown that the S-Ph must be axial in the major isomer; therefore the two possible structures **58a/b** for this isomer are those shown in Figure 22b (*vide infra*). These structures are diastereomeric. There is a weak NOE between the ^{t}Bu protons and H_{eq}; this is much more consistent with structure **58a** with hydrogen bonding to the sulfoximine oxygen. These two arguments, the relative hydrogen-bond acceptor strengths and the NOE, point strongly to **58a** being the structure of the major isomer, with relative configuration *R,R*. Thus the minor isomer **59a** has relative configuration *S,R*, as borne out by NOE connectivities. This diastereoselectivity in the addition of the sulfoximine anion to the aldehyde is opposite to that seen by Hwang *et al.*, who used TMSi protection at nitrogen, rather than Boc.[158] The group reported that, with N-TMSi-S-methyl-S-phenylsulfoximine, the major diastereomeric alcohol has relative configuration *S,R* and the minor diastereoisomer having relative configuration *S,S*.

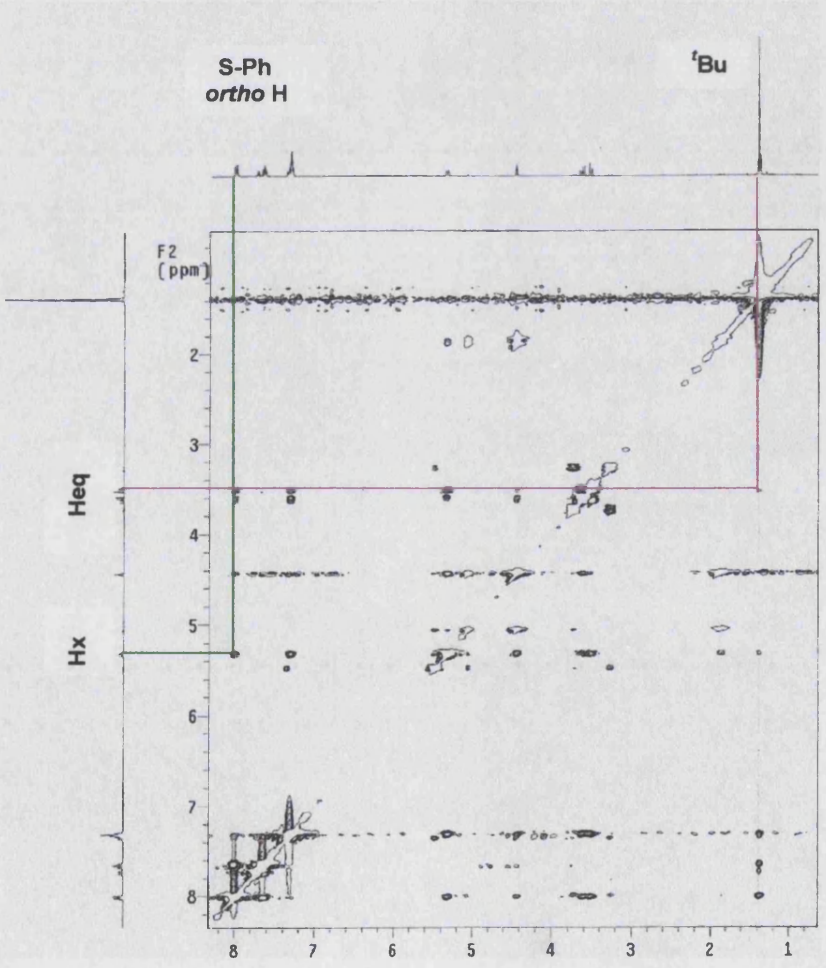

Figure 22a. ^{1}H-^{1}H NOESY spectrum of (±)-2-[N-(*tert*-butoxycarbonyl)-S-phenylsulfonimidoyl]-1-phenyl-ethanol **57a/b**.

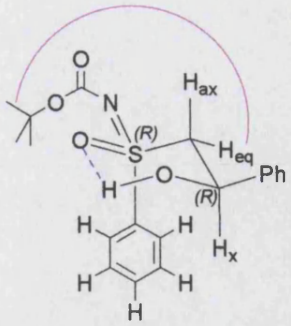

58a (Hydrogen bonding to sulfoximine oxygen)

Major isomer

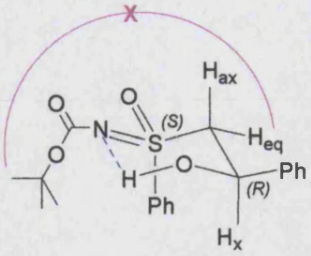

58b (Hydrogen bonding to sulfoximine nitrogen)

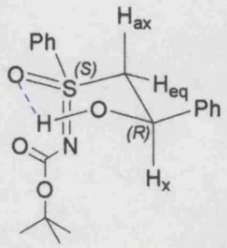

59a Minor isomer

Figure 22b. ^{1}H-^{1}H NOESY spectrum assignment of **57a/b** points strongly to the hydrogen-bonding conformations represented by structures **58a** and **59a**. Lack of NOEs between the *tert*-butyl protons and H_{eq} dismisses the presence of **58b**. (Intramolecular hydrogen bonds – blue; NOEs – purple)

This piece of exciting data prompted further study of the comparative diastereoselectivity of different aromatic aldehydes with electron-withdrawing, electron-donating and heterocyclic properties. Four *para*-substituted aromatic aldehydes were chosen: 4-nitrobenzaldehyde, 4-methoxybenzaldehyde, 4-methyl-benzaldehyde and 5-nitro-thiophene-2-carbaldehyde and they were treated with the carbanion of the N-Boc sulfoximine **(±)-54** under the same conditions as described with benzaldehyde (*vide infra*, Scheme 20). However, the expected addition reaction did not occur. Only the corresponding benzyl alcohols were recovered, complicated with a considerable loss of starting N-Boc sulfoximine. This suggests that the lithiation was not complete and that the residual base reduced the starting aldehydes. Reactions with 4-nitrobenzaldehyde and 4-methoxybenzaldehyde proceeded in very low yield, making determination of diastereoselectivity impossible. Several attempts at extended lithiation times, use of *sec*-BuLi rather than *tert*-BuLi to avoid hydride donation and increased temperature did not alter the outcome. Difficulties in this step called for a halt to this investigation.

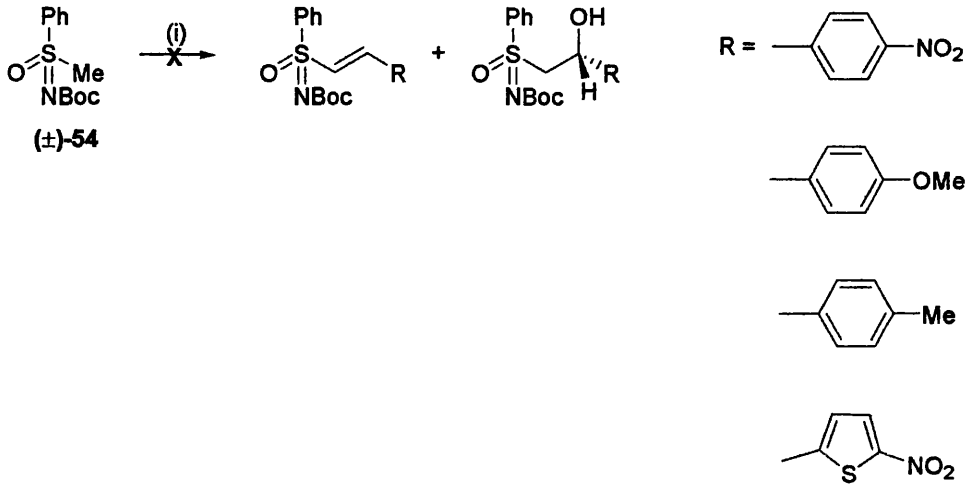

(±)-54

Scheme 20. Attempted addition reactions of **(±)-54** with *para*-substituted aromatic aldehydes. *Reagents and conditions: (i) t-BuLi / s-BuLi, aldehyde, THF, –78°C to RT.*

Attention was then turned to a comparative study on the N-$SiMe_3$ group as described by Hwang *et al.*[158,160] N-TMSi-S-methyl-S-phenylsulfoximine was prepared in two steps: removal of the Boc group of **(±)-54** with trifluoroacetic acid (TFA) gave the trifluoroacetate salt **(±)-55**, which was basified to give S-methyl-S-phenylsulfoximine **(±)-50** (*vide supra*, Scheme 15). Treatment with (trimethylsilyl)diethylamine furnished N-(trimethylsilyl)-S-methyl-S-phenylsulfoximine **(±)-51** in almost quantitative yield (*vide supra*, Scheme 15).[160]

Contrary to the results seen with the N-Boc compound **(±)-54** and those reported by Hwang *et al.*,[158] addition of the corresponding anion of compound **(±)-51** to benzaldehyde afforded only a complex mixture of unidentifiable products (Scheme 21).

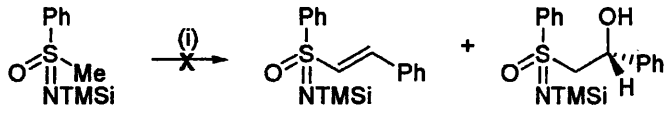

(±)-51 (±)-60 (±)-61

Scheme 21. Attempted anion addition to benzaldehyde with the N-TMSi compound **(±)-51** did not generate the desired products, the alkene **(±)-60** and the diastereomeric alcohol **(±)-61**. *Reagents and conditions: (i) t-BuLi, PhCHO, THF, –78°C.*

When the synthesis of **(±)-54** was attempted on a larger scale, the target could only be obtained as an inseparable mixture (2:3) with $BocNH_2$. As mentioned before, a key component in the iron-catalysed nitrene transfer by $BocN_3$ is the reactive Fe(IV)-nitrene

complex which is attacked by a sulfur nucleophile to form the corresponding sulfoximine. However, when it is attacked by Fe(II), a μ-imido Fe(III) complex is formed; hydrolysis of the latter releases the amide $BocNH_2$ (Scheme 22).[157] Therefore, the presence of $BocNH_2$ in the repeat synthesis of **(±)-54** indicates two possibilities:

1. Inadequate amount of sulfoxide led to residual Fe(IV)-nitrene complex being hydrolysed.
2. Insolubility of $FeCl_2$.

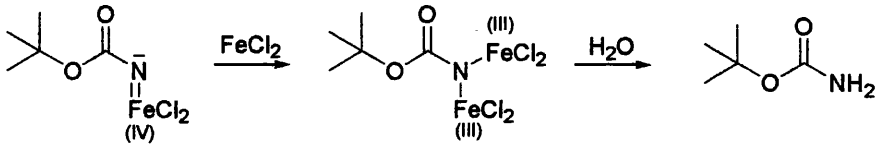

Fe(IV)-nitrene complex **μ-imido Fe(III) complex** **$BocNH_2$**

Scheme 22. $BocNH_2$, a hydrolysed product of $BocN_3$, is formed *via* the attack of the Fe(IV)-nitrene complex by Fe(II).

Modifications of the synthetic method included increasing the sulfoxide concentration to five molar equivalents and by using pentane-2,4-dione to solubilise the Fe(II) catalyst through complexation. Disappointingly, these changes only increased the ratio of product **(±)-54** to $BocNH_2$ to 4:1. Different transition metal catalysts were also employed [CuCl, $RuCl_3$, $Rh_2(OAc)_4$] but they did not improve the outcome.

Since $BocNH_2$ was inseparable from **(±)-54**, it was decided that different protecting groups would be studied and, eventually, the N-Boc group would be introduced by a simple protection on a free NH sulfoximine.

(Fluoren-9-ylmethoxy)carbonyl azide ($FmocN_3$, **63**) is a known compound and readily available from the chloroformate **62** in one simple step (stirring with ice-cold NaN_3 in acetone/water, *vide infra*, Scheme 23).[161] Its application in a nitrene transfer to sulfoxides has not been reported previously. However, when sulfoxide **(±)-47** was allowed to react with $FmocN_3$, only $FmocNH_2$ and starting sulfoxide were recovered (*vide infra*, Scheme 23).

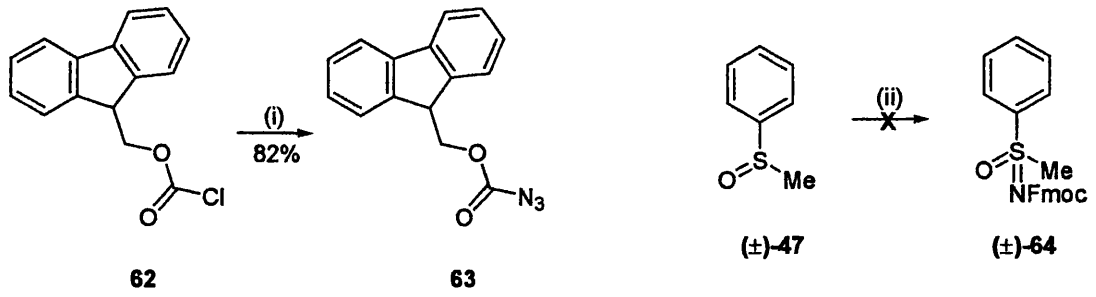

62 63 (±)-47 (±)-64

Scheme 23. $FmocN_3$ **63** was synthesised from the chloroformate **62** in 83% yield; subsequent reaction with sulfoxide (±)-**47** did not give the desired N-Fmoc sulfoximine (±)-**64**. *Reagents and conditions: (i)* NaN_3*, acetone,* H_2O*, 0 °C; (ii)* **63***,* $FeCl_2$*, DCM, 0 °C.*

The N-trifluoroacetyl (N-TFA) group was considered next as it is easily removed by nucleophiles (ammonia, sodium carbonate) to generate the free NH compounds. The rhodium-catalysed iminating method reported by Okamura *et al.* (*vide supra*, Table 5) is a simple one-pot system carried out under mild conditions.[151] All the reagents are stable in air or moisture, thus requiring neither an inert atmosphere nor anhydrous solvents. The iminoiodane, N-(trifluoroacetyl)imino]phenyliodinane [(PhI=$NCOCF_3$)], is formed *in situ* from trifluoroacetamide and iodosobenzene diacetate (Scheme 24). Acetic acid is generated as a by-product from iodosobenzene diacetate and it can reduce the catalytic activity of $Rh_2(OAc)_4$. The basic magnesium oxide serves as an acid scavenger and neutralises the reaction.[162]

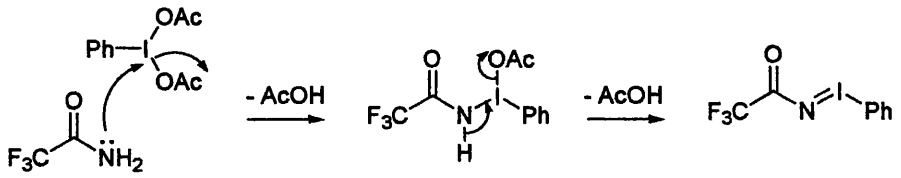

Scheme 24. Mechanism of the formation *in situ* of PhI=$NCOCF_3$ from trifluoroacetamide (CF_3CONH_2) and iodosobenzene diacetate [$PhI(OAc)_2$].

The protocol was followed and N-trifluoroacetyl-S-methyl-S-phenylsulfoximine [(±)-**65**, *vide infra*, Scheme 25] was obtained in moderate yield. Removal of the N-TFA group proceeded smoothly with ammonia/MeOH, giving the free NH compound (±)-**50**. With this new easy access to S-methyl-S-phenylsulfoximine, the introduction of N-TMSi and N-Boc groups gave the corresponding N-substituted sulfoximines (±)-**51** and (±)-**54**, respectively, in excellent yields (*vide infra*, Scheme 25).

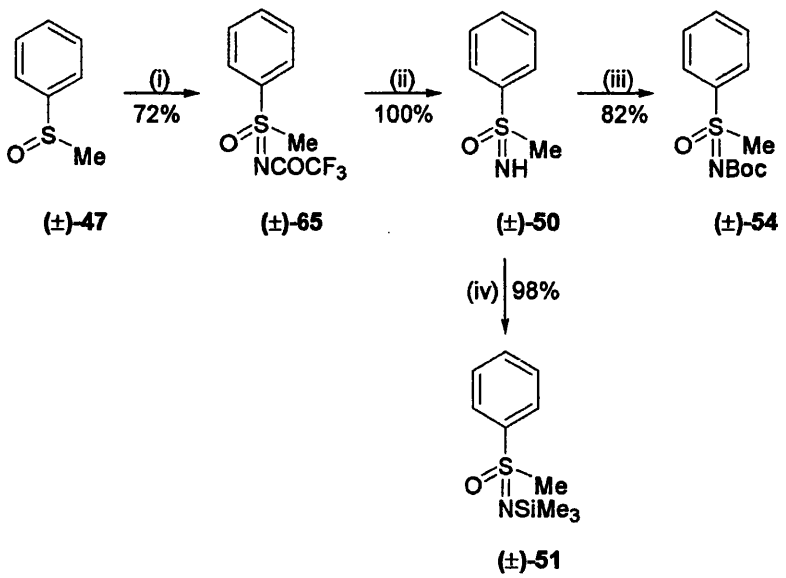

Scheme 25. Synthetic routes to S-methyl-S-phenylsulfoximine **(±)-50**, the N-TMSi **(±)-51** and N-Boc **(±)-54** derivatives. *Reagents and conditions: (i) CF_3CONH_2, MgO, $Rh_2(OAc)_4$, $PhI(OAc)_2$, DCM; (ii) NH_3, MeOH; (iii) NaH, $(Boc)_2O$, THF, 0°C; (iv) Et_2NSiMe_3, MeCN, 65°C.*

Compounds **(±)-51** and **(±)-54** were lithiated as described before and addition of the anions to *S*-glyceraldehyde acetonide **44** was studied. The latter was synthesised from the commercially available 1,2:5,6-diisopropylidene-*D*-mannitol **66** *via* a oxidative cleavage by $NaIO_4$ and $NaHCO_3$ (*vide infra*, Scheme 26).[163] TLC of the addition reaction with N-TMSi compound **(±)-51** indicated that there were no starting materials remaining and showed numerous inseparable species. This finding discouraged further attempts with the N-TMSi derivative.

Many attempts were made to encourage the addition reaction with the N-Boc sulfoximine [**(±)-54**, Scheme 26] but to no avail. They are summarised in Table 6 (*vide infra*). Contrary to the results observed with the N-TMSi compound **(±)-51**, TLC of reactions (*vide infra*, entries 1-4, Table 6) showed that there was no new product formed with the starting sulfoximine compound remaining.

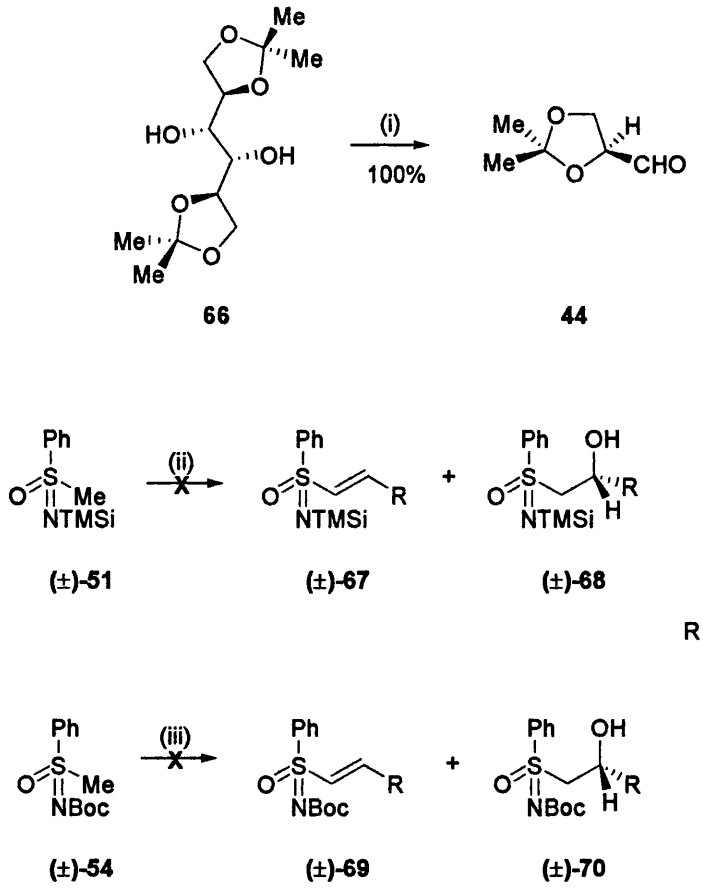

Scheme 26. Synthesis of *S*-glyceraldehyde acetonide **44** and subsequent attempted addition reactions. *Reagents and conditions: (i) $NaHCO_3$, $NaIO_4$, H_2O, DCM; (ii) t-BuLi, **44**, THF, –78°C; (iii) t-BuLi, **44**, THF, various conditions (see Table 6).*

Entry	Lithiation duration (min.)	Reaction temperature (°C)
1	10	–78
2	180	–78
3	180	0
4	60	RT
5*	90	RT

Table 6. Various reaction conditions attempted with the N-Boc sulfoximine (±)-**54** and the *S*-glyceraldehyde acetonide **44**. A ^1H NMR study was performed under the conditions stated in entry 5.

These puzzling results prompted an isotopic labelling study (entry 5, Table 6) to determine the reasons of the failed attempts. A few drops of deuterium oxide (D_2O) were added to the reaction mixture (after lithiation and addition of the aldehyde) and the following outcomes and deductions were possible:

1. If no lithiation occurred, signals of both starting materials should be observed in the ^{1}H NMR spectrum.
2. If lithiation were successful and a carbanion were present but it failed to react with the aldehyde, a diminution in the integral for the S-methyl proton region (δ 3.21) would be observed (Route 1, Scheme 27).
3. If the carbanion were to react with the aldehyde as a base by removing the α-proton, the starting compound **(±)-54** should be recovered (confirmed by the presence of all the S-methyl protons) with the 4-H signal of the aldehyde (δ 4.32) being absent (Route 2, Scheme 27).

Route 1:

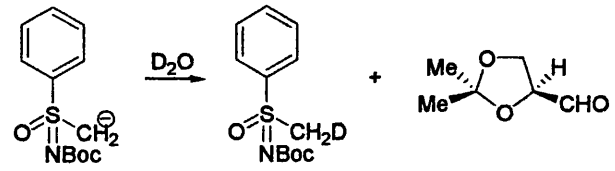

Route 2:

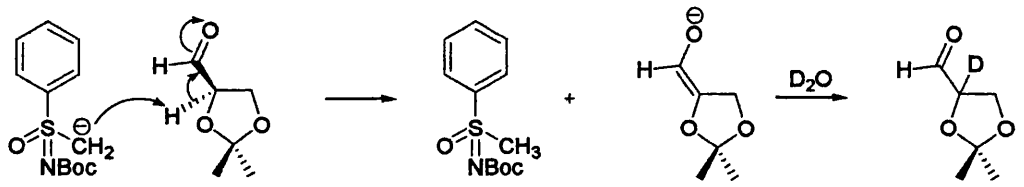

Scheme 27. Mechanistic representation of the isotopic labelling study, determining the possible reaction outcomes.

Interestingly, none of the above outcomes and deductions was observed in the isotopic labelling study (*vide supra*, entry 5, Table 6). Instead, extending the lithiation time to 90 mins and increasing the reaction temperature to room temperature gave a new product on TLC. ^{1}H NMR revealed that the anticipated product had not been formed, but instead the product isolated was tentatively assigned to be compound **71** (*vide infra*, Scheme 28). The diagnostic peaks, which indicate strongly the formation of **71**, are δ 1.49 (*tert*-butyl protons of a Boc group), δ 6.81 (NH), with the absence of the S-methyl protons in the region of δ 2-3.5. Another proposed product, oxirane acetonide **72** was not isolated.

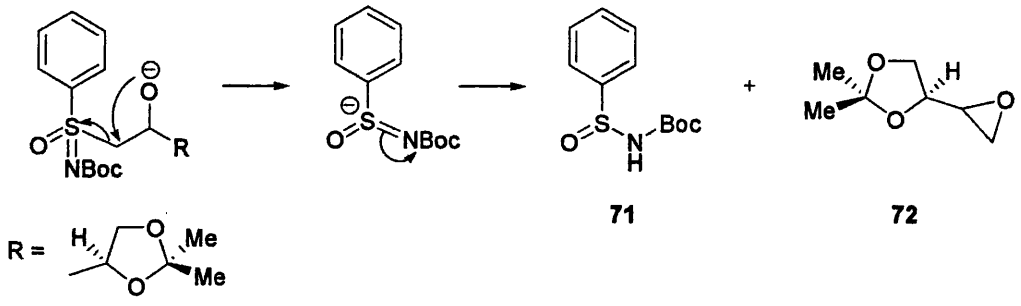

Scheme 28. Proposed mechanism of the synthesis of unexpected by-product **71**.

3.1.4 Synthesis of 3-methylthiobenzonitrile

In parallel with the studies on the addition of the carbanion to the aldehydes, an investigation was carried out on establishing an efficient and reliable sulfoximination method on a 3-substituted aryl sulfoximine. Rhodium-catalysed imination has been shown previously to proceed in good yield and the resulting N-TFA derivative proved to be invaluable in the subsequent adjustment of protecting groups (*vide supra*, Scheme 25). With this strategy in hand, efforts were turned to the synthesis of the required retrosynthetic component, 3-(*S*)-S-methylsulfonimidoyl benzonitrile **45** (*vide supra*, Scheme 13), with an appropriate protecting group at the nitrogen. The precursor to **45**, 3-(methylthio)benzonitrile **78**, is not commercially available and either the 3-cyano group or the methylthio group would have to be introduced to the molecule.

The synthesis of **78** commenced with the introduction of a methylthio group to 3-bromo-benzonitrile **73**. Ornstein *et al.*[164] described the use of dimethyl disulfide as a source of alkylthiolate ion on a 3-bromo phenyl derivative. The group performed a metal-halogen exchange using butyl lithium, followed by quench with dimethyl disulfide, and replacement of the 3-bromo group with a SMe group was achieved in good yield (82%).[164] However, when 3-bromobenzonitrile **73** was subjected to the same conditions, the reaction only led to decomposition of the starting material (*vide infra*, Route A, Scheme 29).

The introduction of a nitrile group in the *meta*-position was next considered. Preparation of aromatic nitriles has been studied extensively. Nitriles are important functional groups with installation of functionalities such as aldehydes, amines, acids and acid derivatives being widely accessible.

One of the most common methods of introducing a nitrile group is by a Sandmeyer reaction. Diazotisation of the corresponding amine gives a diazonium salt, which reacts with copper(I) cyanide *via* a radical mechanism (*vide infra,* Scheme 30). The diazonium ion is reductively cleaved by the cuprous ion, resulting in the formation of an aryl radical. Excess cyanide ions required can be provided by potassium cyanide. The aryl radical then reacts with a cyanide radical from the copper(II) salt, reducing it to the original copper(I) cyanide.[165]

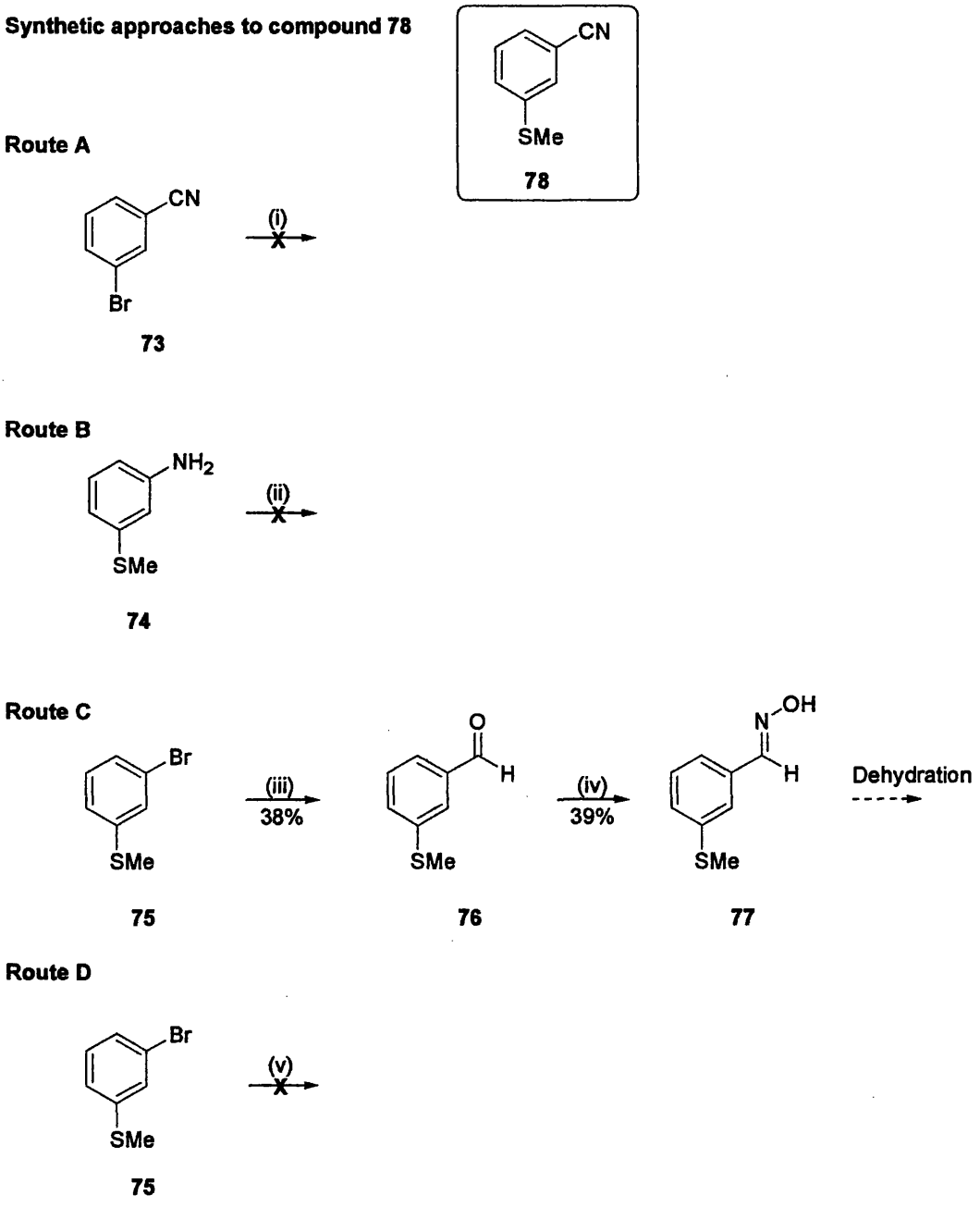

Scheme 29. Attempts to synthesise 3-(methylthio)benzonitrile **78**. *Reagents and conditions: (i) n-BuLi, MeSSMe, THF, –78 °C; (ii) HCl, $NaNO_2$, CuCN, KCN, H_2O, 0-5 °C / HBF_4, $NaNO_2$, CuCN, KCN, H_2O, 0 °C; (iii) n-BuLi, DMF, THF, –78 °C; (iv) NH_2OH·HCl, NaOAc, EtOH, 45 °C; (v) CuCN, DMF, 150 °C.*

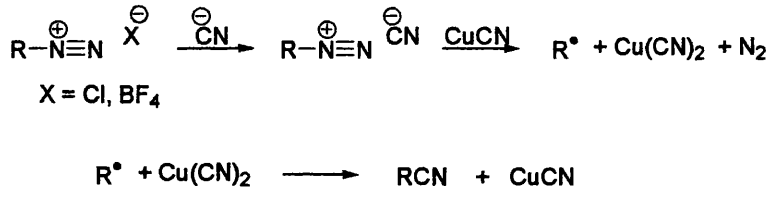

Scheme 30. Sandmeyer reaction.

Attempts to synthesise the nitrile **78** from the standard diazonium chloride method using the Sandmeyer conditions did not proceed as anticipated (*vide supra*, Route B, Scheme 29).[166] The diazonium tetrafluoroborate salt was chosen as the next candidate. It was reasoned that the Sandmeyer reaction might proceed better if the diazonium salt could be isolated and then allowed to react with cyanides. The diazonium tetrafluoroborate was isolated by filtration and subsequently treated with CuCN and KCN. However, TLC of the reaction mixture only revealed numerous highly coloured products and separation of these proved difficult.

An attempt to synthesise a nitrile group from an oxime was pursued. Lithium-bromine exchange with 3-bromothioanisole **75** and quench with dimethylformamide (DMF) gave 3-methylthiobenzaldehyde **76** in low yield (*vide supra*, Route C, Scheme 29). Condensation with hydroxylamine hydrochloride furnished the aldoxime **77**. A subsequent dehydration should afford the nitrile **78**. However, poor yields in this synthetic sequence called for an alternative route to be developed.

Another traditional method of generating an aromatic nitrile is the Rosemund-von Braun reaction, which involves a nucleophilic substitution of the corresponding aryl halide by copper(I) cyanide in DMF. A Cu(III) complex is formed through oxidative addition of the aryl halide. Subsequent reductive elimination gives the aromatic nitrile and cuprous halide (Scheme 31).[167]

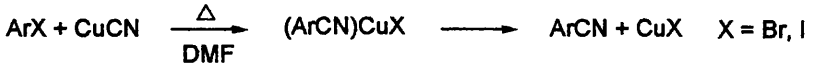

Scheme 31. Rosemund-von Braun reaction.

Procházka *et al.* successfully obtained 3-(methylthio)benzonitrile **78** from 3-bromothioanisole **75** in excellent yield using the Rosemund-von Braun conditions.[167] Surprisingly, under the same reaction conditions, the method could not be repeated

and only decomposition of starting material was observed (*vide supra*, Route D, Scheme 29).

A major drawback of the Rosemund-von Braun reaction is the harsh conditions (150°C for 5-50 h), which makes many sensitive functional groups incompatible with the system. Good progress has been made in the search of alternative procedures. Recent reports concentrate on metal-catalysed cyanation of aryl halides and reactions with palladium [$Pd(OAc)_2$, $Pd_2(dba)_3$ (*dba* = *dibenzylideneacetone*), $Pd(PPh_3)_4$], zinc ($ZnBr_2$) and copper [$Cu(BF_4)_2 \cdot 6H_2O$] catalysts demonstrated higher reaction rates and aryl nitriles were afforded in excellent yields.[168-170] Furthermore, new cyanide reagents have also been investigated, as the cyanide source plays an important part for the applicability of a cyanation reaction. Zinc(II) cyanide [$Zn(CN)_2$] and potassium ferro-cyanide ($K_4[Fe(CN)_6]$) have attracted consideration praise for their role in maintaining cyanide concentration in the catalytic cycle in palladium-catalysed cyanations.[170,171]

Sundermeier *et al.* presented mechanistic studies on the catalytic system.[168] Pd(0) is the active species of palladium catalysts and reaction of Pd(0) with aryl halides is the key step in the cycle (Scheme 32).[169] High concentrations of cyanide ions were reported to affect the palladium catalytic cycle by reacting with Pd(II) species, forming the inactive Pd(II)-CN complexes, thereby reducing the pool of active Pd(0). $Zn(CN)_2$ and $K_4[Fe(CN)_6]$ are both sparingly soluble in most solvent systems which prevents the problem of early exposure of Pd(0) to cyanide.

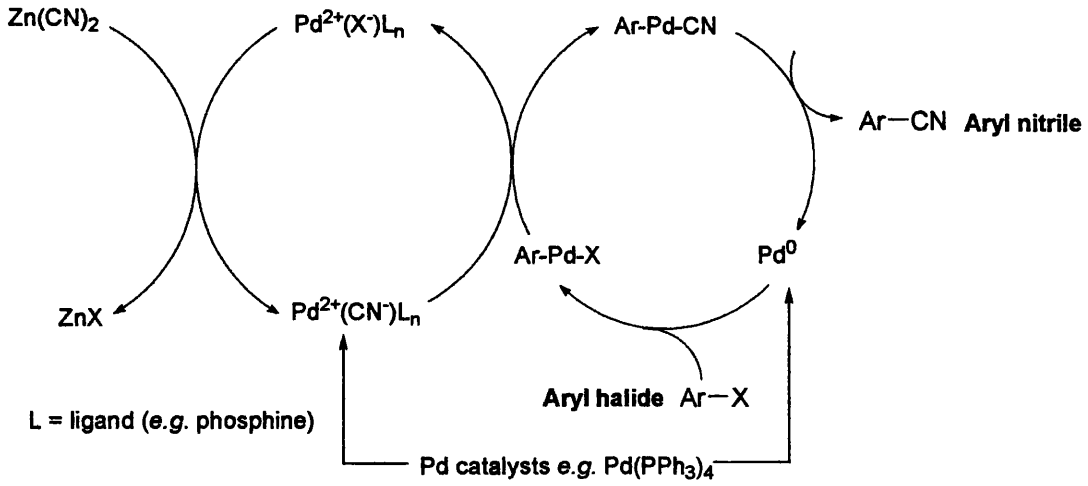

Scheme 32. Proposed mechanism of palladium-catalysed cyanation by Sundermeier *et al.*[168]

$K_4[Fe(CN)_6]$ is a particularly interesting reagent because it is inexpensive, easily handled, commercially available on multi-gram scale and non-toxic. Based on the

positive reviews, an attempt to synthesise compound **78** commenced with the literature method using $K_4[Fe(CN)_6]$ and $Pd(OAc)_2$ in dimethylacetamide (DMA).[170] However, TLC of the reaction mixture indicated that, after 10 h at 120°C, only the starting material was present (Scheme 33).

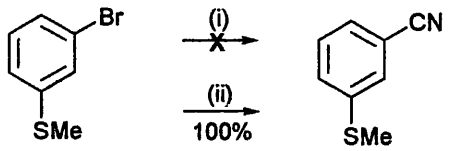

75 **78**

Scheme 33. Synthesis of the important intermediate **78** by palladium-catalysed cyanation with $Zn(CN)_2$. *Reagents and conditions: (i) $K_4[Fe(CN)_6]$, $Pd(OAc)_2$, DMA, 120°C; (ii) $Zn(CN)_2$, $Pd(PPh_3)_4$, DMF, 150°C.*

$Zn(CN)_2$ was next considered as a possible cyanide source. A separate literature method presented by Tatsumi *et al.* was adopted (Scheme 33).[171] The group converted a bromothiophenyl derivative to the corresponding cyano compound in poor yield using a combination of $Zn(CN)_2$ and tetrakis(triphenylphosphine)palladium(0) $[Pd(PPh_3)_4]$ in DMF. Amazingly, using the same reaction conditions, 3-bromothioanisole **75** was converted to the nitrile compound **78** in quantitative yield.

3.1.5 Chiral sulfoxidation

Having successfully obtained compound **78**, the next step was to introduce chirality at the sulfur atom. Chiral sulfoxidation is one of the most important steps in the synthesis of the key intermediate **45**; enantioselective oxidation of the sulfur would give the desired (*S*)-configuration of the sulfoxide and subsequent sulfoximine. 3-Bromothioanisole **78** was used in a model reaction.

Chiral sulfoxidation has been a subject of constant interest for many years and the most acceptable method is the catalytic enantioselective oxidation of prochiral sulfides. In particular, the use of metal catalysts with chiral ligands is a powerful method to generate chiral sulfoxides. Among the numerous reported catalysts such as titanium, iron, and vanadium, the most popular choices are the modified Sharpless reagents, $Ti(OiPr)_4$/(*R,R*)-(+)-diethyl tartrate (DET) (1:4) and $Ti(OiPr)_4$/(*R,R*)-(+)-DET / H_2O (1:2:1), described by Modena *et al.* and Kagan *et al.*, respectively.[172-174] Both systems led to the asymmetric oxidation of sulfides using *tert*-butyl hydroperoxide (TBHP) as oxidant (*vide infra*, Table 7) in similar yields. However, Kagal *et al.* showed that

addition of water to the system dramatically improved the enantioselectivity and the following points were concluded:[172]

1. $Ti(OiPr)_4$ / (*R,R*)-(+)-DET / H_2O / TBHP (1:2:1:1.1) is the best system in terms of yield and enantioselectivity.
2. Water significantly increases enantiomer composition and yield is satisfactory.
3. Optimum reaction temperature is –20°C.
4. The water-modified Sharpless reagent is prepared in DCM at room temperature, with sequential addition of $Ti(OiPr)_4$, DET and water. TBHP is added last. This order is important to avoid precipitation of TiO_2 by early addition of water.

Although this system was first described in 1984 and subsequent reports of use of newer metal catalysts (vanadium and iron) proved positive, the modified Sharpless oxidation still remains a frequent method in chiral sulfoxidation because all the reagents are commercially available, cheap and easy to handle.[172-174] DET is by far the most accessible chiral ligand and both enantiomers are available in multi-gram scales.

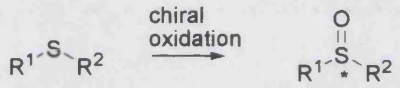

Entry	Metal catalyst	Chiral ligand	Oxidant	R^1	R^2	Yield (%)	ee (%)
1	$Ti(OiPr)_4$[172,174]	(*R,R*)-(+)-DET	TBHP	$PhCH_2$	Me	70	46
2	$Ti(OiPr)_4/H_2O$[172,174]	(*R,R*)-(+)-DET	TBHP	Ph	Me	80	89
3	$Ti(OiPr)_4$[172,174]	*R*-(+)-BINOL	TBHP	Ph	Me	86	63
4	$VO(acac)_2$[174]	Schiff base (*R*)-**a**	H_2O_2	Ph	Me	73	59
5	$Fe(acac)_3$ / 4-methoxybenzoic acid[173,174]	Schiff base (*R*)-**b**	H_2O_2	Ph	Me	66	61

Table 7. Metal-catalysed chiral sulfoxidation. Structures of some unusual chiral ligands are presented in Figure 23 (*vide infra*). (BINOL = binaphthol, acac = acetylacetonate)

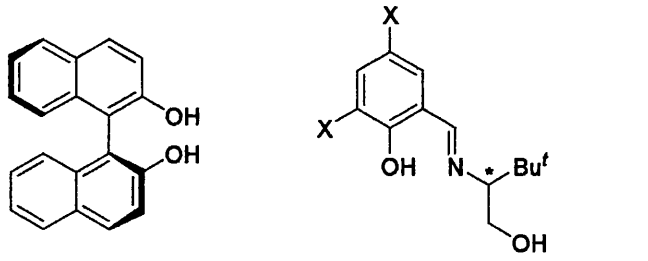

R-(+)-BINOL Schiff bases a: X = Bu^t, b: X = I

Figure 23. Structures of some new chiral ligands utilised in metal-catalysed conditions.

The exact structure of the water-modified Sharpless reagent is still unknown. Fernández *et al.* proposed that the active species is a dimer complex with two titanium atoms connected *via* an η-oxo bridge and delivery of the reactive oxygen is determined by the size of the substituents at the sulfur atom (Figure 24).[172]

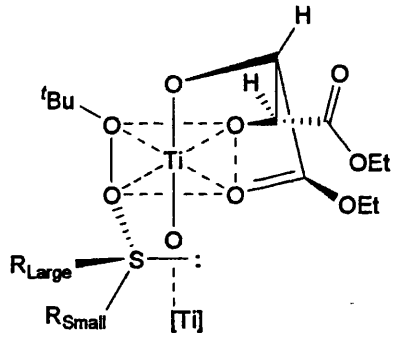

Figure 24. Tentative structure of the catalytically-active Sharpless reagent in chiral sulfoxidation as described by Fernández *et al.*[172]

As shown in Scheme 34 (*vide infra*), 3-bromothioanisole **75** was subjected to the modified Sharpless sulfoxidation conditions using (*S,S*)-(–)-DET as the chiral ligand and the corresponding (*S*)-sulfoxide **79** was afforded in 49% yield. The enantiomeric excess (ee) was measured by polarimetry and the optical rotation $[\alpha]^{20}_{D}$ was found to be –39.6°. Capozzi *et al.* reported a high ee value (97%) for (*R*)-(+)-3-bromophenyl methyl sulfoxide, with an $[\alpha]^{25}_{D}$ of +116.3° using water-modified Sharpless reagents with cumene hydroperoxide.[175] An ee of 33% was calculated for sulfoxide **79**. Some of the enantiomeric purity was lost due to warming of the reaction mixture to ambient temperature when it was left stirring overnight. However, despite careful control of temperature at the subsequent attempt of Sharpless oxidation with target intermediate **78**, TLC of the reaction mixture revealed only the presence of the starting material (*vide infra*, Scheme 34). It was reasoned that the presence of an electron-withdrawing

3-cyano group in **78** might have reduced the nucleophilicity of the sulfur, making the oxidation difficult, although the *meta* relationship of the groups may compromise this explanation.

Since 3-(methylthio)benzonitrile **78** is an essential starting compound in the ongoing synthetic route and chiral sulfoxidation may prove to be difficult in the presence of the nitrile group, it was decided that, like the non-substituted counterparts, enantiomers would be separated at a later stage in the sequence once the sulfoximine moiety is constructed.

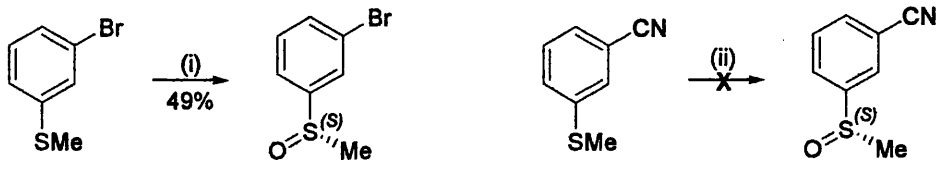

75 **79 (33% ee)** **78** **80**

Scheme 34. Sharpless oxidation converted 3-bromothioanisole **75** to the corresponding *S*-sulfoxide **79** with modest enantiomeric excess (due to raised temperature). The same reaction conditions failed to oxidise target intermediate **78** to the chiral sulfoxide **80**. *Reagents and conditions: (i) $Ti(OiPr)_4$, (S,S)-(–)-DET, H_2O, TBHP, DCM, –20°C to RT; (ii) $Ti(OiPr)_4$, (S,S)-(–)-DET, H_2O, TBHP, DCM, –20°C.*

3.1.6 Addition of carbanions to aldehydes

Bearing this in mind, the synthetic sequence used to synthesise racemic S-methyl-S-phenylsulfoximine **(±)-50** were followed, and 3-(S-methylsulfonimidoyl)-benzonitrile **(±)-83** was obtained in 30% overall yield (*vide infra*, Scheme 35). The lower yields in *m*CPBA-oxidation and rhodium-catalysed imination with the 3-cyano derivatives further support the hypothesis that the existence of a nitrile group reduced the nucleophilicity of the sulfur atom.

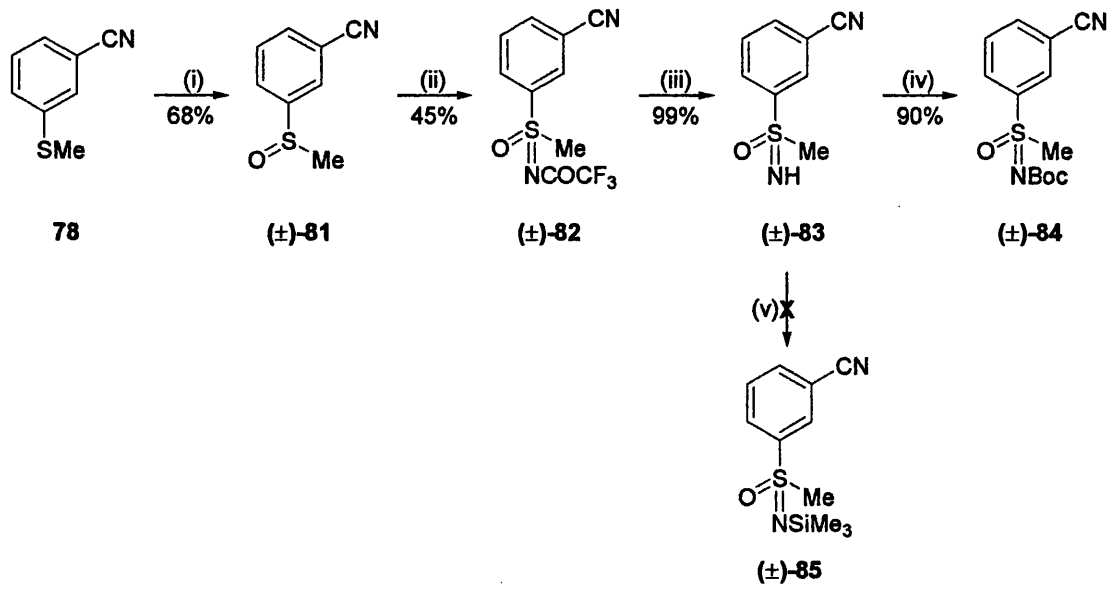

78 (±)-81 (±)-82 (±)-83 (±)-84

(±)-85

Scheme 35. Synthesis of the free NH sulfoximine (±)-**83** and subsequent attempts to protect the nitrogen. *Reagents and conditions: (i) mCPBA, DCM, 0°C; (ii) CF_3CONH_2, MgO, $Rh_2(OAc)_4$, $PhI(OAc)_2$, DCM; (iii) NH_3, MeOH; (iv) NaH, $(Boc)_2O$, THF, 0°C; (v) Et_2NSiMe_3, MeCN, 65°C.*

The intermediate NH sulfoximine (±)-**83** was protected at the nitrogen with a Boc group, giving (±)-**84** in good yield. However, unlike with S-methyl-S-phenylsulfoximine (±)-**50**, a TMSi group could not be introduced at the nitrogen (Scheme 35).

Nevertheless, the carbanion generated at the SMe group of the N-Boc protected sulfoximine (±)-**84** using the strong base, *t*-BuLi, was treated with benzaldehyde and *S*-glyceraldehyde acetonide **44** (*vide infra*, Scheme 36). However, TLC of the reaction mixtures revealed only the presence of starting materials.

As it was unclear whether the failure of this reaction was due to the failure to deprotonate the SMe group or if the anion formed did not react with the electrophilic aldehydes, the reactions were repeated allowing 2 h of lithiation (at –78°C to RT) before the addition of aldehydes. Again, no products were obtained.

The inability to reproduce synthetic steps meant that the route outlined in Scheme 13 (*vide supra*) was no longer viable.

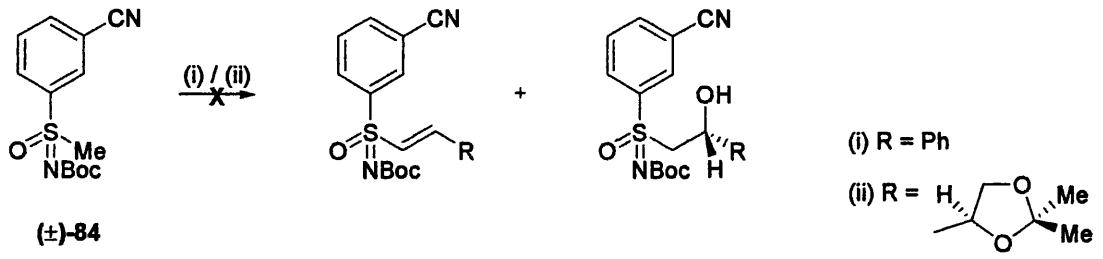

Scheme 36. Attempted anion addition to aldehydes with N-Boc sulfoximine (±)-**84**. *Reagents and conditions: (i) t-BuLi, PhCHO, THF, –78 °C; (ii) t-BuLi, **44**, THF, –78 °C.*

3.2 Route II: introduction of a whole four-carbon unit

3.2.1 Retrosynthesis

Introduction of the ribose mimic **39** as a four-carbon unit as illustrated in Scheme 13 (*vide supra*) relies on the addition of a carbanion of a SMe group (one-carbon unit) to the chiral glyceraldehyde acetonide **44** (three-carbon unit), resulting in a four-carbon unit necessary to form the required stereocentres of the ribosyl moiety. Since this step has been proven to be irreproducible, a new route was devised to introduce all four carboatoms with all chirality already set up at the two carbon chiral centres of a homochiral dioxolane **86** (*vide infra*, Scheme 37). This four-carbon component would be coupled with a sulfur nucleophile **87**. The sulfoximine would be constructed later in the synthesis, with the configuration at the sulfur centre introduced either by separation of diastereoisomers during sulfoximination, or if it is not possible, *via* resolution of racemic free NH sulfoximines using (+)-CSA.[134]

This synthetic sequence (*vide infra*, Scheme 37) avoids the lithiation step and subsequent addition to aldehydes, which proved to be troublesome. The starting dioxolane compound **86** is readily available by literature methods,[176] and 3-bromo-thiophenol **87** is commercially available. Since sulfoximination procedures have now been fully established in the previous retrosynthetic scheme, sulfide **88** will be subjected to the same conditions to afford the corresponding sulfoximine **91**. Acetal hydrolysis gives the diol **92**, which upon an intramolecular Mitsunobu dehydration should generate two ring-closure products: a four-membered ring and a five-membered ring compounds. As five-membered rings are favourable thermodynamically, the resulting product should be the precursor of target compound **39**.

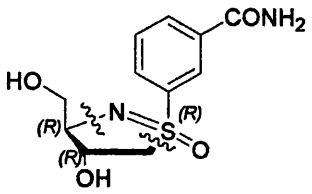

Target compound, 39

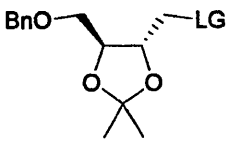

86
LG = leaving group

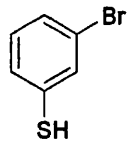

87

Nucleophilic substitution

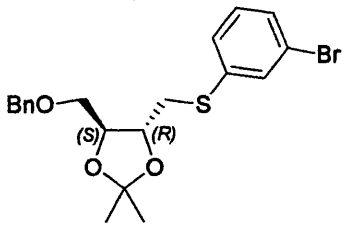

88

SULFOXIMINATION

1. Oxidation
2. Rh(II)-catalysed imination
3. Removal of TFA group

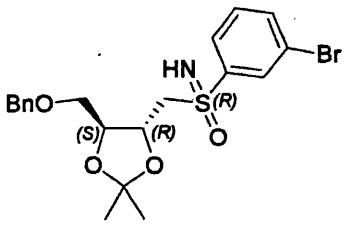

91

Acetal hydrolysis

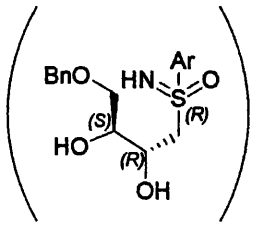

=

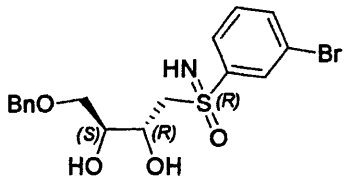

92

1. Mitsunobu ring closure
2. Removal of Bn group
3. FGI (cyanation, hydration of nitrile)

TARGET

Scheme 37. New synthetic approaches to target compound **39**.

3.2.2 Formation of the C–S bond

Accordingly, dioxolane **86** was set as the first target molecule in this new sequence and its synthesis is outlined in Scheme 38. *R,R*-(+)-DET **93** was converted through ketal exchange with 2,2-dimethoxypropane (DMP, **94**) into the C_2-symmetric ester **95** and reduction with lithium aluminium hydride (LAH) gave the corresponding diol **96**.[176,177] The symmetry of diol **96** was disrupted by monobenzylation using an equivalent amount of benzyl bromide to give compound **98**; after investigation of several reaction conditions, it was concluded that freshly-pentane-washed sodium hydride gave the best result in terms of yield (71%) and ratio of mono- and dibenzylation (12:1), the latter being much superior to the statistical mixture.[176,178]

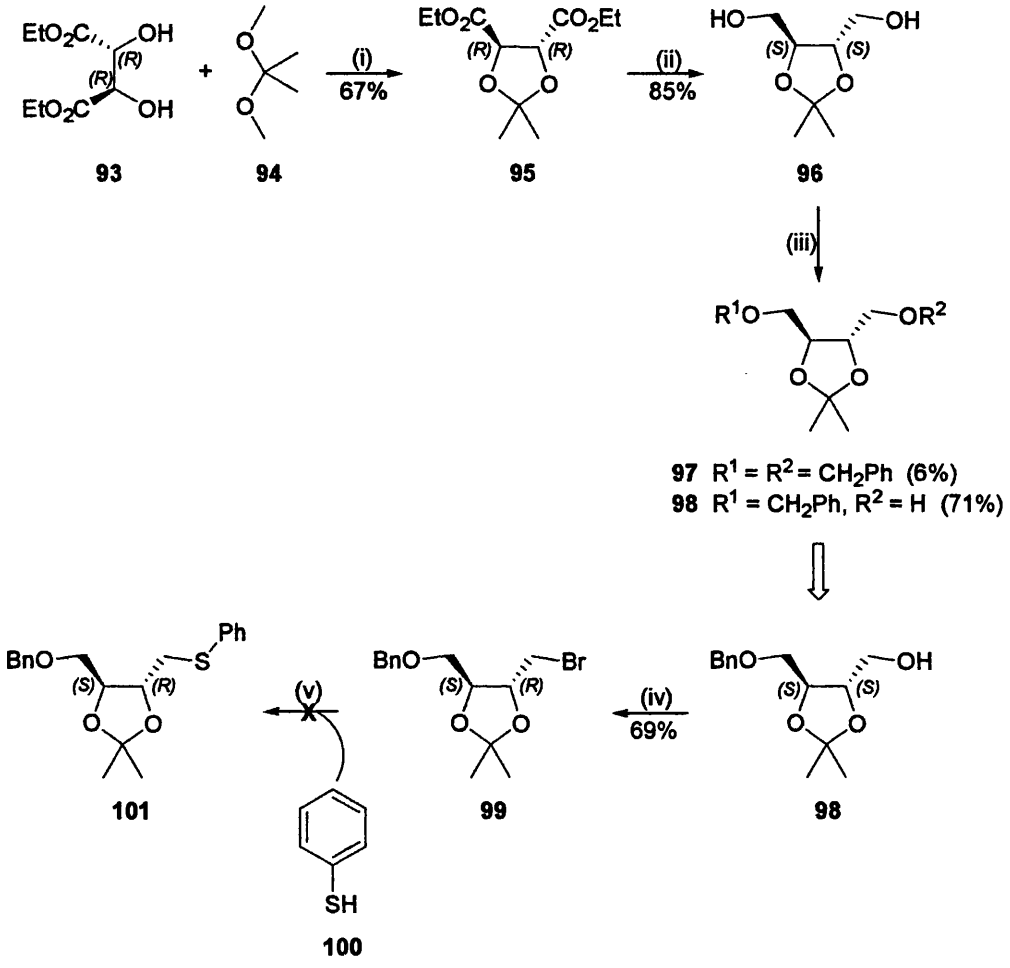

Scheme 38. Attempted synthesis of model dioxolane sulfide **101**. *Reagents and conditions: (i) p-TsOH, DCM, reflux; (ii) $LiAlH_4$, THF, reflux; (iii) NaH, BnBr, DMF, 0 °C; (iv) Ph_3P, CBr_4, THF, 0 °C; (v) LHMDS, **100**, THF, –78 °C.*

Having obtained the monobenzylated dioxolane **98**, the next step would be to replace the free hydroxy group with a reactive leaving group. Treatment with triphenylphosphine (TPP) and carbon tetrabromide afforded the bromomethyl dioxolane **99**.[179] A model reaction was devised to explore subsequent synthetic steps, in which thiophenolate **100** was used as a sulfur nucleophile. Surprisingly, generation of the thiophenolate anion, an exceptionally good nucleophile, with lithium hexamethyldisilazide (LHMDS), and treatment with **99** did not give the desired condensation product **101**. TLC of the reaction mixture indicated that a large amount of thiophenol **100** was still present but the dioxolane compound **99** had been consumed along with generation of a new product spot, which disappeared upon aqueous work-up. This puzzling result may be tentatively explained by a base-catalysed elimination and the enol ether formed may have decomposed in aqueous media (Scheme 39).

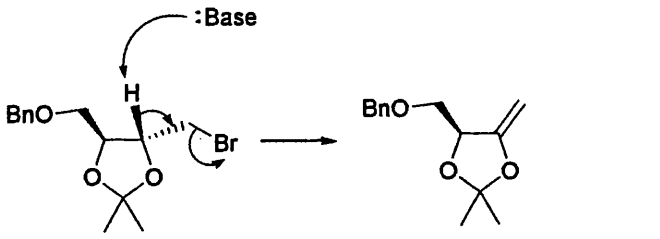

Possible elimination product

Scheme 39. Postulated mechanism of a side reaction in the coupling of bromomethyl dioxolane **99** and thiophenol **100**.

3.2.2.1 Mitsunobu reaction

Consequently, a different approach was sought involving a thio-Mitsunobu reaction between the hydroxymethyl dioxolane derivative **98** and thiophenol **100**. Direct coupling of the two starting compounds using Mitsunobu reagents should afford the desired sulfide **101** under neutral conditions (*vide infra*, Scheme 40).

The Mitsunobu reaction has gained widespread interests in many fields of organic synthesis due to its reliability and applicability. The reaction is very simple with mild conditions and high yields. It was discovered by O. Mitsunobu in 1967 as a dehydration reaction between an alcohol and a carboxylic acid in the presence of diethyl azodicarboxylate (DEAD) and triphenylphosphine (TPP), generating the corresponding C–O ester bond.[180] With secondary alcohols, the largest use of the reaction is inversion of configuration at the alcohol centre and this application was mentioned in Scheme 13 (*vide supra*). Over the years, variants of other acidic nucleophiles to replace a

carboxylic acid have emerged including phenols, thiols/thiophenols and amines for new C–O, C–S and C–N bond formations, respectively.[180,181]

Thio-Mitsunobu reaction

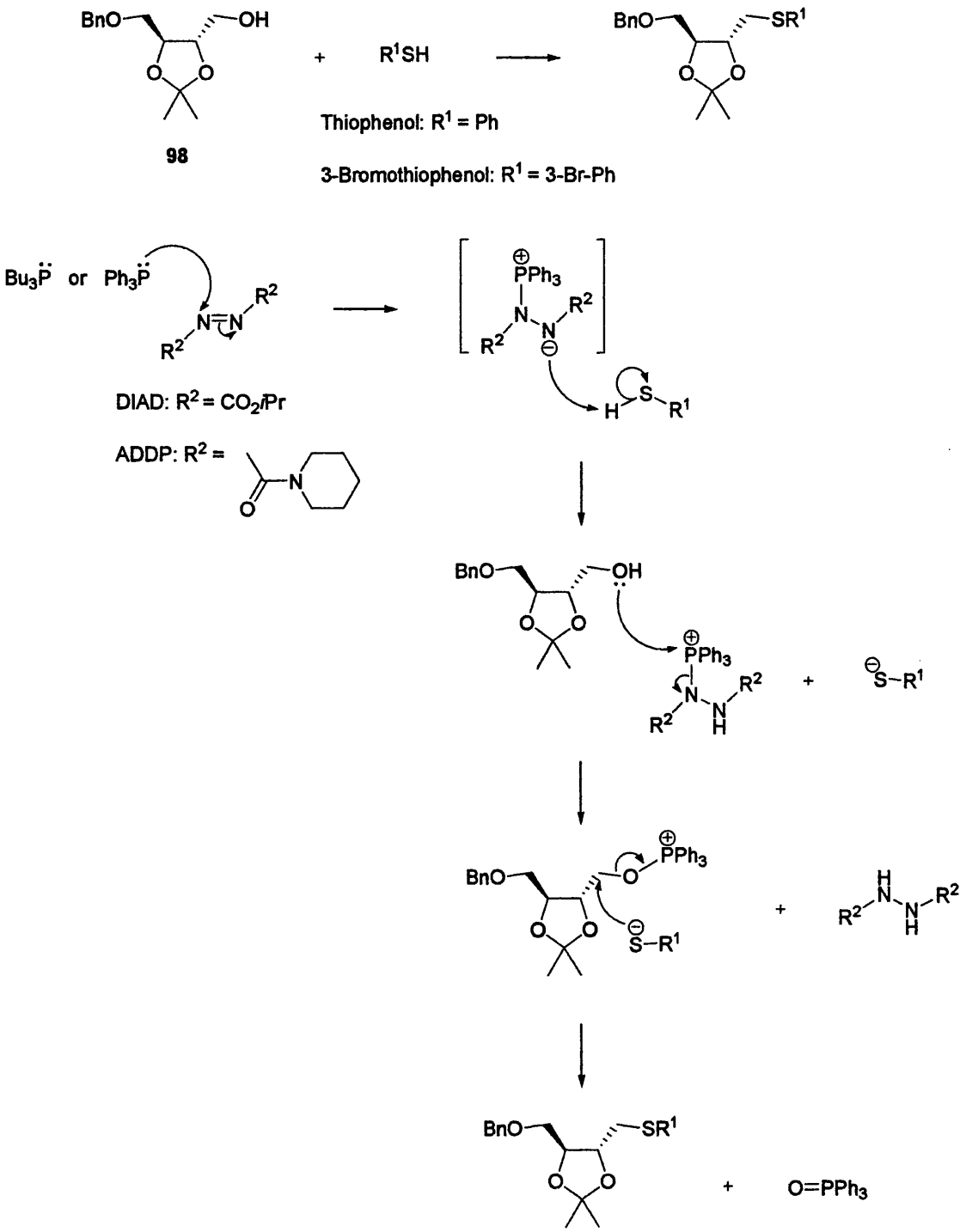

Scheme 40. Mechanism of the thio-Mitsunobu reaction with dioxolane compound **98**.

The mechanism for secondary alcohol substitution and subsequent inversion of configuration is presented in Scheme 41 (*vide infra*).[182] Addition of TPP to DEAD (step

1) gives a zwitterionic quaternary phosphonium adduct, which is protonated by the nucleophilic component (2). Attack by the alcohol (3) forms a highly reactive alkoxy-phosphonium intermediate (4). S_N2 displacement of the phosphonium results in the formation of a new C–O bond with inversion of configuration (5).

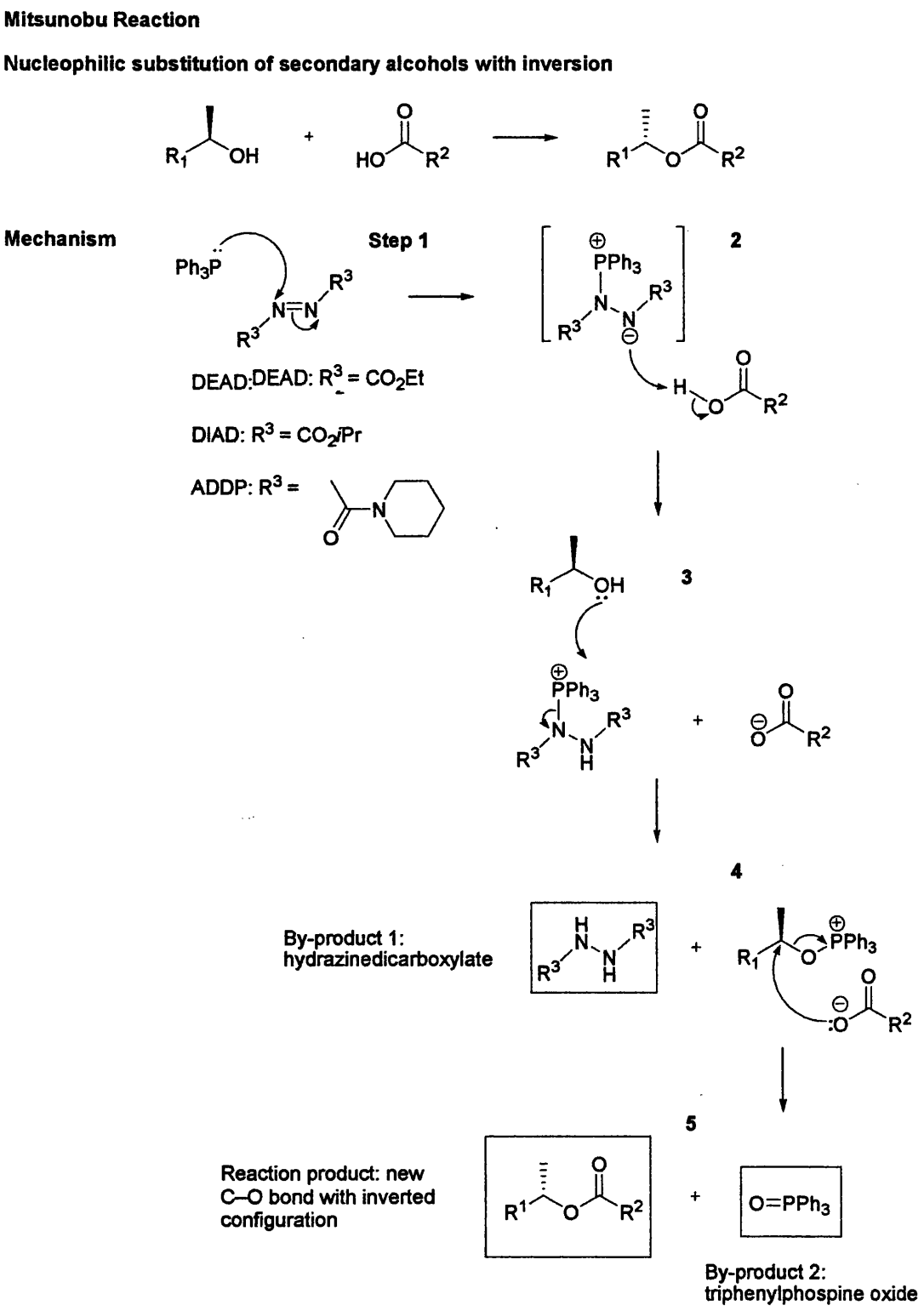

Scheme 41. Mechanism of the Mitsunobu reaction, with inversion of configuration of secondary alcohols.

A major disadvantage of the Mitsunobu reaction lies in the difficulty in the removal of excess reagents and their by-products, diethoxycarbonylhydrazine and triphenylphosphine oxide, formed by hydration of DEAD and oxidation of TPP, respectively. If the reaction can be performed in diethyl ether, both by-products can be precipitated and removed by filtration. However, since most Mitsunobu reactions are carried out in THF, careful column chromatography is often required to isolate the coupled product, which is time-consuming and may lead to deterioration of yield. A number of modified Mitsunobu agents (phosphines and azo compounds) have been recognised to circumvent this problem.

TPP still remains as a traditional reagent and is frequently used, despite the difficult separation of the excess starting material and the oxidised product. Alkylphosphanes such as tributylphosphine (TBP) and trimethylphosphine are popular alternative reagents since their oxidised products can be removed easily by aqueous work-up.[183] Recently, O'Neil *et al.* have demonstrated the utility of 1,2-bis(diphenylphosphino)-ethane (DPPE, Figure 25) as a phosphine reagent in the Mitsunobu reaction due to the greater polarity of the resulting bis(phosphine oxide).[184] This by-product can be easily removed by a simple filtration of the reaction mixture prior to work-up and purification. The group used DPPE in combination with DEAD/DIAD and good yields (59-98% with DEAD, 57% with DIAD) were reported.

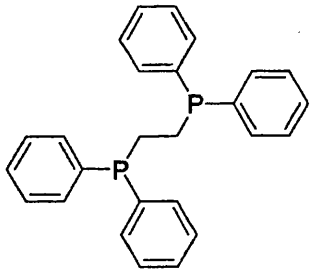

Figure 25. Structure of DPPE.

Diisopropyl azodicarboxylate (DIAD) has replaced DEAD as the more popular choice as a Mitsunobu reagent because it is less toxic, cheaper and easy to handle. Studies have shown that nucleophiles with a p*K*a higher than 11 are likely to contribute to lower reaction yields.[185] A tentative explanation is that with the unavailability of an acidic nucleophile, the alcohol protonates the zwitterionic intermediate, leading to the undesired azodicarboxylate derivative (*vide infra*, Scheme 42). Another drawback of the Mitsunobu reaction is the limitation of compatible nucleophiles. The p*K*a of the conjugate acids of the nucleophiles must be lower than that of the zwitterionic intermediate (p*K*a ~ 13); therefore, only relatively acidic nucleophiles are compatible

with the traditional Mitsunobu reagents. However, a new alternative has found a place in extending the utility of suitable nucleophiles.

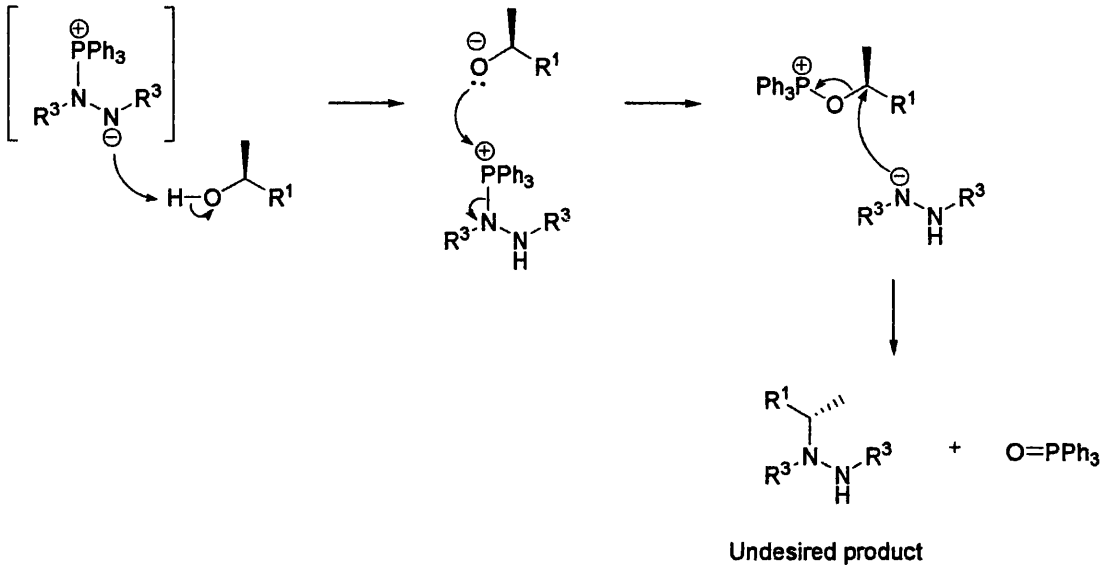

Scheme 42. Possible side-reaction with less acidic nucleophiles (p*K*a > 11).

Reports of the use of 1,1'-(azodicarbonyl)dipiperidine (ADDP) by Dembinski *et al.* provided a more versatile Mitsunobu reagent with higher basicity which works well with a broader range of nucleophiles such as carbon nucleophiles and amides, thus providing new C–C and C–N bond-forming strategies using a Mitsunobu reaction.[185]

For the synthesis of target intermediate **101** with the hydroxymethyl dioxolane **98** and thiophenol **100**, a variety of Mitsunobu conditions were pursued to investigate reaction efficiency. Additionally, a Mitsunobu-like reaction was attempted using TBP, DIAD and diphenyl disulfide (PhSSPh) as the sulfur source, where the latter is reduced to the thiophenolate anion (PhS^-) under the reaction conditions. This procedure was originally reported by Knutsen *et al.* for the synthesis of adenosine analogues using DEAD as the azodicarboxylate reagent, and the C–S bond formation proceeded in moderate yield (57%).[186] The results of attempted Mitsunobu reactions are summarised in Table 8 and the following conclusions were drawn:

1. The order of addition of the reagents does not seem to alter reaction outcome.
2. Reaction with DPPE, a promising new Mitsunobu phosphane, only led to recovery of starting materials.
3. Reaction using diphenyl disulfide (PhSSPh) as an alternative source for aryl-thiolate anion did not proceed as expected.

4. Combination of TBP and ADDP gave the best yield; to achieve efficient stirring, the highly viscous reaction mixture was sonicated.

Entry	Conditions (stated in the order of addition in reaction mixture)	Yield (%)
1	TPP (2 equiv.), DIAD (2 equiv.), thiophenol **100** (1 equiv.), dioxolane **98** (1 equiv.), THF (10 mL)	22
2	TPP (2 equiv.), thiophenol **100** (1 equiv.), DIAD (2 equiv.), dioxolane **98** (1 equiv.), THF (10 mL)	18
3	TBP (1.5 equiv.), ADDP (1.5 equiv.), thiophenol **100** (1.5 equiv.), dioxolane **98** (1 equiv.), THF (10 mL), sonication	44
4	DPPE (0.75 equiv.), DIAD (1.5 equiv.), thiophenol **100** (1.3 equiv.), dioxolane **98** (1 equiv.), THF (10 mL), sonication	-
5	TBP (2 equiv.), DIAD (1.5 equiv.), diphenyl disulfide (1.5 equiv.), dioxolane **98** (1 equiv.), THF (10 mL)	-

Table 8. Various Mitsunobu conditions attempted for the synthesis of sulfide **101**. (TPP = triphenylphosphine, DIAD = diisopropyl azodicarboxylate, TBP = tributylphosphine, ADDP = 1,1'-(azodicarbonyl)-dipiperidine, DPPE = 1,2-bis(diphenylphosphino)ethane)

3.2.2.2 Synthetic approaches to the model phenyl sulfoximine intermediate

Having established the optimum Mitsunobu conditions and obtained the sulfide **101**, it was treated with *m*CPBA at –78°C to give the sulfoxides **102a/b** in excellent yield as a 1:1 mixture of diastereoisomers (*vide infra*, Scheme 43).[187]

The ^{1}H NMR spectrum of **102a/b** showed two sets of signals, indicating the existence of two diastereomeric sulfoxides. The key region lies in the range of δ 2.8 to δ 4.6. In order to improve spectroscopic resolution and separation of signals, ^{1}H NMR analysis was conducted with a 600 MHz spectrometer. With the support of the ^{1}H-^{1}H COSY spectrum, the assignment of the two sets of diastereomeric protons was possible. These spectroscopic data, along with the TLC results (two visible spots in identical sizes), point to a 1:1 diastereomeric ratio (*vide infra*, Figure 26).

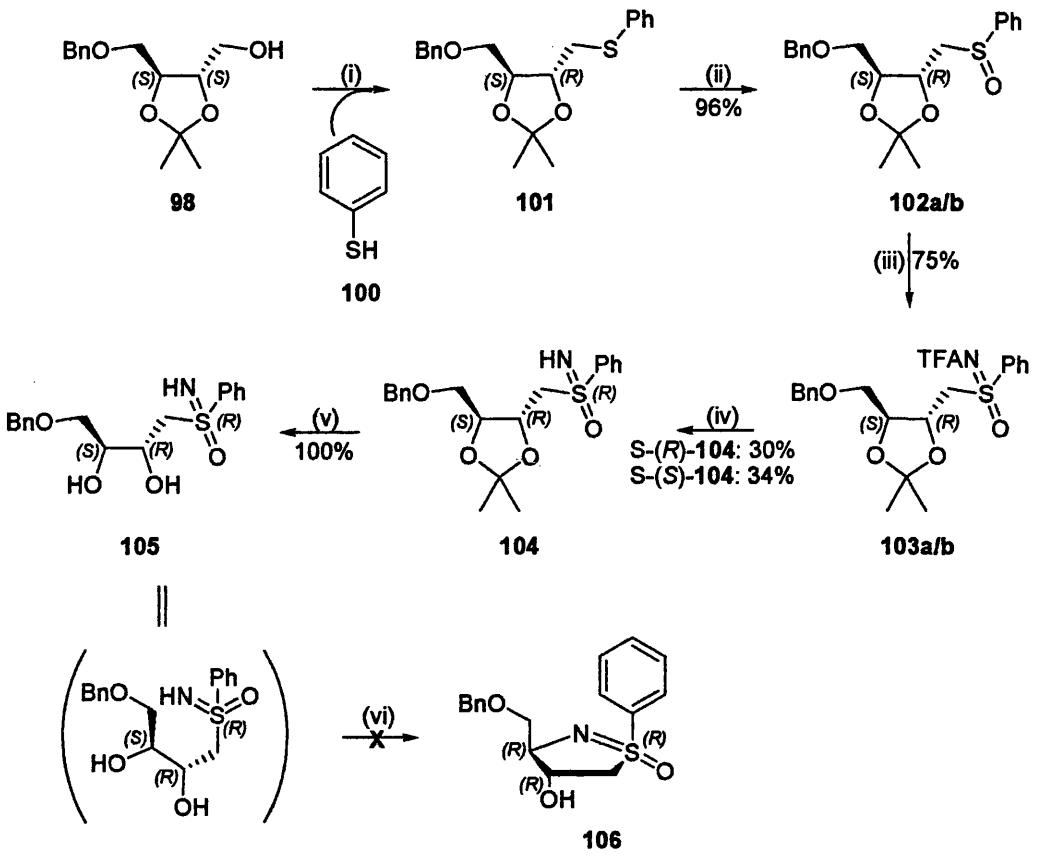

Scheme 43. Synthetic approaches to the model target **106**. *Reagents and conditions: (i) conditions (Table 8); (ii) mCPBA, DCM, –78°C; (iii) CF_3CONH_2, MgO, $Rh_2(OAc)_4$, $PhI(OAc)_2$, DCM; (iv) NH_3, MeOH; (v) HCl, MeOH; (vi) TBP; ADDP, THF, sonication, RT to 45°C.*

The two sets of CMe_2 protons resonated as four singlets at δ 1.37, δ 1.45, δ 1.46 and δ 1.47, each for one and a half protons. In the ^1H spectrum of the starting sulfide **101**, the signals of the CMe_2 protons were shown as two singlets at δ 1.40 and δ 1.44. Therefore, the signals were shifted neither upfield nor downfield in the presence of the remote electronegative sulfoxide oxygen.

The anticipated effect on the SCH_2 protons of the sulfoxide oxygen was relatively small. In the ^1H NMR spectrum of starting sulfide **101**, the SCH_2 protons gave a double doublet signal more upfield (δ 3.19) than the signals for the $BnOCH_2$ protons (δ 3.63). This effect was also observed with sulfoxides **102a/b**. Signals for the SCH_2 protons of both isomers of **102** resonated in the region of δ 2.83 to δ 3.18.

A

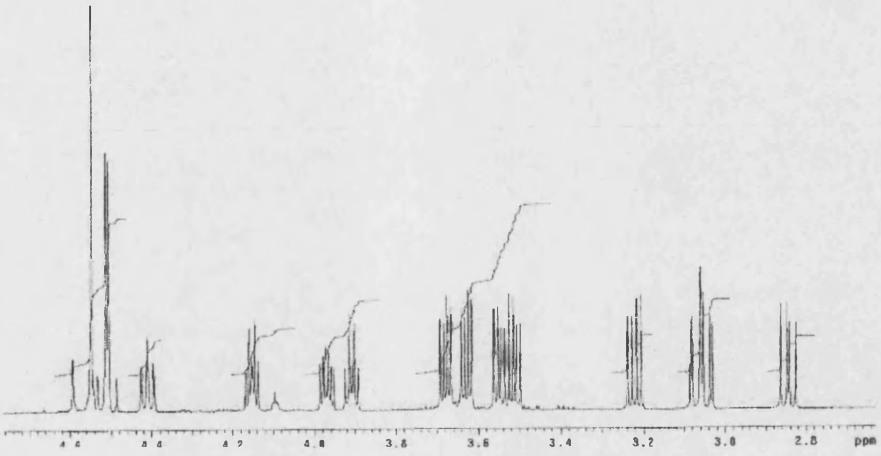

B

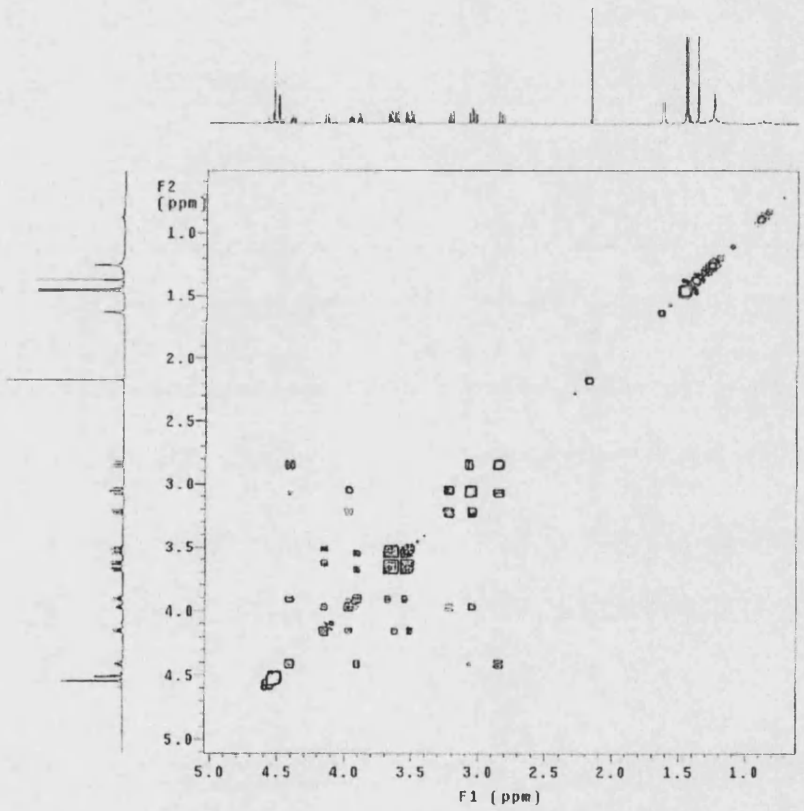

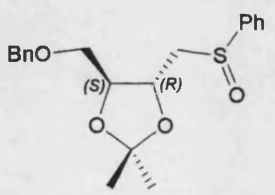

Figure 26. ^{1}H NMR spectra of diastereomeric **102a/b**. (A) is the 1-D ^{1}H NMR spectrum of the key region δ 2.8 to δ 4.6; (B) is the ^{1}H-^{1}H COSY spectrum, showing the cross-peak connections in each diastereoisomer.

From the ^{1}H-^{1}H COSY spectrum (*vide supra*, Figure 26), it was clear that the SCH_2 protons of isomer A appeared as a pair of double doublets at δ 2.84 and δ 3.06, each for half a proton, whereas the two double doublet signals for the SCH_2 protons of isomer B, each for half a proton, were located at δ 3.04 and δ 3.22. With this information, assignment of 5-H for both isomers was also made possible by the cross-peak connections with δ 3.97 and δ 4.41, corresponding to the 5-H for isomer B and A, respectively.

The $BnOCH_2$ proton signals of isomer A appeared as two double doublets integrating for a total of one proton at δ 3.55 and δ 3.68; a cross-peak connection with 4-H at δ 3.91 was observed on the ^{1}H-^{1}H COSY spectrum. The pair of double doublet signals, each for half a proton, at δ 3.51 and δ 3.62 belonged to isomer B, with the signal of its 4-H located at δ 4.15.

The $PhCH_2$ proton signals in the starting sulfide **101** were observed at δ 4.54 and δ 4.57 as a pair of doublets. In the diastereomeric sulfoxides **102a/b**, they appeared as a pair of doublets at δ 4.50 and δ 4.52 for one isomer for a total of one proton. Interestingly, the signal of the $PhCH_2$ protons of the other isomer was a singlet for one proton at δ 4.55. Thus the $PhCH_2$ protons are magnetically inequivalent in **101** and one of the isomer of **102** (as expected for diastereotropic protons) but are accidentally equivalent in the other isomeric **102**.

In isomer A, the 4-H signal (δ 3.91) is relatively upfield from that of 5-H (δ 4.41), whereas in isomer B, the 4-H signal (δ 4.15) is more downfield than that of 5-H (δ 3.97). Therefore, 4-H is more upfield in isomer A than in isomer B, whereas 5-H is more downfield in isomer A than in isomer B. MM2 (Molecular Mechanics) energy-minimised calculations were carried out on the corresponding S-(*R*)- and S-(*S*)-sulfoxides in order to investigate these findings but no apparent reasons could be concluded to explain such effects (*vide infra*, Figure 27).

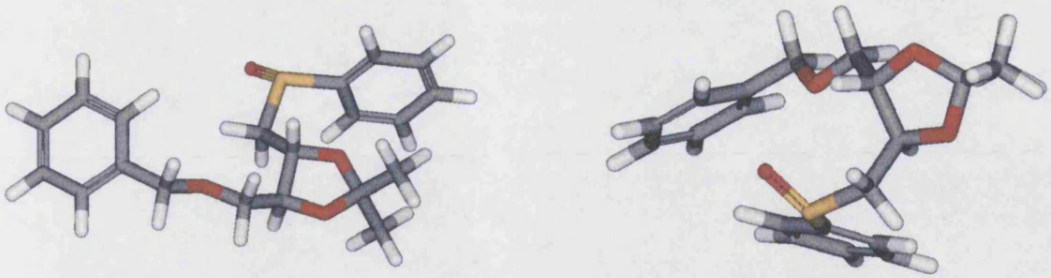

S-(*R*)-102 S-(*S*)-102

Figure 27. MM2-energy minimised models of **S-(*R*)-102** and **S-(*S*)-102**. The red colour refers to oxygen, the yellow refers to sulfur and the grey refers to the carbon atom.

Although the diastereoisomeric **102a/b** could be easily seen by TLC (two spots) and ^{1}H NMR, separation was not attempted as the R*f* values were very similar. Therefore, rather than separating them at this stage, a solution containing a mixture of the isomers in DCM was subjected to the $Rh_2(OAc)_4$-catalysed imination conditions and sulfoxides **102a/b** were converted to the N-TFA sulfoximines **103a/b** in good yield (*vide supra*, Scheme 43).

The ^{1}H NMR spectrum of **103a/b** again showed two sets of signals, indicating the existence of two diastereomeric N-TFA sulfoximines (Figure 28). Due to an extensive overlap of signals in the spectrum, assignment of individual proton signals was extremely difficult. Moreover, the diastereomeric ratio of the N-TFA sulfoximines **103a/b** could not be determined by the integrals of the signals for the $PhCH_2$ protons since only one singlet for two protons appeared in the spectrum. Therefore, a ^{19}F NMR spectrum was used since ^{19}F NMR chemical shifts are very sensitive to changes in environment; this is therefore a useful tool in measuring the diastereomeric ratio. The ^{19}F spectrum showed two singlet signals at δ –76.0 and δ –75.9 in a 3:2 ratio. This is inconsistent with the ^{1}H NMR diastereomeric ratio of 1:1 observed in the starting sulfoxides **102a/b**. This observation indicates that there was a small degree of diastereoselectivity in the imination step.

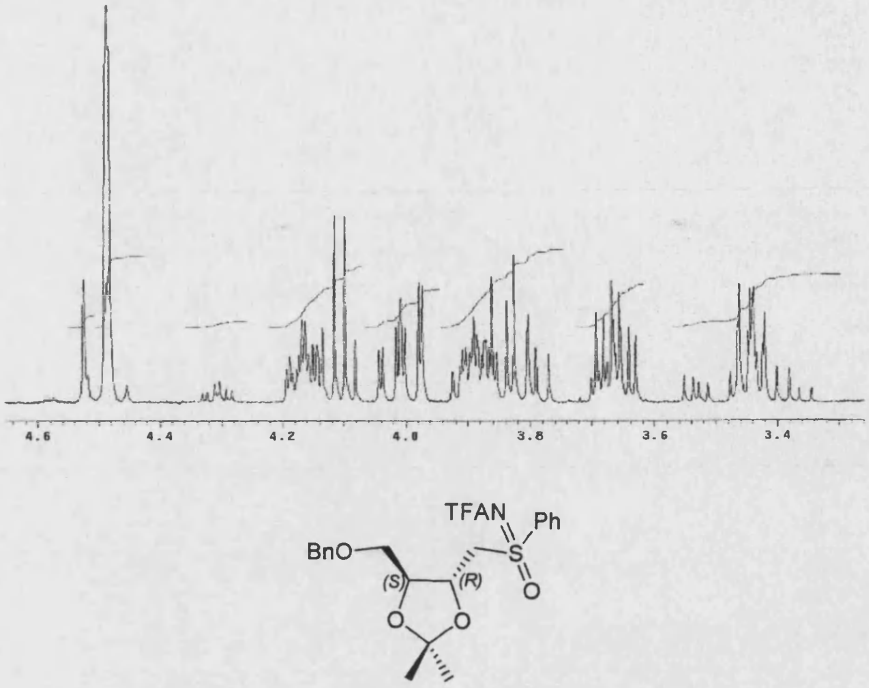

Figure 28. ^{1}H NMR spectrum (key region δ 3.0 to δ 4.6) of diastereomeric N-TFA sulfoximines **103a/b**.

Careful interpretation of coupling constants in the 1H NMR spectrum of **103a/b** allowed a tentative structural assignment of protons and unexpectedly, the signals for the SCH_2 protons appeared more downfield than the $BnOCH_2$ protons. This proton assignment is contrary to that seen in the starting diastereomeric sulfoxides **102a/b**. Further proton and carbon assignments were conducted by the different spectroscopic data from the ^{13}C NMR, 135-DEPT, ^{1}H-^{13}C COSY (HMQC) and long-range ^{1}H-^{13}C COSY (HMBC) spectra. From the HMBC spectrum, cross-peaks between the singlet signal for the $PhCH_2$ protons at δ 4.49 and the signals for a quaternary carbon at δ 137.32/137.35, the *ortho*-carbon for the C-phenyl ring at δ 127.9 and a CH_2 carbon at δ 69.6/69.7, indicating that the latter signal is due to the $BnO\underline{C}H_2$ carbon. Proton signals found to be attached to this carbon were the pair of double doublets at δ 3.42 and δ 3.43, and another pair of double doublets at δ 3.65 and δ 3.66. Therefore, it was assigned that these signals are due to the $BnOCH_2$ protons. Consequently, cross-peaks between the double doublets at δ 3.79, δ 3.81, δ 3.99 and δ 4.03 and the CH_2 carbons at δ 58.5 and δ 59.3 showed that these signals are due to the diastereomeric pair of the SCH_2 groups.

A possible explanation for this downfield shift of the signals for the SCH_2 protons relative to those for the $BnOCH_2$ protons is that the addition of the TFA group caused a marked downfield effect in relation to the starting sulfoxides **102a/b** in the region of the

SCH_2 protons, with the environment for the $BnOCH_2$ protons being relatively unaffected and thus the relative locations of these two groups of protons were opposite to those observed in the starting materials **102a/b**.

Interestingly, TLC of the diastereomeric mixture **103a/b** showed only one visible spot. Therefore, due to identical R*f* values, the two diastereoisomers could not be separated at this stage and a mixture containing both isomers was treated with ammonia to give the corresponding NH sulfoximines in a total yield of 64% (*vide supra*, Scheme 43). Separation of the two diastereoisomers was possible at this stage by careful chromatography and, contrary to the diastereomeric ratio determined from the N-TFA sulfoximines **104a/b**, the diastereomeric NH sulfoximines **S-(*S*)-** and **S-(*R*)-104** were obtained in a ratio of 1:1.1.

The ^1H NMR spectra of both **S-(*R*)-** and **S-(*S*)-104** revealed the following structural information:

1. The singlet signals of the CMe_2 protons of **S-(*R*)-104** were relatively downfield (δ 1.33 and δ 1.37) compared to those of the S-(*S*)-isomer at δ 1.21 and δ 1.29. In both sets of signals, they were shifted relatively downfield in relation to the starting N-TFA sulfoximines **103a/b** where the CMe_2 protons resonated at δ 1.16 to δ 1.26.
2. The signals of the SCH_2 protons were affected the most by removal of the strongly electron-withdrawing TFA group. In the ^1H NMR spectrum of the starting N-TFA compounds **103a/b**, these protons resonated as two double doublets at δ 3.79 and δ 3.81 for one isomer, and at δ 3.99 and δ 4.01 for the other isomer, whereas in the ^1H NMR spectrum of **S-(*R*)-104**, the two double doublet signals for the SCH_2 protons were moved upfield to δ 3.30 and δ 3.45. For the S-(*S*)-isomer, one signal of the SCH_2 protons appeared at δ 3.39 as a double doublet, and the other coincided with the chemical shift for the $BnOCH_2$ protons, forming a multiplet at δ 3.5 to δ 3.54.

Two-dimensional NMR analyses were performed on both isomers, with their COSY spectra showing the expected coupling relationships. In both isomers, cross-peaks connections of the $BnOCH_2$ protons with the double triplet signals at δ 3.90 and δ 3.93 showed that these signals were due to 4-H of **S-(*R*)-** and **S-(*S*)-104**, respectively. Similarly, cross-peaks connected the SCH_2 to the double triplet signals at δ 4.45 and δ 4.31 showed that these were due to 5-H of the (*R*)- and (*S*)-isomer, respectively.

The ^{1}H-^{1}H NOESY spectrum of **S-(*S*)-104** showed the expected connectivities between the $PhCH_2$ protons and the $BnOCH_2$ protons (*vide infra*, Figure 29). NOE connectivities were also observed between the two singlet signals for the CMe_2 protons and the double triplets of 4-H and 5-H. A cross-peak connection between the singlet signal at δ 1.21 and the double triplet of 4-H at δ 3.93 indicates that the former signal was due to the methyl group *trans* to $BnOCH_2$ in the five-membered dioxolane ring. Similarly, a cross-peak between the singlet at δ 1.29 and the double triplet of 5-H at δ 4.31 assigned the former signal to the methyl group *cis* to $BnOCH_2$. NOE connectivities of different intensities were noted between 5-H and the $BnOCH_2$ and SCH_2 protons. A relatively weak cross-peak between 5-H to the double doublet signal for one of the SCH protons at δ 3.39 suggests that this SCH proton is far apart in space to 5-H *i.e.* they are *trans* to each other. This double doublet has coupling constants of J = 14.2, 8.2 Hz, where the former corresponds to the geminal coupling. A coupling constant of J = 8.2 Hz is within the range of an axial/axial coupling. A stronger cross-peak between 5-H and the multiplet at δ 3.50 to δ 3.54 (one SCH proton and one BnOCH proton) indicates that this BnOCH proton and 5-H are close in space to each other.

Similarly, through-space correlations were seen between 4-H and the double doublet signal for one of the $BnOCH_2$ protons and the multiplet at δ 3.50 to δ 3.54. The relatively weak NOE connectivity to the double doublet at δ 3.64 indicates that the BnOCH protons are on the opposite face of the dioxolane ring *i.e.* they are *trans* to 4-H. A stronger cross-peak seen between 4-H and the multiplet at δ 3.50 to δ 3.54 for two protons (a BnOCH proton and a SCH proton) again reveals that the SCH_2 protons and 4-H are on the same face of the dioxolane ring *i.e.* they are *cis* to each other. Weak cross-peaks between 4-H and 5-H confirmed that the protons are on the opposite face of the five-membered dioxolane ring and are thus *trans* to each other. A vicinal coupling constant of ^3J = ~ 8 Hz between 4-H and 5-H further supports this relative configuration.

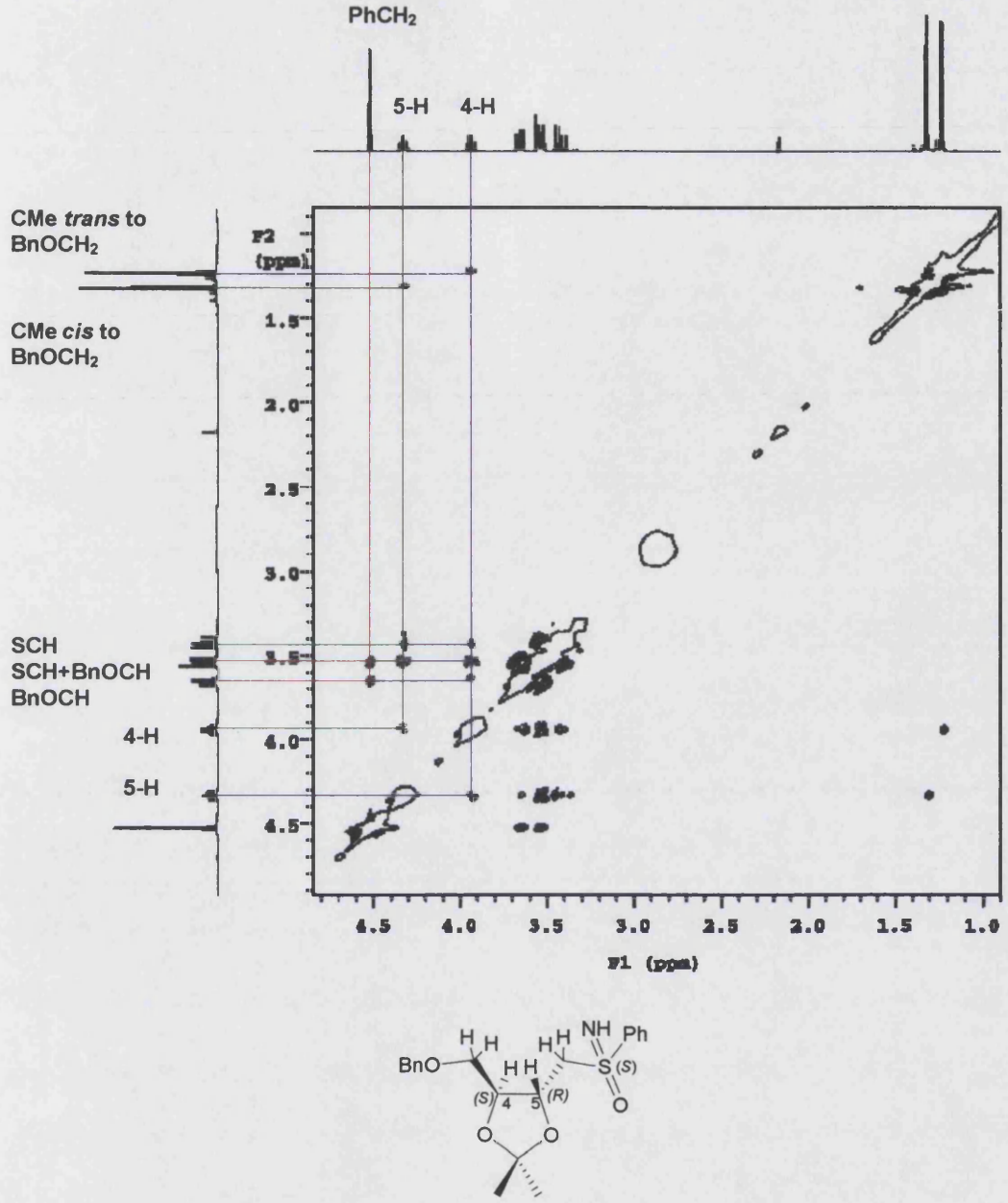

Figure 29. ^{1}H-^{1}H NOESY spectrum of 4*S*,5*R*,S(*S*)-4-(benzyloxymethyl)-2,2-dimethyl-5-(phenyl-sulfonimidoylmethyl)-1,3-dioxolane **S-(*S*)-104**.

The large number of artefacts and the relatively weak NOE connectivities in the NOESY spectrum of **S-(*R*)-104** made interpretation difficult. However, a number of observations could still be identified using coupling constants, since an improved separation of proton signals was seen with the ^{1}H NMR spectrum of **S-(*R*)-104**. A coupling constant of ^{3}J = 8.7 Hz was calculated for one of the SCH_2 protons at δ 3.30 which indicates an axial/axial relationship. A coupling constant of ^{3}J = 2.9 Hz was calculated between the other SCH proton at δ 3.45 and 5-H, which is within the range

of an axial/equatorial coupling. A vicinal coupling of ^3J ~ 7.7 Hz between 4-H and 5-H supports the *trans* configuration of these protons with respect to the five-membered dioxolane ring.

In an attempt to study further the observed coupling constant values and NOE connectivities of both diastereoisomers of **104** in chloroform solution, an assumption was made to an intramolecular hydrogen-bonding interaction between the imino NH and the oxygen atom in the five-membered dioxolane ring in **104**, resulting in a five-/six-membered fused-ring system (Figure 30).

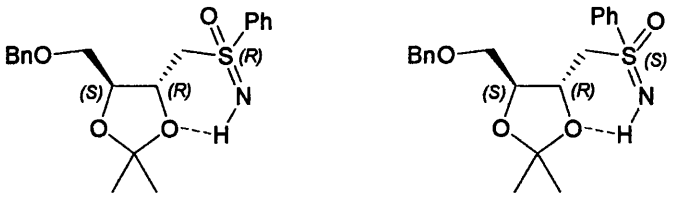

Figure 30. Postulated intramolecular hydrogen-bonding structures of **104** in chloroform. (Hydrogen bonds – blue)

MM2 energy-minimised calculations were also carried out to study the probable structures of these intramolecular hydrogen-bonding systems (*vide infra*, Figure 31). For the (*R*)-isomer, severe ring strain was observed, with the twist-boat six-membered ring deforming the five-membered dioxolane ring; the resulting dihedral angle between 4-H and 5-H was calculated to be 93° (the corresponding dihedral angle in the non-hydrogen-bonded **S-(*R*)-104** = 168°). In the hydrogen-bonded **S-(*S*)-104**, the five-membered dioxolane ring adopted a half-chair conformation and the six-membered ring adopted a twist-boat conformation, with the dihedral angle between 4-H and 5-H = 141° (the corresponding dihedral angle in the non-hydrogen-bonded **S-(*S*)-104** = 169°). Three-bond couplings of ^3J ~ 8 Hz and ^3J ~ 7.7 Hz were calculated between 4-H and 5-H of **S-(*R*)-** and **S-(*S*)-104**, respectively. For the latter, the coupling constant value is consistent with the dihedral angle of 141°, whereas for the (*R*)-isomer, ^3J ~ 8 Hz is inconsistent with the dihedral angle of 93°. With this information and the severe ring strain observed by MM2 calculations, it was concluded that the intramolecular hydrogen-bonding interaction is more likely to exist in the chloroform solution state of **S-(*S*)-104** than that of the (*R*)-isomer.

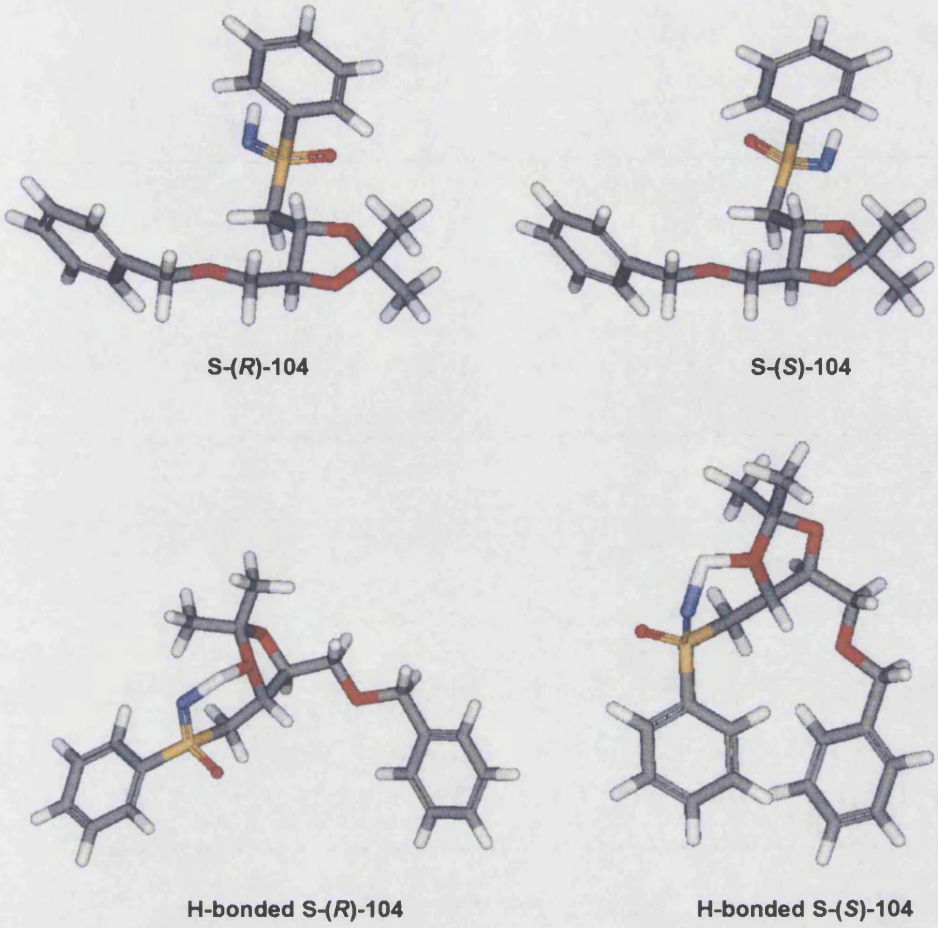

Figure 31. MM2-energy minimised models of the sulfoximines **S-(*R*)-104** and **S-(*S*)-104** with the corresponding intramolecular hydrogen-bonding structures. Dihedral angles (4-H)-(4-C)-(5-C)-(5-H) = 168° and 169° were calculated for **S-(*R*)-104** and **S-(*S*)-104**, respectively. In the hydrogen-bonded system in the (*R*)-isomer, the corresponding dihedral angle was found to be 93°, whereas in the (*S*)-isomer, the corresponding dihedral angle was 141°. The red colour refers to oxygen, the yellow refers to sulfur, the blue refers to nitrogen and the grey refers to the carbon atom.

In addition, cyclohexane undergoes ring-flips to avoid 1,3-diaxial interactions and the preferred conformation of the bulky substituents is equatorial. Therefore, the six-membered ring in the five-/six-membered fused-ring system may also undergo ring-flip and two possible conformations are available for the intramolecular hydrogen-bonding system in **104** (*vide infra*, Scheme 44). Conformer B is the lower-energy conformation since the $BnOCH_2$, methyl group and 5-H are all pseudo-equatorial, whereas in A, these substituents are axial.

Surprisingly, the coupling constant values and the NOE connectivities described above suggest that the conformation in both isomers in chloroform solution is likely to be A. Weak cross-peaks (*i.e.* far apart in space) associated with vicinal coupling constants of

^3J ~ 8-9 Hz, together with the stronger cross-peaks (*i.e.* close in space) associated with vicinal coupling constant of ^3J of 3 Hz (the latter was only observed in **S-(*R*)-104** due to signal overlap in the (*S*)-isomer), were noted between 5-H and the SCH_2 protons in both the (*S*)- and (*R*)-isomers. In B, the conformations of the two substituents are axial/equatorial and equatorial/equatorial (see highlighted protons in Scheme 44). In the higher-energy and disfavoured conformation A, they are axial/equatorial and axial/axial. The coupling constant of ^3J ~ 8-9 Hz is therefore too large to be an axial/equatorial or equatorial/equatorial coupling, and the only possible conformer of this intramolecular hydrogen-bonding system is A.

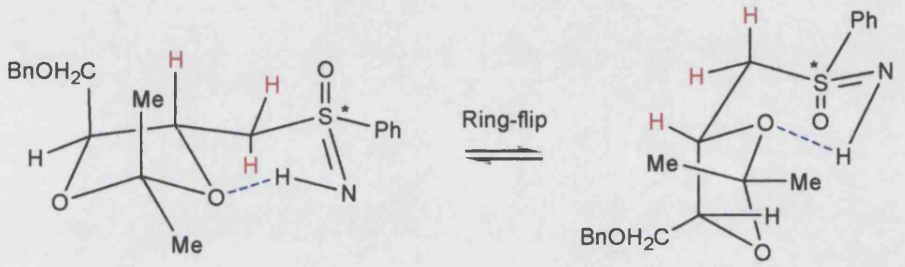

A

axial/equatorial ^3J ~ 3-5 Hz

axial/axial ^3J ~ 8-12 Hz

B

axial/equatorial ^3J ~ 3-5 Hz

equatorial/equatorial ^3J ~ 2-3 Hz

Scheme 44. Conformational change in the fused-ring intramolecular hydrogen-bonding system of **104**. (Hydrogen bonds – blue; 5-H and SCH_2 protons – red)

Since the less polar **S-(*R*)-104** was afforded as an oil, X-ray crystallography determination was not possible. However, the more polar **S-(*S*)-104** was obtained as a solid. Recrystallisation (in EtOH/hexane) and subsequent X-ray analysis of the crystalline **S-(*S*)-104** provided information on the solid-state conformation with probable intermolecular hydrogen-bonding interactions (*vide infra*, Figure 32). It is noteworthy that the comparison of dihedral angles with the corresponding coupling constants from the ^{1}H NMR spectrum might not be consistent since coupling constants were derived from the proposed intramolecular hydrogen-bond conformation in solution in chloroform. Therefore, the conformations in the liquid and solid state might be different. Furthermore, only one set of coupling constants of both SCH_2 and $BnOCH_2$ could be calculated due to the overlapped signals of the protons (the multiplet at δ 3.50 to δ 3.54). A vicinal coupling constant of ^3J ~ 7.9 Hz between 4-H and 5-H corresponds with a dihedral angle (C8-H)-(C8-C)-(C9-C)-(C9-H) = 139°. A three-bond coupling constant of ^3J = 5.3 Hz was calculated between 4-H and one of the $BnOCH_2$ protons at δ 3.64, which is inconsistent to either the dihedral angle (C9-H)-(C9-C)-(C10-C)-(C10-H_A) of

167° or the dihedral angle (C9-H)-(C9-C)-(C10-C)-(C10-H_B) of 74°. A coupling constant of J = 8.2 Hz was calculated for the SCH proton at δ 3.39, which is consistent with the dihedral angle (C8-H)-(C8-C)-(C7-C)-(C7-H_B) of 179°. However, a coupling constant of ^3J = 3.4 Hz calculated between 5-H and one of the SCH protons at δ 3.50 to δ 3.54 is inconsistent to the dihedral angles (C8-H)-(C8-C)-(C7-C)-(C7-H_A) of 65° or (C8-H)-(C8-C)-(C7-C)-(C7-H_B) of 179°. These findings show that the solution and solid conformations are different.

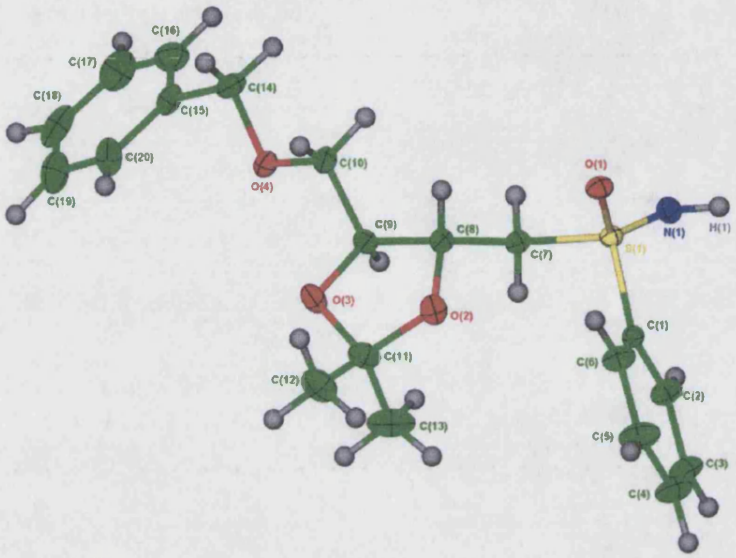

Figure 32. X-ray crystal structure of 4*S*,5*R*,S(*S*)-4-(benzyloxymethyl)-2,2-dimethyl-5-(phenylsulfonimidoyl-lmethyl)-1,3-dioxolane **S-(*S*)-104**, with crystallographic numbering.

Further examination of the dihedral angles was undertaken to explore the details of local conformations in the crystal and their values are summarised in Table 9.

Crystallographic numbering	Dihedral angle (°)
C(14)-O(4)-C(10)-C(9)	173
C(10)-O(4)-C(14)-C(15)	164
O(4)-C(10)-C(9)-C(8)	170
O(4)-C(10)-C(9)-O(3)	75
S(1)-C(7)-C(8)-C(9)	177
S(1)-C(7)-C(8)-O(2)	66
C(6)-C(1)-S(1)-O(1)	14
C(6)-C(1)-S(1)-N(1)	148
C(1)-S(1)-C(7)-C(8)	82

Table 9. Data for dihedral angles obtained from X-ray crystal structure of **S-(*S*)-104**.

As expected, the bulky groups are *anti*-periplanar with respect to the O(4)-C(10) bond with dihedral angles C(14)-O(4)-C(10)-C(9) = 173° and C(10)-O(4)-C(14)-C(15) = 164°. The BnO substituent is *anti*-periplanar with respect to the C(9)-C(8) bond, with dihedral angle O(4)-C(10)-C(9)-C(8) = 170°, but is gauche to O(3) with dihedral angle O(4)-C(10)-C(9)-O(3) = 75°. The bulky sulfoximine-phenyl group is *anti*-periplanar with respect to the C(9)-C(8) bond with dihedral angle S(1)-C(7)-C(8)-C(9) = 177°, but is gauche to O(2) with dihedral angle S(1)-C(7)-C(8)-O(2) = 66°. Interestingly, the sulfoximine oxygen atom is *syn*-periplanar to C(6) with dihedral angle C(6)-C(1)-S(1)-O(1) = 14°. The sulfoximine nitrogen atom is anticlinal to C(6) with dihedral angle C(6)-C(1)-S(1)-N(1) = 148°. The bulky sulfoximine-phenyl group and the dioxolane group are gauche with respect to the S(1)-C(7) bond with dihedral angle C(1)-S(1)-C(7)-C(8) = 82°.

The sulfoximine S=N bond length was found to be 1.517 Å, with a S=O bond length of 1.459 Å. Bond angle was also established and these values are presented in Figure 33 (*vide infra*). They are consistent with those reported by Kumar *et al.*,[188] who studied a range of theoretical isomeric sulfoximines with a formula of $H_2S(=O)=NR$, where R = H, Cl, F, Me. The group reported a calculated bond angle O=S=N = 127.2°. In the sulfoximine of **S-(*S*)-104**, the bond angle O=S=N was calculated to be 121.8°, which is consistent with the literature source.

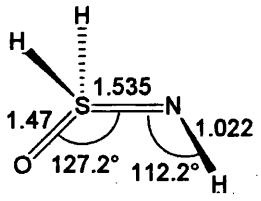

Kumar *et al.*[188] theoretical sulfoximine

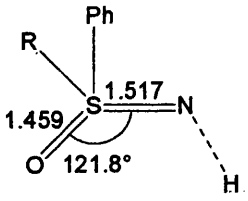

Sulfoximine moiety in **S-(*S*)-104**

Figure 33. Bond angles (°) and bond lengths (Å) of a theoretical sulfoximine group studied by Kumar *et al.* and the measured data of the sulfoximine group in **S-(*S*)-104**.[188]

With the absolute configuration established, acid-hydrolysis of **S-(*R*)-104** with HCl gave the corresponding diol **S-(*R*)-105** in quantitative yield (*vide supra*, Scheme 43). Removal of the acetonide CMe_2 group revealed the two hydroxy groups. The characterisation of **S-(*R*)-105** was supported by the strong OH absorption (3305 cm^{-1}) in the IR spectrum, in addition to the sulfoximine NH absorption observed previously. The ^1H NMR spectrum showed the absence of the CMe_2 acetonide protons together with signals for OH (a broad singlet at δ 2.68), SCH_2 (two double doublets at δ 3.13 and

δ 3.45), $BnOCH_2$ (a multiplet at δ 3.59 to δ 3.63), 3-H (a multiplet at δ 3.69), $PhCH_2$ and 4-H (an overlapped multiplet at δ 4.54 to δ 4.56) and ten aromatic protons. The multiplicity observed in the spectrum may be reasoned by possible intramolecular hydrogen bonding between the two hydroxy groups and the protons on the open chain.

3.2.3 Synthetic approaches to the 3-bromophenyl sulfoximine intermediate

The proposed ring-closure strategy to synthesise the ribosyl moiety in target **39** using a Mitsunobu reaction was based on the knowledge of the reaction giving rise to inversion of configuration in secondary alcohols. However, to date, there are no literature methods describing a Mitsunobu condensation reaction between a sulfoximine NH and a secondary alcohol. A method described by Garofala *et al.*,[189] *i.e.* the use of TBP and ADDP in an interesting intramolecular Mitsunobu cyclisation of a disubstituted pyrrole, was followed but the reaction only led to recovery of the starting diol **S-(*R*)-105**.

The group reasoned the use of a Mitsunobu condensation with the acidic pyrrole NH due to an electron-withdrawing aldehyde *ortho*-substituent and that the TBP/ADDP system is compatible even with weakly acidic protons (p*K*a ~ 13).[190] Therefore, a speculative explanation for the failure of performing an intramolecular Mitsunobu cyclisation in **S-(*R*)-105** is that the sulfoximine NH is not sufficiently acidic to be a good Mitsunobu reagent.

It was decided that the same synthetic sequences were to be applied on the target starting compound, 3-bromothiophenol **87**, to give the corresponding meta-subsituted vicinal diol **92** (*vide infra*, Scheme 45). The presence of the bromine substituent might influence the acidity of the sulfoximine NH and subsequent Mitsunobu reaction outcome.

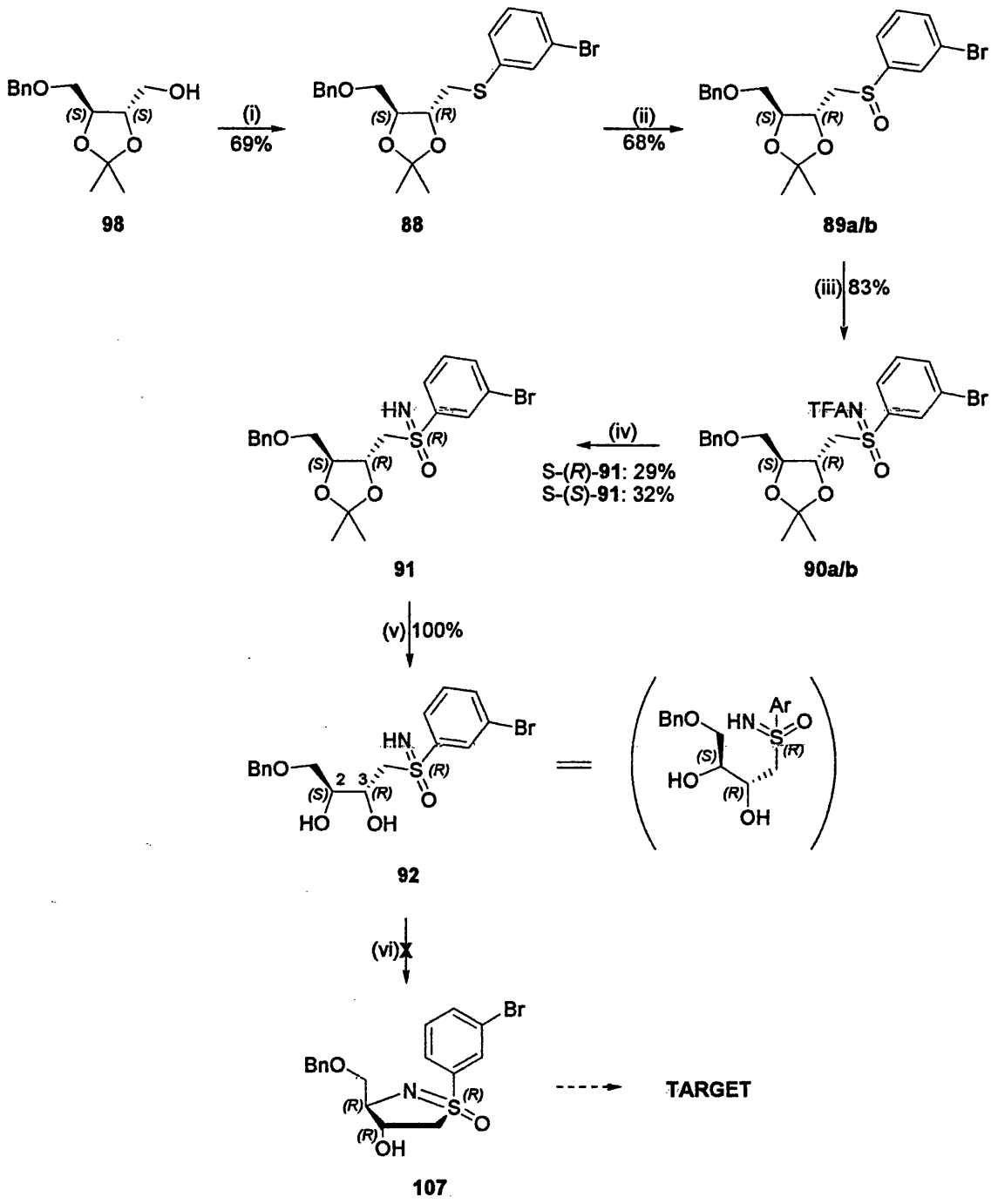

Scheme 45. Synthetic approaches to intermediate **107**. *Reagents and conditions: (i) TBP, ADDP, 3-bromothiophenol **87**, THF, sonication; (ii) mCPBA, DCM, –78°C; (iii) CF_3CONH_2, MgO, $Rh_2(OAc)_4$, $PhI(OAc)_2$, DCM; (iv) NH_3, MeOH; (v) HCl, MeOH; (vi) TBP, ADDP, THF, sonication, RT to 45°C.*

Since the optimum Mitsunobu condensation reaction conditions have already been investigated with the model thiophenol **100**, dioxolane compound **98** was treated with 3-bromothiophenol **87** using the two most efficient systems: TPP/DIAD and TBP/ADDP in THF to give sulfide **88** in 49% and 69% yields, respectively. Subsequent *m*CPBA oxidation gave the corresponding diastereomeric sulfoxides **89a/b** (Scheme 45).

Apart from the apparent changes in the Br-Ph aromatic protons region, the ^{1}H NMR and ^{1}H-^{1}H COSY spectra of **89a/b** were similar to that of the non-substituted sulfoxides **102a/b**. Two separate sets of signals were observed in the ^{1}H NMR spectrum, which pointed to the existence of two diastereomeric sulfoxides. Similar to the ^{1}H NMR analysis of **102a/b**, the key region of the spectrum of **89a/b** lies in the range of δ 2.8 to δ 4.6 and analysis was conducted in a 600 MHz spectrometer to improve resolution and separation of signals. Together with a ^{1}H-^{1}H COSY spectrum, the two sets of diastereomeric protons were assigned (*vide infra*, Figure 34). Furthermore, a diastereomeric ratio of 1:1 was calculated (together with the TLC results, showing two visible spots in identical sizes), indicating that the 3-bromo group did not influence diastereoselectivity.

The two sets of CMe_2 protons gave two singlets each for one and a half protons at δ 1.36 and δ 1.41, with another singlet signal for three protons at δ 1.45. In the ^{1}H spectrum of the starting sulfide **88**, the signals of the CMe_2 protons were shown as two singlets at δ 1.39 and δ 1.43, each for one and a half protons. Therefore, there was no apparent upfield or downfield shift between the two diastereomeric sulfoxides **89a/b** and between the starting material and the sulfoxide products. Expectedly, the presence of the 3-bromo group did not influence the chemical shifts of the CMe_2 protons.

In the ^{1}H NMR spectrum of starting sulfide **88**, the multiplet signal of the SCH_2 protons was more upfield (δ 3.16 to δ 3.19) than the signals for the $BnOCH_2$ protons (δ 3.59 to δ 3.66). This effect, which is similar to that of the non-substituted derivatives, was also observed with sulfoxides **89a/b**. Signals for the SCH_2 protons of both isomers of **89** appeared in the region of δ 2.82 to δ 3.20, revealing that the anticipated downfield effect on the SCH_2 protons of the electronegative sulfoxide oxygen was insignificant.

The ^{1}H-^{1}H COSY spectrum showed that the SCH_2 protons of isomer A gave a pair of double doublets at δ 2.83 and δ 3.06, each for half a proton, whereas the two double doublet signals for the SCH_2 protons of isomer B, each for half a proton, were located at δ 3.04 and δ 3.18. Subsequent assignment of 5-H for both isomers was possible by the cross-peak connections with δ 4.39 and δ 4.00, corresponding to the 5-H for isomer A and B, respectively.

A

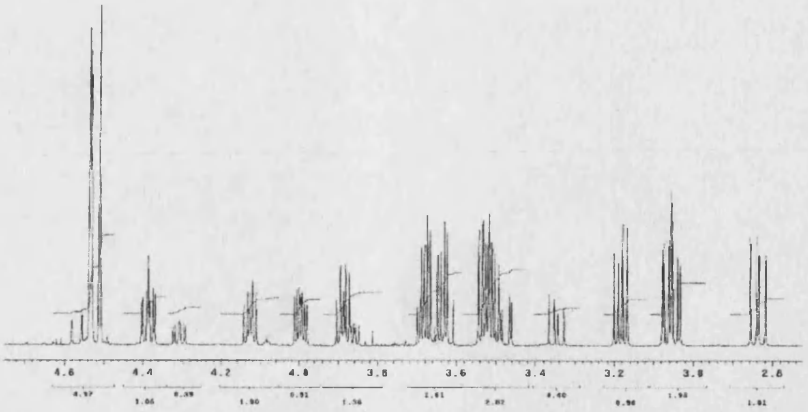

B

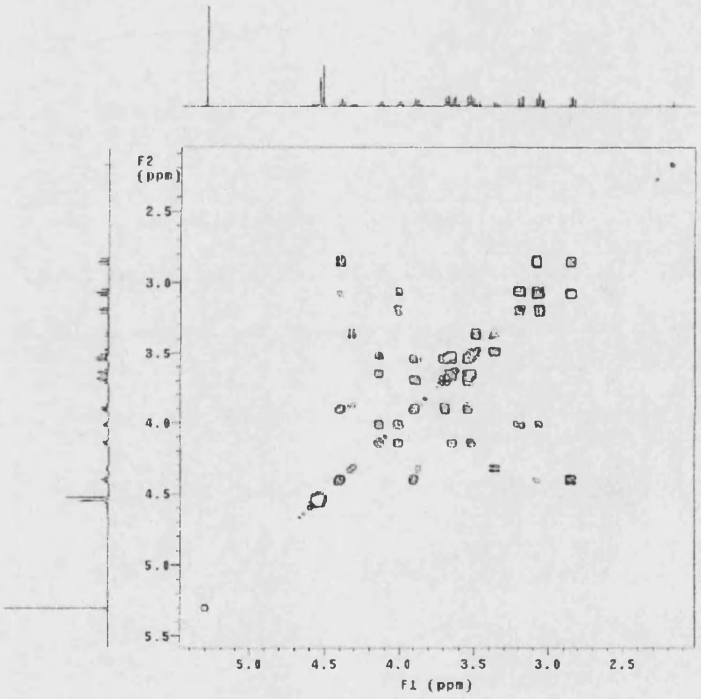

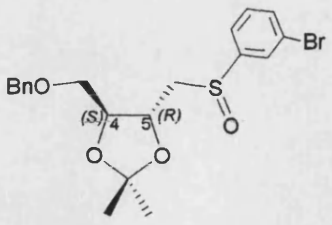

Figure 34. ^{1}H NMR spectra of diastereomeric **89a/b**. (A) is the 1-D ^{1}H NMR spectrum of the key region δ 2.8 to δ 4.6; (B) is the ^{1}H-^{1}H COSY spectrum, showing the cross-peak connections in each diastereoisomer.

The $BnOCH_2$ proton of isomer A gave a double doublet signal for half a proton at δ 3.68, with the other half-proton signal coincided with that of the $BnOCH_2$ half-proton signal of isomer B, resulting in a multiplet at δ 3.46 to δ 3.64. A cross-peak connection between the $BnOCH_2$ protons and 4-H at δ 3.91 was also observed on the ^1H-^1H COSY spectrum. A double doublet signal for half a proton at δ 3.62 belonged to the $BnOCH_2$ proton of isomer B, with the signal of its 4-H located at δ 4.13.

The $PhCH_2$ protons in the starting sulfide **88** gave a singlet at δ 4.57. In the diastereomeric sulfoxides **89a/b**, these proton signals gave a singlet at δ 4.51 for one proton, and at δ 4.52 and δ 4.55 as two doublets each for half a proton. Thus the $PhCH_2$ protons are magnetically inequivalent in **88** and one of the isomeric **89** (as expected for diastereotropic protons), but are accidentally equivalent in the other isomer of **89**.

In isomer A, the 4-H signal (δ 3.89) is more upfield to that of 5-H (δ 4.39), whereas, in isomer B, the 4-H signal (δ 4.13) is slightly more downfield than that of 5-H (δ 4.00). Thus, 4-H is more upfield in isomer A than isomer B, whereas 5-H is significantly more downfield in isomer A than isomer B. The origins of the differences in chemical shifts for both 4-H and 5-H of the diastereomeric sulfoxides **89a/b** were investigated by MM2 energy-minimised calculations on the S-(*R*)- and S-(*S*)-isomers but no apparent reasons could be concluded to explain such effects (Figure 35).

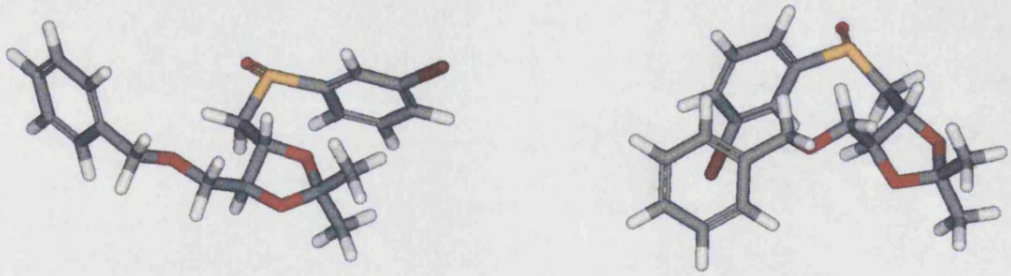

S-(*R*)-89 **S-(*S*)-89**

Figure 35. MM2-energy minimised models of **S-(*R*)-89** and **S-(*S*)-89**. The red colour refers to oxygen, the yellow refers to sulfur, the maroon refers to bromine and the grey refers to the carbon atom.

Subsequently, **89a/b** were converted to the diastereomeric N-TFA sulfoximines **90a/b** *via* Rh(II)-catalysed imination using $PhI(OAc)_2$, $Rh_2(OAc)_4$, MgO and CF_3CONH_2 in DCM (*vide supra*, Scheme 45). TLC of **90a/b** showed two visible spots in identical sizes. Unfortunately, attempts to separate the diastereoisomers chromatographically led to co-elution. Severe signal overlap of the ^1H spectrum made determination of the

diastereomeric ratio difficult. As observed with the non-substituted N-TFA sulfoximines **103a/b**, the diastereomeric ratio of **90a/b** could not be determined by comparing the integrals of the singlet signals normally seen for the $PhCH_2$ protons, since the signals appeared to have coincided with each other, giving one singlet. Therefore, the diastereomeric ratio was determined by a ^{19}F NMR spectrum in which the two singlets for the CF_3 fluorines at δ –76.0 and δ –75.9 were seen, in a 1:1 integral ratio. This finding was different to that of **103a/b,** where asymmetric induction in the imination step slightly disrupted diastereoselectivity and changed the diastereomeric ratio from 1:1 (at the oxidation step) to 3:2. The presence of the 3-bromo substituent might play a role in determining the yields of the individual stereoisomers.

Due to the extensive signal overlap in the ^1H NMR spectrum, interpretation of coupling constants was extremely difficult. As seen in the spectrum of the non-substituted N-TFA sulfoximines **103a/b**, the signals for the SCH_2 protons in **90a/b** appeared more downfield than the $BnOCH_2$ protons. Further proton and carbon assignments were conducted by the different spectroscopic data from the ^{13}C NMR, 135-DEPT and ^1H-^{13}C COSY (HMQC) spectra. Cross-peaks between two SCH_2 carbons at δ 58.4 and δ 59.4 and the various SCH_2 proton signals at δ 3.70 to δ 3.75, δ 3.76, δ 4.05 and δ 4.09, indicate that the signals for the SCH_2 protons in **103a/b** were shifted markedly downfield compared to the starting sulfoxides **102a/b** where these protons resonated at δ 3.04 to δ 3.18. Therefore, the presence of the TFA group caused a marked downfield effect in the region of the SCH_2 protons, with the environment for the $BnOCH_2$ protons being relatively unaffected and thus the relative locations of these two groups of protons were opposite to those in the starting materials **102a/b**.

Removal of the TFA group afforded the free NH sulfoximine **91** as a mixture of diastereoisomers, which were separated chromatographically (*vide supra*, Scheme 45). The NMR spectra of both the S-(*R*)- and S-(*S*)-isomers of **91** were similar, with similar chemical shifts for the CMe_2, SCH_2, $BnOCH_2$, 4-H, 5-H and $PhCH_2$ protons. There was no apparent upfield or downfield shifts between the diastereomeric sulfoximines.

Interestingly, removal of the TFA group which, in the ^1H spectra of the non-substituted S-(*R*)- and S-(*S*)-sulfoximines **104**, led to a marked upfield shift of the double doublet signals of the SCH_2 protons, did not cause this effect in the 3-bromophenyl sulfoximines **S-(*R*)-** and **S-(*S*)-91**. In the starting N-TFA compounds **90a/b**, these protons resonated at δ 3.34 to δ 3.54. In **S-(*R*)-91**, the signals for SCH_2 appeared at δ 3.34 and δ 3.46, whereas in the (*S*)-isomer, they appeared at δ 3.38 and δ 3.54.

Furthermore, the upfield effect observed for the CMe_2 protons between the non-substituted N-TFA sulfoximines **103a/b** and the corresponding NH sulfoximines **S-(*R*)-** and **S-(*S*)-104** was also negligible in the 3-bromo derivatives. In the starting N-TFA sulfoximines **90a/b**, these geminal methyl groups gave four singlet signals, each for one and a half protons, at a range of δ 1.15 to δ 1.28. The signals of the CMe_2 protons of **S-(*R*)-91** appeared as two singlets at δ 1.22 and δ 1.32, each for three protons. In the S-(*S*)-isomer, these protons gave two singlets at δ 1.20 and δ 1.30.

Two-dimensional ^1H NMR analyses provided useful information on the assignment of the spectra of the diastereomeric sulfoximines **S-(*R*)- and S-(*S*)-91**. The COSY spectrum for **S-(*R*)-91** gave the expected coupling relationships, with a cross-peak between the SCH_2 protons and the double-double doublet at δ 4.31, indicating that the latter signal is due to 5-H. A cross-peak between the $BnOCH_2$ protons and the double-double doublet at δ 3.86 was also noted and it was concluded that this signal is due to 4-H. The NOESY spectrum of **S-(*R*)-91** showed the expected connectivities between the $PhCH_2$ protons and the $BnOCH_2$ protons (*vide infra*, Figure 36a/b). A cross-peak between 4-H and the singlet signal of the CMe protons at δ 1.22 indicates that the latter signal was due to the geminal methyl group *trans* to $BnOCH_2$. Similarly, a cross-peak between 5-H and the singlet at δ 1.32 indicates that the latter signal is due to the methyl group *cis* to $BnOCH_2$. Weak connectivities were seen between the two double doublet signals for the SCH_2 protons at δ 3.34 and δ 3.46 and 5-H. A stronger cross-peak noted between 5-H and one of the BnOCH protons at δ 3.53 confirms that 5-H and the $BnOCH_2$ protons are on the same face of the ring *i.e.* they are *cis* to each other. It is noteworthy that the cross-peak between 4-H and its *cis* partner, the SCH_2 protons, was found to be weaker compared to that between 4-H and the $BnOCH_2$. Nevertheless, a weak NOE connectivity between 4-H and 5-H suggests that the protons are on the opposite face of the ring and thus are *trans* to each other, and this finding is supported by a vicinal coupling constant of ^3J = 7.8 Hz between 4-H and 5-H.

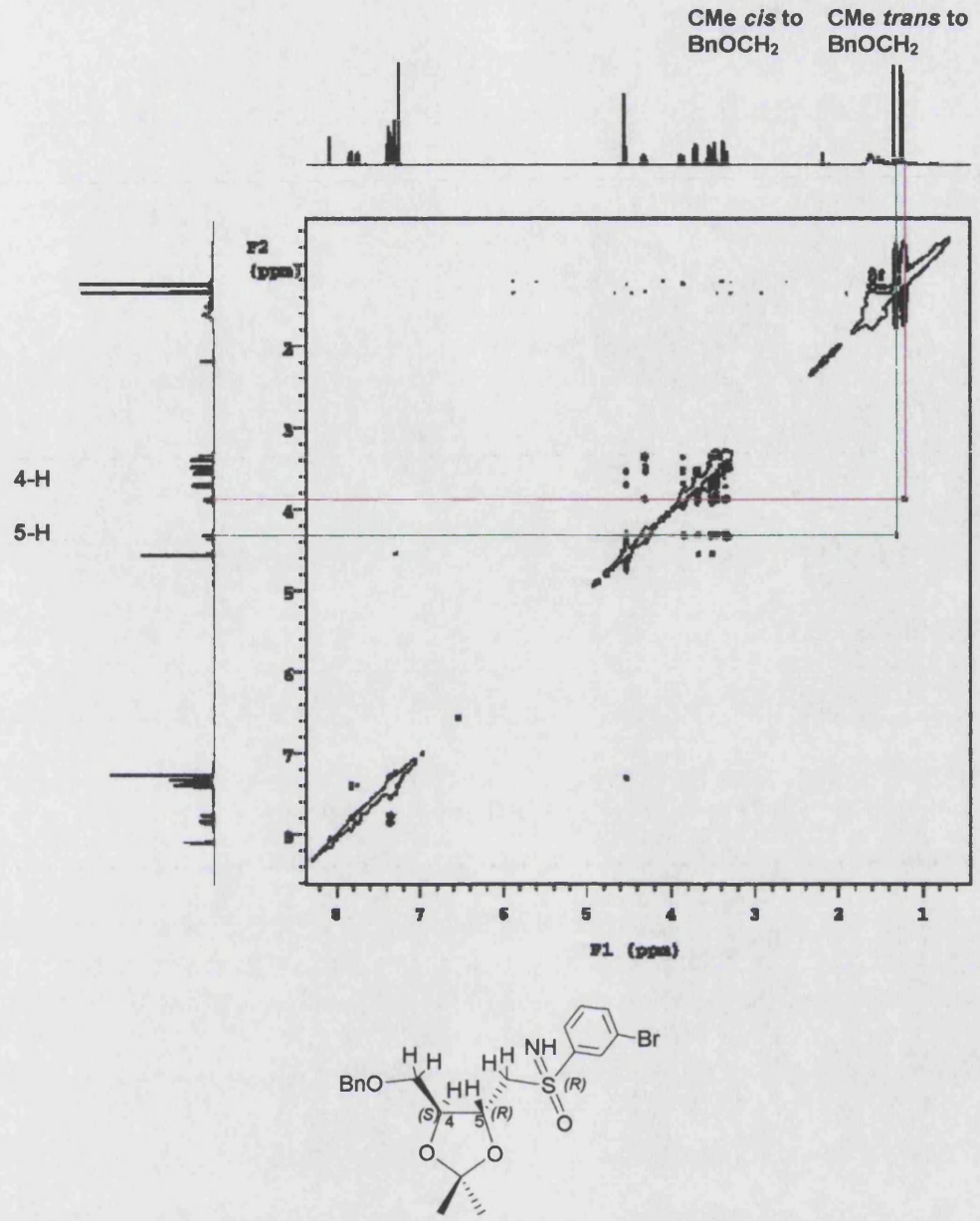

Figure 36a. ^{1}H-^{1}H NOESY spectrum of 4*S*,5*R*,S(*R*)-4-(benzyloxymethyl)-2,2-dimethyl-5-(3-bromophenyl-sulfonimidoylmethyl)-1,3-dioxolane **S-(*R*)-91**.

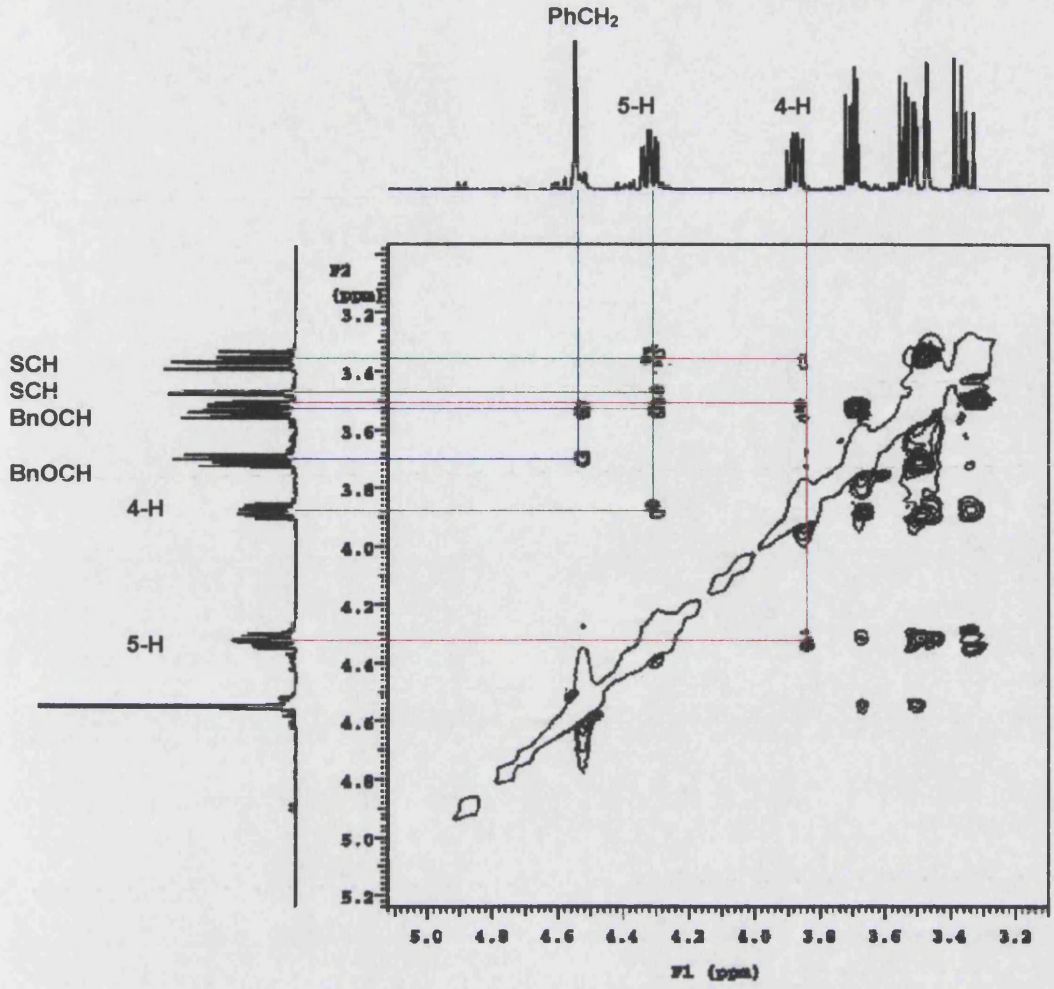

Figure 36b. ^{1}H-^{1}H NOESY spectrum of 4*S*,5*R*,S(*R*)-4-(benzyloxymethyl)-2,2-dimethyl-5-(3-bromophenyl-sulfonimidoylmethyl)-1,3-dioxolane **S-(*R*)-91**.

The COSY spectrum of **S-(*S*)-91** showed the anticipated coupling relationships. Cross-peaks were observed between the two double doublet signals for the SCH_2 protons at δ 3.38 and δ 3.52 and the double-double doublet at δ 4.33, indicating that the latter signal is due to 5-H. Connectivities were also seen between the pair of double doublets for the $BnOCH_2$ protons at δ 3.52 and 3.66 and the double-double doublet at δ 3.89, hence the latter signal is due to 4-H. This was further supported by cross-peaks between 4-H and 5-H.

The NOESY spectrum contains the expected through-space connectivities between the singlet signal for the $PhCH_2$ protons at δ 4.53 and the two double doublets for the $BnOCH_2$ protons (*vide infra*, Figure 37). A cross-peak between 4-H and the singlet for the CMe_2 protons at δ 1.20 indicates that the latter refers to the geminal methyl group *trans* to $BnOCH_2$. Similarly, the cross-peak between 5-H and the remaining CMe singlet δ 1.31 indicates that this signal corresponds to the methyl group *cis* to $BnOCH_2$. Due to

overlapped cross-peaks, interpretation of the relative configuration between the two pairs of *cis*-partners, 4-H and the SCH_2 protons and 5-H and the $BnOCH_2$ protons, was difficult. A weak NOE connectivity between 4-H and 5-H suggests that the protons are on the opposite face of the ring and thus are *trans* to each other, and this finding is supported by a vicinal coupling constant of ^3J = 8.0 between 4-H and 5-H.

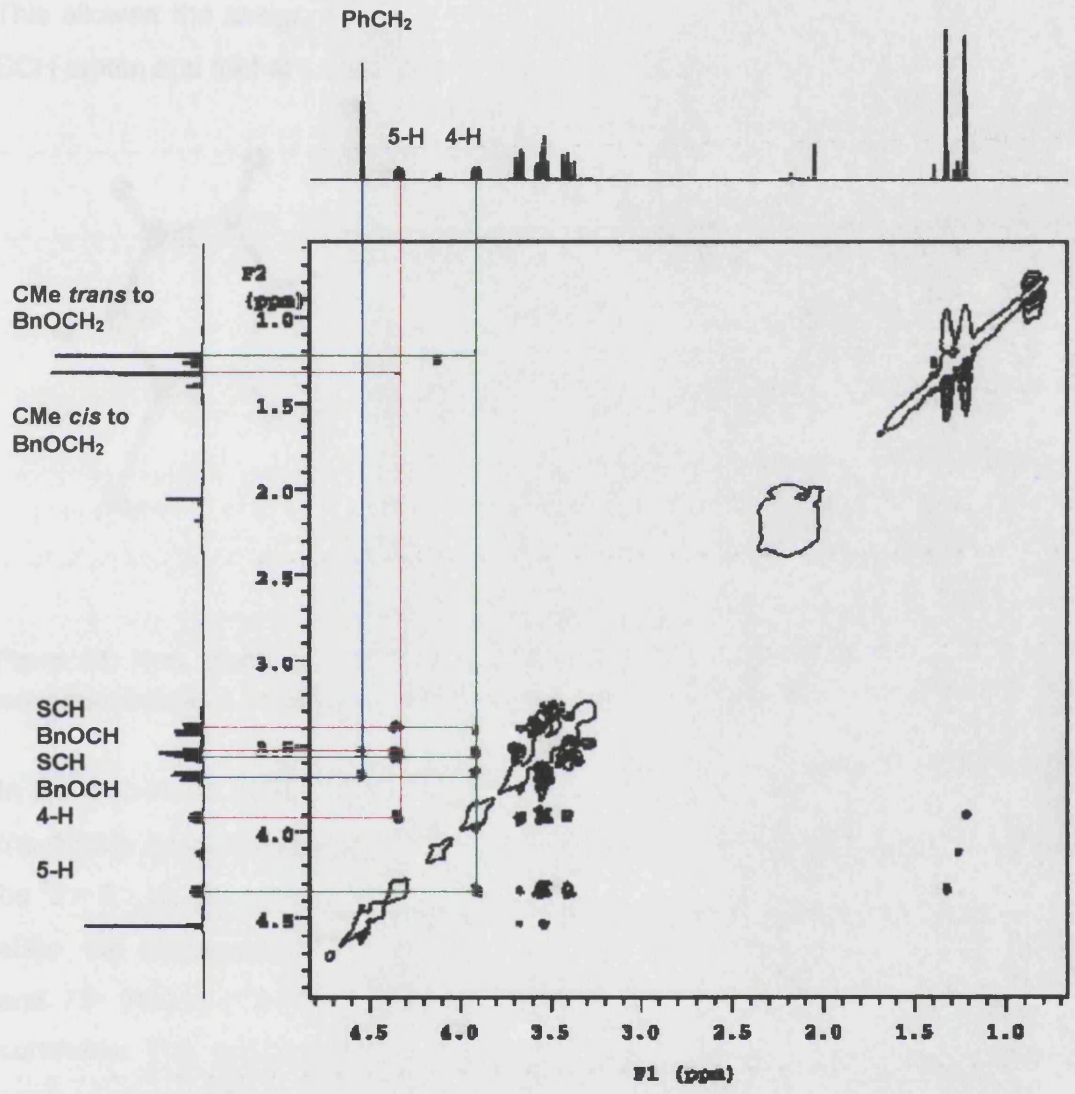

Figure 37. ^{1}H-^{1}H NOESY spectrum of 4*S*,5*R*,S(*S*)-4-(benzyloxymethyl)-2,2-dimethyl-5-(3-bromophenyl-sulfonimidoylmethyl)-1,3-dioxolane **S-(*S*)-91**.

Crystals of **S-(*S*)-91** were grown in an EtOH/hexane system and the X-ray crystallography data provided conclusive information on the relative configurations (*vide infra*, Figure 38). Extensive separation of the proton signals in the ^{1}H NMR spectrum gave all the required coupling constant values, which could be compared with the corresponding dihedral angles calculated in the crystal structure. As mentioned

above, a vicinal coupling constant of ^3J = 8 Hz was measured between 4-H and 5-H. This corresponds to dihedral angle (C8-H)-(C8-C)-(C9-C)-(C9-H) of 147°. A coupling constant of ^3J ~ 8.6 Hz between the double doublet signal at δ 3.38 for one of the SCH_2 protons and 5-H corresponds to the dihedral angle (C8-H)-(C8-C)-(C7-C)-(C7-H_B) of 177°. Similarly, a ^3J value of ~ 3.0 Hz between the double doublet SCH proton signal at δ 3.54 and 5-H corresponds to the dihedral angle (C8-H)-(C8-C)-(C7-C)-(C7-H_A) of 67°. This allowed the assignment of the proton signal at δ 3.38 as arising from the axial SCH proton and that at δ 3.54 from the equatorial SCH.

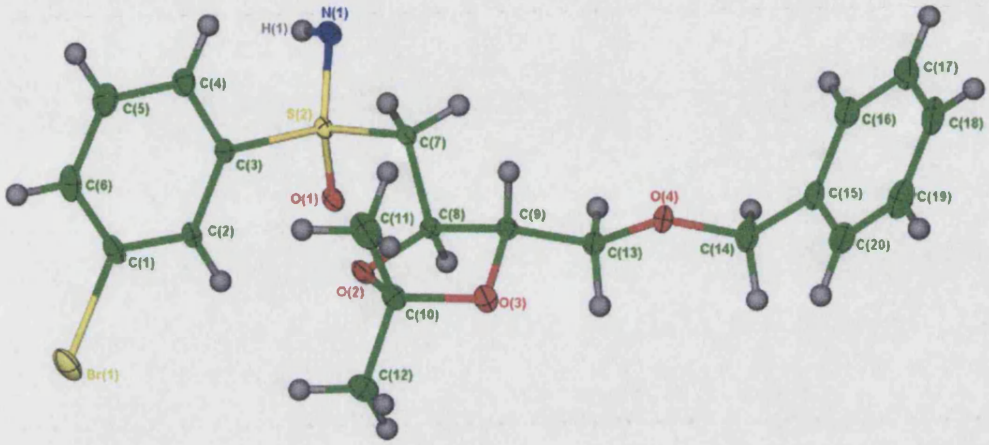

Figure 38. X-ray crystal structure of 4*S*,5*R*,S-(*S*)-4-(benzyloxymethyl)-2,2-dimethyl-5-(3-bromophenyl-sulfonimidoylmethyl)-1,3-dioxolane **S-(*S*)-91**, with crystallographic numbering.

In the chloroform ($CDCl_3$) solution of **S-(*S*)-91**, two vicinal coupling constants between the double doublet BnOCH proton signals at δ 3.52 and δ 3.66 and 4-H were found to be ^3J = 5.1 Hz (for the signal at δ 3.66) and 6.3 Hz (for the signal at δ 3.52). In the solid state, the corresponding dihedral angles are 161° [(C9-H)-(C9-C)-(C13-C)-(C13-H_A)] and 79° [(C9-H)-(C9-C)-(C13-C)-(C13-H_B)], which are inconsistent with the coupling constants. This suggests that, similar to the observations noted with **S-(*S*)-104**, the conformations of **S-(*S*)-91** in the solid state and liquid state are different.

Further examination of the dihedral angles was undertaken to explore the details of local conformations in the crystal of **S-(*S*)-91** and compare to those in the crystal of the phenyl sulfoximine **S-(*S*)-104**. These are summarised in Table 10 (*vide infra*).

Crystallographic numbering in S-(*S*)-104	Dihedral angle (°)	Crystallographic numbering in S-(*S*)-91	Dihedral angle (°)
C(14)-O(4)-C(10)-C(9)	173	C(14)-O(4)-C(13)-C(9)	177
C(10)-O(4)-C(14)-C(15)	164	C(13)-O(4)-C(14)-C(15)	171
O(4)-C(10)-C(9)-C(8)	170	O(4)-C(13)-C(9)-C(8)	164
O(4)-C(10)-C(9)-O(3)	75	O(4)-C(13)-C(9)-O(3)	81
S(1)-C(7)-C(8)-C(9)	177	S(2)-C(7)-C(8)-C(9)	176
S(1)-C(7)-C(8)-O(2)	66	S(2)-C(7)-C(8)-O(2)	67
C(6)-C(1)-S(1)-O(1)	14	C(2)-C(3)-S(2)-O(1)	20
C(6)-C(1)-S(1)-N(1)	148	C(2)-C(3)-S(2)-N(1)	155
C(1)-S(1)-C(7)-C(8)	82	C(3)-S(2)-C(7)-C(8)	76

Table 10. Comparative dihedral angles of the phenyl sulfoximine **S-(*S*)-104** and 3-bromophenyl derivative **S-(*S*)-91**.

As observed in the phenyl sulfoximine **S-(*S*)-104**, the bulky groups in 3-bromophenyl sulfoximine **S-(*S*)-91** are anti-periplanar with respect to the O(4)-C(13) bond with dihedral angles C(14)-O(4)-C(13)-C(9) = 177° and C(13)-O(4)-C(14)-C(15) = 171°. The BnO substituent is *anti*-periplanar with respect to the C(9)-C(8) bond, with dihedral angle O(4)-C(13)-C(9)-C(8) = 164°, but is gauche to O(3) with dihedral angle O(4)-C(13)-C(9)-O(3) = 81°. The sulfoximine-3-bromophenyl group is *anti*-periplanar with respect to the C(9)-C(8) bond with dihedral angle S(2)-C(7)-C(8)-C(9) = 176°, but is gauche to O(2) with dihedral angle S(2)-C(7)-C(8)-O(2) = 67°. The sulfoximine oxygen atom is *syn*-periplanar to C(2) with dihedral angle C(2)-C(3)-S(2)-O(1) = 20°. The imino nitrogen atom is anticlinal to C(2) with dihedral angle C(2)-C(3)-S(2)-N(1) = 155°. The bulky sulfoximine-phenyl group and the dioxolane group are gauche with respect to the S(2)-C(7) bond with dihedral angle C(3)-S(2)-C(7)-C(8) = 76°.

The sulfoximine S=N bond length in **S-(*S*)-91** was found to be 1.512 Å, with a S=O bond length of 1.46 Å. Bond angle was also established and these values are presented in Figure 39 (*vide infra*). The values are similar to those of the non-substituted sulfoximine **S-(*S*)-104**. In the sulfoximine of **S-(*S*)-104**, the bond angle O=S=N was calculated to be 121.8°, whereas in **S-(*S*)-91** the corresponding angle was 122.2°.

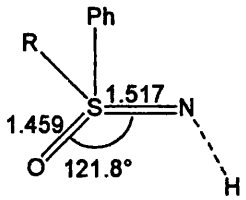

Sulfoximine moiety in **S-(*S*)-104**

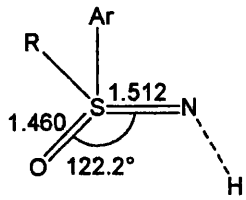

Sulfoximine moiety in **S-(*S*)-91**

Figure 39. Bond angles (°) and bond lengths (Å) of the two sulfoximines in **S-(*S*)-104** and **S-(*S*)-91**.

The next step of the synthesis was an acid-hydrolysis of the cyclic ketal in the S-(*R*)-sulfoximine **91**, which gave the corresponding diol **S-(*R*)-92** in quantitative yield (*vide supra*, Scheme 45). Its IR spectrum showed a strong absorption of OH (3425 cm^{-1}). The ^1H spectrum showed the lack of CMe_2 signals with the signals for OH (two broad singlets at δ 3.00), SCH_2 (a doublet at δ 3.13 and a double doublet at δ 3.45), $BnOCH_2$ (a multiplet at δ 3.59 to δ 3.64), 2-H (a multiplet at δ 3.70), 3-H (a broad singlet at δ 4.55), $PhCH_2$ (two doublets at δ 4.52 and δ 4.54) with nine aromatic protons. **S-(*R*)-92** was subjected to the same intramolecular Mitsunobu cyclisation conditions as those for the model reaction (TBP/ADDP). However, even at extended reaction times, TLC of the reaction mixture revealed only the presence of starting materials. Changes in temperature (RT to 45°C) did not alter this outcome.

Failure of this intramolecular Mitsunobu cyclisation could be explained by the following possibilities:

1. The acidity of a sulfoximine NH was insufficient to take part in the reaction.
2. Formation of a four-membered ring involving the sulfoximine NH and the 3-OH (*vide supra*, Scheme 45).
3. The presence of two adjacent secondary alcohols might cause a diversion of reaction progress and a possible intramolecular cyclisation between the two OH groups, resulting in an oxirane.

To test the possible involvement of the hydroxy groups, a series of experiments was devised to protect the 3-OH selectively while leaving the 2-OH free for cyclisation to occur with the NH of the sulfoximine.

The wide application of the 4-methoxybenzyl (PMB) group for hydroxy group protection has been highlighted by Johansson *et al.*[190] It is a useful protecting group since it is often removable in the presence of other protecting groups such as benzyl ethers (OBn), by oxidation with 2,3-dichloro-5,6-dicyanobenzoquinone (DDQ) or by acidolysis

with TFA. The PMB group is usually prepared, like the Bn group, by etherification using the corresponding benzyl halide and a base. However, alternative synthesis of PMB groups *via* a diastereoselective reductive ring-opening of 4-methoxybenzylidene acetals has attracted considerable interest because of the potential regioselectivity. The 1,3-dioxane of the benzylidene acetal is ring-opened by a reducing agent, giving a mixture of two diastereoisomers. The traditional Lewis-acidic reducing agents include $LiAlH_4$-$AlCl_3$ in THF, $NaCNBH_3$-Me_3SiCl in acetonitrile and diisobutylaluminium hydride (DIBAL-H) in DCM. Regioselectivity is influenced by the steric bulk of the substituents at the oxygen atoms and the approaching electrophiles. The reducing agents named above are all sterically demanding, causing an attack on the less sterically bulky oxygen, and the more hindered alcohol is protected with the PMB group.[190]

Riley *et al.* described the use of 4-methoxybenzylidene acetal as a protecting group for the hydroxy groups in ribofuranosides.[191] Upon protection of the 2'-OH and 3'-OH groups using 4-methoxybenzaldehyde dimethyl acetal, the resulting 4-methoxy-benzylidene derivative was afforded as a mixture of diastereoisomers. Cleavage of the acetal with DIBAL-H (best yielding reagent) proceeded with no regioselectivity and both the 2'- and 3'-*O*-(4-methoxybenzyl) ethers were obtained (1:1 ratio).

The investigation commenced with the N-TFA sulfoximines **90a/b** (*vide infra*, Scheme 46a) since nitrogen requires protection at this stage of the synthesis to avoid the PMB group being inserted at the nitrogen atom, with a view to separate the stereoisomers at the sulfur at an appropriate stage throughout the sequence. Therefore, **90a/b** would first be hydrolysed to the corresponding diol compounds **108a/b**. Treatment with acetal **110** would give the 2,3-*O*-(4-methoxy)benzylidene derivatives **111a/b**, and subsequent reductive cleavage of the acetal with DIBAL-H in DCM should give a mixture of 2- and 3-*O*-*p*-methoxybenzyl ethers **112a/b** and **113a/b**, respectively. Removal of the TFA group in **113a/b** and possible separation of diastereoisomers gives the resulting S-(*R*)-sulfoximine **114**, with the 2-OH free to participate in the subsequent step. Intra-molecular Mitsunobu cyclisation would give the cyclic product **115** and subsequent removal of protecting groups and FGI (cyanation and hydration of nitrile) should afford the target compound **39**.

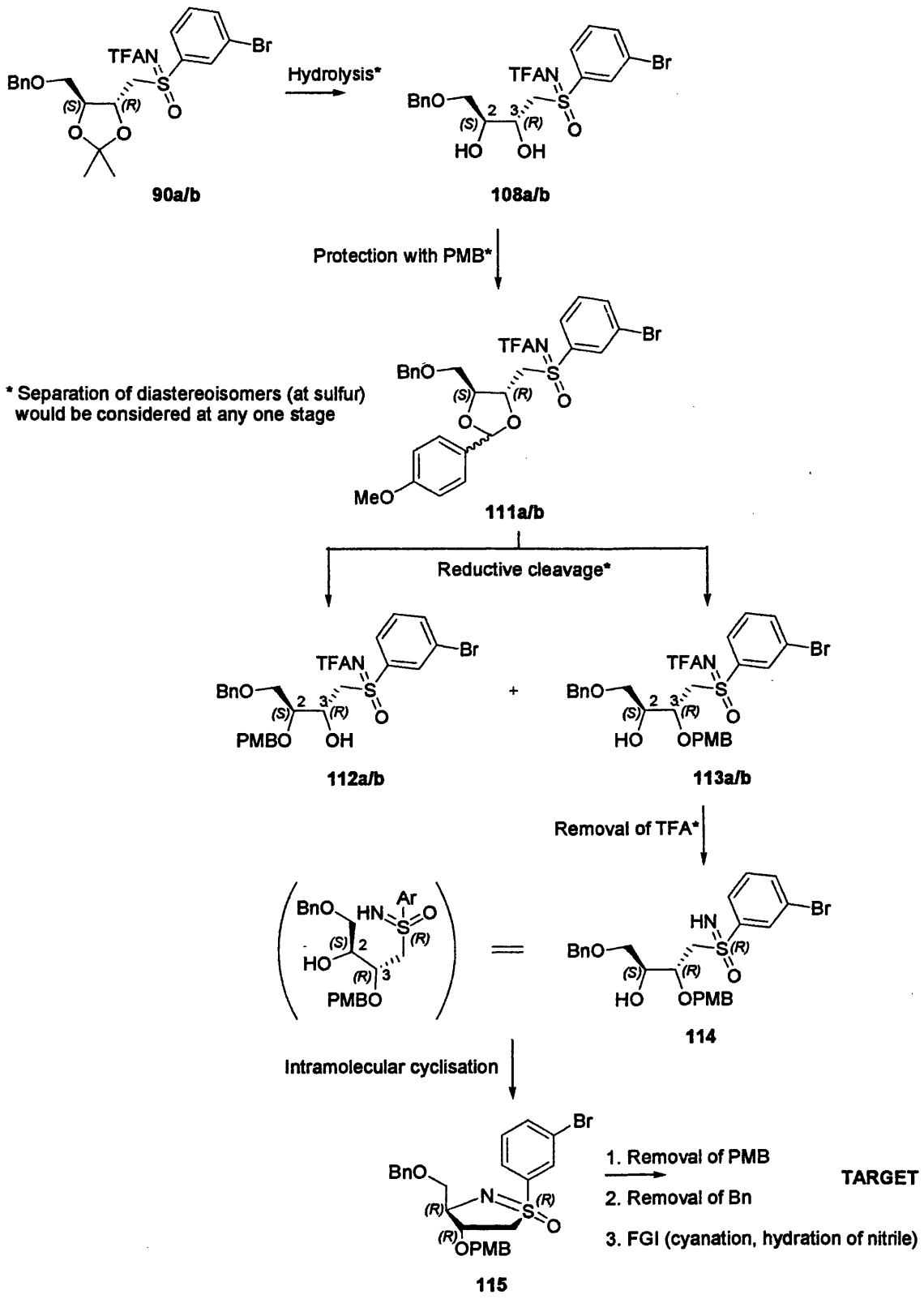

Scheme 46a. Synthetic approaches to target benzamide 2-deoxyriboside analogue **39** *via* PMB-protected dioxolane derivatives **111a/b**, allowing the required 2-OH free for cyclisation.

By protecting the 3-OH selectively, a number of issues could be addressed:

1. The possible influence of the extra hydroxy group in the Mitsunobu reaction in the formation of a four-membered ring;
2. If this extra hydroxy group affects the formation of the Mitsunobu phosphonium intermediate.

In addition, since there are no known literature reports on the use of a sulfoximine NH group in Mitsunobu reactions, the presence of only one free hydroxy group and one sulfoximine NH as two reactive possibilities in **114** would allow the investigation of the compatibility of a sulfoximine NH as a potential nucleophilic component in Mitsunobu reactions.

If sulfoximines are to be proven as poor nucleophilic Mitsunobu reagents, a different and comparatively longer route for the synthesis of **115** could also be derived from **113a/b**. Replacement of the 2-OH with a reactive leaving group and subsequent removal of the TFA protecting group would result in an intermediate for a conventional S_N2 reaction, giving the ring-closed product **115** (Scheme 46b).

Different strategy using 113a/b:

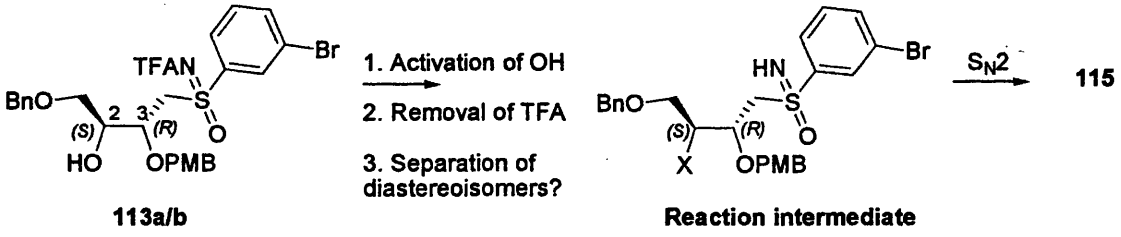

113a/b **Reaction intermediate**

Scheme 46b. A different route starting from **113a/b** *via* a conventional S_N2 reaction would also give the cyclised product **115**.

4-Methoxybenzaldehyde dimethyl acetal **110** is usually derived from the corresponding aldehyde **109** using trimethyl orthoformate/*p*-TsOH or MeOH/*p*-TsOH (*vide infra*, Scheme 47). Recently, De *et al.* reported the use of ruthenium(III) chloride as a Lewis acid catalyst in the synthesis of **110** with MeOH.[192] It was found that, with a catalytic amount of $RuCl_3$, conversion was completed in 5 h, yielding **110** in 84%. Acetalisation is a common protecting method of carbonyl groups and Lewis acid catalysts are often used, and De *et al.* applied this knowledge to the synthesis of various acetals.

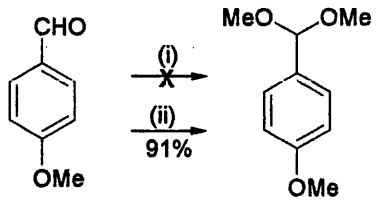

109 **110**

Scheme 47. Synthesis of 4-methoxybenzaldehyde dimethyl acetal **110**. *Reagents and conditions: (i) $RuCl_3$, MeOH, reflux; (ii) trimethyl orthoformate, p-TsOH, reflux.*

However, subjecting 4-methoxybenzaldehyde **109** to the same conditions described by De *et al.* failed to produce the corresponding acetal **110**.[192] TLC of the reaction mixture after 48 h showed only traces of a new product, with the majority of the starting aldehyde **109** still present (Scheme 47).

The traditional method using trimethyl orthoformate and *p*-TsOH was followed as described by Johansson *et al.* (Scheme 47),[190] and 4-methoxybenzaldehyde dimethyl acetal **110** was obtained in excellent yield.

With the acetal compound **110** in hand, attention was then turned to synthesise the required N-TFA diols **108a/b** and pursue the subsequent steps in the study. Acid-hydrolysis of the acetal of dioxolanes **90a/b** gave **108a/b** in moderate yield (*vide infra*, Scheme 48). Unexpectedly, the NMR spectra of **108a/b** showed the existence of only one diastereoisomer. In particular, the ^{13}C spectrum revealed only one set of signals. Three CH_2 carbon signals were observed at δ 59.6, δ 71.5 and δ 73.7 which represent the SCH_2, $BnO\underline{C}H_2$ and $Ph\underline{C}H_2$ carbons, respectively. Moreover, as only one singlet at δ –76.0 was seen in the ^{19}F spectrum, it was concluded that only one TFA group was present in the compound and thus there was only one diastereoisomer. Repeated attempts at recrystallisation to obtain a crystalline product failed.

Since X-ray analysis was not available for **108a/b**, the configuration at the sulfur atom was unclear. Nevertheless, it was decided that this compound would be subjected to the subsequent reaction with acetal **110**. The resulting benzylidene derivatives **111a/b** should be obtained as a mixture of diastereoisomers (as described by Riley *et al.*[191]) and separation of diastereoisomers and X-ray analysis might be possible at this stage. Disappointingly, the attempted acid-catalysed reaction of **108a/b** with the acetal **110** was unsuccessful. Increasing reaction temperature to 100°C and extending reaction duration to 36 h failed to give the benzylidene derivatives **111a/b**. TLC of the reaction

mixture indicated presence of only starting materials and no considerable progress was shown after 36 h.

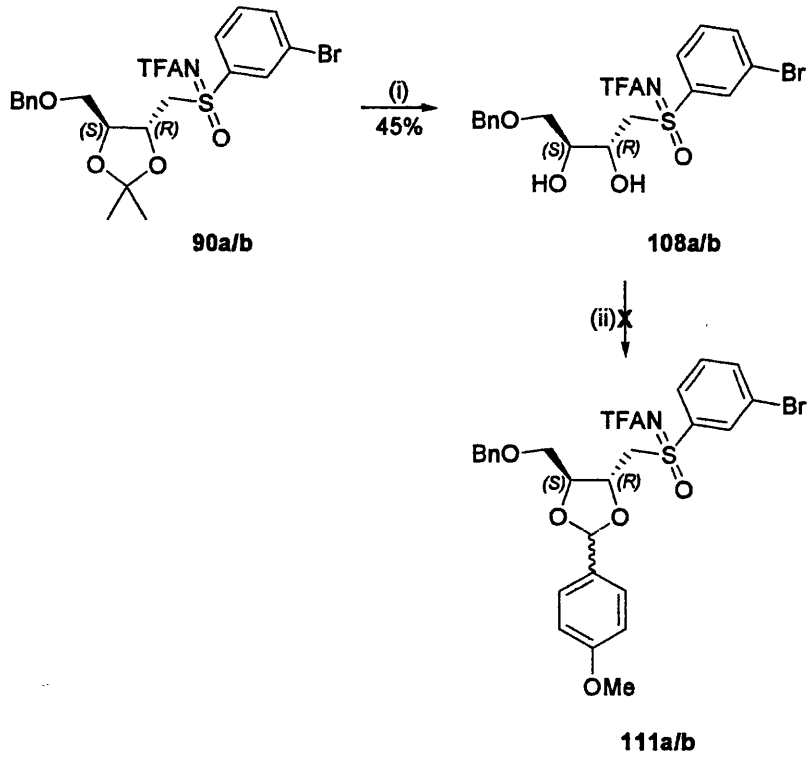

Scheme 48. Attempted synthesis of the benzylidene derivatives **111a/b**. *Reagents and conditions: (i) HCl, MeOH; (ii)* ***110****, p-TsOH, DMF, 70°C to 100°C.*

An alternative procedure to discriminate between the two secondary alcohols in the sulfoximine diol **S-(*R*)-92** was sought to protect 3-OH selectively and expose the free 2-OH and the sulfoximine NH for subsequent S_N2 ring-closure reaction (*vide infra*, Scheme 49). Reaction of **S-(*R*)-92** with DMP would give either a five-membered ring dioxolane **S-(*R*)-91**, which was synthesised previously (*vide supra*, Scheme 45), or a six-membered ring product. The two hydroxy groups in the latter would be discriminated. Replacement of the free 2-OH with a reactive leaving group and subsequent removal of the acetal would expose the sulfoximine NH. Similar to the PMB strategy, a S_N2 reaction between the NH and 2-OH would give the ribosyl derivative **107** (*vide infra*, Scheme 49).

It was reasoned that the third alternative product, a seven-membered ring product, would be thermodynamically unfavourable and the possibility of its formation would be small. Furthermore, the five- and six-membered products could be differentiated by ^1H NMR analysis from the coupling constants of the SCH_2 protons, since the six-membered product resembles a chair-conformation.

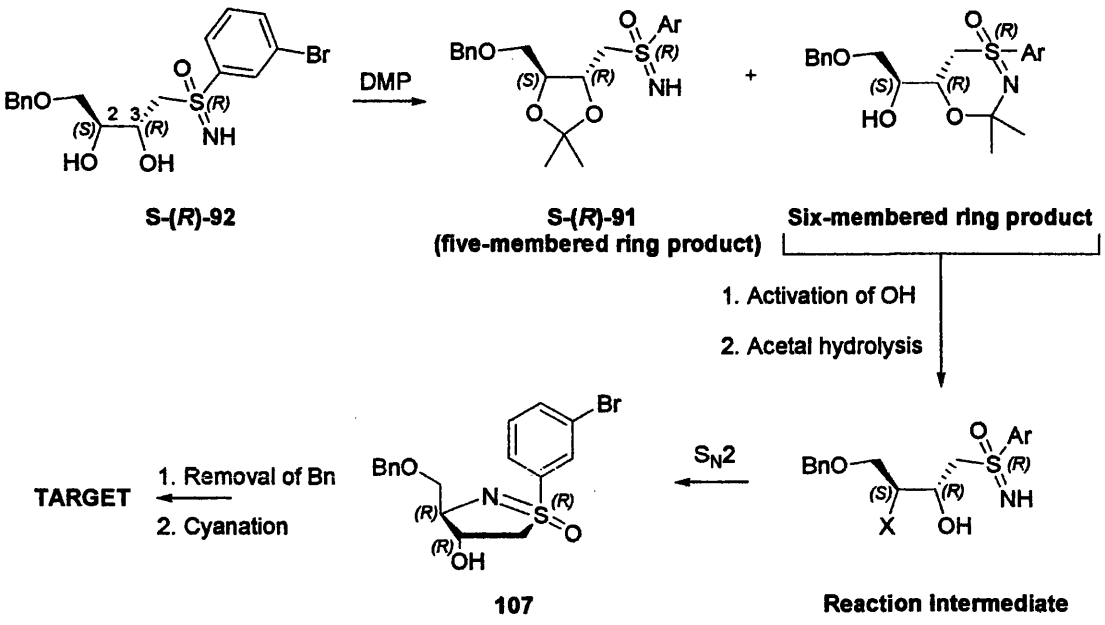

Scheme 49. Alternative synthetic approaches to target **39** *via* an acid-catalysed PMB cyclisation.

Treatment of **S-(*R*)-92** with DMP and *p*-TsOH in refluxing $CHCl_3$ gave three products in a 3:1:1 ratio (Scheme 50). The ^1H NMR spectrum of the major product showed that it contained the previously-afforded five-membered ring dioxolane **S-(*R*)-91**, with the signals of CMe_2 (two singlets at δ 1.22 and δ 1.32), SCH_2 (double doublet at δ 3.34, J = 14.5, 8.6 Hz; double doublet at δ 3.47, J = 14.5, 2.7 Hz), $BnOCH_2$ (double doublet at δ 3.52, J = 9.8, 6.3 Hz; double doublet at δ 3.68, J = 9.8, 4.7 Hz), 4-H (double-double doublet at δ 3.89, J = 7.8, 6.3, 4.7 Hz), 5-H (double triplet at δ 4.31, J = 2.7, 8.6 Hz), $PhCH_2$ (singlet at δ 4.53), and the S-Ph *ortho*-proton (triplet at δ 8.08, J = 1.7 Hz) all being extremely similar or identical to those from the ^1H NMR spectrum of dioxolane **S-(*R*)-91**.

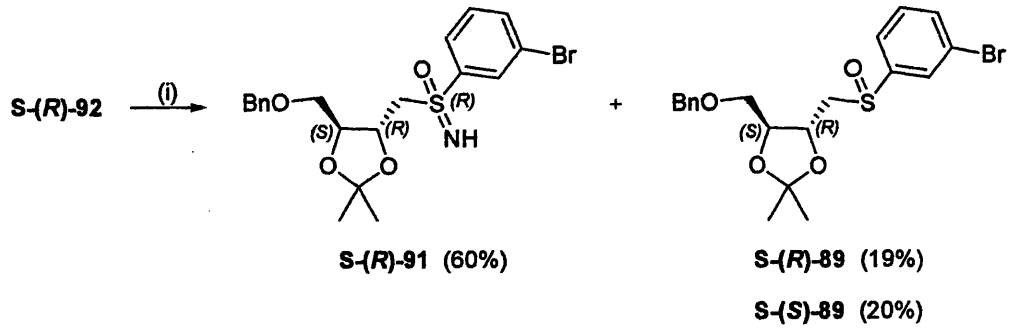

Scheme 50. Attempted DMP-reaction of the diol **S-(*R*)-92**. *Reagents and conditions: (i) DMP, p-TsOH, $CHCl_3$, reflux.*

Unexpectedly, this reaction also led to the formation of the diastereomeric sulfoxides **89a/b** which could be separated chromatographically. Comparision of the ^{1}H NMR spectra of the two isolated minor products with that of the previously synthesised diastereomeric sulfoxides **89a/b** showed that spectrum of each of these minor products was identical to one of the two sets of signals in **89a/b**. This finding was further supported by the mass spectrum of one of the minor products, showing a probable molecular weight of 438. An even molecular weight number corresponds to a lack of nitrogen in the molecule.

There are two speculative mechanisms for the formation of the diastereomeric sulfoxides. Reduction of the sulfoximine **S-(*R*)-91** would give the corresponding sulfoxide **S-(*R*)-89**, and subsequent epimerisation at the sulfur atom leads to the generation of the S-(*S*)-isomer. However, since epimerisation at a sulfur centre is usually achieved in only harsh conditions (heat in concentrated acid), it is highly unlikely that the relatively mild reaction conditions used (a catalytic amount of *p*-TsOH in refluxing $CHCl_3$) could cause this loss of chirality at the sulfur centre.

Therefore, the loss of the imino NH in **S-(*R*)-92** did not proceed with retention or inversion of configuration at the sulfur. The exact mechanism for this loss of stereochemical integrity remains unclear.

Chapter 4 Results and Discussion II

Synthetic approaches to a 2-deoxy-*D*-ribose-1α-phosphate analogue

4.1 Retrosynthesis

Following the success with the synthesis of a sulfide dioxolane precursor to the target benzamide 2-deoxyriboside analogue **39**, the same synthetic strategy was used to prepare a different target compound: the 2-deoxy-*D*-ribose-1α-phosphate analogue **37**. The two targets are structurally similar, differing only at the sulfur substituents: the former contains an aromatic carboxamide group, whereas the latter has a carboxymethyl chain (Scheme 51).

Mitsunobu reaction between an alcohol of the dioxolane derivative **98** and a sulfur nucleophile has been proven to proceed smoothly, with thiophenol and 3-bromo-thiophenol giving positive results. Therefore, to synthesise the carboxymethyl side-chain of target **37**, the same strategy could be used using an alkyl sulfur nucleophile. Methyl mercaptoacetate **116** was chosen as a reagent; reaction with dioxolane **98** should give the extracyclic C–S bond in the alkylsulfide dioxolane precursor **117** (Scheme 51).

Mitsunobu reactions of the dioxolane 98 and aromatic sulfur nucleophiles

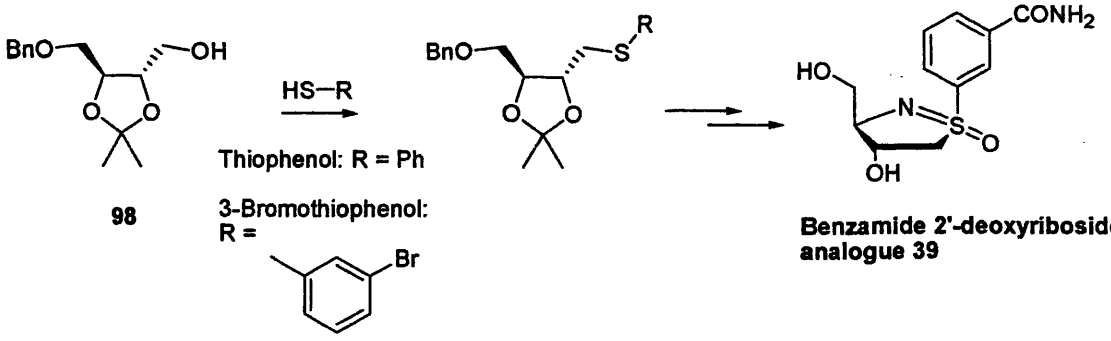

98

Benzamide 2'-deoxyriboside analogue 39

Proposed synthesis of target 37

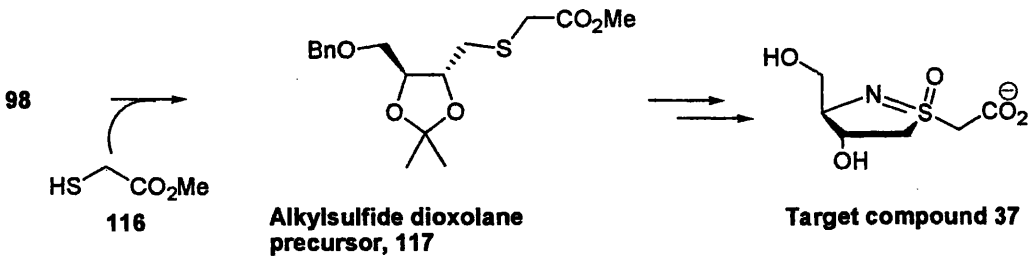

Alkylsulfide dioxolane precursor, 117

Target compound 37

Scheme 51. Proposed extracyclic C–S bond formation *via* a Mitsunobu reaction of dioxolane **98** and methyl mercaptoacetate **116**.

4.2 Synthesis

The proposed synthetic sequence to the target compound **37** is outlined in Scheme 52. Mitsunobu condensation of methyl mercaptoacetate **116** and dioxolane **98** gives the sulfide **117**. Hydrolysis of the acetal generates the diol **118**. An intramolecular cyclisation *in situ* between the OH and the ester carbonyl carbon would give the six-membered ring derivative **119**. Introduction of the sulfoximine moiety is followed by an intramolecular Mitsunobu cyclisation. Since there is only one secondary alcohol available for ring closure, the reaction should proceed to form the fused ring (5/6) system in **121**. The ester bond linkage is hydrolysed and subsequent removal of the Bn group would give the final target compound **37**.

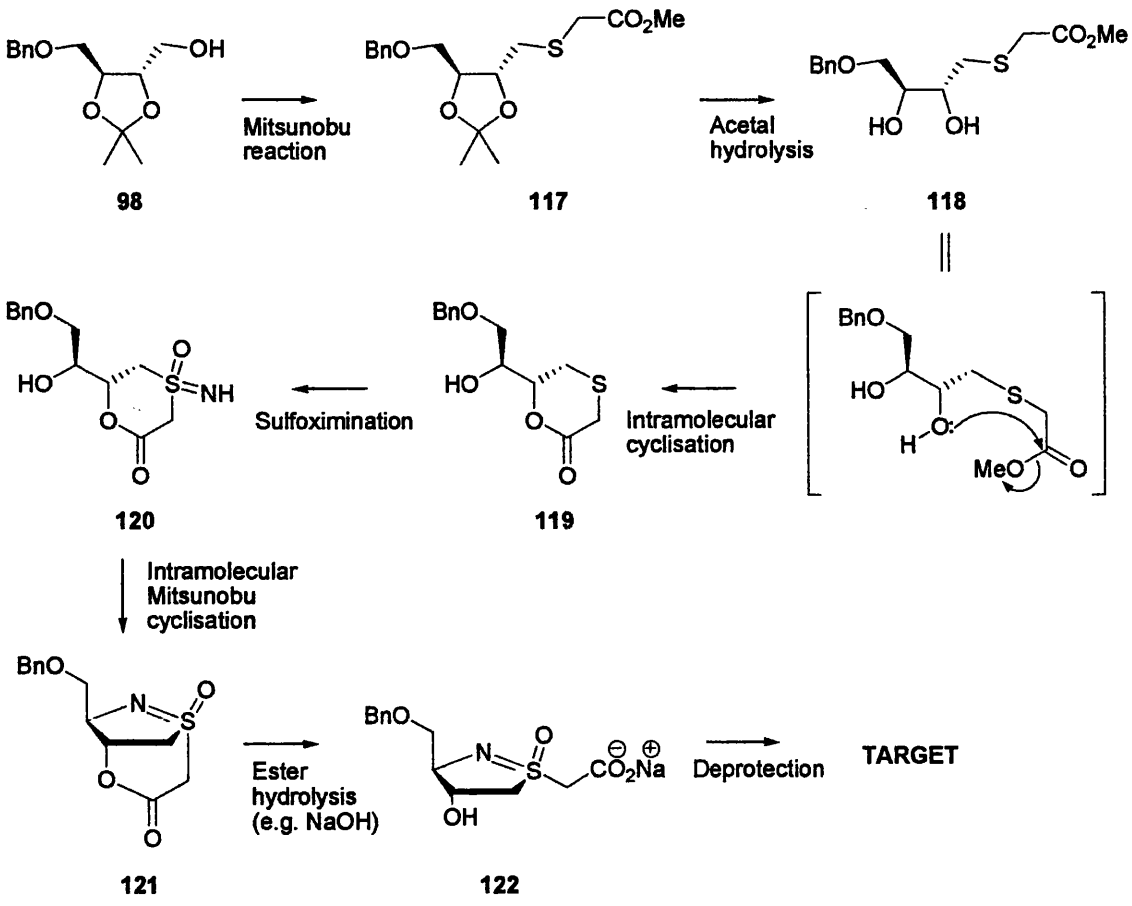

Scheme 52. Proposed synthetic approaches to target compound **37**.

Methyl mercaptoacetate **116** and the dioxolane compound **98** were subjected to a variety of Mitsunobu conditions (*vide infra*, Route A, Scheme 53). They are summarised in Table 11 (*vide infra*). None of the reactions furnished the desired product **117**, including the previously effective ADDP/TBP system (*vide infra*, entry 3,

Table 11), which worked well with thiophenol and 3-bromothiophenol. The reactions failed to progress even under extended reaction duration and elevated temperature. TLC of reaction mixtures showed only the presence of starting materials in all cases.

Entry	Conditions (stated in the order of addition in reaction mixture)	Yield (%)
1	TPP (2 equiv.), DIAD (2 equiv.), methyl mercaptoacetate **116** (1 equiv.), dioxolane **98** (1 equiv.), THF (10 mL)	-
2	TPP (2 equiv.), methyl mercaptoacetate **116** (1 equiv.), DIAD (2 equiv.), dioxolane **98** (1 equiv.), THF (10 mL)	-
3	TBP (1.5 equiv.), ADDP (1.5 equiv.), methyl mercaptoacetate **116** (1.5 equiv.), dioxolane **98** (1 equiv.), THF (10 mL)	-
4	DPPE (0.75 equiv.), DIAD (1.5 equiv.), methyl mercaptoacetate **116** (1.3 equiv.), dioxolane **98** (1 equiv.), THF (10 mL)	-

Table 11. Attempted Mitsunobu reaction conditions. (TPP = triphenylphosphine, DIAD = diisopropyl azodicarboxylate, TBP = tributylphosphine, ADDP = 1,1'-(azodicarbonyl)dipiperidine, DPPE = 1,2-bis(diphenylphosphino)ethane)

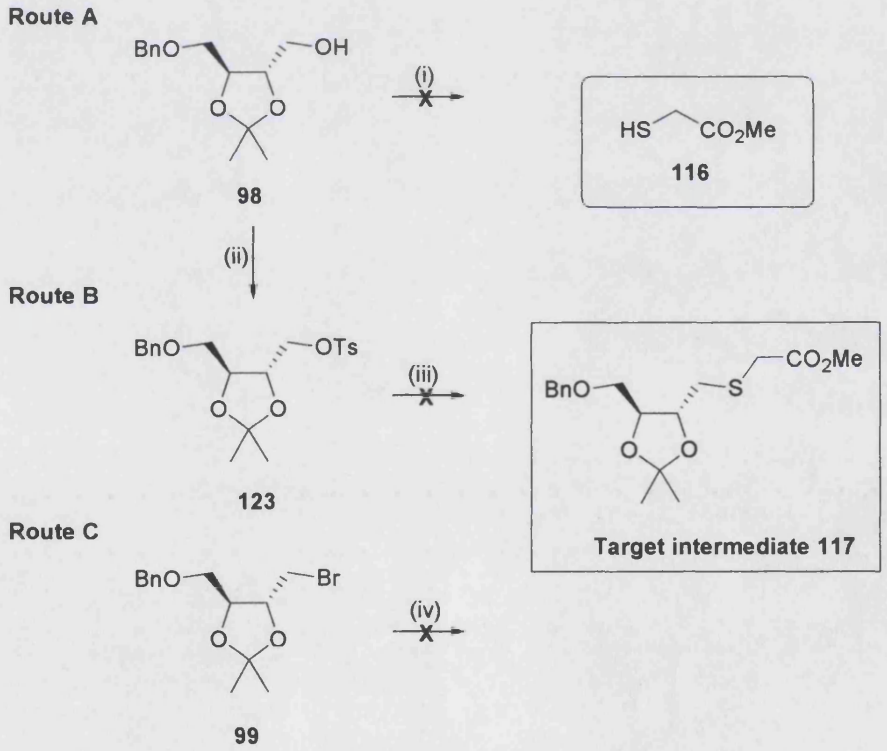

Scheme 53. Attempts to synthesise sulfide intermediate **117** using methyl mercaptoacetate **116** and a variety of dioxolane derivatives. *Reagents and conditions: (i) see Table 11; (ii) p-TsCl, Et_3N, DMAP, DCM; (iii) LHMDS, THF, –78 °C / t-BuOK, MeOH, 75 °C / t-BuOK, DMF, 150 °C; (iv) NaH, DMF, 0 °C.*

It was postulated that a more efficient leaving group was required to increase the reactivity of the OH in **98**. A tosylate derivative was considered first (Route B, Scheme 53); tosylates (*p*-toluenesulfonate esters) are good substrates for substitution reactions with nucleophiles and they are better leaving groups than the corresponding alcohols. Tosylate **123** was prepared from the alcohol **98** using *p*-toluenesulfonyl chloride (*p*-TsCl), triethylamine and 4-dimethylaminopyridine (DMAP).

With the tosylate compound **123** in hand, a series of base-catalysed nucleophilic substitutions with methyl mercaptoacetate was attempted but to no avail. In all cases, TLC of the reaction mixtures indicated only the presence of starting materials. Changes in base [LHMDS, potassium *tert*-butoxide (*t*-BuOK)], solvent (THF, MeOH, DMF), temperature and duration did not alter the outcome. Substituting DMF as an alternative solvent and heating the reaction to reflux for 72 h gave a complex mixture.

An alternative approach of generating the thiolate *in situ* by hydrolysis of a thioester was also investigated. Thioacetates are often prepared from the corresponding halides and potassium thioacetate in one simple step, and treatment with base (sodium hydroxide) gives the thiolate anion.[193] Using this method, thioacetate **126** was obtained in quantitative yield. However, treatment of **126** with sodium hydroxide and subsequent addition of the tosylate **123** to the reaction mixture led only to the recovery of starting materials (Scheme 54).

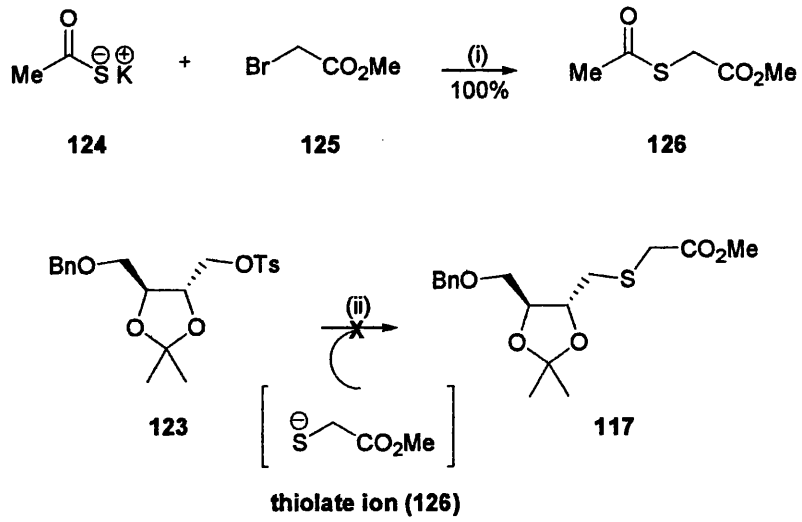

Scheme 54. Attempted synthesis of target intermediate **117** using thioacetate derivative **126**. *Reagents and conditions: (i) MeOH; (ii)* ***126****, NaOH, MeOH.*

Bromide was investigated next to be a potential leaving group. However, treatment of the bromomethyl dioxolane **99** (*vide supra*, Scheme 38) with methyl mercaptoacetate **116** and sodium hydride also failed to furnish the target intermediate **117** (*vide supra*, Route C, Scheme 53).

The above results called a halt to the synthesis of target **37** as it is fully demonstrated that the coupling of the thio ester to the dioxolane derivative is impossible even under harsh conditions. This is puzzling, since methyl mercaptoacetate is sterically less crowded than thiophenol and 3-bromothiophenol, and its approach to the electrophilic dioxolane should be favoured.

It was speculated that, since both thiophenol and 3-bromothiophenol are planar but methyl mercaptoacetate anion contains a tetrahedral carbon ($\underline{C}H_2S^-$), the local shape of approaching nucleophiles might play an important role in the outcome of the reactions.

Chapter 5 Results and Discussion III

Towards the synthesis of a PARP-1 transition-state analogue and a 2-deoxy-*D*-ribose analogue

5.1 Retrosynthesis

The second series of target compounds to be investigated are the 2-deoxy-*D*-ribose analogue **38a** and the PARP-1 transition-state analogue **40**. As in the previous targets studied, the anomeric carbon of this ribonucleoside analogue has been replaced by a tetrahedral sulfoximine. However, the structural scaffolding of this transition-state mimic is centred on the extracyclic S=N bond, which mimics the C–N bond stretch observed when NAD^+ is docked into the substrate-binding site of PARP-1.

Scheme 55 (*vide infra*) illustrates how targets of more than one type can be produced by a single carefully-planned synthetic sequence. Disconnection of C–N bond of the transition-state analogue **40** led to two starting compounds: a 3-substituted benzamide and the 2-deoxy-*D*-ribose mimic **38a**. The forward metal-catalysed N-arylation of sulfoximines has been studied. Palladium-catalysed N-arylation of sulfoximines was first reported by Bolm and Hildebrand using aryl bromides and aryl iodides as substrates.[194,195] Different palladium catalysts and chelating phosphine ligands, the most reported being the $Pd(OAc)_2$/BINAP [2,2'-bis(diphenylphosphino)-1,1'-binaphthyl] system, were studied by the group and N-arylated sulfoximines were obtained in good yields. Furthermore, the reactions to convert enantiomerically pure sulfoximines to the arylated derivatives proceeded with retention of configuration at sulfur. A subsequent method reported by Harmata *et al.* demonstrated the use of $Pd(OAc)_2$ with aryl chlorides.[196] Recently, the Bolm group studied the use of copper catalysts in N-arylation of sulfoximines.[197,198] They used CuI and base (Cs_2CO_3, CsOAc) with aryl bromides and aryl iodides, and also $Cu(OAc)_2$ with arylboronic acids for N-arylations of sulfoximines.[198]

References for the construction of a chiral 3,4-substituted tetrahydrothiophene are limited. However, in contemplating the syntheses of **38a**, it was envisioned that the critical intermediate, the homochiral *R,R*-tetrahydrothiophene **127**, could be formed through an asymmetric 1,3-dipolar cycloaddition similar to a published strategy. Karlsson and Högberg described an efficient method to synthesise chiral tetrahydrothiophenes *via* C–C bond forming asymmetric 1,3-dipolar cycloadditions of thiocarbonyl ylides.[199,200] Upon reductive cleavage of the chiral auxiliary, the resulting *trans*-3,4-disubstituted tetrahydrothiophenes were obtained in high diastereomeric ratios and in high yields.

By adopting this method, the C-3 and C-4 stereocentres of target compound **38a** would be established at an early stage in a stereoselective manner. Stereocontrol at the sulfur atom to introduce the third chiral centre is viable using chiral sulfoxidation, resolution of diastereomeric sulfoximines using (+)-CSA or chromatographic separation of diastereoisomers after sulfoximination.[134]

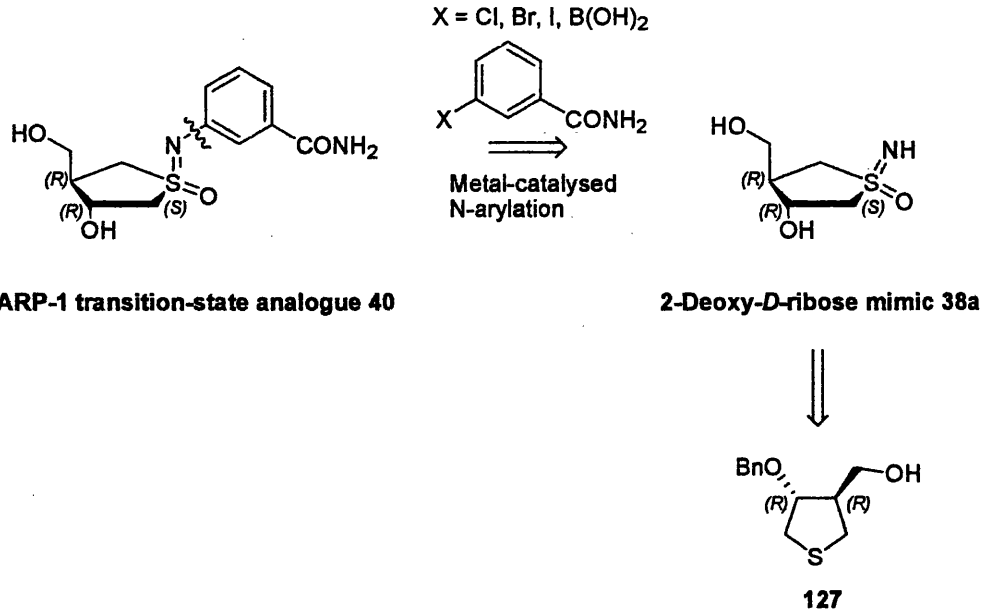

PARP-1 transition-state analogue 40

2-Deoxy-*D*-ribose mimic 38a

Scheme 55. Retrosynthetic analysis of target compounds **38a** and **40**.

5.2 Asymmetric 1,3-dipolar cycloaddition

Cycloadditions belong to the family of pericyclic reactions. One famous example is the Diels-Alder reaction, where a diene and a dienophile form a six-membered ring. 1,3-Dipolar cycloaddition is a [3 + 2] reaction where two components, a 1,3-dipole (ylide) and a dipolarophile, react together to form a five-membered heterocycle (*vide infra*, Scheme 56).

Similar to a dienophile in the Diels-Alder reaction, a cycloaddition dipolarophile is a reactive alkene containing two π-electrons. Many examples of dipolarophiles include simple alkenes, α,β-unsaturated ketones, aldehydes and esters, alkynes and allylic derivatives.

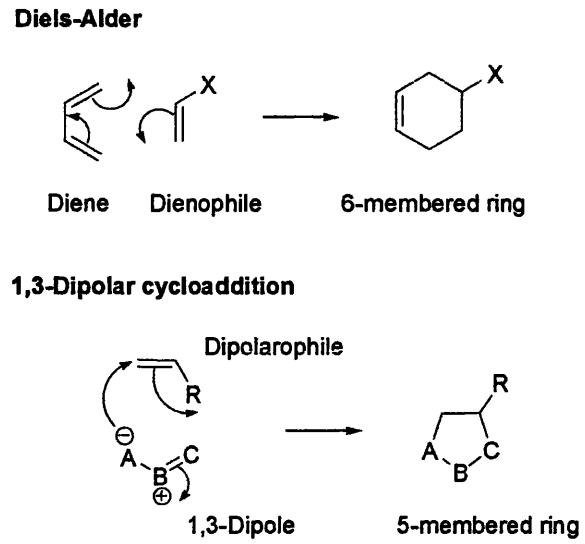

Scheme 56. Mechanisms of the Diels-Alder reaction and the 1,3-dipolar cycloaddition.

The 1,3-dipole, or an ylide, is a 'four-π-electron-component' with an electrophilic end and a nucleophilic end. Many types of ylides exist containing nitrogen, carbon, sulfur or oxygen atoms and the ylides can contain one or more heteroatoms.

The cycloaddition reaction involves the four π-electrons of the ylide and the two π-electrons of the dipolarophile in a concerted manner. The configurations of the chiral dipolarophiles have a major impact on the outcome of the diastereomeric products: *trans*-dipolarophiles give *trans*-cycloadduct, and *cis*-dipolarophiles will thus yield the *cis* isomer (Scheme 57).

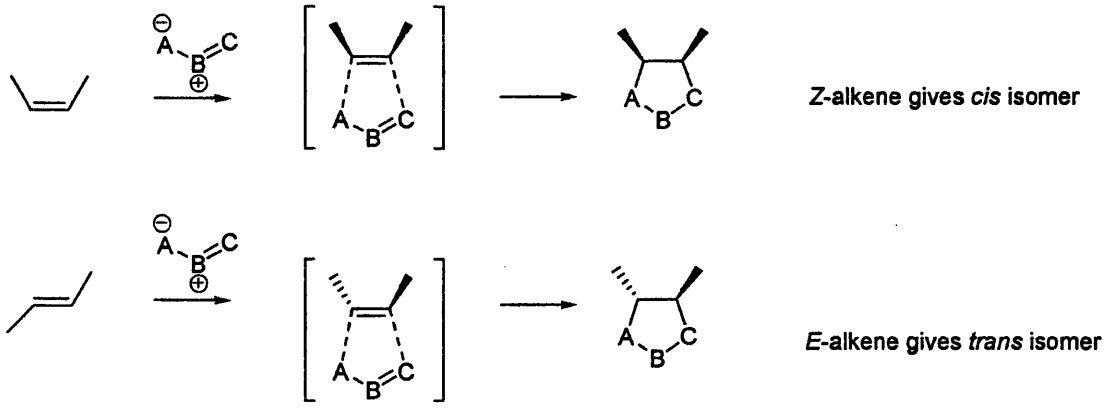

Scheme 57. Configuration of the dipolarophiles directly influence the geometry of the cycloadduct.

As described by Karlsson and Högberg, the asymmetric 1,3-dipolar cycloaddition reaction would involve a monohetero sulfur ylide with a (*E*)-dipolarophile linked to a

chiral auxiliary, (1*S*)-(–)-2,10-camphorsultam (*vide infra*, Scheme 58).[200] The sulfur ylide precursor, chloromethyl trimethylsilylmethyl sulfide, was desilylated with CsF, triggering an elimination to give the 1,3-dipole. Use of a chiral auxiliary gave high diastereoselectivities for a variety of dipolarophiles and allowed construction of enantiopure tetrahydrothiophenes. The reaction gave exclusively the two *trans*-diastereoisomers in excellent yield (88%) and high diastereoselectivity (87:13). The major (3*R*,4*S*)-isomer was generated together with the separable minor (3*S*,4*R*)-isomer. This method was, at the time, the first reported asymmetric 1,3-dipolar cycloaddition of a thiocarbonyl ylide with chiral dipolarophiles, resulting in *trans*-3,4-disubstituted tetrahydrothiophenes.

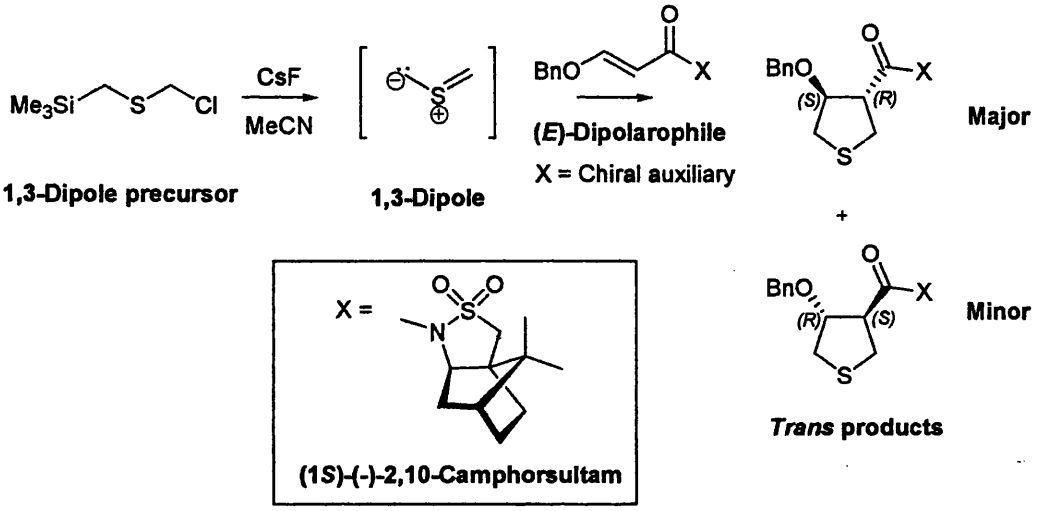

Scheme 58. Asymmetric 1,3-dipolar cycloaddition of a thiocarbonyl ylide and chiral benzyloxy dipolarophile, as demonstrated by Karlsson and Högberg.[200]

The diastereoselectivity observed when reacting a ylide with a camphorsultam-derived dipolarophile was explained by Karlsson and Hogberg using a model depicted in Figure 40 (*vide infra*).[201] The group reasoned that the camphorsultam-linked dipolarophile reacts with 1,3-dipoles in a conformation where the sulfone oxygens of the sultam are *trans*-located to the carbonyl oxygen in relation to the C–N amide bond. To avoid possible interactions and steric clashes with the axial sulfone oxygen (Oα), attack of the ylide has to occur on the opposite side to that occupied by Oα. Thus, the major isomer obtained is the (3*R*,4*S*)-isomer.

This procedure was adopted and modified for the synthesis of the homochiral tetrahydrothiophene intermediate **127**, using (*E*)-benzyloxy-α,β-unsaturated acid linked

to (1*R*)-(+)-2,10-camphorsultam as a chiral dipolarophile to give the desired relative configuration at C-3 and C-4.

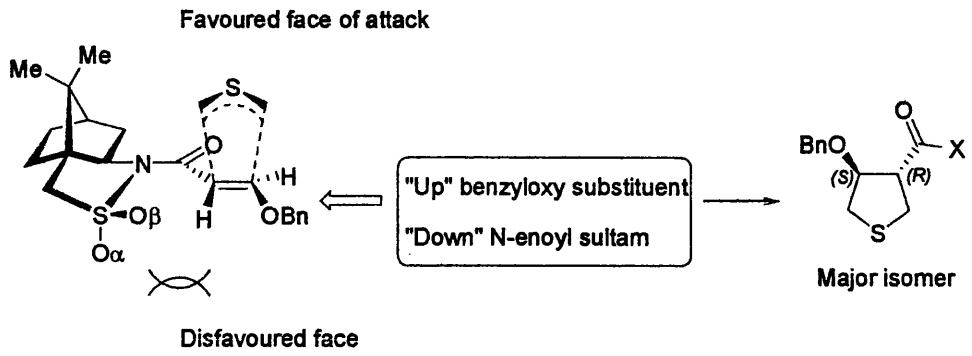

Figure 40. Proposed diastereoselectivity mediated by (1*S*)-(–)-2,10-camphorsultam by Karlsson and Högberg.[201]

5.2.1 Synthesis of the (*E*)-dipolarophile

Karlsson and Högberg prepared the chiral dipolarophile **132** using a one-pot synthesis: benzyl alcohol **128** and methyl propynoate **129** were treated with N-methylmorpholine to give the crude ester **130**, which, upon hydrolysis *in situ* by potassium hydroxide, gave the acrylic acid **131** (Scheme 59).[200] However, attempts to repeat this conjugate addition were unsuccessful. TLC of the reaction mixture prior to hydrolysis revealed the presence of an excess of benzyl alcohol, with little amounts of methyl propynoate and product, indicating that the Michael addition failed to proceed.

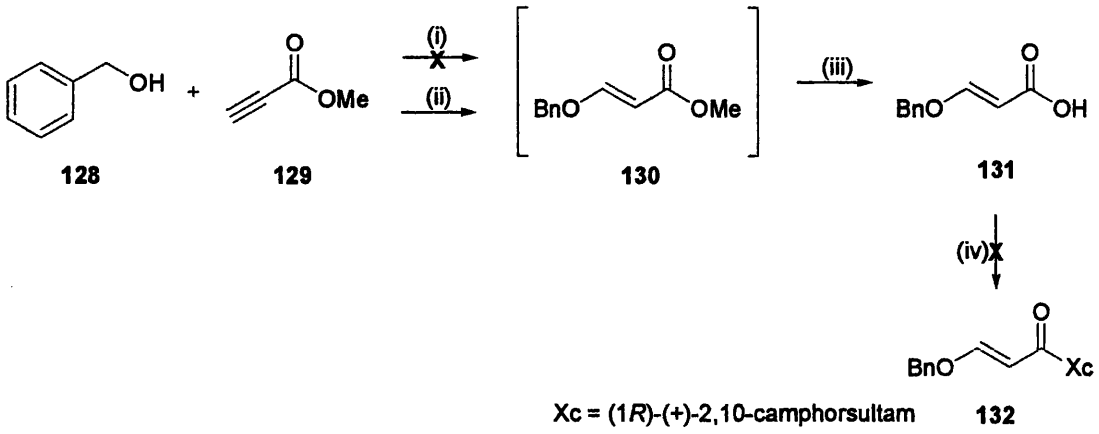

Scheme 59. Attempted synthesis of chiral (*E*)-benzyloxyacrylate dipolarophile **132**. *Reagents and conditions: (i) N-methylmorpholine, Et_2O; (ii) TBP, DCM; (iii) KOH, benzyl alcohol, propan-2-ol; (iv) conditions (vide infra, Scheme 61).*

A different catalyst was sought to encourage the conjugate addition. Trialkylphosphines have found a place as useful catalysts in addition of alcohols to electron-deficient alkynes.[202] Inanaga *et al.* examined the use of several phosphine catalysts in the addition of benzyl alcohol to methyl propynoate and tributylphosphine (TBP) was found to be the best reagent due to its high nucleophilicity.[203] The reaction mechanisms were postulated to involve initial addition of the phosphine to the β-carbonyl of the propiolate to give a zwitterionic enolate intermediate which then deprotonates the alcohol. Subsequent addition of the benzyl alkoxide anion and phosphine elimination gives the ester **130** with (*E*)-stereoselectivity and regenerates the catalyst (Scheme 60).

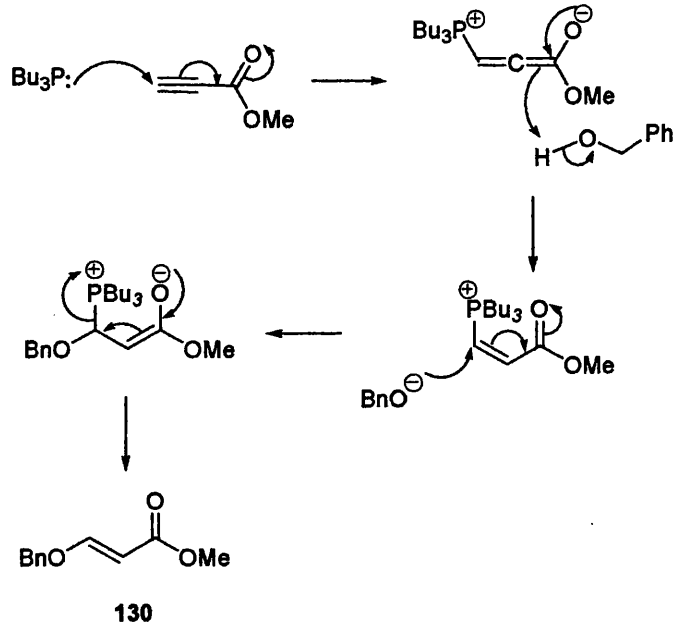

130

Scheme 60. Proposed mechanism of TBP-catalysed conjugate addition reaction by Inanaga *et al.*[203]

Following the method of Inanaga *et al.*,[203] (*E*)-3-benzyloxypropenoic acid **131** was obtained in good yield (*vide supra*, Scheme 59). The ^{1}H NMR spectrum of **131** showed two doublets for the alkene protons, one at δ 5.29 corresponding to the CH next to the carbonyl group, and one further downfield at δ 7.74 for the CH next to the ether oxygen. Their coupling constants corresponded to those seen in *trans* double bond (J = 12.8 Hz).

Karlsson and Högberg converted the unsaturated acid **131** to the corresponding acid chloride **133** using thionyl chloride, and reaction with camphorsultam and MeMgBr gave the chiral dipolarophile **132** (*vide infra*, Scheme 61).[200] Several attempts were made to synthesise this acid chloride, using a variety of reagents (thionyl chloride, oxalyl choride) in different solvents (DCM, toluene) and temperatures (RT to 85°C). In

order to examine the formation of the acid chlorides, samples of the reaction mixtures were quenched with methanol to give the methyl ester, which was shown by TLC. However, these acid chlorides failed to react with the magnesium salt of the camphorsultam. Moreover, decomposition of the starting materials was noted from TLC of the reaction mixture, which made the recovery of the expensive camphorsultam extremely difficult.

Following this discouragement, a different leaving group, pentafluorophenoxy (OPFP), was considered. Pentafluorophenyl esters are usually stable crystalline compounds and they are relatively easy to prepare using pentafluorophenol (PFPOH) and *N,N*-dicyclohexylcarbodiimide (DCC); the pentafluorophenoxide anion makes an excellent leaving group from these active esters. Synthesis of the PFP ester **134** proceeded swiftly and it was subsequently subjected to amidation with the camphorsultam under the same conditions as described above (Scheme 61) but the reaction gave only an unidentifiable solid.

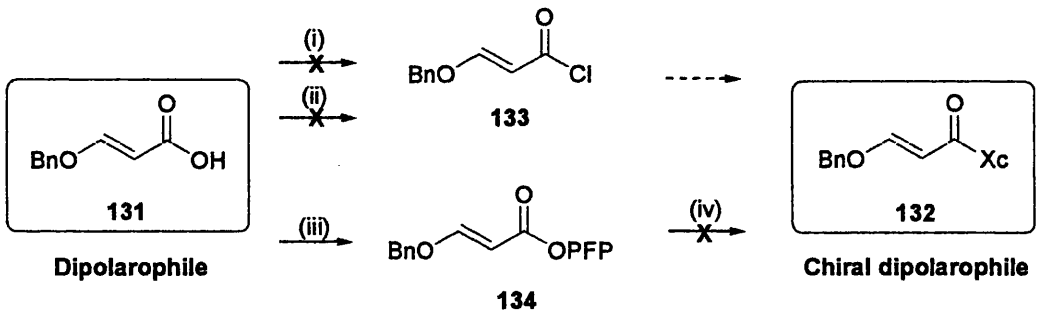

Scheme 61. Attempts at synthesising the chiral dipolarophile linked with (1*R*)-(+)-2,10-camphorsultam (Xc). *Reagents and conditions: (i) $SOCl_2$, DMF, DCM, 85°C; (ii) $(COCl)_2$, DMF, DCM, 85°C / $(COCl)_2$, DMF, toluene, RT; (iii) PFPOH, DCC, EtOAc, 0°C; (iv) (1R)-(+)-2,10-camphorsultam, MeMgBr, THF, 0°C.*

The prohibitive cost of camphorsultam deterred further investigation. Instead a more economical choice of chiral auxiliary, *L*-menthol **135**, which is used frequently as a chiral auxiliary, was adopted as the reagent of choice.[204,205] It is commercially available in both enantiomers and is cheap. The synthetic routes to the new chiral dipolarophile **136** are presented in Scheme 62 (*vide infra*). Attempted condensation of the PFP ester **134** with *L*-menthol **135** using Et_3N failed. Therefore, a direct coupling of the acid **131** with *L*-menthol **135** using DCC and DMAP was performed and gave product **136** as a colourless oil. The ^1H NMR spectrum showed a downfield shift of the menthol H-1 (δ 3.39) to δ 4.77, corresponding with the attachment of a carbonyl group to the menthol oxygen.

Despite the failed attempts to synthesise a camphorsultam-linked chiral dipolarophile, a new reagent was successfully obtained using *L*-menthol as a potential chiral auxiliary. Having established a functional protocol for the preparation of this modified chiral dipolarophile, attention was then turned to construct a sulfur 1,3-dipole using the reaction sequence conducted by Karlsson and Högberg.[200]

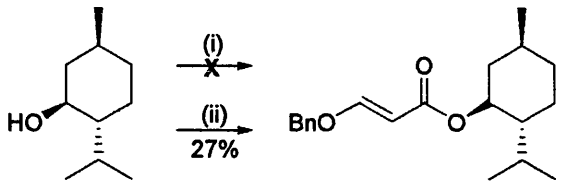

135 **136**

New chiral dipolarophile

Scheme 62. Synthesis of a new chiral dipolarophile **136** using *L*-menthol **135** as a chiral auxiliary. *Reagents and conditions: (i)* ***134****, Et_3N, Et_2O; (ii)* ***131****, DCC, DMAP, DCM, 0 °C.*

5.2.2 Synthesis of a sulfur ylide

Karlsson and Högberg reported that, since thiocarbonyl ylides are often reactive, short-lived species, they have to be prepared *in situ* from a precursor.[200] Chloromethyl trimethylsilylmethyl sulfide **137** has been shown to be a useful thiocarbonyl ylide precursor by Hosomi *et al.*[206] CsF-catalysed elimination of Me_3SiCl from this precursor gave the desired sulfur 1,3-dipole which readily underwent 1,3-dipolar cycloaddition reaction with different dipolarophiles and gave the corresponding adducts in good yields [Scheme 63 and Scheme 58 (*vide supra*)].

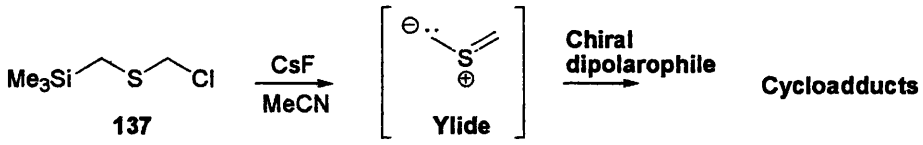

137

Scheme 63. Karlsson and Högberg synthesis of a sulfur 1,3-dipole and subsequent 1,3-dipolar cycloaddition.[200]

A literature method by Block *et al.* for the synthesis of the ylide precursor **137** was investigated (*vide infra*, Scheme 64).[207] The chloromethyl compound **138** was treated with thiourea, and the solid S-alkylisothiouronium salt **139** was obtained in quantitative yield. It was subsequently hydrolysed with aqueous base to give the thiol **140**. The presence of **140** was detected by the strong odour. However, isolation of this volatile

thiol by distillation proved to be extremely difficult due to its low boiling point. All attempts to isolate the compound were unsuccessful.

Therefore, a new strategy was adopted to increase molecular weight and thus the boiling point by using a larger aromatic silyl group. Similar reaction of $PhMe_2SiCH_2Cl$ **141** with thiourea gave the isothiouronium salt **142**, which was hydrolysed to give the thiol **143** (Scheme 64). This thiol appeared to be easily autoxidised to the disulfide. Thus, after evaporation of the solvent, the crude **143** was directly and rapidly treated with 1,3,5-trioxane and dry HCl.[208] Generation of the product **144** was detected in the crude reaction mixture *via* ^1H NMR. However, it was not isolable by short-path distillation and the product present quickly decomposed at raised temperature.

Attempted synthesis of chloromethyl trimethylsilylmethyl sulfide 137

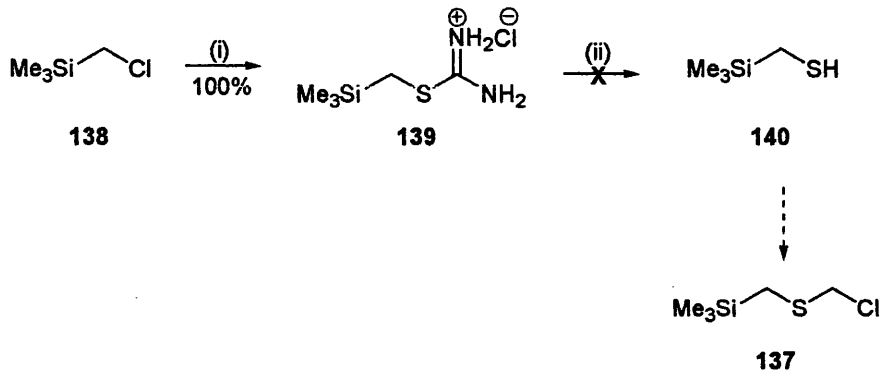

138 **139** **140** **137**

Synthesis of new, less volatile sulfur ylide precursor 144

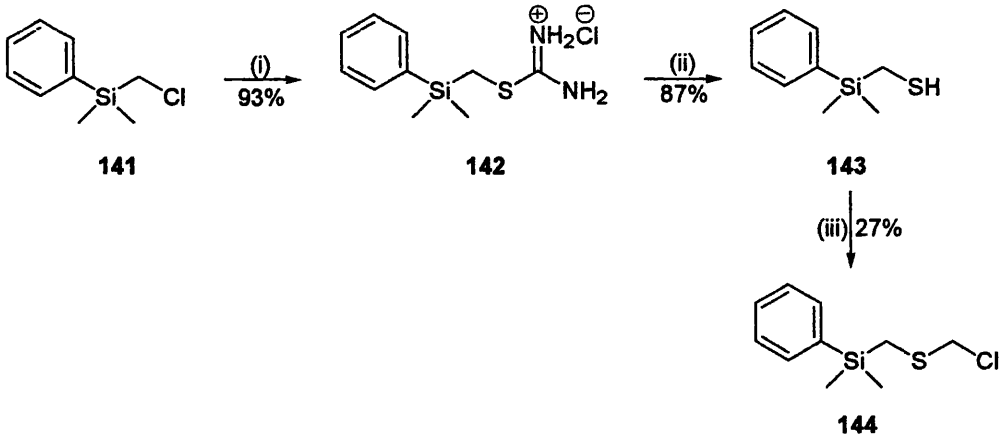

141 **142** **143** **144**

Scheme 64. Synthetic approaches to a sulfur 1,3-dipole. *Reagents and conditions: (i) thiourea, NaI, EtOH, reflux; (ii) 40% aq. NaOH; (iii) 1,3,5-trioxane, dry HCl, –10°C.*

Nevertheless, CsF-catalysed 1,3-dipolar cycloaddition reaction with the menthol-linked dipolarophile **136** and the crude ylide precursor **144** was attempted but the reaction did

not give the desired products (**145a/b**, Scheme 65), with TLC of the reaction mixture indicating decomposition of starting materials.

The complications in the isolation of the sulfur 1,3-dipole and the relatively lower yields observed for the previous steps warranted exploration of a new strategy.

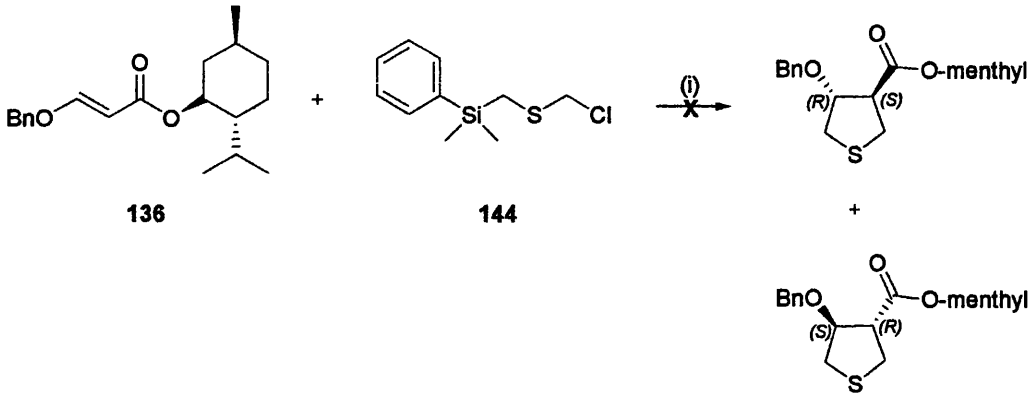

Scheme 65. Attempted 1,3-dipolar cycloaddition reaction with new chiral dipolarophile **136** and new sulfur ylide precursor **144**. *Reagents and conditions: (i) CsF, MeCN.*

5.3 Halocyclisation

Attention was turned to investigate literature methods in synthesising a racemic tetrahydrothiophene skeleton, with the possibility of introducing enantiomeric purity at a later stage. Initial attempts involved the generation of a monobrominated tetrahydrothiophene derivative from unsaturated sulfides, as described by Ren *et al.*[209,210] Alkenylbenzyl sulfides were found to react with iodine or bromine at room temperature to give five-membered ring cycloadducts (*vide infra*, Scheme 66).

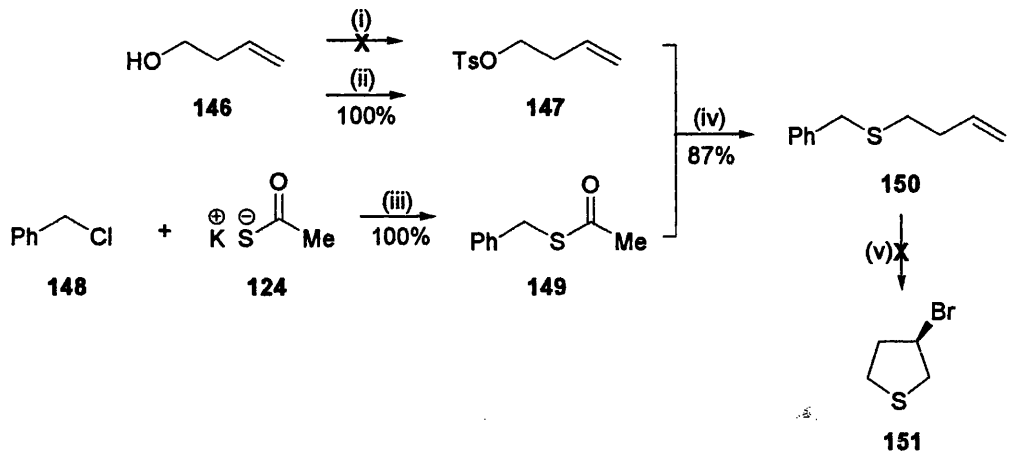

Scheme 66. Synthetic approaches to the monobrominated tetrahydrothiophene **151**. *Reagents and conditions: (i) pyridine, p-TsCl, DCM; (ii) LHMDS, p-TsCl, THF, –78°C; (iii) MeOH; (iv) NaOH, MeOH; (v) Br_2, DCM, RT to 70°C.*

The mechanism of this reaction was demonstrated by Ren *et al.* and it is illustrated in Scheme 67.[209,210] It was concluded that the halogen attacks an unsaturated sulfide by coordinating to the double bond to produce a halonium ion. Sulfur behaves as a nucleophile and addition to the electrophilic complex would give a cyclic benzyl-sulfonium ion. A final dealkylation step, found to be irreversible by the group, by the halide ion would produce benzyl halide and a five-membered ring product. Furthermore, Ren *et al.* also discovered that bromine is superior to iodine in these cyclisation reactions in terms of reaction rates. Iodocyclisations proceeded more slowly and required several days for completion.[210]

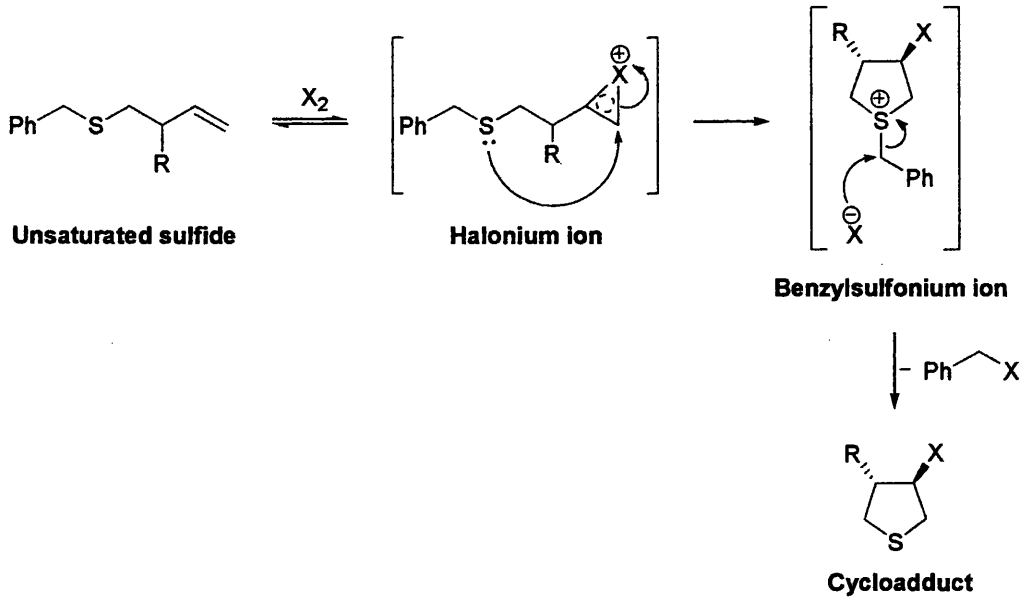

Scheme 67. Synthesis of halogenated tetrahydrothiophenes by Ren *et al.*[209,210]

This method would first be followed to synthesise the monobrominated tetrahydrothiophene **151** in order to clarify synthetic difficulties. Once the reaction conditions have been studied, a disubstituted tetrahydrothiophene would be synthesised using the corresponding unsaturated sulfide.

Synthesis of 3-butenyl benzyl sulfide **150** commenced from commercially available 3-buten-1-ol **146**, benzyl chloride **148** and potassium thioacetate **124** for the preparation of two starting components: butenyl tosylate **147** and benzyl thioester **149** (*vide supra*, Scheme 66).[210]

3-Buten-1-ol **146** was tosylated under traditional conditions (pyridine, *p*-TsCl) but the reaction failed to give the desired product (*vide supra*, Scheme 66).[210] TLC of the reaction mixture showed that the reaction never showed considerable progress and only traces of a new product were formed. Therefore, a stronger base, LHMDS, was used to encourage the conversion and tosylate **147** was furnished in quantitative yield (*vide supra*, Scheme 66). Reaction of benzyl chloride **148** and potassium thioacetate **124** afforded benzyl thioacetate **149** (*vide supra*, Scheme 66),[193] which was subsequently treated with tosylate **147** to give the benzyl sulfide **150** in good yield (87%). Disappointingly, attempted bromination of this benzyl sulfide failed. At elevated temperature, only decomposition of starting materials was observed.

Failure to synthesise the brominated tetrahydrothiophene **151** using the Ren *et al.*[210] protocol indicated that an alternative cyclisation strategy was required.

5.4 Dieckmann condensation

The Claisen condensation is described as a base-catalysed condensation of two esters containing α-hydrogens, forming β-ketoesters. The Dieckmann condensation is the intramolecular version of the Claisen condensation where the two esters are linked within the same molecule, giving cyclic β-ketoesters. Shinkwin *et al.* reported the use of a Dieckmann condensation in the synthesis of a disubstituted tetrahydrothiophene derivative as depicted in Scheme 68 (*vide infra*).[211] The group discovered that, upon treatment of the dimethyl ester **153** with sodium ethoxide, **154** was afforded as the major product, with the isomeric compound **155** as the minor product, in poor overall yields (14% and 10%, respectively). Additionally, keto-enol tautomerism was observed in the ^{1}H NMR spectrum of **154** and not in the minor product **155**.

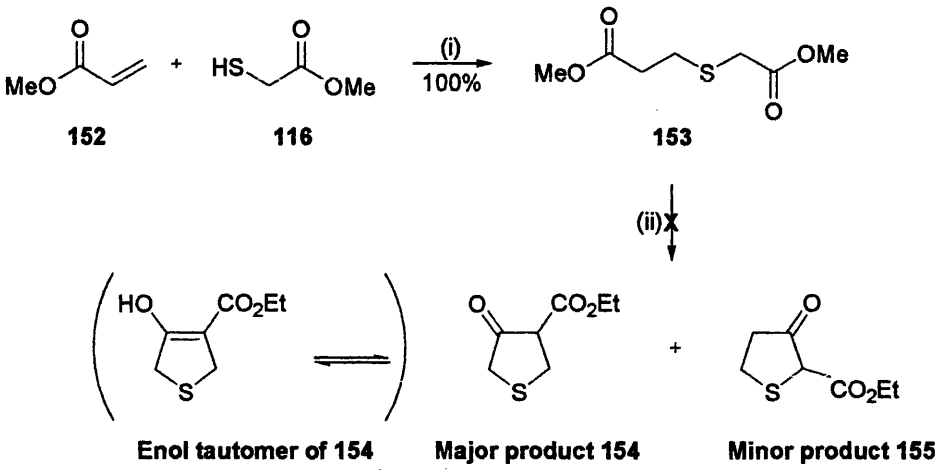

152 **116** **153**

Enol tautomer of 154 **Major product 154** **Minor product 155**

Scheme 68. Attempted synthesis of ethyl 4-oxotetrahydrothiophene-3-carboxylate **154** using the Shinkwin *et al.* method.[211] *Reagents and conditions: (i) piperidine, 45°C; (ii) NaOEt, EtOH, reflux.*

Woodward *et al.* interpreted the formation of isomer **155**, which was formed rapidly as a major product as low temperature (*i.e.* a kinetic product), was due to anion stabilisation by sulfur. However, at elevated temperature the major product was the isomer **154** (*i.e.* a thermodynamic product). The mechanisms of their formation are shown in Scheme 69.[212]

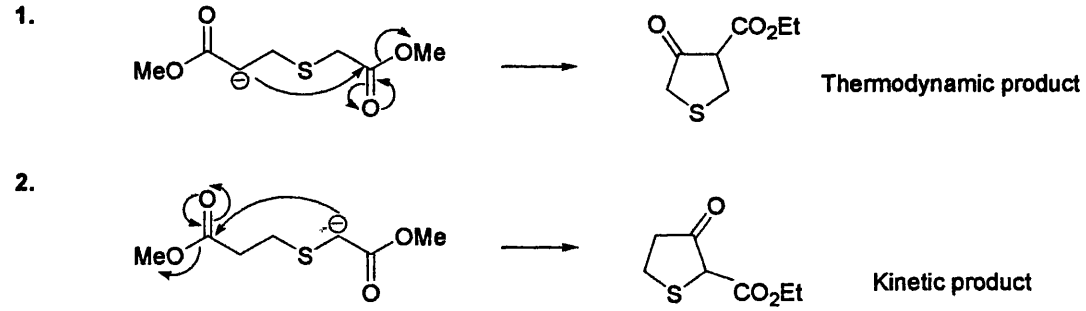

Scheme 69. Proposed mechanism of the formation of isomeric β-ketoesters **154** and **155**.[212]

Following the methods by Shinkwin *et al.*,[211] Dieckmann reagent **153** was obtained in quantitative yield from methyl acrylate **152** and methyl mercaptoacetate **116** with piperidine (Scheme 68). However, subsequent condensation using sodium ethoxide only afforded a mixture of unidentifiable products.

A different approach presented by Baraldi *et al.* was followed using methyl mercapto-acetate **116** and acrylonitrile **156** (Scheme 70).[213] This one-pot synthesis gave the required 3-oxotetrahydrothiophene-4-carbonitrile **(±)-157** *via* a Dieckmann-like condensation of the cycloadduct intermediate (formed *in situ*) in 50% yield. This

method provides the product **(±)-157** in good yield and avoids the possibility of the formation of regioisomers, as the cyano group has a stronger acidifying effect on its α–protons and is a weaker electrophile than CO_2Me. Thus **(±)-157** could be obtained in multi-gram scale.

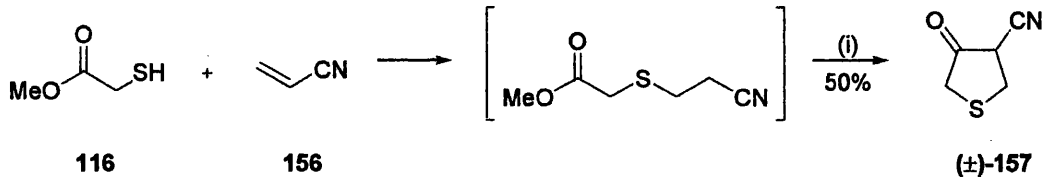

116 **156** **(±)-157**

Scheme 70. Dieckmann-like condensation of the Michael adduct between methyl mercaptoacetate **116** and acrylonitrile **156** gave **(±)-157** in moderate yield (50%). *Reagents and conditions: (i) NaOMe, MeOH, reflux.*

5.5 Synthesis of 3-benzyloxy-4-hydroxymethyltetrahydrothiophene

With **(±)-157** being readily accessible, many functional-group transformations could be performed to give the required functional groups at C-3 and C-4. The first step was to reduce the ketone to an alcohol. Hoffmann *et al.* described an asymmetric yeast reduction of methyl-4-oxotetrahydrothiophene-3-carboxylate and the corresponding alcohol was obtained as the (3*R*,4*R*)-isomer in 7 days.[214] This method was followed using **(±)-157** (*vide infra*, Scheme 71) but the reaction failed to show any progress even at raised temperature and extended reaction duration (10 days).

A non-enantioselective approach was sought with the aim to introduce the required relative configuration at a later stage. Reduction of **(±)-157** with $NaBH_4$ in EtOH was anticipated to give a 1:1 mixture of diastereomeric alcohols, as described by Baraldi *et al* (*vide infra*, Scheme 71).[215] However, a 2:3 mixture of products, which were separable by chromatography, was obtained instead. The more polar, minor product was unidentifiable. The ^1H NMR spectrum of the major compound showed only one set of proton signals, indicating that it is solely one diastereomeric alcohol **(±)-158**. The minor product was not the diastereomeric *cis* alcohol.

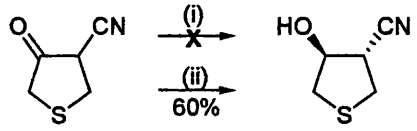

(±)-157 (±)-158

Scheme 71. Reductions of tetrahydrothiophene (±)-157. *Reagents and conditions: (i) bakers' yeast, sucrose, H_2O, RT to 50°C; (ii) $NaBH_4$, EtOH, 0°C.*

The ^1H NMR spectrum and subsequent two-dimensional NMR analyses of **(±)-158** were conducted in a 600 MHz spectrometer to improve separation of the proton signals. Assignment of the proton signals was made possible by the ^1H-^1H COSY spectrum. A strong cross-peak between the double doublet at δ 2.88 and the double doublet at δ 3.23 indicate that this pair of double doublets is due to the two geminal protons in the tetrahydrothiophene ring. A cross-peak was also noted between the signal at δ 2.88 and the quintet signal for 3-H at δ 4.71. It was reasoned that for a quintet signal to appear on the spectrum with such high downfield effect, it must be next to the electronegative oxygen of the OH with four neighbouring protons *i.e.* 3-H. This assignment was confirmed by the cross-peak between this quintet and the broad doublet for OH at δ 2.95. Therefore, the two double doublets at δ 2.88 and δ 3.23 must be the geminal protons at the 2-position to give a COSY cross-peak with 3-H. Correlation was observed between the multiplet for one proton at δ 3.09 and the multiplet for two protons at δ 3.17 to δ 3.20, indicating that the signal for the remaining pair of geminal protons at the 5-position coincided with the signal for 4-H. The location of both pairs of geminal CH_2 protons was confirmed using a ^1H-^{13}C COSY (HMQC) spectrum, which, together with a ^{13}C-DEPT spectrum, indicated that there are two CH_2 carbons in the molecule, as expected, with signals at δ 30.5 and δ 37.1. Cross-peaks between the latter and the signal for the 2-H geminal protons (as assigned in the ^1H-^1H COSY spectrum) show that these protons were attached to a CH_2 carbon. Therefore, the CH_2 carbon signal at δ 30.5 must be due to the carbon at the 5-position, and cross-peaks between this signal and the two multiplets at δ 3.09 and δ 3.17 to δ 3.20 confirm that these signals are due to the geminal CH_2 protons at the 5-position. Since the latter multiplet δ 3.17 to δ 3.20 integrates for two protons, the remaining proton must be that of 4-H and this was confirmed by a cross-peak in the HMQC spectrum between the carbon signal at δ 39.9 and the mutiplet.

Since the ^1H and ^{13}C NMR spectra indicated the presence of only one diastereoisomer, the NOESY spectrum was studied to establish the relative configuration of alcohol

(±)-158 (Figure 41). However, overlap of connectivities and the presence of artefacts in the tetrahydrothiophene ring region of δ 2.8 to δ 3.3 made interpretation of the conformation and configuration difficult. A cross-peak was observed between 3-H and the OH as expected. Interestingly, the cross-peak between 3-H and 4-H was very weak, suggesting that these protons are far apart in space and thus might be *trans* to each other. The lack of a cross-peak between the 2-H at δ 2.88 and 3-H indicates that they are remote in space to each other and thus it is likely that this 2-H proton is the pseudo-axial geminal proton at the 2-position.

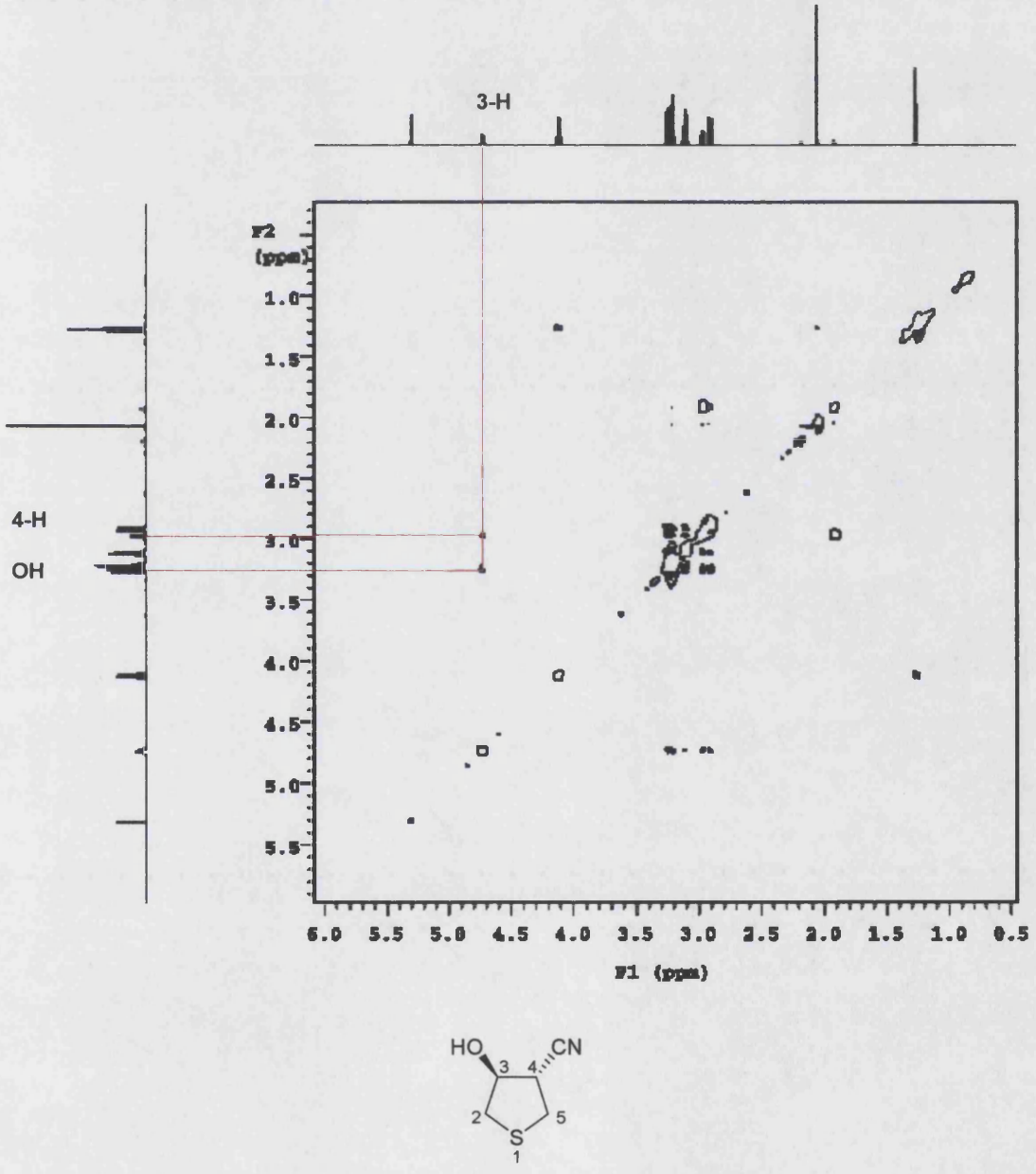

Figure 41. ^{1}H-^{1}H NOSEY spectrum of (±)-*trans*-3-hydroxytetrahydrothiophene-4-carbonitrile **(±)-158**.

Although the ^1H NMR analysis indicated that alcohol **(±)-158** was only one diastereoisomer, it was unclear, at this stage, which diastereoisomer this was. Therefore, it was decided that alcohol **(±)-158** would be used in a series of experiments to explore different chemical approaches to a tetrahydrothiophene compound with the required functional groups at C-3 and C-4. Once synthetic difficulties have been clarified and an efficient sequence has been devised, it would be possible to study the configuration at C-3 and C-4 at a later stage by ^1H and ^{13}C NMR analysis or X-ray crystallography on crystalline products.

1. Synthetic approaches to the 2-deoxy-*D*-ribose analogue template

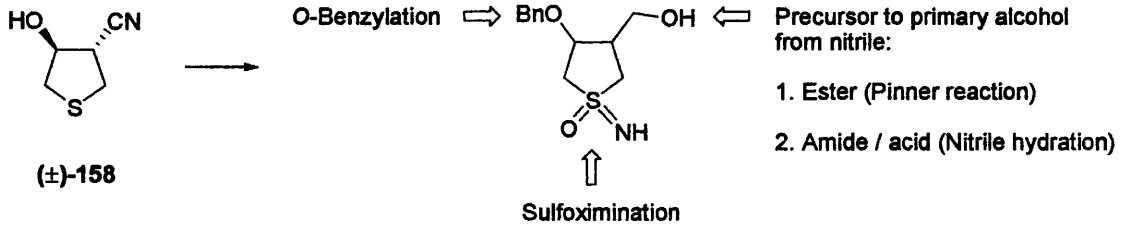

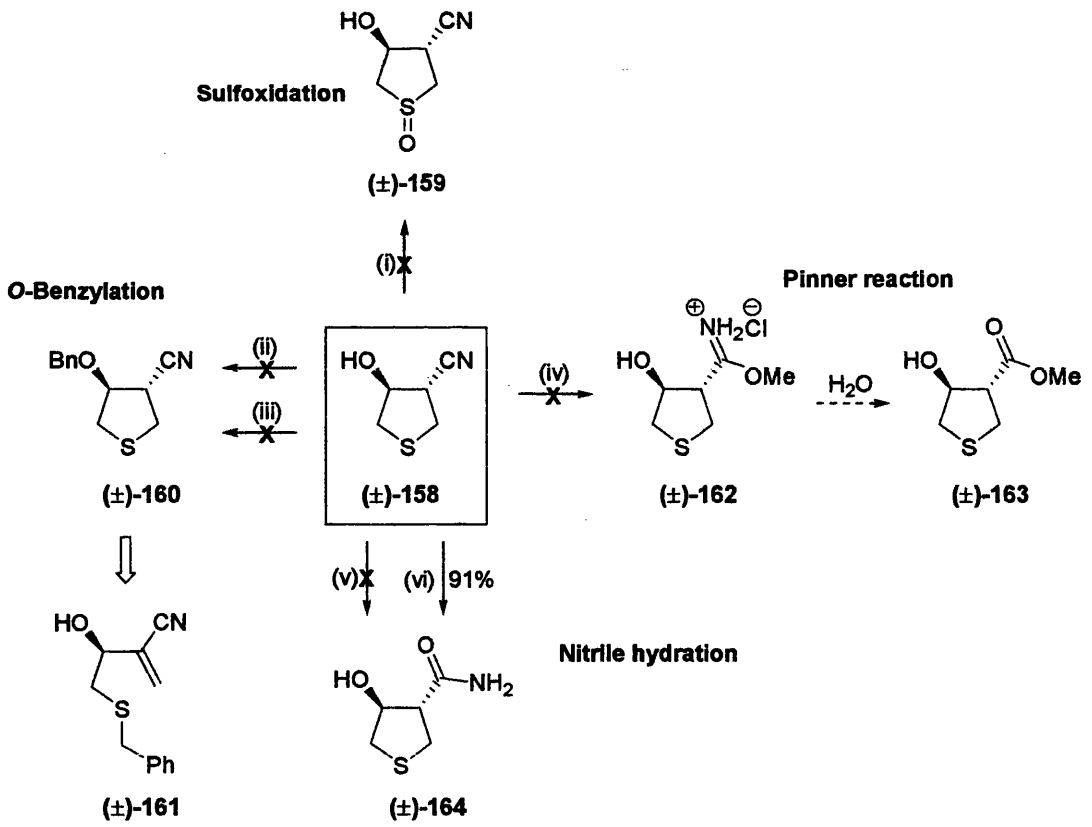

Scheme 72. Attempted functional group introductions for **(±)-158**. *Reagents and conditions: (i) mCPBA, DCM, 0°C; (ii) LHMDS, BnBr, THF, –78°C; (iii) K_2CO_3, BnBr, THF; (iv) dry HCl, MeOH; (v) 35% aq. H_2O_2, NaOH, EtOH, H_2O, 50°C; (vi) HCl, 50°C.*

Many attempts were made to perform functional group transformations on **(±)-158** as illustrated in Scheme 72 (*vide supra*). Oxidation with *m*CPBA did not furnish the corresponding sulfoxide **(±)-159** and led only to decomposition of the starting compound **(±)-158**.

An attempt was made to protect the secondary alcohol as the *O*-benzyl derivative. The alkoxide was formed by treatment with LHMDS but subsequent reaction with benzyl bromide did not give the anticipated product **(±)-160** (*vide supra*, Scheme 72). The ^{1}H NMR spectrum of the obtained product showed the signals for two distinctive alkenyl protons as two doublets for two protons at δ 6.02. A pair of double doublets for two protons appeared in the region normally occupied by the 2- and 5-protons of the five-membered tetrahydrothiophene ring, at δ 2.63 and δ 2.84. Furthermore, a broad singlet signal of an OH coincided with the latter, confirming that the *O*-benzylation did not occur as anticipated. A sharp singlet at δ 3.77 for two protons reveals the presence of a benzyl CH_2 group at a chemical shift appropriate for SCH_2Ph. The singlet also suggested that the benzyl group was remote from any chiral centre.

These 1-D ^{1}H NMR data, together with the low-resolution mass spectrum, showed that the product was a structural isomer of the expected benzyloxy tetrahydrothiophene. Two-dimensional NMR analyses were carried out to elucidate its structure. In the ^{1}H-^{1}H COSY spectrum, the cross-peak between the double doublets at δ 2.63 and δ 2.84 confirmed that these signals are due to the geminal protons. There were also COSY correlations between these peaks and the multiplet at δ 4.15. The chemical shift of the latter corresponds more to the C<u>H</u>OH of an allylic alcohol than a simple secondary saturated alcohol. The NOESY spectrum was particularly informative. As expected, there were NOESY cross-peaks between the signals at δ 2.63, δ 2.84 and δ 4.15 of the previously-identified $SCH_2CH(R)O$ spin system (*vide infra*, Figure 42). A cross-peak was seen between the singlet at δ 3.77 and the signal for the phenyl protons, confirming the presence of an S-benzyl group. Thus the product is likely to contain $PHCH_2SCH_2CH(R)O$. No NOE connectivities were seen from the alkene signals to other protons, indicating that they are remote in space. These data, together with the observation of a nitrile band in the IR and the high-resolution MS data, indicated that the structure was the ring-opened product **(±)-161**, as shown in Scheme 73 (*vide infra*).

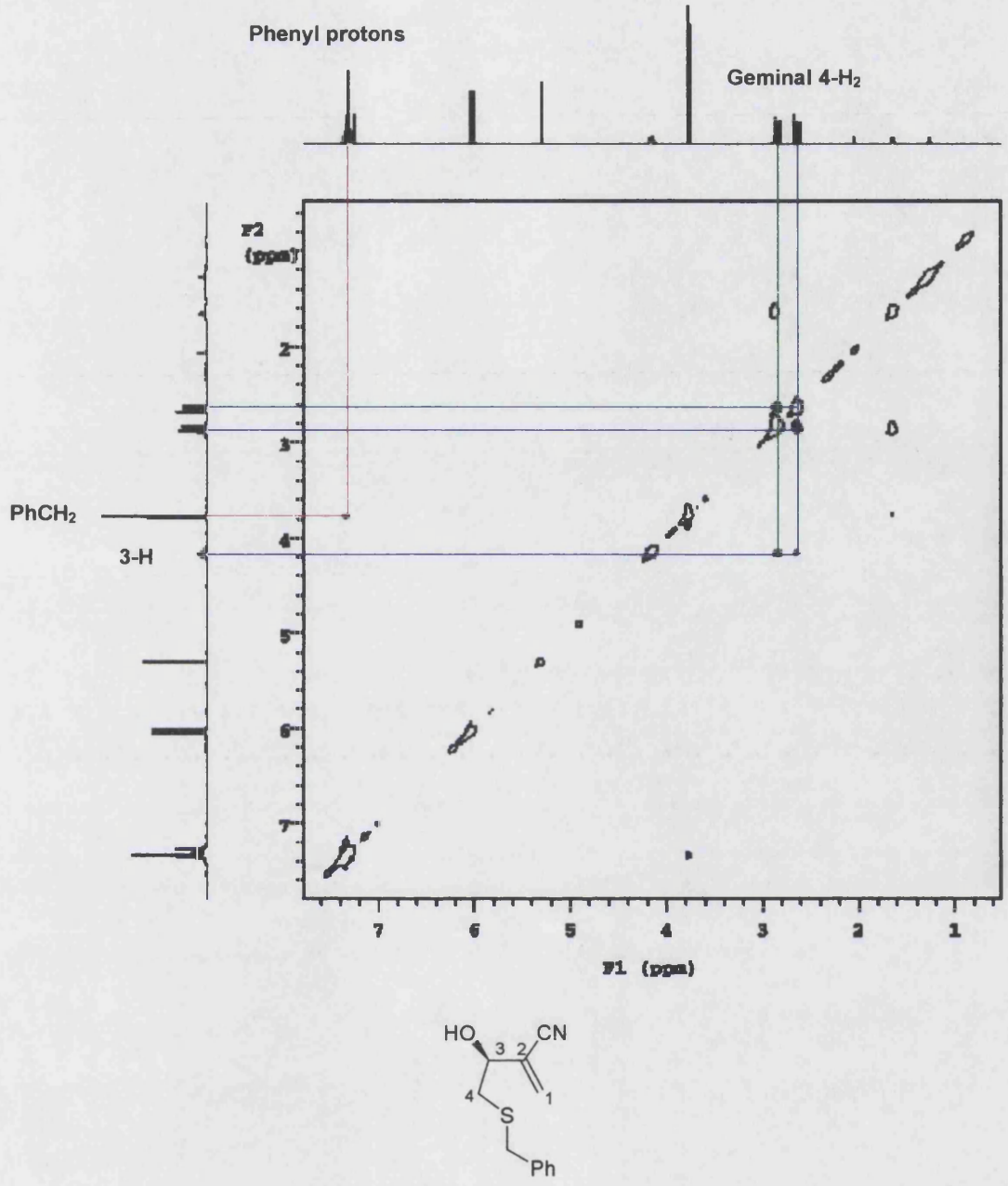

Figure 42. ^{1}H-^{1}H NOESY spectrum of 4-benzylthio-3-hydroxy-2-methylenebutanenitrile **(±)-161**.

Since LHMDS is a relatively strong base, it was postulated that removal of 4-H of **(±)-158** by the oxygen anion formed led to the elimination product **(±)-161** by a reverse aldol-like process (*vide infra*, Route A, Scheme 73). Therefore, a weaker base (K_2CO_3) was employed in the subsequent attempt. Interestingly, the same alkenyl product was obtained. Since the ring-opening could be triggered by even a weak base, it was concluded that this side-reaction was caused by the nucleophilic attack of the sulfur to BnBr. In Route A (*vide infra*, Scheme 73), the alkoxide is readily generated by the strong base $^{-}N(SiMe_3)_2$. This alkoxide is *cis* to the acidic proton α to the nitrile,

facilitating the generation of a carbanion-like intermediate and triggering the elimination. The thiolate formed would then react rapidly with the benzyl bromide. However, RS^- is only a moderate leaving group and rapid elimination by Route A is unlikely to be triggered by the weaker base K_2CO_3. Thus Route B (Scheme 73) is proposed to be the mechanism followed. Nucleophilic attack of the sulfide on the benzyl bromide would give an intermediate sulfonium. This is now an excellent leaving group for the elimination triggered either by direct removal of the C–H or by initial formation of the alkoxide and subsequent intramolecular proton transfer.

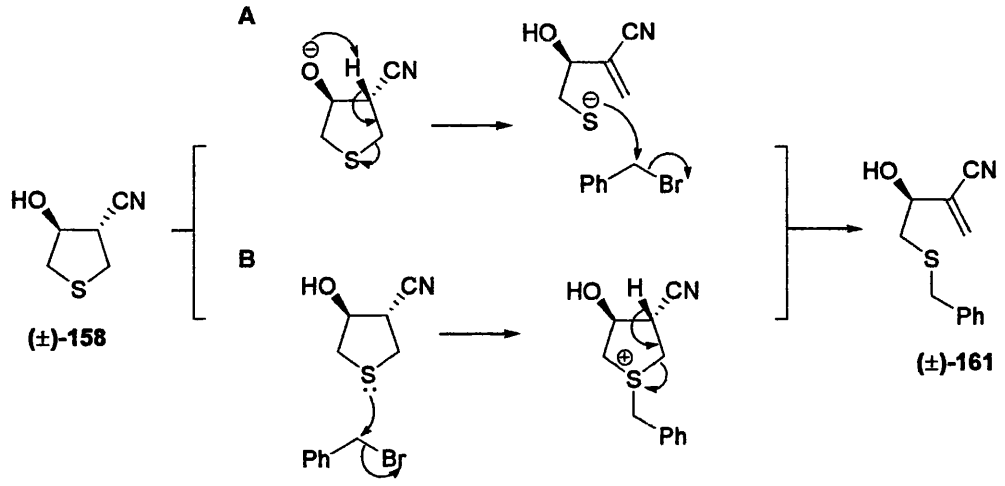

Scheme 73. Proposed mechanisms of the base-catalysed ring-opening of **(±)-158**, leading to the formation of alkenyl compound **(±)-161**. Route A refers to the mechanism initially proposed upon reaction with a strong base (LHMDS). However, despite the use of a weaker base (K_2CO_3), the same ring-opened product was observed, leading to the conclusion that Route B is the mechanism followed.

Attempted conversion of the nitrile to the methyl ester **(±)-163** using Pinner reaction conditions (dry HCl, MeOH) led only to the decomposition of starting material (*vide supra*, Scheme 72). Pinner reaction is the reaction of nitriles with alcohols *via* the formation of an imino ether hydrochloride salt (imidate) **(±)-162** catalysed by acid. Imidate salts are relatively unstable compounds and are quickly hydrolysed in water to form the corresponding esters.

Hydration of the nitrile **(±)-158** to amide **(±)-164** was attempted using two methods (*vide supra*, Scheme 72). Watson *et al.* described a H_2O_2/NaOH system as a useful method for hydration of aromatic nitriles, giving the corresponding amides in almost quantitative yield.[79] According to Payne and Williams,[216] nucleophilic addition of the peroxide ion (HOO^-), a much more powerful nucleophile than HO^-, to the carbon atom of the nitrile triple bond forms a peroxyimine intermediate (*vide infra*, Scheme 74). The

latter is then capable of oxidising another molecule of H_2O_2 to give the corresponding amide. However, reaction of nitrile **(±)-158** under the same conditions failed to give the amide **(±)-164** and led to decomposition of the starting material (*vide supra*, Scheme 72).

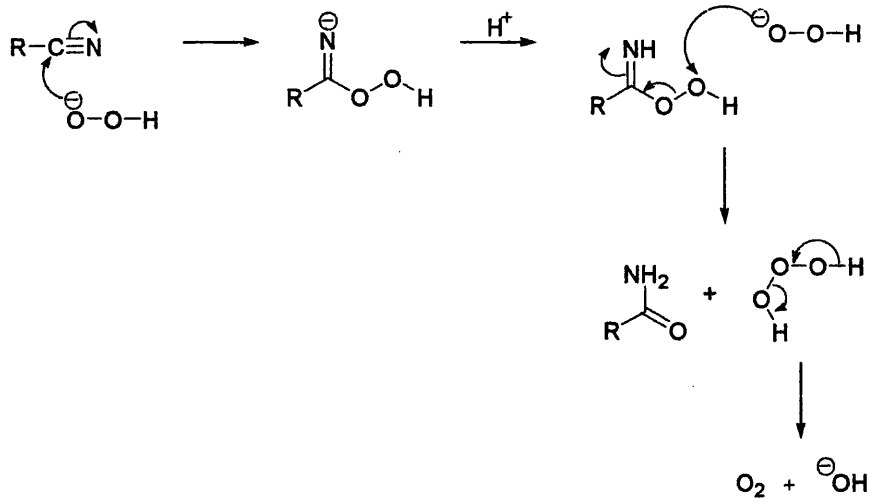

Scheme 74. Proposed mechanism of the hydrogen peroxide-assisted hydrolysis of nitriles by Payne and Williams.[216]

Acid-hydrolysis of the nitrile compound **(±)-158** generated 4-hydroxytetrahydro-thiophene-3-carboxamide **(±)-164** (*vide supra*, Scheme 72). Work-up of this reaction was studied: Dehli *et al.* reported a HCl hydrolysis of a cyclopentanecarbonitrile derivative and the reaction mixture was neutralised with NaOH and $NaHCO_3$, and the corresponding amide was afforded in 96% yield by continuous extraction of the neutralised reaction mixture with EtOAc.[217] This work-up procedure was followed and gave the amide **(±)-164** in moderate yield (40%). An alternative work-up was sought to improve yield. It was postulated that the formation of a slurry mixture at the neutralisation stage and the need for continuous extraction with an organic solvent might contribute to the loss of product. Thefore, HCl was removed directly *in vacuo*, and the evaporation residue was triturated with Et_2O to give **(±)-164** in a much higher yield.

The ^1H NMR spectrum of **(±)-164** showed two broad singlets each for one proton at δ 7.00 and δ 7.40, indicating the presence of a carboxamide NH_2. The OH proton resonated at δ 5.29 as a sharp doublet for one proton. The NH signal at δ 7.40 is due to intramolecular hydrogen bonding (with either the OH oxygen or the carbonyl oxygen), leading to a downfield effect of the NH proton. One of the geminal 2-H protons gave a

double doublet at δ 2.60. With this information and the ^{1}H-^{1}H COSY spectrum, assignment of protons was possible. A cross-peak between the 2-H at δ 2.60 and the double doublet at δ 2.91 for one proton indicates that the latter signal is due to the partner 2-H proton. This was confirmed by the ^{1}H-^{13}C COSY (HMQC) spectrum, showing the two CH_2 carbon signals at δ 29.9 and δ 36.4. Cross-peaks between the two 2-H protons and the carbon signal at δ 36.4 show that these protons were directly attached to a CH_2 carbon. Therefore, the remaining CH_2 carbon at δ 29.9 must be C-5, and correlation between this carbon and the multiplet at δ 2.81 to δ 2.89 in the HMQC spectrum indicates that these protons are the geminal 5-H protons. A cross-peak between the 2-H protons and the quintet at δ 4.32 indicates that the latter is due to 3-H. Cross-peaks were also noted between 3-H and OH. A cross-peak was observed between 3-H and a double doublet at δ 2.71, indicating that this signal is due to 4-H.

The NOESY spectrum of **(±)-164** showed the expected connectivity between the 2-H proton at δ 2.60 and its geminal partner at δ 2.91. Interestingly, no connectivities were observed between the remaining protons in the tetrahydrothiophene ring (5-H protons, 3-H, 4-H), with only weak NOE connections between the two carboxamide NH_2 protons. Thus the NOESY spectrum did not allow determination of the relative configuration.

Therefore, to aid the assignment of the relative configuration of compound **(±)-164** and thus of the precursor nitrile **(±)-158**, a ^{1}H NMR study was performed by the formation of a bicyclic system. Condensation of **(±)-164** with 2,2-dimethoxypropane (DMP) under acid catalysis gave an inseparable mixture of two compounds in a 3:2 ratio (*vide infra*, Scheme 75). ^{1}H NMR analysis of the mixture indicated that the major product was the thienooxazinone **(±)-165**. The spectrum of the minor product showed a tetrahydro-thiophene ring, two C-methyl groups, one OH doublet, one broad singlet and a methoxy group. Its structure is therefore proposed to be the non-ring-closed intermediate **(±)-166**.

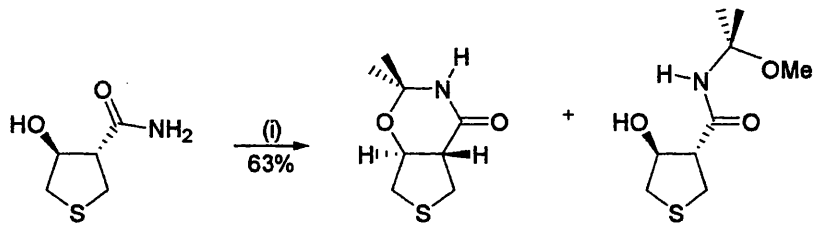

(±)-164 (±)-165 Major (±)-166 Minor

Scheme 75. Configuration of compound (±)-**164** was assigned *via* the formation of the oxazin-2-one derivative (±)-**165**. A non-ring-closed product (±)-**166** was also generated in the DMP/*p*-TsOH reaction. *Reagents and conditions: (i) DMP, p-TsOH, acetone, reflux.*

There was extensive overlap of NMR signals in the region δ 2.4 to δ 3.2, making measurement of individual coupling constants difficult. However, the 7a-proton of the bicycle (±)-**165** gave a discrete double triplet signal at δ 4.17, with coupling constants of J = 6.2 Hz, 10.5 Hz. Since 7a-H cannot couple to *both* protons at the 7-position with large coupling constants of J = 10.5 Hz, owing to Karplus considerations, one of the J = 10.5 Hz couplings must be between 7a-H and 4a-H. This value of J = 10.5 Hz indicates that these protons are both axial with respect to the six-membered ring and thus must be *trans* to each other, confirming the *trans* relative configuration of the precursor amide (±)-**164** and the precursor nitrile (±)-**158**.

Two-dimensional NMR analyses were also performed on the mixture of (±)-**165** and (±)-**166**. The COSY spectrum showed the expected coupling relationships. In particular, a cross-peak connected the doublet signal at δ 5.23 to the 3-H in the monocycle (±)-**166**, confirming that the former is due to the OH. The NOESY spectrum was informative (*vide infra*, Figure 43). For both compounds, cross-peaks indicating through-space connectivity were seen between the C-Me signals and the NH singlets. This allowed assignment of the broad singlet at δ 7.61 as arising from the NH of the monocycle (±)-**166** and that at δ 8.10 to the NH of the bicycle (±)-**165**. In (±)-**166**, there was also a cross-peak connecting the NH and the 3-H signal but the corresponding cross-peak (NH–7a-H) was absent for (±)-**165**. These observations are consistent with the control of the orientation of the N–H bond in the oxazinone ring holding it away from the 7a-H. Interestingly, in (±)-**165**, there is a cross-peak connecting 7a-H with the C-Me signal at δ 1.40, confirming that this signal is due to the methyl group *cis* to the 7a-H.

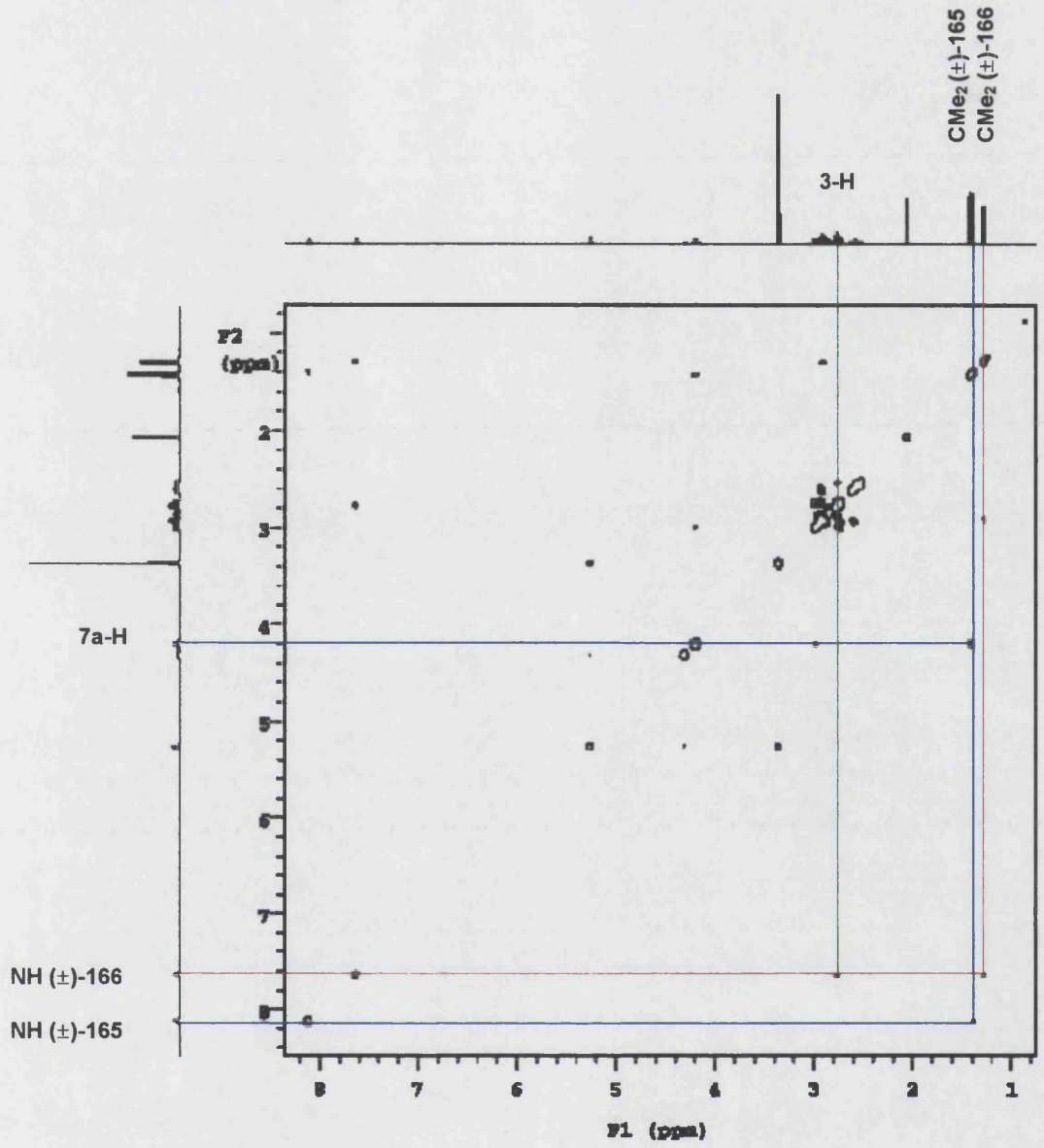

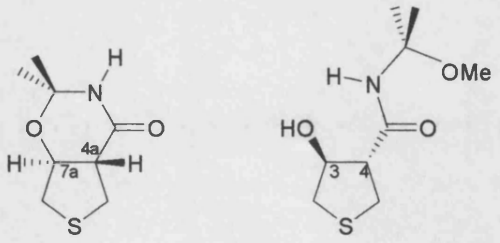

(±)-165 (±)-166

Figure 43. ^{1}H-^{1}H NOESY spectrum of (±)-*trans*-2,2-dimethylhexahydrothieno[3,4-e][1,3]oxazin-4-one **(±)-165** and (±)-*trans*-3-hydroxy-N-(1-methoxy-1-methylethyl)tetrahydrothiophene-4-carboxamide **(±)-166**.

MM2 energy-minimised calculations were also carried out to confirm the relative configuration of **(±)-165**. For the *trans*-model where 7a-H and 4a-H are *trans*-diaxial to

each other with respect to the six-membered ring [**(3)**, Figure 44], dihedral angle (4a-H)-(4a-C)-(7a-C)-(7a-H) of 177° was calculated which is consistent with the coupling constant of ^{3}J = 10.5 Hz. Two *cis*-compounds were similarly studied and dihedral angles (4a-H)-(4a-C)-(7a-C)-(7a-H) of 50° and 8° were calculated for the *cis*-diaxial [**(1)**, Figure 44] and *cis*-diequatorial [**(2)**, Figure 44] bicycles, respectively. These are inconsistent with the coupling constant ^{3}J of 10.5 Hz. In addition, modelling of structure **(2)** revealed severe ring strain, with the five-membered tetrahydrothiophene ring to be twisted out-of-plane, making this structure highly unfavourable.

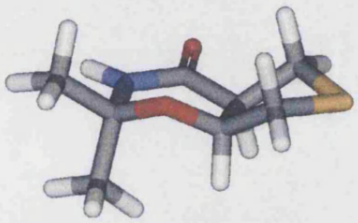

(1)

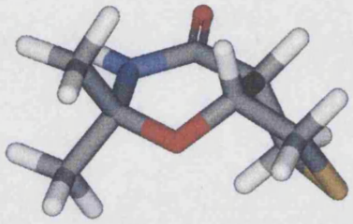

(2)

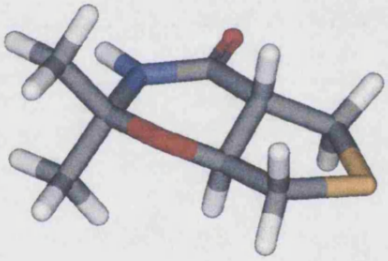

(3)

Figure 44. MM2-energy minimised models of the three relative configurations of **(±)-165**. The red colour refers to oxygen, the yellow refers to sulfur, the blue refers to nitrogen and the grey refers to the carbon atom. Structure **(1)** represents a *cis*-configuration with dihedral angle (4a-H)-(4a-C)-(7a-C)-(7a-H) = 8°. Structure **(2)** represents a *cis*-configuration with dihedral angle (4a-H)-(4a-C)-(7a-C)-(7a-H) = 50°. Structure **(3)** is a *trans*-configuration with dihedral angle (4a-H)-(4a-C)-(7a-C)-(7a-H) = 177°.

Although the NMR data suggested that amide **(±)-164** is only one diastereoisomer, it was not clear whether this is the *cis*- or *trans*-isomer. Therefore, crystals were grown in an EtOAc/EtOH system and X-ray analysis was conducted to study the relative configuration at C-3 and C-4. It is notable that, even though the bulk sample was racemic, individual crystals contained one enantiomer only. X-ray crystallography data of **(±)-164** provided information on the relative configuration as illustrated in Figure 45 (*vide infra*). A vicinal coupling constant of ^{3}J ~ 7.9 Hz was measured between 3-H and 4-H, which is consistent with dihedral angle (C3-C)-(C3-H)-(C4-C)-(C4-H) = 172°,

indicating a *trans*-diaxial configuration. A three-bond coupling constant of ^{3}J ~ 7.3 Hz was measured between 3-H and one of the geminal protons at C(2). This is consistent with dihedral angle (C3-H)-(C3-C)-(C2-C)-(C2-H_A) = 162°. Dihedral angle (C3-H)-(C3-C)-(C2-C)-(C2-H_B) = 42° was calculated between 3-H and the other geminal proton at C(2), and this is also consistent with a three-bond coupling constant of ^{3}J ~ 5.9 Hz. Due to overlap of proton signals in the ^{1}H NMR spectrum, coupling constants could not be determined between 4-H and the geminal protons at C(5). The corresponding dihedral angles (C4-H)-(C4-C)-(C5-C)-(C5-H_A) = 36° and (C4-H)-(C4-C)-(C5-C)-(C5-H_B) = 156° were calculated. The two substituents are gauche with respect to the C(3)-C(4) bond with dihedral angle C(41)-C(4)-C(3)-O(3) = 67°.

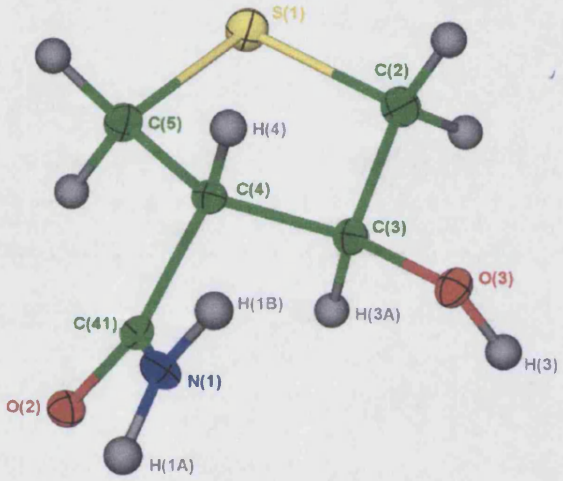

Figure 45. X-ray crystal structure of (±)-*trans*-3-hydroxytetrahydrothiophene-4-carboxamide **(±)-164**, with crystallographic numbering.

Interestingly, despite the presence of neighbouring primary carboxamide and alcohol groups, no intramolecular hydrogen bonding was observed in the crystal of **(±)-164**. Intermolecular hydrogen-bonding interactions were observed in the crystal structure of **(±)-164** from the three hydrogen-bond donors (two N–H bonds and one O–H) and both hydrogen-bond acceptors (carbonyl C=O and alcohol O). The N–H *cis* to the carbonyl oxygen makes a hydrogen bond to the alcohol oxygen of an adjacent molecule B whereas the N–H *trans* to the carbonyl oxygen hydrogen bonds to the carbonyl oxygen of a third molecule C. A hydrogen bond between the carbonyl oxygen and an N–H of molecule B completes a hydrogen-bonded ring in the structure. Finally, a chain is formed by the hydrogen bond between the O–H and a carbonyl oxygen of a fourth molecule D above (*vide infra*, Figure 46).

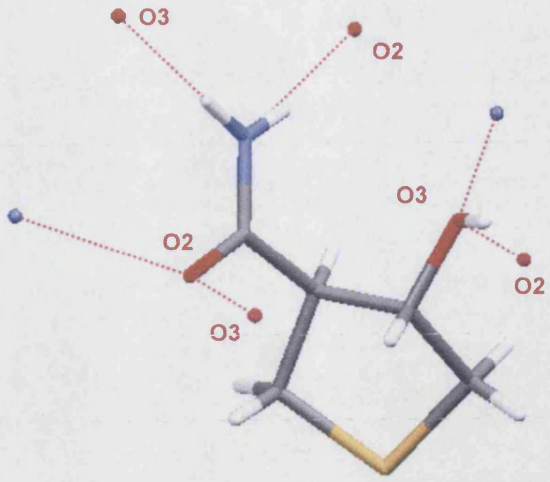

Figure 46. X-ray crystal structure of **(±)-164**, showing the intermolecular hydrogen-bonding interactions. The red colour refers to oxygen, the yellow refers to sulfur, the blue refers to nitrogen and the grey refers to the carbon atom.

Having obtained this key amide intermediate **(±)-164** and assigned the relative configuration, further approaches to perform functional group transformations were explored. The primary goal was to develop reliable and efficient synthetic routes to the required functional groups at C-3 and C-4 in the racemic series, so that the single enantiomer could be prepared later.

2. Synthetic approaches to the 2-deoxy-*D*-ribose analogue template

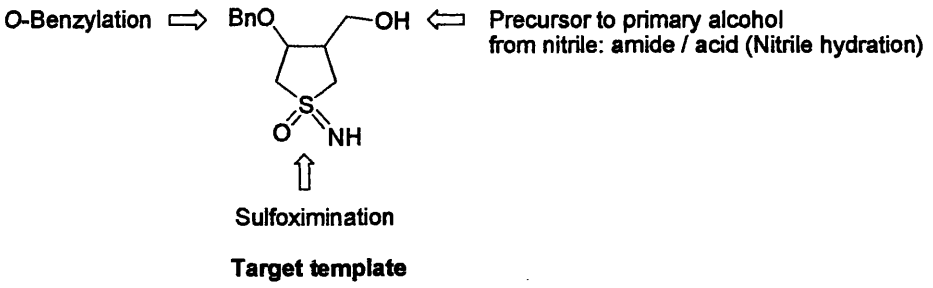

Pathway A

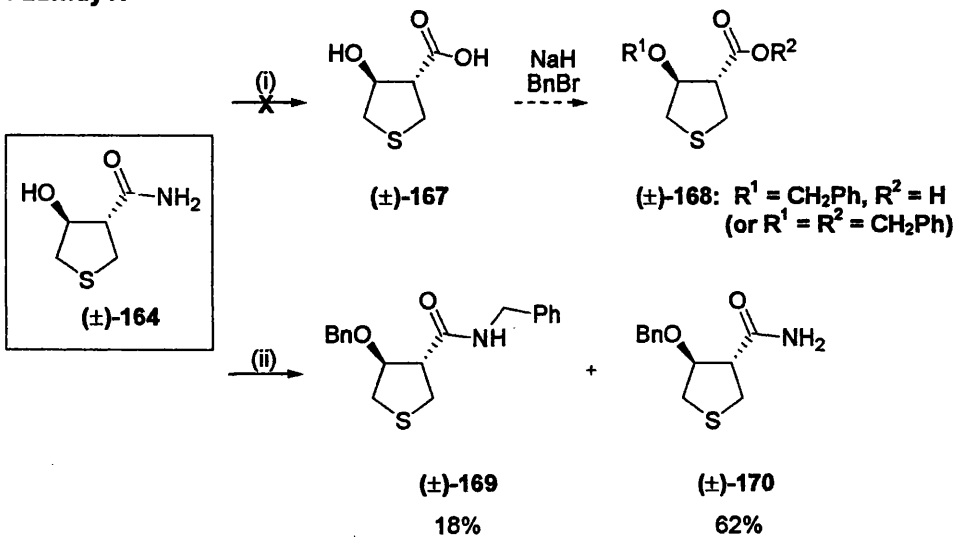

Pathway B

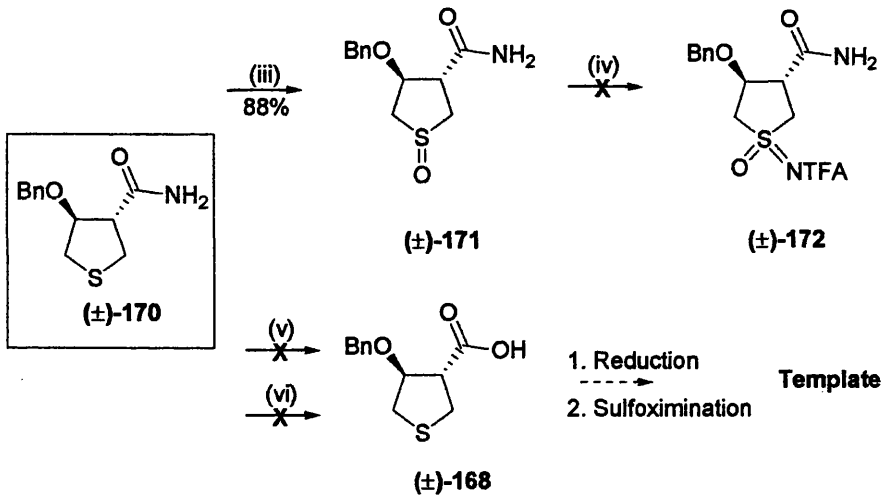

Scheme 76. Synthetic approaches to the 2-deoxy-*D*-ribose analogue **38a**. *Reagents and conditions: (i) HCl, 50°C; (ii) NaH, BnBr, DMF, 0°C; (iii) mCPBA, DCM, -40°C; (iv) CF_3CONH_2, $Rh_2(OAc)_4$, MgO, $PhI(OAc)_2$, DCM; (v) HCl, 50°C; (vi) TFA, H_2O, 130°C.*

Initial investigations concentrated on converting the amide group to an acid with or without prior *O*-benzylation at the 3-OH. Reduction of the acid intermediate **(±)-168** to a primary alcohol, followed by sulfoximination, would lead to the 2-deoxy-*D*-ribose analogue **38a** [*vide supra*, step (i), Pathway A, Scheme 76]. The synthetic sequence commenced with acid-hydrolysis of carboxamide **(±)-164** [*vide supra*, step (i), pathway A, Scheme 76]. The corresponding carboxylic acid derivative **(±)-167** formed would then be *O*-benzylated to give the mono- and the dibenzylated tetrahydrothiophenes. Both derivatives could be reduced to give the desired tetrahydrothiophene derivative with a primary alcohol at C-4 and *O*-benzylation at the 3-OH. However, the acid-hydrolysis failed to generate the carboxylic acid compound **(±)-167** and the reaction led only to decomposition of the starting material.

Therefore, it was decided that the protection of the 3-OH of **(±)-164** would be performed and the resulting amide compounds **(±)-169** and **(±)-170** could be hydrolysed to the carboxylic acids. As reported previously (*vide supra*, Section 3.2.2), *O*-benzylation using an equivalent amount of benzyl bromide and freshly-washed (in pentane) sodium hydride gave the best result in terms of yield of the monobenzylated product and ratio of mono- and dibenzylation. The strong base sodium hydride is capable of removing both OH and NH protons but, since only one equivalent was used, it was expected that only the more acidic OH proton would be abstracted. Since only the alkoxide and amide-derived anions could be nucleophilic enough to react with the benzyl bromide, some nitrogen-based anion must have been formed to give the corresponding secondary amide. However, in this current synthesis, both the mono- and dibenzylated compounds could be used in the subsequent hydrolysis of the amide to the carboxylic acid, since the nitrogen (and its appended benzyl group) would be lost from both substrates. Therefore, compound **(±)-164** was treated with an equivalent amount of benzyl bromide and the reaction gave the di- and monobenzylated products **(±)-169** and **(±)-170** in 18% and 62% yields, respectively [*vide supra*, step (ii), pathway A, Scheme 76]. It is noteworthy that the S-benzylation and reverse aldol-like ring-opening seen with the corresponding nitrile compound **(±)-158** (*vide supra*, Scheme 73) did not occur during benzylation of the amide **(±)-164**. Perhaps the benzyl electrophile is consumed rapidly by both the oxygen and nitrogen nucleophiles before it can react at the sulfur. Moreover, the reverse aldol will be less favoured in the present carboxamide system, as the carboxamide carbonyl is less able to stabilise the intermediate α-anion than is the nitrile.

Sulfoximination was studied using the monobenzylated amide compound **(±)-170**. Oxidation with *m*CPBA gave the corresponding sulfoxide **(±)-171** in good yield [*vide supra*, step (iii), pathway B, Scheme 76].[218] The ^{1}H NMR spectrum of the sulfoxides showed the presence of two diastereoisomers in a 7:1 ratio. Both diastereoisomers retained the *trans* relationship at the C3–C4 bond and must therefore arise from different configurations at the chiral sulfur atom. It could not be determined whether the major isomer had the sulfoxide oxygen *cis* to the carboxamide or to the benzyl ether; arguments could be put forward for the formation of either through hydrogen-bonding of the peroxyacid to the amide carbonyl oxygen or to the ether oxygen leading to two alternative modes of stereocontrol. The diastereomeric mixture of sulfoxides was then subjected to the usual Rh(II)-catalysed imination conditions [*vide supra*, step (iv), pathway B, Scheme 76] to generate the cyclic sulfoximine **(±)-172**, but no reaction was evident.

Attempted acid-hydrolysis, with aqueous hydrochloric acid and with aqueous trifluoro-acetic acid, of the amide of compound **(±)-170** led only to decomposition of starting materials, rather than affording the desired carboxylic acid **(±)-168** [*vide supra*, steps (v) and (vi), pathway B, Scheme 76].

The failure to introduce a sulfoximine moiety and to synthesise an appropriate primary alcohol precursor at the C-4 centre meant that the route outlined in Scheme 54 (*vide supra*) was no longer viable. Since the above route of conversion to the carboxylic acid, followed by reduction to the primary alcohol, was not possible, the reverse sequence of reduction of the amide, followed by conversion of the primary amine to a primary alcohol (*e.g.* by nitrosation) was investigated. Reduction of the carboxamide **(±)-170** with LAH in boiling THF gave the primary amine **(±)-173** (Scheme 77). For ease of isolation, this was benzoylated *in situ* (after the aqueous quench) and the benzamide **(±)-174** was obtained in good yield.

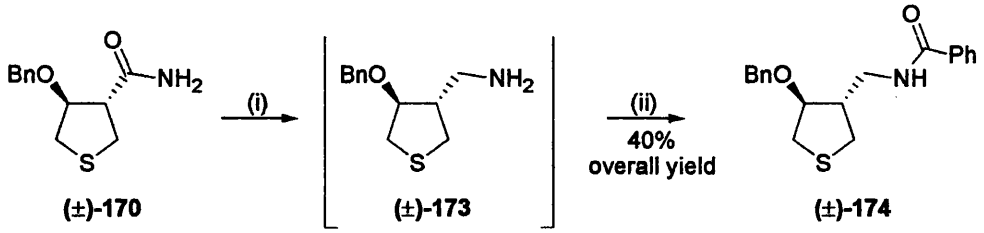

Scheme 77. Synthesis of the benzamide compound **(±)-174**. *Reagents and conditions: (i) $LiAlH_4$, THF, reflux; (ii) Et_3N, BzCl, DCM.*

In this section of the project, appropriately 3,4-disubstituted tetrahydrothiophene intermediates have been successfully synthesised through a key Dieckmann cyclisation. These have the correct *trans* stereochemical relationship between the protected 3-oxygen substituent and the one-carbon unit at C-4. It only remains to develop methods for imination at the sulfoxide and conversion of the carboxamide to a CH_2OH group.

Chapter 6 Conclusions

6.1 Conclusions

Various synthetic strategies were explored towards potential inhibitors for TP, PARP-1 and IMPDH, incorporating a sulfoximine group. These target compounds include the 2-deoxy-*D*-ribose-1α-phosphate analogue **37** and the 2-deoxy-*D*-ribose analogue **38a** as TP inhibitors, the benzamide 2-deoxyriboside mimic **39** and the transition-state analogue **40** for the inhibition of PARP-1, and upon conversion to the corresponding dinucleotide with adenosine, **39** is expected to be an inhibitor of IMPDH. The design of these cyclic sulfoximine mimics of ribosides and 2-deoxyribosides centres on the replacement of the anomeric carbon by the tetrahedral sulfoximine.

The initial synthetic plan relied on addition of an anion derived from a S-methyl-sulfoximine to a protected glyceraldehyde. The targets contain three chiral centres, one of which was supplied in the glyeraldehyde, one supplied as the sulfoximine and one being generated during the addition step. Some diastereocontrol may have been expected. Model reactions were investigated to study this novel addition. Several routes were investigated to produce sulfoximines from sulfoxides but the most effective was found to be the rhodium-catalysed oxidative imination of sulfoxides with trifluoro-acetamide and iodosobenzene diacetate. Treatment of anions derived from N-Boc-protected and N-$SiMe_3$-protected S-methyl-S-phenyl sulfoximines with a range of aldehydes gave only low yields of the required secondary alcohols, along with some products of elimination. These additions were also found to be difficult to reproduce, with frequent degradation of the substrates and reduction of the aldehydes.

In an alternative scheme, a four-carbon unit, carrying two of the chiral centres, was to be attached to the sulfur of a 3-substituted thiophenol; the sulfoximine was then to be generated and cyclised to the target riboside mimic. Diethyl *R,R*-tartrate supplied the four-carbon unit with the correct configurations and was readily converted into 4*S*,5*S*-4,5-di(hydroxymethyl)-2,2-dimethyl-1,3-dioxolane. This C_2-symmetric compound was desymmetrised by monobenzylation and the remaining primary alcohol was replaced by phenylthio- and 3-bromophenylthio groups by a thio-Mitsunobu coupling. Sulfoxidation proceeded without diastereocontrol but imination at sulfur gave separable diastereoisomers of the sulfoximines. These were identified by X-ray crystallography. Removal of the acetal protection revealed the vicinal diol but two preliminary attempts to use an intramolecular Mitsunobu reaction did not give the cyclised product. Thus the required carbon and sulfur framework of the target compounds has been assembled

successfully, with appropriate functionality and with the correct configurations at all the chiral centres. It only remains to develop a cyclisation method to complete this sequence.

Synthetic approaches to the second series of targets, such as **38a** and **40**, were also studied. The first strategy involved assembly of the tetrahydrothiophene ring from a C–C unit and a C–S–C unit through a dipolar cycloaddition. The C–C dipolarophile was to carry a chiral auxiliary. (*E*)-3-Benzyloxypropenoic acid was synthesised but could not be converted into the corresponding N-acyl-camphorsultam. The menthyl ester, however, was accessible. The 1,3-dipole, $H_2C{=}S^+{-}CH_2^-$ was to be generated *in situ* from a silylmethyl chloromethyl sulfide by desilylation with fluoride. However, the trimethylsilyl reagent was too volatile to be isolated. Increasing the molecular weight (and therefore decreasing the volatility) by having larger substituents on the silicon led to severe synthetic difficulties. Attempted 1,3-dipolar cycloaddition of a crude sulfur 1,3-dipole and a representative chiral dipolarophile only led to decomposition of starting materials.

Following an alternative strategy, a Dieckmann cyclisation furnished the racemic 3-oxo-tetrahydrothiophene-4-carbonitrile **(±)-157**. Reduction of the ketone gave a single diastereoisomer of the secondary alcohol. An attempt to protect the alcohol by benzylation led to an interesting S-benzylation and retro-aldol-like ring-opening. However, hydration of the nitrile gave the crystalline carboxamide, which was demonstrated by a careful NMR study and an X-ray-crystal determination to have the required *trans* relative configuration. Studies showed that the secondary alcohol could be protected without risk of the retro-aldol ring-opening and that the sulfur could be oxidised to the sulfoxide but imination at sulfur remains to be effected. In this sequence, it only remains to develop methods for imination at the sulfoxide and conversion of the carboxamide to a CH_2OH group.

Much interesting chemistry was achieved in the synthetic approaches to all the named target compounds. This thesis has presented the use of sulfoximine chemistry in drug design, with major advances in several synthetic sequences. A solid foundation has been laid for later workers to complete the syntheses and evaluate the biological activities of the target cyclic sulfoximine riboside mimics. Further investigation of the potential role of sulfoximines in the design of nucleoside derivatives should lead to exciting findings. The search for selective and efficient chemotherapeutic agents continues.

Experimental

General Procedures

All melting points were determined using a Reichert-Jung Thermo Galen Kofler block and are uncorrected. IR spectra were recorded on a Perkin-Elmer RXI FT-IR spectrometer, either as a liquid (film) or as a KBr disc (KBr). ν_{max} values are given in cm^{-1}. Optical rotations ([α]) were measured in a 1.0 dm cell on an Optical Activity Ltd. polarimeter and concentrations (c) were expressed in g/100 mL. NMR spectra were recorded on either a Jeol-Varian GX 270 (270.05 MHz ^{1}H; 67.8 MHz ^{13}C), Varian Mercury EX 400 (399.65 MHz ^{1}H; 100.4 MHz ^{13}C; 376.05 MHz ^{19}F) or Varian Unity Inova 600 MHz (^{1}H NMR only) spectrometers. Tetramethylsilane was used as an internal standard for samples dissolved in $CDCl_3$ and $(CD_3)_2SO$. NMR spectra are reported in p.p.m. downfield from tetramethylsilane. Multiplicities are indicated by s (singlet), d (doublet), t (triplet), q (quartet), qn (quintet), m (multiplet) and br (broad). Coupling constants (*J*) are expressed in Hz. Where indicated, 2-D experiments were used to assign ^{1}H and ^{13}C NMR signals. Mass spectra were obtained by either Electron Impact (EI), Electrospray (ES) or Fast Atom Bombardment (FAB) (with *m*-nitrobenzyl alcohol as the matrix) at the University of Bath Mass Spectrometry Service using a VG 7070 mass spectrometer, the University of Bath Department of Pharmacy and Pharmacology High Resolution Mass Spectrometry Service using a Bruker microOTOF™ and the EPSRC Mass Spectrometry Service, Swansea. Microanalysis was carried out at the School of Pharmacy, University of London, Microanalysis Service. Thin layer chromatography (TLC) was performed on silica gel 60 F_{254}-coated aluminium sheets (Merck) and visualisation was accomplished by UV light (254 nm), iodine vapour, solutions of iron(III) chloride, 2,4-dinitrophenylhydrazine, phosphomolybdic acid, potassium permanganate or ninhydrin. Flash column chromatography was performed using silica gel 60 (0.040-0.063 mm, Merck) as the stationary phase.

All reagents for chemical synthesis were purchased from Sigma-Aldrich and Lancaster Chemical Company and were used without further purification. Experiments were conducted at ambient temperature, unless otherwise stated. Where experiments were repeated, only one description was provided. Solutions in organic solvents were dried using anhydrous $MgSO_4$ and solvents were evaporated under reduced pressure using a Büchi rotary evaporator. THF was freshly distilled under nitrogen from sodium and benzophenone.

(±)-S-Methyl-S-phenylsulfoxide (47)

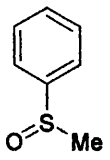

$NaIO_4$ (10.7 g, 50 mmol) in water (15 mL) was added slowly to thioanisole (**46**, 6.2 g, 50 mmol) in MeOH (100 mL). The mixture was stirred vigorously overnight then filtered. Drying and evaporation yielded **47** (6.5 g, 93%) as a colourless oil: TLC R_f = 0.1 (EtOAc / hexane, 2:3); IR ν_{max} (film) 1301 cm^{-1}; ^1H NMR (400 MHz, $CDCl_3$) δ 2.69 (3 H, s, CH_3), 7.47-7.56 (3 H, m, Ph 3,4,5-H_3), 7.64-7.67 (2 H, m, Ph 2,6-H_2); ^{13}C NMR (100 MHz, $CDCl_3$) δ 44.0 (CH_3), 123.5 (Ph 4-CH), 129.4 (Ph 3,5-C_2), 131.1 (Ph 2,6-C_2), 145.7 (Ph 1-C_q); HRMS (FAB+) *m/z* 141.0369 (M + H) ($^{12}C_7H_9OS$ requires 141.0374).

N-*tert*-Butoxycarbonyl azide (53)

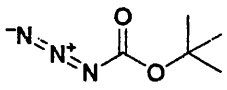

$NaNO_2$ (1.17 g, 17 mmol) in water (10 mL) was added to *tert*-butyl carbazate (**52**, 2.02 g, 15 mmol), acetic acid (1.75 g) and water (2.4 mL) at 0°C during 1 h. After a further 1 h, water (2.4 mL) was added and the oil was extracted into DCM. The organic extract was washed with water and aq. $NaHCO_3$ (1 M) and dried. Concentration gave **53** (1.75 g, 82%) as a yellow oil which was used in the next step without further purification: IR ν_{max} (film) 1731, 2132 cm^{-1}.

(±)-N-*tert*-Butoxycarbonyl-S-methyl-S-phenylsulfoximine (54)

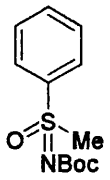

Method A: Compound **53** (1.75 g, 12 mmol) was added to **47** (1.70 g, 12 mmol) in dry DCM at 0°C. $FeCl_2$ (1.51 g, 12 mmol) was added. The mixture was warmed to RT

and stirred overnight, then poured into water and extracted with DCM (x 2). The organic layers were washed with water and dried. Evaporation and chromatography (DCM / EtOAc, 1:1) gave **54** (1.62 g, 53%) as a white solid: TLC R_f = 0.7 (DCM / EtOAc, 1:1); mp 66-67°C (lit.[153] mp 65-67°C); IR ν_{max} (KBr) 1657 cm^{-1}; ^1H NMR (400 MHz, $CDCl_3$) δ 1.33 [9 H, s, $C(CH_3)_3$], 3.21 (3 H, s, CH_3), 7.59-7.71 (3 H, m, Ph 3,4,5-H_3), 7.99 (2 H, m, Ph 2,6-H_2); ^{13}C NMR (100 MHz, $CDCl_3$) δ 28.0 [$(CH_3)_3$], 44.7 (SCH_3), 80.6 (C_q), 127.4 (2 x CH), 129.6 (2 x CH), 133.7 (CH), 138.9 (C_q), 157.6 (C=O); HRMS (FAB+) *m/z* 256.1016 (M + H) ($^{12}C_{12}H_{17}NO_3S$ requires 256.1007), 182 [M – $OC(CH_3)_3$].

Method B: NaH (60% in mineral oil, 133 mg, 3.32 mmol, pre-washed in dry pentane) was added to a solution of compound **50** (370 mg, 2.38 mmol) in dry THF (0.5 mL) and the mixture was stirred for 30 min. Di-*tert*-butyl dicarbonate (1.04 g, 4.76 mmol) was added and the reaction mixture was stirred overnight. The mixture was quenched with aq. NH_4Cl (sat.) and extracted with DCM (x 3). The organic layers were collected and dried. Evaporation and chromatography (DCM / EtOAc, 1:1) afforded **54** (500 mg, 82%) as a white solid. The data were identical to those above.

(±)-S-Methyl-S-phenylsulfoximine trifluoroacetate salt (55)

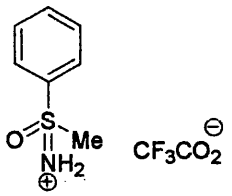

Compound **54** (500 mg, 1.96 mmol) was treated with TFA (5 mL) in DCM (5 mL) at 0°C. The mixture was warmed to RT and stirred for 60 min. Evaporation and trituration (Et_2O) gave **55** (150 mg, 28%) as pale buff crystals: TLC R_f = 0.2 (DCM / EtOAc, 1:1); mp 73-75°C; IR ν_{max} (KBr) 1678, 3435 cm^{-1}; ^1H NMR (400 MHz, $CDCl_3$) δ 3.51 (3 H, s, CH_3), 7.66-7.68 (2 H, t, *J* = 7.5 Hz, Ph 3,5-H_2), 7.76-7.79 (1 H, t, *J* = 7.5 Hz, Ph 4-H), 8.04-8.06 (2 H, d, *J* = 7.5 Hz, Ph 2,6-H_2), 8.89 (2 H, br s, NH_2); ^{13}C NMR (100 MHz, $CDCl_3$) δ 44.1 (CH_3), 115.1 (CF_3, q, *J* = 285 Hz), 128.3 (2 x CH), 130.1 (2 x CH), 135.5 (CH), 136.2 (C_q), 161.2 ($CF_3\underline{C}O_2$, q, *J* = 37.5 Hz); HRMS (FAB+) *m/z* 156.0485 (M – CF_3CO_2) ($^{12}C_7H_{10}NOS$ requires 156.0483).

(±)-S-Methyl-S-phenylsulfoximine (50)

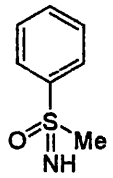

Method A: To a solution of **55** (130 mg, 0.48 mmol) in MeOH (1 mL) was treated with Na_2CO_3 (aq. sat.) to pH 7 and the mixture extracted with DCM (x 4). The organic layers were collected and dried. Evaporation and chromatography (MeOH / EtOAc, 7:3) afforded **50** (85 mg, 98%) as a pale yellow oil: TLC R_f = 0.2 (DCM / EtOAc, 1:1); IR ν_{max} (film) 1031, 3400 (NH) cm^{-1}; ^1H NMR (400 MHz, $CDCl_3$) δ 3.03 (1 H, br s, NH), 3.10 (3 H, s, CH_3), 7.52-7.65 (3 H, m, Ph 3,4,5-H_3), 8.01 (2H, m, Ph 2,6-H_2); ^{13}C NMR (100 MHz, $CDCl_3$) δ 46.2 (CH_3), 127.7 (2 x CH), 129.3 (2 x CH), 133.1 (CH), 143.5 (C_q); HRMS (FAB+) *m/z* 156.0488 (M + H) ($^{12}C_7H_{10}NOS$ requires 156.0483).

Method B: Compound **65** (1.00 g, 3.97 mmol) was stirred with NH_3 (35% in water, 10 mL) in MeOH (25 mL) for 16 h. Evaporation and chromatography (EtOAc / MeOH, 7:3) gave **50** (616 mg, 100%) as a yellow oil. The data were identical to those above.

(±)-N-(Trimethylsilyl)-S-methyl-S-phenylsulfoximine (51)

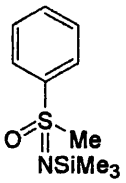

To **50** (100 mg, 0.65 mmol) in MeCN (1 mL) at 65°C was added dropwise Et_2NSiMe_3 (105 mg, 0.72 mmol). The mixture was stirred at 65°C for 4 h and at RT for 3 d. Evaporation gave **51** (145 mg, 98%) as a pale buff liquid: TLC R_f = 0.2 (EtOAc / hexane, 7:3); IR ν_{max} (film) 847, 1077 cm^{-1}; ^1H NMR (400 MHz, $CDCl_3$) δ 0.05 (9 H, s, $SiMe_3$), 2.98 (3 H, s, CH_3), 7.46-7.56 (3 H, m, Ph 3,4,5-H_3), 7.91 (2 H, m, Ph 2,6-H_2); ^{13}C NMR (100 MHz, $CDCl_3$) δ 2.3 ($SiCH_3$), 49.3 (SCH_3), 127.0 (2 x CH), 128.9 (2 x CH), 129.3 (2 x CH), 132.2 (C_q).

(±)-N-(*tert*-Butoxycarbonyl)-S-phenyl-S-[(*E*)-2-phenylethenyl]sulfoximine (56) and (±)-2-[N-(*tert*-butoxycarbonyl)-S-phenylsulfonimidoyl]-1-phenylethanol (57a/b)

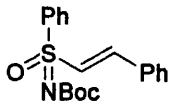

(56)

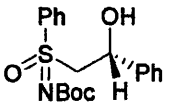

(57a/b)

Compound **54** (250 mg, 0.98 mmol) was treated with *t*-BuLi (1.7 M in pentane, 0.58 mL, 0.98 mmol) in dry THF at –78°C under N_2 for 2 h. Benzaldehyde (104 mg, 0.98 mmol) in dry THF (1.0 mL) was added and the mixture was allowed to reach RT overnight. Evaporation residue, in EtOAc was washed with water (x 2) and dried. Evaporation and chromatography (EtOAc / hexane, 2:8) afforded first, in elution order, **56** (11 mg, 3%) as a white solid: TLC R_f = 0.4 (EtOAc / hexane, 2:3); mp 33-35°C; ^{1}H NMR (400 MHz, $CDCl_3$) δ 1.37 [9 H, s, $C(CH_3)_3$], 6.87 (1 H, d, *J* = 15.3 Hz, PhCH), 7.28-7.44 (5 H, m, C-Ph-H_5), 7.46-7.61 (3 H, m, S-Ph 3,4,5-H_3), 7.66 (1 H, d, *J* = 15.3 Hz, SCH), 7.95-8.00 (2 H, m, S-Ph 2,6-H_2); ^{13}C NMR (100 MHz, $CDCl_3$) (HMQC) δ 28.0 [$(CH_3)_3$], 80.6 [$\underline{C}(CH_3)_3$], 125.5 (PhCH), 127.5 (2 x CH), 128.6 (2 x CH), 129.1 (2 x CH), 129.5 (2 x CH), 131.3 (CH), 132.1 (C_q), 133.3 (CH), 139.2 (C_q), 143.3 (SCH), 157.3 (C=O); MS (FAB+) *m/z* 344 (M + H), 243 (M – Boc).

Further elution gave **57a/b** as a 7:1 mixture of diastereoisomers (220 mg, 62%) as a colourless oil: TLC R_f = 0.3 (EtOAc / hexane, 2:3); ^{1}H NMR (400 MHz, $CDCl_3$) δ 1.34 [1.12 H, s, minor $C(CH_3)_3$], 1.36 [7.88 H, s, major $C(CH_3)_3$], 3.22 (0.12 H, dd, *J* = 14.0, 1.2 Hz, minor C$\underline{H}$H), 3.48 (0.88 H, dd, *J* = 14.2, 2.0 Hz, major C$\underline{H}$H), 3.59 (0.88 H, dd, *J* = 14.2, 9.9 Hz, major CH$\underline{H}$), 3.72 (0.12 H, dd, *J* = 14.2, 9.9 Hz, minor CH$\underline{H}$), 4.40 (0.88 H, d, *J* = 2.0 Hz, major OH), 5.03 (0.12 H, d, *J* = 1.2 Hz, minor OH), 5.30 (0.88 H, d, *J* = 9.9 Hz, major CHPh), 5.45 (0.12 H, d, *J* = 9.9 Hz, minor CHPh), 7.27-7.33 (5 H, m, C-Ph-H_5), 7.61-7.73 (3 H, m, S-Ph 3,4,5-H_3), 7.98-8.00 (2 H, m, S-Ph 2,6-H_2); ^{13}C NMR (100 MHz, $CDCl_3$) δ 28.0 [$(CH_3)_3$], 64.4 (CH_2), 68.5 (PhCH) 81.1 [$\underline{C}(CH_3)_3$], 125.8 (Ph 3,5-C_2), 128.0 (Ph 2,6-C_2), 128.6 (Ph 4-CH), 128.8 (S-Ph 3,5-C_2), 129.8 (S-Ph 2,6-C_2), 134.1 (S-Ph 4-CH), 137.8 (Ph 1-C_q), 157.1 (C=O); HRMS (FAB+) *m/z* 362.1432 (M + H) ($^{12}C_{19}H_{24}NO_4S$ requires 362.1426).

Fluoren-9-ylmethyloxycarbonyl azide (63)

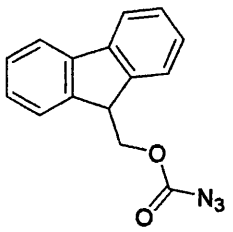

To NaN_3 (520 mg, 8.0 mmol) in water (2 mL) at 0°C was added slowly fluoren-9-yl-methyl chloroformate (**62**, 1.35 g, 5.2 mmol) in acetone (2.5 mL). The mixture was stirred at 0°C for 2 h and at RT for a further 2 h. Filtration and recrystallisation (acetone) afforded **63** (1.14 g, 82%) as colourless crystals: TLC R_f = 0.8 (EtOAc / hexane, 2:3); mp 82-83°C (lit.[161] mp 83-85°C); IR ν_{max} (KBr) 1716 (C=O), 2140 (N_3), 2197 cm^{-1}; ^1H NMR (270 MHz, $CDCl_3$) δ 4.26 (1 H, t, *J* = 7.4 Hz, 9-H), 4.48 (2 H, d, *J* = 7.4 Hz, CH_2), 7.33 (2 H, dt, *J* = 1.2, 7.4 Hz, fluorene 3,6-H_2), 7.43 (2 H, t, *J* = 7.4 Hz, fluorene Ph 2,7-H_2), 7.59 (2 H, d, *J* = 7.5 Hz, fluorene 4,5-H_2), 7.78 (2 H, d, *J* = 7.5 Hz, fluorene 1,8-H_2); ^{13}C NMR (68 MHz, $CDCl_3$) δ 46.6 (CH), 70.4 (CH_2), 120.3 (2 x CH), 125.2 (2 x CH), 127.4 (2 x CH), 128.1 (2 x CH), 140.1 (2 x C_q), 143.0 (2 x C_q), 163.1 (C=O); MS (FAB+) *m/z* 179 (M – $OCON_3$), 165 (M – CH_2OCON_3).

(±)-N-(Trifluoroacetyl)-S-methyl-S-phenylsulfoximine (65)

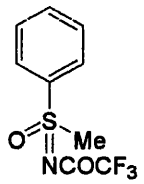

To a suspension of compound **47** (1.40 g, 10.0 mmol), trifluoroacetamide (2.26 g, 20.0 mmol), MgO (1.60 g, 40.0 mmol) and $Rh_2(OAc)_4$ (110 mg, 2.5 mol %) in DCM (50 mL) was added $PhI(OAc)_2$ (4.83 mg, 15.0 mmol) and the mixture was stirred for 16 h. The suspension was filtered (Celite®); evaporation and chromatography (EtOAc/hexane, 2:3) gave **65** (1.80 g, 72%) as a white solid: TLC R_f = 0.4 (EtOAc / hexane, 2:3); mp 77-78°C (lit.[151] mp 76.5-77.5°C); IR ν_{max} (KBr) 1131, 1189 (CF_3), 1242, 1662 (C=O) cm^{-1}; ^1H NMR (400 MHz, $CDCl_3$) δ 3.46 (3 H, s, CH_3), 7.66 (2 H, m, Ph 3,5-H_2), 7.76 (1 H, m, Ph 4-H), 8.00 (2 H, m, Ph 2,6-H_2); ^{13}C NMR (100 MHz, $CDCl_3$) δ 44.3 (CH_3), 115.8 (C_q), 127.1 (2 x CH), 130.1 (2 x CH), 134.9 (CH), 136.5 (C_q), 163.9 (C=O); ^{19}F

NMR (376 MHz, $CDCl_3$) δ –76.0 (3 F, s, CF_3); HRMS (FAB+) *m/z* 252.0303 (M + H) ($^{12}C_9H_8NO_2F_3S$ requires 252.0306), 182 (M – CF_3).

S-2,2-Dimethyl-1,3-dioxolane-4-carboxaldehyde (44)

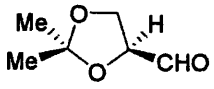

Saturated aqueous $NaHCO_3$ (0.20 mL) was added to 1,2:5,6-diisopropylidene-*D*-mannitol (**66**, 250 mg, 0.96 mmol) in DCM (4.5 mL). $NaIO_4$ (810 mg, 3.80 mmol) was added and the mixture was stirred for 1.5 h and then filtered. Drying and evaporation afforded **44** (260 mg, 100%) as a colourless liquid: TLC R_f = 0.4 (DCM / EtOAc, 1:1); IR ν_{max} (film) 845, 1216, 1375, 1736 (C=O) cm^{-1}; ^1H NMR (400 MHz, $CDCl_3$) δ 1.34 (3 H, s, CH_3), 1.41 (3 H, s, CH_3), 4.03 (1 H, dd, *J* = 8.8, 4.7 Hz, 5-H), 4.10 (1 H, dd, *J* = 8.8, 7.5 Hz, 5-H), 4.32 (1 H, ddd, *J* = 7.5, 4.7, 1.9 Hz, 4-H), 9.64 (1 H, d, *J* = 1.9 Hz, CHO); ^{13}C NMR (100 MHz, $CDCl_3$) (HMQC) δ 25.0 (CH_3), 26.1 (CH_3), 65.4 (CH_2), 79.7 (CH), 111.1 [$C(CH_3)_3$], 201.7 (CHO); $[\alpha]^{20}_D$ = +62° (c = 1.2, EtOAc) [lit.[163] $[\alpha]^{25}_D$ = +80° (c = 1.5, EtOAc)].

3-(Methylthio)benzaldehyde (76)

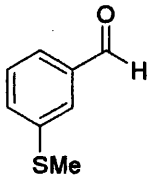

3-Bromothioanisole (**75**, 203 mg, 1 mmol) was treated with n-BuLi (2.5 M in hexane, 1.2 mL, 3 mmol) in dry THF at –78°C under N_2 for 2 h. Dry DMF (0.23 mL, 219 mg, 3 mmol) in dry THF (1.0 mL) was added and the mixture was allowed to reach RT overnight. The evaporation residue, in EtOAc was washed with aq. $NaHCO_3$ (1 M) and brine and dried. Evaporation and chromatography (EtOAc / hexane, 1:10) gave **76** (58 mg, 38%) as a pale yellow liquid: TLC R_f = 0.7 (EtOAc / hexane, 2:3); ^1H NMR (400 MHz, $CDCl_3$) δ 2.54 (3 H, s, CH_3), 7.45 (1 H, t, *J* = 7.4, Ph 5-H), 7.51 (1 H, m, Ph 4-H), 7.62 (1 H, dt, *J* = 7.4, 1.5 Hz, Ph 6-H), 7.73 (1 H, t, *J* = 1.5 Hz, Ph 2-H), 10.0 (1 H, s,

CHO); ^{13}C NMR (100 MHz, $CDCl_3$) δ 29.8 (CH_3), 126.1 (Ph 6-CH), 126.8 (Ph 2-CH), 128.9 (Ph 5-CH), 129.3 (Ph 4-CH), 136.9 (Ph 1-C_q), 140.5 (Ph 3-C_q), 192 (C=O).

3-(Methylthio)benzaldehyde oxime (77)

$NH_2OH.HCl$ (48 mg, 0.69 mmol) and sodium acetate (94 mg, 1.20 mmol) in water (5 mL) were added to compound **76** (58 mg, 0.38 mmol) in EtOH (5 mL) and heated at 45°C overnight. Water was added and the mixture was extracted with EtOAc. The organic layer was washed with water, dried and evaporated to give **77** (25 mg, 39%) as pale yellow crystals: TLC R_f = 0.9 (EtOAc / hexane, 2:3); mp 53-54°C (lit.[219] mp 54-56°C); ^1H NMR (270 MHz, $CDCl_3$) δ 2.50 (3 H, s, CH_3), 4.68 (1 H, s, OH), 7.27-7.32 (3 H, m, Ph-H_3), 7.47 (1 H, m, Ph 2-H), 8.09 (1 H, s, N=CH).

3-(Methylthio)benzonitrile (78)

3-Bromothioanisole (**75**, 1.00 g, 4.92 mmol), $Zn(CN)_2$ (580 mg, 4.92 mmol) and $Pd(PPh_3)_4$ (284 mg, 5 mol %) in DMF (10 mL) were boiled under N_2 for 3 d. The cooled suspension was filtered (Celite®), diluted with EtOAc, washed with 5% aq. $Na_2S_2O_3$, 10% aq. K_2CO_3, water and brine and dried. Evaporation and chromatography (EtOAc / hexane, 1:4) gave **78** (735 mg, 100%) as a yellow oil: TLC R_f = 0.5 (EtOAc / hexane, 1:4); IR ν_{max} (film) 908, 2232, 2254 (CN) cm^{-1}; ^1H NMR (400 MHz, $CDCl_3$) δ 2.52 (3 H, s, CH_3), 7.30-7.47 (4 H, m, Ph-H_4); ^{13}C NMR (100 MHz, $CDCl_3$) δ 60.3 (CH_3), 112.9 (Ph 1-C_q), 118.3 (C≡N), 128.1 (Ph 6-CH), 128.6 (Ph 5-CH), 129.2 (Ph 2-CH), 130.2 (Ph 4-CH), 140.8 (Ph 3-C_q); HRMS (FAB+) *m/z* 150.0301 (M + H) ($^{12}C_8H_8NS$ requires 150.0377), 149.0299 (M) ($^{12}C_8H_7NS$ requires 149.0299).

(*S*)-(–)-3-Bromophenyl methyl sulfoxide (79)

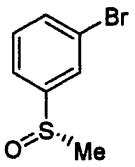

$Ti(OiPr)_4$ (711 mg, 2.5 mmol) and (*S,S*)-(–)-diethyl tartrate (1.03 g, 5 mmol) were stirred in dry DCM (25 mL) for 15 min followed by addition of water (0.04 mL, 2.5 mmol). 3-Bromothioanisole (**75**, 508 mg, 2.5 mmol) was added after 20 min. The mixture was cooled to –20°C and aq. ^tBuOOH (70%, 248 mg, 2.75 mmol) was added. After 3 h, water (328 mg, 18 mmol) was introduced and the mixture was vigorously stirred at –20°C for 1 h and at RT overnight. The white gel formed was filtered (Celite®) and washed well with DCM. The filtrate was treated with 5% aq. NaOH overnight, washed with brine and water and dried. Evaporation and chromatography (EtOAc / hexane, 1:4) gave **79** (270 mg, 49%) as a pale yellow oil: TLC R_f = 0.1 (EtOAc / hexane, 1:4); ^1H NMR (400 MHz, $CDCl_3$) δ 2.73 (3 H, s, CH_3), 7.37 (1 H, t, *J* = 7.5 Hz, Ph 5-H), 7.52 (1 H, dt, *J* = 7.5, 1.4 Hz, Ph 6-H), 7.60 (1 H, dt, *J* = 7.5, 1.4 Hz, Ph 4-H), 7.79 (1 H, m, Ph 2-H); $[\alpha]^{20}_D$ = –38.6° (c = 0.07, acetone), 33% ee. [lit.[175] $[\alpha]^{25}_D$ for (*R*)-(+)-isomer = +116.3° (c = 1.2, acetone), 97% ee]

(±)-3-(Methylsulfinyl)benzonitrile (81)

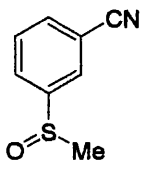

Compound **78** (735 mg, 4.92 mmol) was treated with *m*CPBA (849 mg, 4.92 mmol) in DCM at 0°C for 2 h. The mixture was diluted with DCM (10 mL) and washed with aq. $NaHCO_3$ (1 M) and water and dried. Evaporation and chromatography (DCM / EtOAc, 7:3) afforded **81** (550 mg, 68%) as a pale yellow solid: TLC R_f = 0.3 (DCM / EtOAc, 1:1); mp 68-72°C; IR ν_{max} (KBr) 911, 2254 (CN) cm^{-1}; ^1H NMR (400 MHz, $CDCl_3$) δ 2.76 (3 H, s, CH_3), 7.67 (1 H, dt, *J* = 0.5, 7.8 Hz, Ph 5-H), 7.87 (1 H, dt, *J* = 7.8, 1.6 Hz, Ph 4-H), 7.90 (1 H, dt, *J* = 7.8, 1.6 Hz, Ph 6-H), 7.94 (1 H, dt, *J* = 0.5, 1.6 Hz, Ph 2-H); ^{13}C NMR (100 MHz, $CDCl_3$) δ 44.0 (CH_3), 113.9 (C_q), 117.5 (C_q), 127.2 (CH), 127.7 (CH), 130.2 (CH), 134.4 (CH), 147.9 (C_q); HRMS (EI+) *m/z* 165.0245 (M) ($^{12}C_8H_7NOS$

requires 165.0248), 150 (M – CH_3), 134 (M – OCH_3), 102 (M – $SOCH_3$); HRMS (FAB+) *m/z* 166.0324 (M + H) ($^{12}C_8H_8NOS$ requires 166.0327).

(±)-3-[N-(Trifluoroacetyl)-S-(methylsulfonimidoyl)]benzonitrile (82)

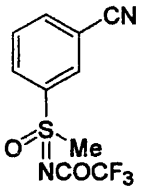

To a suspension of compound **81** (70.0 mg, 0.42 mmol), trifluoroacetamide (95.0 mg, 0.84 mmol), MgO (67.7 mg, 1.68 mmol) and $Rh_2(OAc)_4$ (4.60 mg, 2.5 mol %) in DCM (5 mL) was added $PhI(OAc)_2$ (203 mg, 0.63 mmol) and the mixture was stirred for 16 h. The suspension was filtered (Celite®); evaporation and chromatography (DCM / EtOAc, 7:3) gave **82** (52.0 mg, 45%) as a white solid: TLC R_f = 0.4 (DCM / EtOAc, 7:3); mp 125-128°C; IR ν_{max} (KBr) 911, 1171 (CF_3), 1379, 2254 (CN) cm^{-1}; ^1H NMR (400 MHz, $CDCl_3$) δ 3.49 (3 H, s, CH_3), 7.82 (1 H, dt, *J* = 0.5, 7.8 Hz, Ph 5-H), 8.02 (1 H, dt, *J* = 7.8, 1.2 Hz, Ph 4-H), 8.21 (1 H, dt, *J* = 7.8, 1.2 Hz, Ph 6-H), 8.29 (1 H, dt, *J* = 0.5, 1.2 Hz, Ph 2-H); ^{13}C NMR (100 MHz, $CDCl_3$) δ 44.1 (CH_3), 114.9 (C_q), 116.3 (C_q), 130.9 (CH), 131.1 (CH), 131.2 (CH), 137.8 (CH), 138.7 (C_q); ^{19}F NMR (376 MHz, $CDCl_3$) δ –76.0 (3 F, s, CF_3); HRMS (FAB+) *m/z* 294.0517 (M + NH_4) ($^{12}C_{10}H_{11}N_3O_2F_3S$ requires 294.0519), 277.0239 (M + H) ($^{12}C_{10}H_8N_2O_2F_3S$ requires 277.0259), 207 (M – CF_3).

(±)-3-(S-Methylsulfonimidoyl)benzonitrile (83)

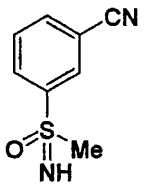

Compound **82** (52.0 mg, 0.21 mmol) was stirred with NH_3 (35% in water, 1.0 mL) in MeOH (5 mL) for 2 h. Evaporation and chromatography (MeOH / EtOAc, 7:3) gave **83** (37.5 mg, 99%) as a pale yellow oil: TLC R_f = 0.3 (DCM / EtOAc, 1:1); IR ν_{max} (film) 756, 2237, 3020, 3402 cm^{-1}; ^1H NMR (400 MHz, $CDCl_3$) δ 2.75 (1 H, br s, NH), 3.11 (3 H, s, CH_3), 7.69 (1 H, dt, *J* = 0.5, 7.9 Hz, Ph 5-H), 7.88 (1 H, dt, *J* = 7.9, 1.5 Hz, Ph

4-H), 8.22 (1 H, dt, J = 7.9, 1.5 Hz, Ph 6-H), 8.29 (1 H, t, J = 1.5 Hz, Ph 2-H); ^{13}C NMR (100 MHz, $CDCl_3$) δ 45.8 (CH_3), 113.7 (C_q), 117.1 (C_q), 130.3 (CH), 131.4 (CH), 131.7 (CH), 136.2 (CH), 145.1 (C_q); HRMS (FAB+) *m/z* 181.0432 (M + H) ($^{12}C_8H_8N_2OS$ requires 181.0430).

3-[(±)-N-*tert*-Butoxycarbonyl-S-methylsulfonimidoyl)]benzonitrile (84)

NaH (60% in mineral oil, 93 mg, 2.32 mmol, pre-washed with dry pentane) was added to compound **83** (300 mg, 1.66 mmol) in dry THF (2.5 mL) and the mixture was stirred for 30 min. Di-*tert*-butyl dicarbonate (725 mg, 3.32 mmol) was added and the reaction mixture was stirred overnight. The mixture was quenched with sat. aq. NH_4Cl and extracted with DCM (x 3). The organic layers were collected and dried. Evaporation and chromatography (DCM / EtOAc, 1:1) afforded **84** (420 mg, 90%) as a white solid: TLC R_f = 0.7 (DCM / EtOAc, 1:1); mp 148-150°C; IR ν_{max} (KBr) 770, 1642, 2251 cm^{-1}; ^{1}H NMR (400 MHz, $CDCl_3$) δ 1.39 [9 H, s, $C(CH_3)_3$], 3.27 (3 H, s, CH_3), 7.76 (1 H, t, J = 7.8 Hz, Ph 5-H), 7.96 (1 H, dt, J = 7.8, 1.4 Hz, Ph 4-H), 8.21 (1 H, dt, J = 8.1, 1.6 Hz, Ph 6-H), 8.28 (1 H, t, J = 1.6 Hz, Ph 2-H); ^{13}C NMR (100 MHz, $CDCl_3$) δ 26.7 [$(CH_3)_3$], 44.0 (SCH_3), 81.8 [$\underline{C}(CH_3)_3$], 114.2 (C_q), 116.1 (C_q), 130.3 (CH), 131.2 (CH), 131.5 (CH), 136.3 (CH), 140.8 (C_q), 158.2 (C_q); HRMS (FAB+) *m/z* 281.0955 (M + H) ($^{12}C_{13}H_{17}N_2O_3S$ requires 281.0954), 165 (M – NBoc), 102 (C_6H_4-CN).

(4*R*,5*R*)-Diethyl 2,2-dimethyl-1,3-dioxolane-4,5-dicarboxylate (95)

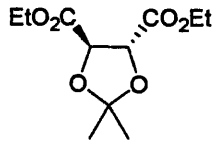

Diethyl (*R*,*R*)-2,3-dihydroxybutanedioate (**93**, 15.0 g, 70 mmol), 2,2-dimethoxypropane (**94**, 32 g, 320 mmol) and 4-toluenesulfonic acid monohydrate (198 mg, 1.02 mmol) in DCM (200 mL) were boiled under reflux in a Soxhlet apparatus for 7 d through

activated 4 Å molecular sieves (33 g). Anhydrous Na_2CO_3 (83 mg, 1.0 mmol) was added. Filtration, drying, evaporation and chromatography (EtOAc / hexane, 2:3) afforded **95** with some ester interchange, yielding ethyl methyl and dimethyl esters (total usable esters 12 g, *ca.* 67%) as a pale buff oil. TLC R_f = 0.4 (EtOAc / hexane, 2:3); IR ν_{max} (film) 1385, 1753 (C=O), 2988, 3055 cm^{-1}; **95**: ^1H NMR (400 MHz, $CDCl_3$) δ 1.26 (6 H, t, *J* = 7.2 Hz, 2 x $CH_2C\underline{H}_3$), 1.43 [6 H, s, $(CH_3)_2$], 4.21 (4 H, q, *J* = 7.2 Hz, $C\underline{H}_2CH_3$), 4.75 (2 H, s, 4,5-H_2); **ethyl methyl ester:** ^1H NMR (400 MHz, $CDCl_3$) δ 1.19 (3 H, t, *J* = 7.2 Hz, $CH_2C\underline{H}_3$), 1.43 [6 H, s, $(CH_3)_2$], 3.76 (3 H, s, OCH_3), 4.05 (2 H, q, *J* = 7.2 Hz, $C\underline{H}_2CH_3$), 4.72 (1 H, s, 4-H), 4.74 (1 H, s, 5-H); **dimethyl ester**: ^1H NMR (400 MHz, $CDCl_3$) δ 1.43 [6 H, s, $(CH_3)_2$], 3.76 (6 H, s, 2 x OCH_3), 4.71 (2H, s, 4,5-H_2); ^{13}C NMR (100 MHz, $CDCl_3$) (HMQC) δ 14.0 ($CH_2\underline{C}H_3$), 26.2 x 3 [$(CH_3)_2$], 52.7 x 2 (OCH_3), 61.8 x 2 ($\underline{C}H_2CH_3$), 76.8, 77.0 (4-CH + 5-CH), 113.6, 113.7 x 2 [$\underline{C}(CH_3)_2$], 169.5, 169.6 (C=O); HRMS (FAB+) *m/z* 247.1182 [M (**95**) + H] ($^{12}C_{11}H_{19}O_6$ requires 247.1154), 233.2 (**ethyl methyl ester** + H), 217.2 (**dimethyl ester** – H).

4*S*,5*S*-Di(hydroxymethyl)-2,2-dimethyl-1,3-dioxolane (96)

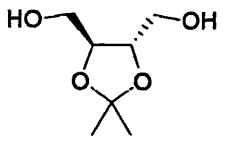

$LiAlH_4$ (2.0 M in THF, 103 mmol, 51.5 mL) was added during 1.5 h to **95** (12 g, 49 mmol) in dry THF (80 mL) and the mixture was boiled under reflux for a further 5 h. It was then cooled to 0°C and water (10 mL), aq. NaOH (4 M, 10 mL) and water (30 mL) were added cautiously in turn. The aluminium salts were removed by filtration. Evaporation of the filtrate gave crude **96**. The aluminium salts were extracted with boiling 1,4-dioxane (3 x 100 mL) and removed by filtration; evaporation of the extracts gave further product (6.7 g, 85 %) as a pale yellow oil: TLC R_f = 0.2 (EtOAc / hexane, 2:3); IR ν_{max} (film) 3370 (OH) cm^{-1}; ^1H NMR (400 MHz, $CDCl_3$) δ 1.40 [6 H, s, $(CH_3)_2$], 2.83 (2 H, br s, 2 x OH), 3.69-3.73 (4 H, m, 2 x CH_2); ^{13}C NMR (100 MHz, $CDCl_3$) δ 26.9 [$(CH_3)_2$], 62.0 (2 x CH_2), 78.1 (2 x CH), 109.2 [$\underline{C}(CH_3)_2$]; HRMS (FAB+) *m/z* 163.0966 (M + H) ($^{12}C_7H_{15}O_4$ requires 163.0970), 147 (M + H – O); $[\alpha]^{20}_D$ = +4.4° (c 4.0, $CHCl_3$) [lit.[177] $[\alpha]^{20}_D$ = +4.1° (c 5.0, $CHCl_3$)].

4*S*,5*S*-Di(benzyloxymethyl)-2,2-dimethyl-1,3-dioxolane (97) and 4*S*,5*S*-4-benzyloxymethyl-5-hydroxymethyl-2,2-dimethyl-1,3-dioxolane (98)

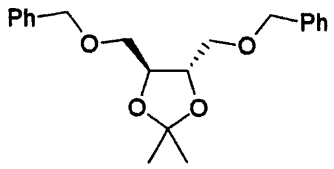

(97)

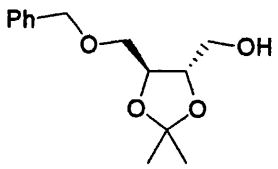

(98)

Sodum hydride (60% dispersion in mineral oil, 1.9 g, 46 mmol, pre-washed with dry pentane) was stirred in dry DMF (20 mL) at 0°C under N_2 for 30 min. Compound **96** (6.7 g, 42 mmol) in dry DMF (20 mL) was then added dropwise and the reaction mixture was stirred for a further 30 min before benzyl bromide (7.35 g, 43 mmol) was added. The reaction mixture was stirred for 1.5 h at RT and was then poured into ice-water (250 mL) and extracted with Et_2O (x 3). The combined extracts were washed with water and brine. Drying, evaporation and chromatography [pet. ether (40-60°C) / Et_2O, 1:1] gave **97** (500 mg, 6 %) as a pale yellow oil: TLC R_f = 0.8 [pet. ether (40-60°C) / Et_2O, 1:1]; IR ν_{max} (film) 650, 735, 910, 1454, 2988, 3054 cm^{-1}; ^1H NMR (400 MHz, $CDCl_3$) δ 1.44 [6 H, s, $(CH_3)_2$], 3.61-3.62 (4 H, m, 2 x $BnOCH_2$), 4.05 (2 H, s, 4,5-H_2), 4.55 (2 H, d, *J* = 12.3 Hz, 2 x PhCH), 4.59 (2 H, d, *J* = 12.3 Hz, 2 x PhCH), 7.27-7.38 (10 H, m, 2 x Ph-H_5); ^{13}C NMR (100 MHz, $CDCl_3$) (HMQC) δ 26.9 [$(CH_3)_2$], 70.6 (2 x $BnOCH_2$), 73.4 (4-CH + 5-CH), 77.4 (2 x $PhCH_2$), 109.6 [$\underline{C}(CH_3)_2$], 127.6 (CH), 128.3 (CH), 137.9 (C_q); HRMS (FAB+) *m/z* 343.1939 (M + H) ($^{12}C_{21}H_{27}O_4$ requires 343.1909).

Further elution gave **98** (3.6 g, 71%) as a pale yellow oil: TLC R_f = 0.2 (hexane / Et_2O, 1:1); IR ν_{max} (film) 701, 740, 910, 1454, 2989, 3055, 3468 (OH) cm^{-1}; ^1H NMR (400 MHz, $CDCl_3$) δ 1.40 (3 H, s, CH_3), 1.41 (3 H, s, CH_3), 2.40 (1 H, br s, OH), 3.55 (1 H, dd, *J* = 9.8, 5.5 Hz, BnOCH), 3.65-3.69 (2 H, m, C<u>H</u>OH + BnOCH), 3.75 (1 H, dd, *J* = 11.7, 4.3 Hz, C<u>H</u>OH), 3.93 (1 H, m, 5-H), 4.05 (1 H, m, 4-H), 4.57 (2 H, s, $PhCH_2$), 7.26-7.36 (5 H, m, Ph-H_5); ^{13}C NMR (100 MHz, $CDCl_3$) (HMQC) δ 26.8 (CH_3), 26.9 (CH_3), 62.3 (CH_2OH), 70.2 ($BnOCH_2$), 73.6 ($PhCH_2$), 76.5 (5-CH), 79.5 (4-CH), 109.3 [$\underline{C}(CH_3)_2$], 127.7 (2 x CH), 127.8 (2 x CH), 128.4 (CH), 137.5 (C_q); HRMS (FAB+) *m/z* 253.1435 (M + H) ($^{12}C_{14}H_{21}O_4$ requires 253.1440), 237 (M + H – O); $[\alpha]^{20}_D$ = +7.9° (c 3.2, $CHCl_3$) [lit.[178] $[\alpha]^{23}_D$ = +8.3° (c 2.9, $CHCl_3$)].

4*S*,5*R*-4-(Benzyloxymethyl)-5-(bromomethyl)-2,2-dimethyl-1,3-dioxolane (99)

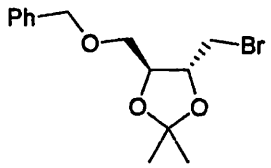

To **98** (280 mg, 1.12 mmol) and CBr_4 (409 mg, 1.23 mmol) in dry THF (2 mL) was added dropwise Ph_3P (353 mg, 1.34 mmol) in dry THF (1 mL) at 0°C under N_2 and the mixture was stirred for 3 h. Evaporation and chromatography (hexane / Et_2O, 1:1) gave **99** (240 mg, 69%) as a colourless oil: TLC R_f = 0.9 (hexane / Et_2O, 1:1); IR ν_{max} (film) 601, 740, 910, 1422, 2987, 3054 cm^{-1}; ^1H NMR (400 MHz, $CDCl_3$) δ 1.43 (3 H, s, CH_3), 1.45 (3 H, s, CH_3), 3.46-3.54 (2 H, m, $BrCH_2$), 3.62-3.69 (2 H, m, $BnOCH_2$), 4.04-4.12 (2 H, m, 4,5-H_2), 4.59 (2 H, s, $PhCH_2$), 7.30-7.38 (5 H, m, Ph-H_5); ^{13}C NMR (100 MHz, $CDCl_3$) δ 27.1 (CH_3), 27.2 (CH_3), 32.6 ($BrCH_2$), 70.4 ($BnOCH_2$), 73.6 ($PhCH_2$), 77.2 (5-CH), 78.8 (4-CH), 110.0 [$\underline{C}(CH_3)_2$], 127.7 (2 x CH), 127.8 (2 x CH), 128.4 (CH), 137.7 (C_q); HRMS (FAB+) *m/z* 317.0563 (M + H) ($^{12}C_{14}H_{20}O_3{}^{81}Br$ requires 317.0575); 316.0503 (M) ($^{12}C_{14}H_{19}O_3{}^{81}Br$ requires 316.0497), 235 (M – ^{81}Br), 220 (M – $CH_2{}^{81}Br$); $[\alpha]^{20}_D$ = +3.6° (c 1.7, $CHCl_3$).

4*S*,5*R*-4-(Benzyloxymethyl)-2,2-dimethyl-5-(phenylthiomethyl)-1,3-dioxolane (101)

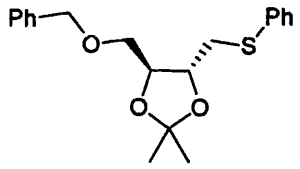

Method A: A cooled (0°C) solution of thiophenol (**100**, 218 mg, 1.98 mmol) and **98** (500 mg, 1.98 mmol) in dry THF (3 mL) was added to a cooled (0°C) solution of triphenylphosphine (1.04 g, 3.96 mmol) and diisopropyl azodicarboxylate (800 mg, 3.96 mmol) in dry THF (7 mL) under Ar and the reaction mixture was allowed to warm to RT and stirred overnight. Evaporation and chromatography [pet. ether (40-60°C) / Et_2O, 1:1] gave **101** (150 mg, 22%) as a yellow oil: TLC R_f = 0.7 [pet. ether (40-60°C) / Et_2O, 1:1]; IR ν_{max} (film) 738, 1265, 1422, 2986, 3054 cm^{-1}; ^1H NMR (400 MHz, $CDCl_3$) δ 1.40 (3 H, s, CH_3), 1.44 (3 H, s, CH_3), 3.19 (1 H, d, *J* = 4.3 Hz, SCH), 3.20 (1 H, d, *J* = 4.3 Hz, SCH), 3.63 (2 H, d, *J* = 4.7 Hz, $BnOCH_2$), 4.04-4.09 (2 H, m, 4,5-H_2), 4.54 (1 H, d, *J*

= 14.9 Hz, PhCH), 4.57 (1 H, d, *J* = 14.9 Hz, PhCH), 7.16-7.36 (10 H, m, Ph-H_{10}); ^{13}C NMR (100 MHz, $CDCl_3$) δ 27.1 (CH_3), 27.2 (CH_3), 36.7 (SCH_2), 70.7 ($BnOCH_2$), 73.5 ($PhCH_2$), 77.0 (5-CH), 79.4 (4-CH), 109.7 [$\underline{C}(CH_3)_2$], 126.2 (2 x CH), 127.8 (2 x CH), 128.4 (2 x CH), 128.9 (2 x CH), 129.2 (2 x CH), 135.8 (C_q), 137.8 (C_q); HRMS (FAB+) *m/z* 345.1522 (M + H) ($^{12}C_{20}H_{24}O_3S$ requires 345.1519), 329 (M – CH_3), 109 (PhSH), 91 (Bn); $[\alpha]^{20}_D$ = +4.4° (c 2.0, $CHCl_3$).

Method B: A cooled (0°C) solution of thiophenol (**100**, 567 mg, 5.15 mmol) and triphenylphosphine (2.70 g, 10.3 mmol) in dry THF (7 mL) was stirred for 30 min under Ar and diisopropyl azodicarboxylate (2.08 g, 10.3 mmol) was added and the mixture was stirred for a further 30 min. **98** (1.30 g, 5.15 mmol) in dry THF (3 mL) was then added and the reaction mixture was allowed to warm to RT and stirred overnight. Evaporation and column chromatography [pet. ether (40-60°C) / Et_2O, 1:1] afforded **101** (320 mg, 18%) as a yellow oil. The data were identical to those above.

Method C: To a cooled (0°C) solution of tributylphosphine (601 mg, 2.97 mmol) and 1,1'-(azodicarbonyl)dipiperidine (749 mg, 2.97 mmol) in dry THF (7 mL) was added thiophenol (**100**, 327 mg, 2.97 mmol) under Ar and the reaction vessel was sonicated for 30 min. While being sonicated, **98** (500 mg, 1.98 mmol) in dry THF (3 mL) was added and the reaction mixture was stirred at RT overnight. Filtration, evaporation and chromatography (hexane / Et_2O, 5:1) gave **101** (300 mg, 44%) as a yellow oil. The data were identical to those above.

4*S*,5*R*,S(±)-4-(Benzyloxymethyl)-2,2-dimethyl-5-(phenylsulfinylmethyl)-1,3-dioxolane (102a/b)

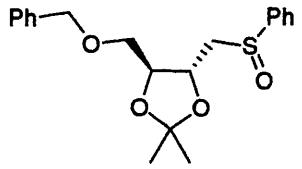

Compound **101** (180 mg, 0.52 mmol) was treated with *m*CPBA (111 mg, 0.52 mmol) in DCM (15 mL) at –78°C for 5 h. The mixture was diluted with DCM (10 mL) and washed with aq. $NaHCO_3$ (1 M) and water. Drying and evaporation gave **102a/b** (180 mg, 96%) as a 1:1 mixture of diastereoisomers as a yellow oil: TLC R_f = 0.7 (DCM / EtOAc, 1:1); IR ν_{max} (film) 739, 1265, 3054 cm^{-1}; ^1H NMR (600 MHz, $CDCl_3$) δ 1.37 (1.5 H, s, CH_3),

1.45 (1.5 H, s, CH_3), 1.46 (1.5 H, s, CH_3), 1.47 (1.5 H, s, CH_3), 2.84 [0.5 H, dd, *J* = 13.2, 9.8 Hz, SCH (isomer A)], 3.04 [0.5 H, dd, *J* = 13.2, 4.2 Hz, SCH (isomer B)], 3.06 [0.5 H, dd, *J* = 13.2, 2.2 Hz, SCH (isomer A)], 3.22 [0.5 H, dd, *J* = 13.2, 7.2 Hz, SCH (isomer B)], 3.51 [0.5 H, dd, *J* = 10.1, 5.7 Hz, BnOCH (isomer B)], 3.55 [0.5 H, dd, *J* = 9.8, 5.7 Hz, BnOCH (isomer A)], 3.62 [0.5 H, dd, *J* = 9.8, 4.9 Hz, BnOCH (isomer B)], 3.68 [0.5 H, dd, *J* = 9.5, 5.3 Hz, BnOCH (isomer A)], 3.91 [0.5 H, dt, *J* = 5.3, 8.3 Hz, 4-H (isomer A)], 3.97 [0.5 H, m, 5-H (isomer B)], 4.15 [0.5 H, dt, *J* = 5.3, 8.3 Hz, 4-H (isomer B)], 4.41 [0.5 H, ddd, *J* = 9.8, 8.3, 2.3 Hz, 5-H (isomer A)], 4.50 (0.5 H, d, *J* = 12.1 Hz, PhCH), 4.52 (0.5 H, d, *J* = 12.1 Hz, PhCH), 4.55 (1 H, s, $PhCH_2$), 7.23-7.35 (5 H, m, Ph-H_5), 7.50-7.53 (3 H, m, S-Ph 3,4,5-H_3), 7.65-7.67 (2 H, m, S-Ph 2,6-H_2); ^{13}C NMR (100 MHz, $CDCl_3$) (HMQC, HMBC) δ 26.8 (CH_3), 26.9 (CH_3), 27.0 (CH_3), 27.2 (CH_3), 60.2 [SCH_2 (isomer B)], 62.2 [SCH_2 (isomer A)], 69.6 [$BnOCH_2$ (isomer B)], 70.0 [$BnOCH_2$ (isomer A)], 73.2 [5-CH (isomer A)], 73.5 [$PhCH_2$ (isomer B)], 73.7 [$PhCH_2$ (isomer A)], 73.9 [5-CH (isomer B)], 78.6 [4-CH (isomer B)], 79.0 [4-CH (isomer A)], 110.0 [$\underline{C}(CH_3)_2$], 110.2 [$\underline{C}(CH_3)_2$], 123.8 (CH), 124.3 (CH), 127.6 (CH), 127.7 (CH), 127.8 (CH), 128.4 (CH), 129.2 (CH), 129.3 (CH), 131.2 (S-Ph 4-CH), 131.3 (S-Ph 4-CH), 137.6 (C-Ph 1-C_q), 137.7 (C-Ph 1-C_q), 143.5 [S-Ph 1-C_q (isomer B)], 144.5 [S-Ph 1-C_q (isomer A)]; MS (FAB+) *m/z* 361 (M + H), 303 (M + H – Me_2CO); $[\alpha]^{20}_D$ = +4.4° (c 2.0, $CHCl_3$).

4*S*,5*R*,S(±)-4-(Benzyloxymethyl)-2,2-dimethyl-5-[N-(trifluoroacetyl)phenyl-sulfonimidoylmethyl]-1,3-dioxolane (103a/b)

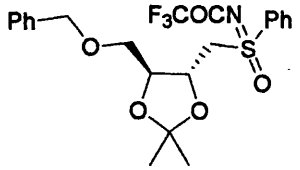

To a suspension of compounds **102a/b** (180 mg, 0.5 mmol), trifluoroacetamide (113 mg, 1.0 mmol), MgO (80.6 mg, 2.0 mmol) and $Rh_2(OAc)_4$ (5.52 mg, 2.5 mol %) in DCM (10 mL) was added $PhI(OAc)_2$ (242 mg, 0.75 mmol) and the mixture was stirred for 6 d. The suspension was filtered (Celite®); evaporation and chromatography [pet. ether (40-60°C) / Et_2O, 1:1] afforded **103a/b** (176 mg, 75%) as a 3:2 mixture of diastereoisomers as a pale yellow oil: TLC R_f = 0.2 [pet. ether (40-60°C) / Et_2O, 1:1]; IR ν_{max} (film) 705, 739, 1173 (CF_3), 1265, 1422 cm^{-1}; ^1H NMR (400 MHz, $CDCl_3$) δ 1.16 (1.8 H, CH_3), 1.21 (1.2 H, CH_3), 1.25 (1.8 H, CH_3), 1.26 (1.2 H, CH_3), 3.42 (dd, *J* = 9.6,

6.8 Hz, BnOCH) and 3.43 (dd, J = 9.7, 6.8 Hz, BnOCH) for a total of one proton, 3.65 (dd, J = 10.7, 4.7 Hz, BnOCH) and 3.66 (dd, J = 10.2, 4.7 Hz, BnOCH) for a total of one proton, 3.79 (dd, J = 14.1, 8.6 Hz, SCH) and 3.81 (dd, J = 14.4, 9.7 Hz, SCH) for a total of one proton, 3.86-3.92 (1 H, m, 4-H), 3.99 (dd, J = 11.2, 2.3 Hz, SCH) and 4.03 (dd, J = 11.2, 2.2 Hz, SCH) for a total of one proton, 4.14-4.19 (1 H, m, 5-H), 4.49 (2 H, s, $PhCH_2$), 7.23-7.37 (5 H, m, Ph-H_5), 7.54-7.60 (2 H, m, S-Ph 3,5-H_2), 7.70 (1 H, t, J = 8 Hz, S-Ph 4-H), 7.94 (2 H, d, J = 8 Hz, S-Ph 2,6-H_2); ^{13}C NMR (100 MHz, $CDCl_3$) (HMQC, HMBC) δ 26.4 (CH_3), 26.6 (CH_3), 58.5 (SCH_2), 59.3 (SCH_2), 69.6 ($BnOCH_2$), 69.7 ($BnOCH_2$), 72.9 (5-CH), 73.3 (5-CH), 73.6 ($PhCH_2$), 73.7 ($PhCH_2$), 78.1 (4-CH), 78.2 (4-CH), 110.8 [$\underline{C}(CH_3)_2$], 127.7 (CH), 127.8 (CH), 127.9 (C-Ph 2-CH or 6-CH), 128.0 (CH), 128.2 (S-Ph 2-CH or 6-CH), 128.3 (CH), 128.47 (CH), 128.49 (CH), 128.53 (C-Ph 3-CH or 5-CH), 129.0 (CH), 129.5 (S-Ph 3-CH or 5-CH), 134.6 (S-Ph 4-CH), 134.8 (S-Ph 4-CH), 135.3 (S-Ph 1-C_q), 135.4 (S-Ph 1-C_q), 137.32 (C-Ph 1-C_q), 137.35 (C-Ph 1-C_q); ^{19}F NMR (376 MHz, $CDCl_3$) δ –76.0 (1.8 F, s), –75.9 (1.2 F, s); HRMS (FAB+) *m/z* 472.1382 (M + H) ($^{12}C_{22}H_{25}NO_5F_3S$ requires 472.1406), 472 (M + H – O), 414 (M + H – Me_2CO); $[\alpha]^{20}_D$ = +5.1° (c 2.6, $CHCl_3$).

4*S*,5*R*,S(*R*)- and 4*S*,5*R*,S(*S*)-4-(Benzyloxymethyl)-2,2-dimethyl-5-(phenylsulfonimidoylmethyl)-1,3-dioxolane (104)

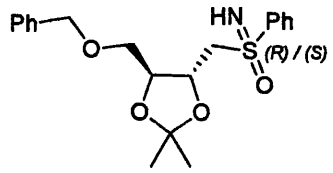

Compounds **103a/b** (176 mg, 0.37 mmol) were stirred with NH_3 (35% in water, 2 mL) in MeOH (5 mL) overnight. Evaporation and chromatography (EtOAc / hexane, 2:3) yielded **S-(*R*)-104** (42 mg, 30%) as a pale yellow oil: TLC R_f = 0.5 (EtOAc / hexane, 7:3); IR ν_{max} (film) 733, 2926, 3332 cm^{-1}; ^1H NMR (400 MHz, $CDCl_3$) δ 1.33 (3 H, s, CH_3), 1.37 (3 H, s, CH_3), 3.10 (1 H, br s, NH), 3.30 (1 H, dd, J = 13.6, 8.7 Hz, SCH), 3.45 (1 H, dd, J = 13.6, 2.9 Hz, SCH), 3.53 (1 H, dd, J = 9.8, 5.8 Hz, BnOCH), 3.67 (1 H, dd, J = 9.8, 5.3 Hz, BnOCH), 3.90 (1 H, dt, J = 7.7, 5.3 Hz, 4-H), 4.45 (1 H, dt, J = 2.9, 8.7 Hz, 5-H), 4.51 (2 H, s, $PhCH_2$), 7.27-7.35 (5 H, m, Ph-H_5), 7.48-7.52 (2 H, m, S-Ph 3,5-H_2), 7.57-7.61 (1 H, m, S-Ph 4-H), 7.98-8.01 (2 H, m, S-Ph 2,6-H_2); ^{13}C NMR (100 MHz, $CDCl_3$) (HMQC) δ 26.8 (CH_3), 26.9 (CH_3), 61.3 (SCH_2), 70.0 ($BnOCH_2$), 73.6 ($PhCH_2$), 73.7 (5-CH), 78.7 (4-CH), 110.4 [$\underline{C}(CH_3)_2$], 127.6 (2 x CH), 127.7 (CH), 128.4

(2 x CH), 128.5 (S-Ph 2-CH and 6-CH), 129.0 (S-Ph 3-CH and 5-CH), 133.1 (S-Ph 4-CH), 137.6 (C_q), 141.5 (C_q); MS (FAB+) *m/z* 376 (M + H); HRMS (ES+) *m/z* 775 (2 M + Na), 399 (M + Na), 375 (M); $[\alpha]^{20}_D$ = +8.4° (c 2.3, $CHCl_3$).

Further elution gave **S-(*S*)-104** (47 mg, 34%) as a white solid: TLC R_f = 0.4 (EtOAc / hexane, 7:3); mp 86-88°C; IR ν_{max} (KBr) 734, 2934, 2990, 3332 cm^{-1}; ^1H NMR (400 MHz, $CDCl_3$) δ 1.21 (3 H, s, CH_3), 1.29 (3 H, s, CH_3), 3.39 (1 H, dd, *J* = 14.2, 8.2 Hz, SCH), 3.50-3.54 (2 H, m, SCH + BnOCH), 3.64 (1 H, dd, *J* = 9.7, 5.3 Hz, BnOCH), 3.93 (1 H, dt, *J* = 7.6, 5.3 Hz, 4-H), 4.31 (1 H, dt, *J* = 3.4, 8.2 Hz, 5-H), 4.51 (2 H, s, $PhCH_2$), 7.26-7.35 (5 H, m, Ph-H_5), 7.45-7.50 (2 H, m, S-Ph 3,5-H_2), 7.55-7.60 (1 H, m, S-Ph 4-H), 7.94-7.97 (2 H, m, S-Ph 2,6-H_2); ^{13}C NMR (100 MHz, $CDCl_3$) (HMQC) δ 26.7 (CH_3), 26.8 (CH_3), 61.0 (SCH_2), 69.9 ($BnOCH_2$), 73.5 (5-CH), 73.6 ($PhCH_2$), 78.6 (4-CH), 110.1 [$\underline{C}(CH_3)_2$], 127.6 (2 x CH), 127.7 (CH), 128.4 (2 x CH), 128.5 (S-Ph 2-CH and 6-CH), 128.8 (S-Ph 3-CH and 5-CH), 133.0 (S-Ph 4-CH), 137.6 (C_q), 141.5 (C_q); MS (FAB+) *m/z* 376 (M + H); $[\alpha]^{20}_D$ = +7.8° (c 2.3, $CHCl_3$).

2*S*,3*R*,S(*R*)-1-(Benzyloxy)-4-(phenylsulfonimidoyl)butane-2,3-diol (105)

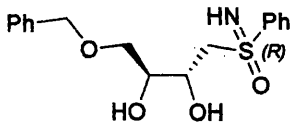

Compound **S-(*R*)-104** (38 mg, 0.1 mmol) was treated with aq. HCl (9 M, 1 mL) in MeOH (5 mL) for 4 h. Evaporation and chromatography (EtOAc / MeOH, 7:3) afforded **105** (37 mg, 100%) as a pale yellow oil: TLC R_f = 0.8 (EtOAc / MeOH, 7:3); IR ν_{max} (film) 3305 (OH) cm^{-1}; ^1H NMR (400 MHz, $CDCl_3$) δ 2.68 (1 H, br, OH), 3.13 (1 H, dd, *J* = 13.8, 1.7 Hz, SCH), 3.45 (1 H, dd, *J* = 13.8, 10.1 Hz, SCH), 3.59-3.63 (2 H, m, $BnOCH_2$), 3.69 (1 H, m, 3-H), 4.54-4.56 (3 H, m, $PhCH_2$ + 4-H), 7.27-7.35 (5 H, m, Ph-H_5), 7.53-7.58 (2 H, m, S-Ph 3,5-H_2), 7.64 (1 H, m, S-Ph 4-H), 7.98 (2 H, m, S-Ph 2,6-H_2); ^{13}C NMR (100 MHz, $CDCl_3$) (HMQC, HMBC) δ 59.8 (SCH_2), 66.4 (4-CH), 71.0 ($BnOCH_2$), 72.4 (3-CH), 73.5 ($PhCH_2$), 127.7 (2 x CH), 127.8 (CH), 128.1 (2 x CH), 128.5 (S-Ph 2-CH and 6-CH), 129.4 (S-Ph 3-CH and 5-CH), 133.5 (S-Ph 4-CH), 137.7 (C_q), 142.6 (C_q); MS (FAB+) *m/z* 336 (M + H); HRMS (ES+) *m/z* 693 (2 M + Na), 671 (2 M + H), 336.1264 (M + H) ($^{12}C_{17}H_{23}NO_4S$ requires 336.1264); MS (ES–) *m/z* 372/370 (M + Cl); MS (EI+) *m/z* 336 (M + H), 244 (M – Bn), 214 (M – $BnOCH_2$), 91 (Bn); $[\alpha]^{20}_D$ = +5.5° (c 1.3, $CHCl_3$).

4*S*,5*R*-4-(Benzyloxymethyl)-2,2-dimethyl-5-(3-bromophenylthiomethyl)-1,3-dioxolane (88)

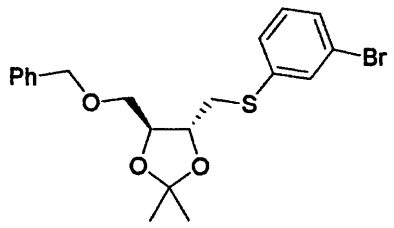

Method A: A cooled (0°C) solution of 3-bromothiophenol (**87**, 374 mg, 1.98 mmol) and **98** (500 mg, 1.98 mmol) in dry THF (5 mL) was added to a cooled (0°C) solution of triphenylphosphine (1.04 g, 3.96 mmol) and diisopropyl azodicarboxylate (800 mg, 3.96 mmol) in dry THF (7 mL) under Ar and the reaction mixture was allowed to warm to RT and stirred overnight. Evaporation and chromatography (hexane / Et_2O, 5:1) gave **88** (410 mg, 49%) as a yellow oil: TLC R_f = 0.7 (hexane / Et_2O, 5:1); ^1H NMR (400 MHz, $CDCl_3$) δ 1.39 (3 H, s, CH_3), 1.43 (3 H, s, CH_3), 3.16-3.19 (2 H, m, SCH_2), 3.59-3.66 (2 H, m, $BnOCH_2$), 4.03-4.05 (2 H, m, 4,5-H_2), 4.57 (2 H, s, $PhCH_2$), 7.08 (1 H, t, *J* = 8.0 Hz, Ar 5-H), 7.22 (1 H, ddd, *J* = 8.1, 1.8, 1.0 Hz, Ar 6-H), 7.42-7.46 (5 H, m, Ph-H_5), 7.48-7.51 (2 H, m, Ar 2,4-H_2); ^{13}C NMR (100 MHz, $CDCl_3$) (HMQC) δ 27.0 (CH_3), 27.1 (CH_3), 36.3 (SCH_2), 70.5 ($BnOCH_2$), 73.6 ($PhCH_2$), 77.2 (5-CH), 79.1 (4-CH), 110.0 [$\underline{C}(CH_3)_2$], 122.8 (C_q), 127.3 (CH), 127.8 (2 x CH), 128.4 (2 x CH), 129.0 (CH), 130.2 (CH), 131.2 (CH), 132.3 (CH), 137.7 (C_q), 138.5 (C_q); $[\alpha]^{20}_D$ = +6.1° (c 2.5, $CHCl_3$).

Method B: To a cooled (0°C) solution of tributylphosphine (670 mg, 3.31 mmol) and 1,1'-(azo-dicarbonyl)dipiperidine (835 mg, 3.31 mmol) in dry THF (7 mL) was added 3-bromothiophenol (**87**, 625 mg, 3.31 mmol) under Ar and the reaction mixture was sonicated for 30 min. While the mixture was being sonicated, **98** (558 mg, 2.21 mmol) in dry THF (3 mL) was added and the reaction mixture was stirred at RT overnight. Filtration, evaporation and chromatography (hexane / Et_2O, 5:1) gave **88** (650 mg, 69%) as a yellow oil. The data were identical to those above.

4*S*,5*R*,S(±)-4-(Benzyloxymethyl)-2,2-dimethyl-5-(3-bromophenylsulfinylmethyl)-1,3-dioxolane (89a/b)

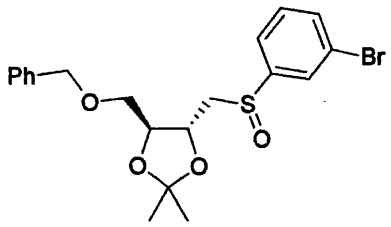

Compound **88** (1.06 g, 2.5 mmol) was treated with *m*CPBA (559 mg, 2.5 mmol) in DCM at –78°C for 5 h. The mixture was diluted with DCM (10 mL) and washed with aq. $NaHCO_3$ (1 M) and water. Drying and evaporation gave **89a/b** (1.62 g, 68%) as a 1:1 mixture of diastereoisomers as a yellow oil: TLC R_f = 0.2 [pet. ether (40-60°C) / Et_2O, 1:1]; ^1H NMR (600 MHz, $CDCl_3$) δ 1.36 (1.5 H, s, CH_3), 1.41 (1.5 H, s, CH_3), 1.45 (3 H, CH_3), 2.83 [0.5 H, dd, *J* = 13.2, 9.9 Hz, SCH (isomer A)], 3.04 [0.5 H, dd, *J* = 13.4, 3.4 Hz, SCH (isomer B)], 3.06 [0.5 H, dd, *J* = 13.0, 3.6 Hz, SCH (isomer A)], 3.18 [0.5 H, dd, *J* = 13.4, 7.0 Hz, SCH (isomer B)], 3.46-3.54 [1 H, m, BnOCH (both isomers)], 3.62 [0.5 H, dd, *J* = 10.1, 4.6 Hz, BnOCH (isomer B)], 3.68 [0.5 H, dd, *J* = 9.6, 4.6 Hz, BnOCH (isomer A)], 3.89 [0.5 H, m, 4-H (isomer A)], 4.00 [0.5 H, ddd, *J* = 8.1, 7.2, 4.2 Hz, 5-H (isomer B)], 4.13 [0.5 H, dt, *J* = 8.1, 10.4 Hz, 4-H (isomer B)], 4.39 [0.5 H, ddd, *J* = 10.1, 8.3, 2.3 Hz, 5-H (isomer A)], 4.51 (1 H, s, $PhCH_2$), 4.52 (0.5 H, d, *J* = 12.0 Hz, PhCH), 4.55 (0.5 H, d, *J* = 12.0 Hz, PhCH), 7.23-7.84 (9 H, Ph-H_5 + Ar-H_4); ^{13}C NMR (100 MHz, $CDCl_3$) (HMQC) δ 26.8 (CH_3), 26.91 (CH_3), 26.94 (CH_3), 27.1 (CH_3), 60.0 [SCH_2 (isomer B)], 62.3 [SCH_2 (isomer A)], 69.5 (CH_2), 70.0 (CH_2), 73.2 [5-CH (isomer A)], 73.59 [5-CH (isomer B)], 73.66 ($PhCH_2$), 73.70 ($PhCH_2$), 78.5 [4-CH (isomer B)], 78.9 [4-CH (isomer A)], 110.1 [$\underline{C}(CH_3)_2$], 110.3 [$\underline{C}(CH_3)_2$], 122.4 (CH), 122.9 (CH), 123.4 (C_q), 123.6 (C_q), 127.6 (CH), 127.78 (CH), 127.81 (CH), 128.42 (CH), 128.45 (CH), 128.46 (CH), 130.6 (CH), 130.8 (CH), 132.0 (CH), 132.1 (CH), 134.20 (CH), 134.24 (CH), 137.5 (C_q), 137.6(C_q), 145.8 (C_q), 146.8 (C_q); $[\alpha]^{20}_D$ = +3.7° (c 2.0, $CHCl_3$).

4*S*,5*R*,S(±)-4-(Benzyloxymethyl)-2,2-dimethyl-5-[N-(trifluoroacetyl)-3-bromo-phenylsulfonimidoylmethyl]-1,3-dioxolane (90a/b)

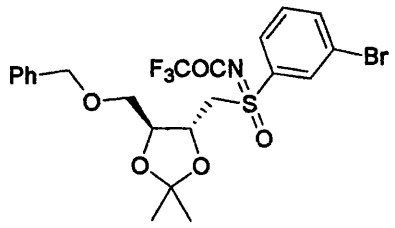

To a suspension of compounds **89a/b** (1.62 g, 3.69 mmol), trifluoroacetamide (834 mg, 7.38 mmol), MgO (595 mg, 14.8 mmol) and $Rh_2(OAc)_4$ (41.0 mg, 2.5 mol %) in DCM (50 mL) was added $PhI(OAc)_2$ (1.78 g, 5.54 mmol) and the mixture was stirred for 6 days. The suspension was filtered (Celite®); evaporation and chromatography [pet. ether (40-60°C)/Et_2O, 1:1] afforded **90a/b** (1.69 g, 83%) as a 1:1 mixture of diastereoisomers as a pale yellow oil: TLC R_f = 0.2 [pet. ether (40-60°C) / Et_2O, 1:1]; IR ν_{max} (film) 733, 908, 1176 (CF_3), 1216 (CF_3), 1383 [$C(CH_3)_2$], 1746 (C=O) cm^{-1}; ^1H NMR (400 MHz, $CDCl_3$) δ 1.15 (1.5 H, s, CH_3), 1.21 (1.5 H, s, CH_3), 1.26 (1.5 H, s, CH_3), 1.28 (1.5 H, s, CH_3), 3.43-3.54 (1 H, m, BnOCH), 3.66 (0.5 H, dd, *J* = 8.2, 4.8 Hz, BnOCH), 3.68 (0.5 H, dd, *J* = 8.2, 4.8 Hz, BnOCH), 3.70-3.75 (0.5 H, m, SCH), 3.76 (0.5 H, dd, *J* = 14.6, 9.8 Hz, SCH), 3.83-3.91 (1 H, m, 4-H), 4.05 (0.5 H, dd, *J* = 10.0, 2.2 Hz, SCH), 4.09 (0.5 H, dd, *J* = 9.9 Hz, 2.3 Hz, SCH), 4.14-4.22 (1 H, m, 5-H), 4.51 (2 H, s, $PhCH_2$), 7.27-7.40 (5 H, m, Ph-H_5), 7.43 (1 H, dt, *J* = 1.9, 8.0 Hz, Ar 5-H), 7.72-7.85 (2 H, m, Ar 4,6-H_2), 8.08 (0.5 H, t, *J* = 1.6 Hz, Ar 2-H), 8.11 (0.5 H, t, *J* = 1.9 Hz, Ar 2-H); ^{13}C NMR (100 MHz, $CDCl_3$) (HMQC) δ 26.4 (CH_3), 26.5 (CH_3), 26.6 (CH_3), 58.6 (SCH_2), 59.4 (SCH_2), 69.5 ($BnOCH_2$), 69.6 ($BnOCH_2$), 72.9 (5-CH), 73.4 (5-CH), 73.8 ($PhCH_2$), 77.97 (4-CH), 78.02 (4-CH), 110.8 [$\underline{C}(CH_3)_2$], 110.9 [$\underline{C}(CH_3)_2$], 123.3 (C_q), 126.7 (CH), 126.8 (CH), 127.8 (CH), 128.0 (CH), 128.1 (CH), 128.5 (CH), 128.6 (CH), 130.83 (Ar 5-CH), 130.85 (Ar 5-CH), 131.3 (Ar 2-CH), 131.4 (Ar 2-CH), 137.2 (C_q), 137.3 (C_q), 137.4(C_q), 137.5 (C_q), 137.7 (CH), 137.8 (CH); ^{19}F NMR (376 MHz, $CDCl_3$) δ –76.0 (1.5 F, s), –75.9 (1.5 F, s); $[\alpha]^{20}_D$ = +4.3° (c 1.4, $CHCl_3$).

4*S*,5*R*,S(*R*)- and 4*S*,5*R*,S(*S*)-4-(Benzyloxymethyl)-2,2-dimethyl-5-(3-bromophenyl-sulfonimidoylmethyl)-1,3-dioxolane (91)

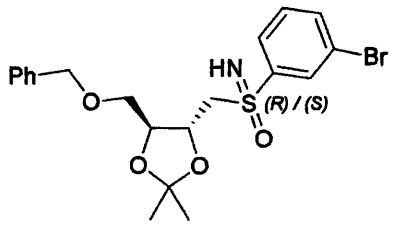

Compounds **90a/b** (2.00 g, 3.63 mmol) were stirred with NH_3 (35% in water, 5 mL) in MeOH (20 mL) overnight. Evaporation and chromatography (EtOAc / hexane, 7:3) yielded **S-(*R*)-91** (472 mg, 29%) as a pale yellow oil: TLC R_f = 0.6 (EtOAc / hexane, 7:3); ^{1}H NMR (400 MHz, $CDCl_3$) δ 1.22 (3 H, s, CH_3), 1.32 (3 H, s, CH_3), 3.34 (1 H, dd, *J* = 14.5, 9.0 Hz, SCH), 3.46 (1 H, dd, *J* = 14.5, 2.7 Hz, SCH), 3.52 (1 H, dd, *J* = 9.8, 6.3 Hz, BnOCH), 3.69 (1 H, dd, *J* = 9.8, 5.1 Hz, BnOCH), 3.86 (1 H, ddd, *J* = 7.8, 6.3, 4.7 Hz, 4-H), 4.31 (1 H, ddd, *J* = 8.6, 7.8, 2.7 Hz, 5-H), 4.53 (2 H, s, $PhCH_2$), 7.29-7.37 (5 H, m, Ph-H_5), 7.38 (1 H, t, *J* = 7.8 Hz, Ar 5-H), 7.75 (1 H, ddd, *J* = 7.8, 2.0, 0.8 Hz, Ar 4-H or Ar 6-H), 7.82 (1 H, ddd, 7.8, 2.0, 0.8 Hz, Ar 6-H or Ar 4-H), 8.08 (1 H, t, *J* = 1.9 Hz, Ar 2-H); ^{13}C NMR (100 MHz, $CDCl_3$) (HMQC) δ 26.7 (CH_3), 26.8 (CH_3), 59.7 (SCH_2), 69.9 ($BnOCH_2$), 73.6 (5-CH), 73.7 ($PhCH_2$), 78.4 (4-CH), 110.3 [$\underline{C}(CH_3)_2$], 122.8 (C_q), 126.9 (Ar 6-CH or Ar 4-CH), 127.7 (2 x CH), 127.9 (CH), 128.5 (2 x CH), 130.4 (Ph 5-CH), 131.6 (Ar 2-CH), 136.7 (Ar 4-CH or Ar 6-CH), 137.5 (C_q), 141.6 (C_q); HRMS (ES+) *m/z* 456.0642 (^{81}Br-M + H), 455.0585 (^{81}Br-M), 454.0669 (^{79}Br-M + H) ($^{12}C_{20}H_{25}{}^{79}BrNO_4S$ requires 454.0682), 453.0604 (^{79}Br-M); $[\alpha]^{20}_D$ = +3.2° (c 1.5, $CHCl_3$).

Further elution gave **S-(*S*)-91** (530 mg, 32%) as a white solid: TLC R_f = 0.5 (EtOAc / hexane, 7:3); mp 75-77°C; ^{1}H NMR (400 MHz, $CDCl_3$) δ 1.20 (3 H, s, CH_3), 1.31 (3 H, s, CH_3), 2.32 (1 H, br s, NH), 3.38 (1 H, dd, *J* = 14.3, 8.7 Hz, SCH), 3.52 (1 H, dd, *J* = 9.5, 6.3 Hz, BnOCH), 3.54 (1 H, dd, *J* = 14.3, 3.0 Hz, SCH), 3.66 (1 H, dd, *J* = 9.5, 5.1 Hz, BnOCH), 3.89 (1 H, ddd, *J* = 8.0, 6.3, 5.1 Hz, 4-H), 4.33 (1 H, ddd, *J* = 8.5, 8.0, 2.9 Hz, 5-H), 4.53 (2 H, s, $PhCH_2$), 7.27-7.39 (5 H, m, Ph-H_5), 7.36 (1 H, t, *J* = 8.0 Hz, Ar 5-H), 7.70 (1 H, ddd, *J* = 8.0, 2.1, 1.0 Hz, Ar 4-H or Ar 6-H), 7.90 (1 H, ddd, *J* = 8.0, 2.1, 1.0 Hz, Ar 6-H or Ar 4-H), 8.14 (1 H, t, *J* = 1.9 Hz, Ar 2-H); ^{13}C NMR (100 MHz, $CDCl_3$) (HMQC) δ 26.7 (CH_3), 26.8 (CH_3), 61.0 (SCH_2), 69.9 ($BnOCH_2$), 73.7 ($PhCH_2$ + 5-CH), 78.4 (4-CH), 110.3 [$\underline{C}(CH_3)_2$], 122.7 (C_q), 127.2 (Ar 6-CH or Ar 4-CH), 127.7 (2 x CH), 127.9 (CH), 128.5 (2 x CH), 130.3 (Ar 5-CH), 131.8 (Ar 2-CH), 136.0 (Ar 4-CH or Ar

6-CH), 137.5 (C_q), 144.3 (C_q); Anal. Calcd. for $C_{20}H_{24}BrNO_4S$: C, 52.87; H, 5.32; N, 3.08. Found: C, 52.82; H, 5.22; N, 3.06; $[\alpha]^{20}_D$ = +2.6° (c 1.5, $CHCl_3$).

2*S*,3*R*,S(*R*)-1-(Benzyloxy)-4-(3-bromophenylsulfonimidoyl)butane-2,3-diol (92)

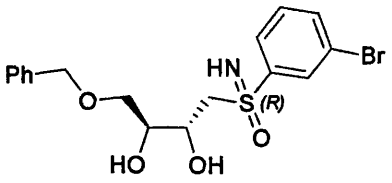

Compound **S-(*R*)-91** (200 mg, 0.44 mmol) was treated with aq. HCl (9 M, 1 mL) in MeOH (5 mL) for 4 h. Evaporation and chromatography (EtOAc / MeOH, 7:3) afforded **92** (180 mg, 100%) as a pale yellow solid: TLC R_f = 0.8 (EtOAc / MeOH, 7:3); mp 73-76°C; IR ν_{max} (KBr) 3425 (OH) cm^{-1}; ^1H NMR (400 MHz, $CDCl_3$) δ 3.00 (2 H, br, 2 x OH), 3.13 (1 H, d, *J* = 14 Hz, SCH), 3.45 (1 H, dd, *J* = 13.9, 10.1 Hz, SCH), 3.59-3.64 (2 H, m, $BnOCH_2$), 3.70 (1 H, m, 2-H), 4.52 (1 H, d, *J* = 11.7 Hz, PhCH), 4.54 (1 H, d, *J* = 11.7 Hz, PhCH), 4.55 (1 H, br d, *J* = 10 Hz, 3-H), 7.27-7.36 (5 H, m, Ph-H_5), 7.43 (1 H, t, *J* = 7.9 Hz, Ar 5-H), 7.75 (1 H, ddd, *J* = 8.0, 1.9, 0.8 Hz, Ar 4-H or Ar 6-H), 7.91 (1 H, ddd, *J* = 8.0, 1.9, 0.8 Hz, Ar 6-H or Ar 4-H), 8.12 (1 H, t, *J* = 1.8 Hz, Ar 2-H); ^{13}C NMR (100 MHz, $CDCl_3$) δ 59.9 (SCH_2), 66.5 (3-CH), 71.0 ($BnOCH_2$), 72.3 (2-CH), 73.6 ($PhCH_2$), 123.4 (C_q), 126.7 (Ar 6-CH or Ar 4-CH), 127.9 (2 x CH), 128.0 (CH), 128.6 (2 x CH), 130.9 (Ar 5-CH), 131.1 (Ar 2-CH), 136.7 (Ar 4-CH or Ar 6-CH), 137.6 (C_q), 141.0 (C_q); Anal. Calcd. for $C_{17}H_{20}BrNO_4S$: C, 49.28; H, 4.87; N, 3.38. Found: C, 49.48; H, 4.61; N, 2.95; $[\alpha]^{20}_D$ = +2.5° (c 1.7, $CHCl_3$).

2*S*,3*R*,S-1-(Benzyloxymethyl)-4-[N-(trifluoroacetyl)-3-bromophenylsulfonimidoyl]-butane-2,3-diol (108)

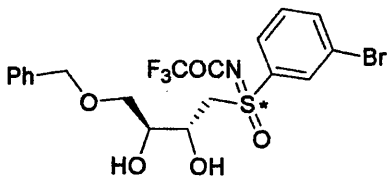

Configuration at sulfur not known since crystalline product (thus X-ray crystal data) could not be obtained

Compounds **90a/b** (1.50 g, 2.73 mmol) were treated with aq. HCl (9 M, 4 mL) in MeOH (15 mL) for 4 h. Evaporation and chromatography ($CHCl_3$ / MeOH, 10:1) afforded **108**

(620 mg, 45%) as a single diastereoisomer (unknown configuration at sulfur) as a pale yellow solid: TLC R_f = 0.5 ($CHCl_3$ / MeOH, 10:1); mp 84-85°C; IR ν_{max} (KBr) 736, 1293 (CF_3), 1314 (CF_3), 1407, 1454, 2867, 2924, 3436 (OH) cm^{-1}; ^1H NMR (400 MHz, $CDCl_3$) δ 3.11 (2 H, br s, OH), 3.33 (1 H, dd, *J* = 14.4, 3.1 Hz, SCH), 3.44 (1 H, dd, *J* = 14.6, 8.9 Hz, SCH), 3.58 (2 H, d, *J* = 5.1 Hz, $BnOCH_2$), 3.73 (1 H, dt, *J* = 2.9, 5.1 Hz, 2-H), 4.31 (1 H, dt, *J* = 8.9, 2.9 Hz, 3-H), 4.49-4.53 (2 H, m, $PhCH_2$), 7.23-7.37 (5 H, m, Ph-H_5), 7.44 (1 H, t, *J* = 7.9 Hz, Ar 5-H), 7.77 (1 H, ddd, *J* = 7.9, 1.9, 1.0 Hz, Ar 4-H or Ar 6-H), 7.84 (1 H, ddd, *J* = 7.9, 1.9, 1.0 Hz, Ar 6-H or Ar 4-H), 8.07 (1 H, t, *J* = 1.9 Hz, Ar 2-H); ^{13}C NMR (100 MHz, $CDCl_3$) (HMQC) δ 59.6 (SCH_2), 67.1 (3-CH), 71.3 (2-CH), 71.5 ($BnOCH_2$), 73.7 ($PhCH_2$), 123.2 (C_q), 126.6 (Ar 6-CH or Ar 4-CH), 127.8 (2 x CH), 128.0 (CH), 128.5 (2 x CH), 130.8 (Ar 5-CH), 130.9 (Ar 2-CH), 137.0 (Ar 4-CH or Ar 6-CH), 137.2 (C_q), 141.4 (C_q); ^{19}F NMR (376 MHz, $CDCl_3$) δ –76.0 (3 F, s, CF_3); $[\alpha]^{20}_D$ = +3.1° (c 2.1, $CHCl_3$).

4-Methoxybenzaldehyde dimethyl acetal (110)

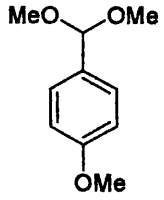

A mixture of 4-methoxybenzaldehyde (**109**, 5.61 g, 41 mmol) and 4-toluenesulfonic acid monohydrate (39 mg, 21 mmol) in trimethyl orthoformate (50 mL) was heated at 78°C for 4 h. The evaporation residue, in DCM, was washed with aq. $NaHCO_3$ (1 M) and dried. Evaporation gave **110** (6.81 g, 91%) as a colourless liquid: TLC R_f = 0.6 (hexane / EtOAc, 10:1); IR ν_{max} (film) 823, 2832 (OCH_3), 2938 cm^{-1}; ^1H NMR (400 MHz, $CDCl_3$) δ 3.30 [6 H, s, $C(OCH_3)_2$], 3.79 (3 H, s, OCH_3), 5.34 [1 H, s, $C\underline{H}(OCH_3)_2$], 6.88 (2 H, d, *J* = 8.9 Hz, Ph 3,5-H_2), 7.34 (2 H, dd, *J* = 8.9, 0.6 Hz, Ph 2,6-H_2); ^{13}C NMR (100 MHz, $CDCl_3$) (HMQC) δ 52.5 (2 x CH_3), 55.2 (CH_3), 103.0 (CH), 113.4 (Ph 3,5-C_2), 127.8 (Ph 2,6-C_2), 130.3 (Ph 1-C_q), 159.6 (Ph 4-C_q).

[4*S*,5*R*-5-(Benzyloxymethyl)-2,2-dimethyl-1,3-dioxolan-4-yl]methyl tosylate (123)

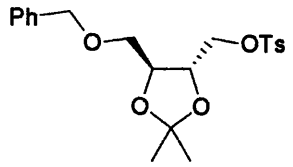

To a solution of **98** (500 mg, 1.98 mmol), DMAP (24.0 mg, 0.26 mmol) and triethylamine (401 mg, 3.96 mmol) in dry DCM (3 mL) was added toluene-4-sulfonyl chloride (566 mg, 2.97 mmol) at 0°C under N_2 and the reaction mixture was sonicated for 15 minutes and then stirred overnight. The evaporation residue, in EtOAc, was washed with water, brine and 5% aq. citric acid. Drying and evaporation afforded **123** (730 mg, 91%) as a pale yellow oil: TLC R_f = 0.5 [pet. ether (40-60°C) / Et_2O, 1:1]; IR ν_{max} (film) 738, 1266, 1365 (SO_3), 1711, 2988, 3055 cm^{-1}; ^1H NMR (400 MHz, $CDCl_3$) δ 1.32 (3 H, s, CH_3), 1.36 (3 H, s, CH_3), 2.42 (3 H, s, $ArCH_3$), 3.52 (1 H, dd, *J* = 10.2, 4.7 Hz, BnOCH), 3.60 (1 H, dd, *J* = 10.2, 4.7 Hz, BnOCH), 3.97-4.09 (3 H, m, TsOCH + 4,5-H_2), 4.19 (1 H, dd, *J* = 10.2, 3.1 Hz, TsOCH), 4.53 (2 H, s, $PhCH_2$), 7.28-7.36 (7 H, m, Ph-H_5 + Ar 3,5-H_2), 7.75 (2 H, d, *J* = 8.2 Hz, Ar 2,6-H_2); ^{13}C NMR (100 MHz, $CDCl_3$) (HMQC) δ 21.7 ($ArCH_3$), 26.7 (CH_3), 26.9 (CH_3), 69.3 ($TsOCH_2$), 70.0 ($BnOCH_2$), 73.6 ($PhCH_2$), 76.7 (4-CH + 5-CH), 110.2 [$\underline{C}(CH_3)_2$], 127.6 (2 x CH), 127.8 (CH), 128.0 (2 x CH), 128.4 (2 x CH), 129.8 (2 x CH), 132.7 (C_q), 137.6 (C_q), 144.9 (C_q); $[\alpha]^{20}_D$ = +8.6° (c 2.8, $CHCl_3$).

Methyl 2-(acetylthio)acetate (126)

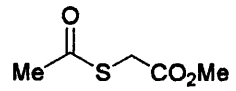

Methyl bromoacetate (**125**, 1.53 g, 10 mmol) was added to a vigorously stirred solution of potassium thioacetate (**124**, 1.14 g, 10 mmol) in MeOH (80 mL) under N_2. The mixture was stirred overnight and the organic layer was extracted with DCM and washed with water. Evaporation afforded **126** (1.46 g, 100%) as a colourless liquid: TLC R_f = 0.5 (hexane / EtOAc, 10:1); IR ν_{max} (film) 1135, 1300, 1436, 1744 (C=O), 2956, 3000 cm^{-1}; ^1H NMR (400 MHz, $CDCl_3$) δ 2.37 (3 H, s, CH_3CO), 3.69 (2 H, s, CH_2), 3.72 (3 H, s, CO_2CH_3); ^{13}C NMR (100 MHz, $CDCl_3$) δ 30.1 (CH_3), 31.2 (CH_2), 52.8 (CH_3), 169.2 (ester C=O), 193.8 (thioester C=O).

(*E*)-3-Benzyloxypropenoic acid (131)

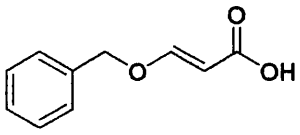

Methyl propynoate (**129**, 8.18 g, 84 mmol) was added to benzyl alcohol (**128**, 11.2 g, 84 mmol) in DCM (20 mL), followed by Bu_3P (2.1 g, 8.4 mmol) and the mixture was stirred overnight. Propan-2-ol (120 mL), water (120 mL) and aq. KOH (20%, 72 mL) were added and the mixture was stirred overnight. The solution was diluted with water (50 mL) and extracted with Et_2O (x 2). The aq. phase was acidified with aq. HCl (9 M) and extracted with Et_2O. The organic phase was washed (water) and dried. Evaporation and recrystallisation (EtOAc / hexane) afforded **131** (10.0 g, 67%) as pale yellow crystals: TLC R_f = 0.4 (EtOAc / hexane, 2:3); mp 116-117°C (lit.[200] mp 117-118°C); IR ν_{max} (KBr) 1609, 1668, 2500-3200 cm^{-1}; ^1H NMR (400 MHz, $CDCl_3$) δ 4.91 (2 H, s, $PhCH_2$), 5.29 (1 H, d, *J* = 12.8 Hz, C<u>H</u>CO_2H), 7.32-7.41 (5 H, m, Ph-H_5), 7.75 (1 H, d, *J* = 12.8 Hz, BnOCH); ^{13}C NMR (100 MHz, $CDCl_3$) δ 73.2 (CH_2), 96.8 (CH), 127.8 (CH), 128.7 (2 x CH), 128.8 (2 x CH), 135.0 (C_q), 164.1 (CH), 173.7 (C=O); HRMS (FAB+) *m/z* 179.0706 (M + H) ($^{12}C_{10}H_{11}O_3$ requires 179.0708), 91.0 (Bn).

Pentafluorophenyl (*E*)-3-benzyloxypropenoate (134)

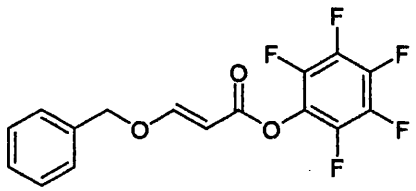

Pentafluorophenol (1.03 g, 5.62 mmol) was added to **131** (1.05 g, 5.62 mmol) in EtOAc at 0°C during 15 min. DCC (1.16 g, 5.62 mmol) was then added and the mixture was stirred at 0°C overnight. The suspension was filtered (Celite®) and the solid was washed with cold EtOAc. The combined organic phases were kept at 4°C for 48 h and filtered. Evaporation afforded **134** (1.20 g, 62%) as white crystals which were used in the next step without further purification: TLC R_f = 0.9 (EtOAc / hexane, 2:3); mp 98-100°C; IR ν_{max} (KBr) 1750 cm^{-1}; ^1H NMR (400 MHz, $CDCl_3$) δ 5.02 (2 H, s, $PhCH_2$), 5.55 (1 H, d, *J* = 12.5 Hz, C<u>H</u>CO_2), 7.38-7.41 (5 H, m, Ph-H_5), 7.92 (1 H, d, *J* = 12.5 Hz, BnOCH); ^{13}C NMR (100 MHz, $CDCl_3$) δ 73.9 (CH_2), 94.3 (CH), 127.9 (CH), 128.9 (2 x

CH), 129.0 (2 x CH), 134.5 (C_q), 163.3 (C=O), 165.7 (CH); ^{19}F NMR (376 MHz, $CDCl_3$) δ –162.8 (2 F, m, 3',5'-F_2), –158.7 (1 F, t, *J* = 21.7 Hz, 4'-F), –152.8 (2 F, m, 2',6'-F_2); HRMS (FAB+) *m/z* 345.0573 (M + H) ($^{12}C_{16}H_{10}O_3F_5$ requires 345.0550), 161.1 (M – OC_6F_5), 91 (Bn).

(1*R*,2*S*,5*R*)-Menthyl (*E*)-3-benzyloxypropenoate (136)

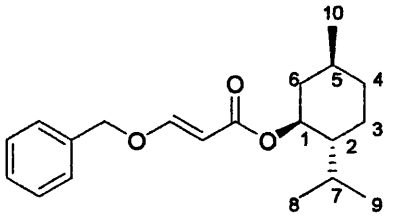

DCC (1.16 mg, 5.62 mmol) was added to **131** (1.00 g, 5.62 mmol) and *L*-menthol (**135**, 0.88 g, 5.62 mmol) in dry DCM. The mixture was stirred at 0°C for 10 min and DMAP (0.69 g, 5.62 mmol) was added. The mixture was stirred at 0°C for 2 h and at RT for 16 h. The suspension was filtered (Celite®) and the filtrate was washed with water and aq. $CuSO_4$ and kept at 4°C for 48 h. Filtration, drying, evaporation and chromatography (EtOAc / hexane, 1:4) gave **136** (0.48 g, 27%) as a colourless oil: TLC R_f = 0.7 (EtOAc / hexane, 1:4); IR ν_{max} (film) 1705 cm^{-1}; ^{1}H NMR (400 MHz, $CDCl_3$) δ 0.77 (3 H, d, *J* = 6.6 Hz, menthol C^{10}-H_3), 0.90 (6 H, dd, *J* = 6.6, 2.7 Hz, menthol $C^{8,9}$-H_6), 0.98-2.04 (10 H, m, menthol-H_{10}), 4.77 (1 H, dt, *J* = 4.3, 17.2 Hz, menthol C^1-H), 4.88 (2 H, s, $PhCH_2$), 5.30 (1 H, d, *J* = 12.7 Hz, $CHCO_2$), 7.32-7.39 (5 H, m, Ph-H_5), 7.66 (1 H, d, *J* = 12.7 Hz, BnOCH); ^{13}C NMR (100 MHz, $CDCl_3$) δ 16.0 (CH_3), 20.8 (CH_3), 22.1 (CH_3), 23.6 (CH_2), 26.4 (CH), 31.4 (CH), 34.3 (CH_2), 41.1 (CH_2), 47.2 (CH), 72.7 (CH_2), 73.5 (CH), 97.7 (CH), 127.8 (CH), 128.6 (2 x CH), 128.7 (2 x CH), 135.3 (C_q), 161.8 (CH), 167.3 (C=O); HRMS (FAB+) *m/z* 317.2137 (M + H) ($^{12}C_{20}H_{29}O_3$ requires 317.2117), 179 (M – menthyl), 91 (Bn); $[\alpha]^{20}_D$ = –59.8° (c = 5, $CHCl_3$).

S-(Trimethylsilylmethyl)isothiouronium chloride (139)

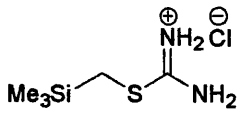

Chloromethyltrimethylsilane (**138**, 2.0 g, 16 mmol), thiourea (2.4 g, 32 mmol) and NaI (5 mg) were boiled under reflux in dry EtOH (20 mL) for 48 h. Evaporation and trituration (Et_2O) gave **139** (3.20 g, 100%) as a white solid which was used in the next step without further purification: mp 140-142°C (lit.[220] mp 141.5-143°C); ^1H NMR [270 MHz, $(CD_3)_2SO$] δ 0.15 [9 H, s, $(CH_3)_3Si$], 2.42 (2 H, s, CH_2), 7.11 (2 H, br s, NH_2), 9.11 (2 H, br s, NH_2).

S-[(Dimethylphenylsilyl)methyl]isothiouronium chloride (142)

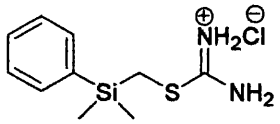

Chloromethyldimethylphenylsilane (**141**, 3.72 g, 20 mmol), thiourea (1.52 g, 20 mmol), and NaI (5 mg) were boiled under reflux in dry EtOH (30 mL) for 5 d. Evaporation and trituration (Et_2O) afforded **142** (4.86 g, 93%) as a white solid which was used in the next step without further purification: mp 113-115°C; ^1H NMR (400 MHz, $CDCl_3$) δ 0.45 [6 H, s, $(CH_3)_2Si$], 2.12 (1 H, br s, NH), 2.67 (2 H, s, CH_2), 7.35-7.42 (3 H, m, Ph 3,4,5-H_3), 7.50-7.55 (2 H, m, Ph 2,6-H_2), 7.91 (1 H, br s, NH), 9.16 (1 H, br s, NH); ^{13}C NMR (100 MHz, $CDCl_3$) δ 16.1 (CH_2), 128.1 (2 x CH), 130.2 (CH), 133.7 (2 x CH), 134.9 (C_q), 174.1 (C_q); MS (FAB+) *m/z* 227 (M), 225 (M), 147 [M – $HSC(NH_2)=NH_2$].

Dimethylphenylsilylmethanethiol (143)

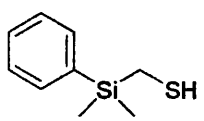

Compound **142** (4.86 g, 20 mmol) was stirred with aq. NaOH (40%, 100 mL, 1 mol) under N_2 overnight. The aqueous layer was washed with Et_2O and acidified with aq.

HCl (9 M). This was then extracted with Et_2O (x 3) and washed with brine. Drying and evaporation yielded **143** (3.45 g, 87%) as a pale yellow liquid: ^{1}H NMR (270 MHz, $CDCl_3$) δ 0.37 [6 H, s, $(CH_3)_2Si$], 1.08 (1 H, t, *J* = 7.2 Hz, SH), 1.84 (2 H, d, *J* = 7.2 Hz, CH_2), 7.35-7.37 (3 H, m, Ph 3,4,5-H_3), 7.50-7.57 (2 H, m, Ph 2,6-H_2). No further data could be obtained due to fast oxidation.

Chloromethyl (dimethylphenylsilylmethyl) sulfide (144)

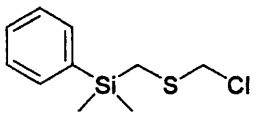

HCl was bubbled through 1,3,5-trioxane (1.02 g, 11 mmol) and **143** (3.45 g, 19 mmol) at –10°C until saturated. After 12 h at 0°C, the mixture was dried over anhydrous $CaCl_2$ at 0°C for 2 h to give crude **144** (1.29 g, 29%) as a pale yellow oil: ^{1}H NMR (270 MHz, $CDCl_3$) δ 0.40 [6 H, s, $(CH_3)_2Si$], 2.25 (2 H, s, CH_2Si), 4.67 (2 H, s, CH_2Cl), 7.36-7.43 (3 H, m, Ph 3,4,5-H_3), 7.55-7.59 (2 H, m, Ph 2,6-H_2). No further data could be obtained owing to decomposition.

But-3-enyl tosylate (147)

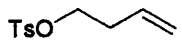

$LiN(SiMe_3)_2$ (1.0 M in THF, 6.93 mL, 6.93 mmol) was added to but-3-en-1-ol (**146**, 500 mg, 6.93 mmol) in dry THF (5 mL) at –78°C under Ar during 30 min. Toluene-4-sulfonyl chloride (1.32 g, 6.93 mmol) was added and the mixture was allowed to reach RT during 16 h. The evaporation residue, in EtOAc, was washed with aq. HCl (1 M), aq. $NaHCO_3$ (1 M), water and brine and was dried. Evaporation gave **147** (1.56 g, 100%) as a pale buff oil: TLC R_f = 0.4 (EtOAc / hexane, 2:3); IR ν_{max} (film) 821, 907, 1184, 1420, 1600 cm^{-1}; ^{1}H NMR (400 MHz, $CDCl_3$) δ 2.31-2.38 (2 H, m, $C\underline{H}_2CH{=}CH_2$), 2.41 (3 H, s, CH_3), 4.02 (2 H, t, *J* = 6.7 Hz, $TsOCH_2$), 5.01-5.06 (2 H, m, $C{=}CH_2$), 5.64 (1 H, m, $C\underline{H}{=}CH_2$), 7.31 (2 H, d, *J* = 8.6 Hz, Ph 3,5-H_2), 7.75 (2 H, d, *J* = 8.6 Hz, Ph 2,6-H_2); ^{13}C NMR (100 MHz, $CDCl_3$) δ 21.5 (CH_3), 33.0 (CH_2), 69.3 (CH_2), 118.1 (CH_2), 127.7 (2 x CH), 129.7 (2 x CH), 132.3 (CH), 132.8 (C_q), 144.7 (C_q); MS (FAB+) *m/z* 227 (M + H), 173 (M – $CH_2CH_2CH{=}CH_2$).

S-Benzyl thioacetate (149)

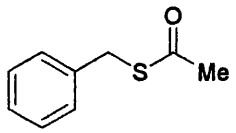

Benzyl chloride (**148**, 1.27 g, 10 mmol) was added to a vigorously stirred solution of potassium thioacetate (**124**, 1.14 g, 10 mmol) in MeOH (80 mL) under N_2. The mixture was stirred at RT overnight and the organic layer was extracted with DCM and washed with water. Evaporation afforded **149** (1.70 g, 100%) as a colourless liquid: TLC R_f = 0.7 (EtOAc / hexane, 1:4); IR ν_{max} (film) 1691 (C=O) cm^{-1}; ^1H NMR (400 MHz, $CDCl_3$) δ 2.32 (3 H, s, CH_3), 4.12 (2 H, s, CH_2), 7.24-7.40 (5 H, m, Ph-H_5); ^{13}C NMR (100 MHz, $CDCl_3$) δ 30.0 (CH_2), 33.1 (CH_3), 127.0 (CH), 128.4 (2 x CH), 128.6 (2 x CH), 137.4 (C_q), 194.7 (C=O).

4-(Benzylthio)but-1-ene (150)

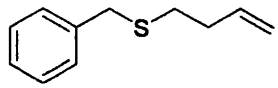

To **147** (500 mg, 2.20 mmol) in MeOH (10 mL) at 0°C was added slowly NaOH (0.5 M in water, 4.40 mL, 2.20 mmol)) and **149** (366 mg, 2.20 mmol) under N_2 and the mixture was stirred at RT for 4 h. Evaporation and chromatography (EtOAc / hexane, 1:10) gave **150** (340 mg, 87%) as a colourless oil: TLC R_f = 0.8 (EtOAc / hexane, 1:4); IR ν_{max} (film) 825, 970, 1467 cm^{-1}; ^1H NMR (270 MHz, $CDCl_3$) δ 2.25-2.34 (2 H, m, $C\underline{H}_2CH{=}CH_2$), 2.47 (2 H, t, J = 7.3 Hz, $BnSCH_2$), 3.72 (2 H, s, $PhCH_2$), 4.99-5.07 (2 H, m, $C{=}CH_2$), 5.78 (1 H, m, $C\underline{H}{=}CH_2$), 7.25-7.32 (5 H, m, Ph-H_5).

Methyl 3-(methoxycarbonylmethylthio)propanoate (153)

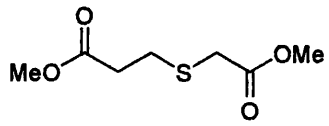

Methyl propenoate (**152**, 2.25 g, 26 mmol) was added during 30 min to methyl mercaptoacetate (**116**, 2.65 g, 25 mmol) and piperidine (0.025 mL) at 40°C. Piperidine (0.05 mL) was then added dropwise over 10 min. The mixture was warmed to 50°C for 5 min and cooled and Et_2O was added. The organic layer was washed with water and brine and dried. Evaporation yielded **153** (5.00 g, 100%) as a colourless oil: TLC R_f = 0.4 (EtOAc / hexane, 1:4); IR ν_{max} (film) 1741 (C=O) cm^{-1}; ^1H NMR (400 MHz, $CDCl_3$) δ 2.63 (2 H, t, *J* = 7.3 Hz, $MeO_2C\underline{H_2}CH_2$), 2.87 (2 H, t, *J* = 7.3 Hz, $CH_2C\underline{H_2}S$), 3.23 (2 H, s, SCH_2CO), 3.69 (3 H, s, CH_3), 3.74 (3 H, s, CH_3); ^{13}C NMR (100 MHz, $CDCl_3$) δ 27.4 (CH_2), 33.3 (CH_2), 33.9 (CH_2), 51.7 (CH_3), 52.3 (CH_3), 170.6 (C=O), 171.9 (C=O); MS (FAB+) *m/z* 193 (M + H), 192 (M), 165 (M – OMe), 133 (M – CO_2Me).

(±)-3-Oxotetrahydrothiophene-4-carbonitrile (157)

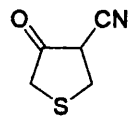

Na (1.32 g, 57 mmol) was stirred with dry MeOH (20 mL) at 0°C for 45 min. Methyl mercaptoacetate (**116**, 2.16 g, 20 mmol) was added dropwise. Acrylonitrile (**156**, 4.30 g, 81 mmol) was then added and the mixture was boiled under reflux for 1 h. The evaporation residue, in Et_2O, was washed with water (x 2). The aqueous layers were acidified with aq. HCl (10%) and extracted with Et_2O (x 4). The organic layers were dried. Evaporation and chromatography (EtOAc / hexane, 2:3) gave **157** (1.28 g, 50%) as a yellow solid: TLC R_f = 0.3 (EtOAc / hexane, 2:3); mp 71-73°C (lit.[213] mp 71-72°C); IR ν_{max} (KBr) 1742 (C=O), 2245 (CN), 2360 cm^{-1}; ^1H NMR (400 MHz, $CDCl_3$) δ 3.25 (1 H, m, 4-H), 3.34 (1 H, dd, *J* = 11.9, 7.9 Hz, 5-H), 3.40 (2 H, s, 2-H_2), 3.65 (1 H, dd, *J* = 10.9, 7.9 Hz, 5-H); ^{13}C NMR (100 MHz, $CDCl_3$) δ 29.4 (CH_2), 36.3 (CH_2), 41.1 (CH), 114.7 (C≡N), 201.1 (C=O).

(±)-*Trans*-3-Hydroxytetrahydrothiophene-4-carbonitrile (158)

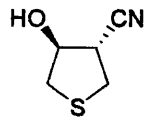

$NaBH_4$ (380 mg, 10 mmol) was added to **157** (1.27 g, 10 mmol) in EtOH (10 mL) at 0°C and the mixture was stirred at RT for 1 h. It was then cooled to 0°C and acidified with AcOH to pH 6. The evaporation residue, in EtOAc, was washed with water and brine and was dried. Evaporation and chromatography (EtOAc / hexane, 2:3) yielded **158** (780 mg, 60%) as a pale yellow oil: TLC R_f = 0.4 (EtOAc / hexane, 1:4); IR ν_{max} (film) 2246 (C≡N), 3435 (OH) cm^{-1}; ^1H NMR (600 MHz, $CDCl_3$) δ 2.88 (1 H, dd, *J* = 11.7, 4.7 Hz, 2-H), 2.95 (1 H, br d, *J* = 5.9 Hz, OH), 3.09 (1 H, m, 5-H), 3.17-3.20 (2 H, m, 4,5-H_2), 3.23 (1 H, dd, *J* = 11.7, 4.7 Hz, 2-H), 4.71 (1 H, qn, *J* = 4.7 Hz, 3-H); ^{13}C NMR (100 MHz, $CDCl_3$) (HMQC) δ 30.5 (5-CH_2), 37.1 (2-CH_2), 39.9 (4-CH), 76.7 (3-CH), 118.9 (C≡N); MS (FAB+) *m/z* 130 (M + H), 112 (M – OH); HRMS (EI+) *m/z* 129.0254 (M) ($^{12}C_5H_7NOS$ requires 129.0248).

(±)-4-Benzylthio-3-hydroxy-2-methylenebutanenitrile (161)

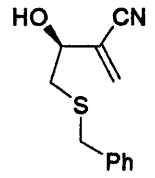

Method A: To **158** (200 mg, 1.56 mmol) in dry THF (5 mL) was added $LiN(SiMe_3)_2$ (1.0 M in THF, 1.87 mL, 1.87 mmol) at –78°C under Ar and the mixture was stirred for 30 min. Benzyl bromide (320 mg, 1.87 mmol) was added and the mixture was allowed to reach RT during 16 h. The evaporation residue, in EtOAc, was washed with water and dried. Evaporation and chromatography (EtOAc / hexane, 2:3) afforded **161** (120 mg, 35%) as a pale yellow oil: TLC R_f = 0.2 (EtOAc / hexane, 2:3); IR ν_{max} (film) 908, 2253 (CN), 3435 (OH) cm^{-1}; ^1H NMR (400 MHz, $CDCl_3$) δ 2.63 (1 H, dd, *J* = 14.3, 8.4 Hz, 4-H), 2.84 (1 H, dd, *J* = 14.3, 8.4 Hz, 4-H), 2.85 (1 H, d, *J* = 4.0 Hz, OH), 3.77 (2 H, s, $PhCH_2$), 4.15 (1 H, m, 3-H), 6.02 (2 H, dd, *J* = 12.6, 1.3 Hz, 1-H_2), 7.37-7.26 (5 H, m, Ph-H_5); ^{13}C NMR (100 MHz, $CDCl_3$) (HMQC) δ 36.4 ($PhCH_2$), 37.6 (4-CH_2), 69.6 (3-CH), 116.6 (C≡N), 124.4 (2-C_q), 127.5 (CH), 128.8 (2 x CH), 128.9 (2 x CH), 130.9

(1-CH_2), 137.4 (Ph 1-C_q); HRMS (FAB+) *m/z* 220.0791 (M + H) ($^{12}C_{12}H_{13}NOS$ requires 220.0791), 202 (M – OH), 91 (Bn).

Method B: To **158** (40 mg, 0.31 mmol) in dry THF (1 mL) was added K_2CO_3 (26 mg, 0.37 mmol) at –78°C under Ar and the mixture was stirred for 30 min. Benzyl bromide (75 mg, 0.37 mmol) was added and the mixture was allowed to reach 20°C during 16 h. The evaporation residue, in EtOAc, was washed with water and dried. Evaporation and chromatography (EtOAc / hexane, 2:3) afforded **161** (30 mg, 44%) as a pale yellow oil. The data were identical to those above.

(±)-*Trans*-3-Hydroxytetrahydrothiophene-4-carboxamide (164)

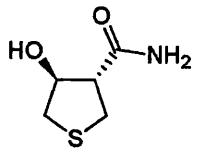

Compound **158** (340 mg, 2.63 mmol) was stirred in aq. HCl (9 M, 5.26 mL) at 50°C for 2 h. Evaporation (with addition of toluene and EtOH to aid evaporation of water) and trituration (Et_2O) yielded **164** (350 mg, 91%) as a white solid: TLC R_f = 0.3 ($CHCl_3$ / MeOH, 9:1); mp 120-123°C; IR ν_{max} (KBr) 1635 (C=O), 3446 (OH) cm^{-1}; ^1H NMR [400 MHz, $(CD_3)_2SO$] δ 2.60 (1 H, dd, *J* = 10.6, 7.3 Hz, 2-H), 2.71 (1 H, dd, *J* = 15.9, 7.9 Hz, 4-H), 2.81-2.89 (2 H, m, 5-H_2), 2.91 (1 H, dd, *J* = 10.2, 5.9 Hz, 2-H), 4.32 (1 H, *ca.* qn, *J* = 7 Hz, 3-H), 5.29 (1 H, d, *J* = 5.1 Hz, OH), 7.00 (1 H, br s, NH), 7.40 (1 H, br s, NH); ^{13}C NMR [100 MHz, $(CD_3)_2SO$] (HMQC) δ 29.9 (5-CH_2), 36.4 (2-CH_2), 54.0 (4-CH), 76.3 (3-CH), 173.4 (C=O); HRMS (EI+) *m/z* 148.0427 (M + H) ($^{12}C_5H_9NO_2S$ requires 148.0427), 147 (M), 129 (M – OH – H), 85 (M + H – OH – $CONH_2$).

(±)-*Trans*-2,2-Dimethylhexahydrothieno[3,4-e][1,3]oxazin-4-one (165) and (±)-*Trans*-3-hydroxy-N-(1-methoxy-1-methylethyl)tetrahydrothiophene-4-carboxamide (166)

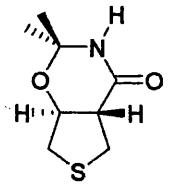

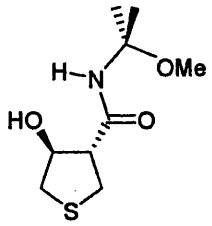

(165) **(166)**

Compound **164** (130 mg, 0.88 mmol) and 4-toluenesulfonic acid monohydrate (2.0 mg, 0.01 mmol) were boiled under reflux with 2,2-dimethoxypropane (4 mL) and acetone (2 mL) for 15 h. The evaporation residue, in EtOAc, was washed with water and aq. $NaHCO_3$ and was dried. Evaporation and chromatography (EtOAc / hexane, 4:1) gave **165** and **166** as an inseparable mixture (104 mg, 3:2 ratio) as a white solid: TLC R_f = 0.4 (EtOAc / hexane, 4:1); mp 112-113°C; IR (KBr) ν_{max} 1668 (C=O), 3394, (NH) cm^{-1}; **165:** ^1H NMR [400 MHz, $(CD_3)_2SO$] δ 1.37 (3 H, s, CH_3), 1.40 (3 H, s, CH_3), 2.69-2.77 (2 H, m) and 2.86-3.00 (3 H, m) (4a,5,5,7,7-H_5), 4.17 (1 H, dt, *J* = 6.2, 10.5 Hz, 7a-H), 8.10 (1 H, br s, NH); **166:** ^1H NMR [400 MHz, $(CD_3)_2SO$] δ 1.26 (3 H, s, CH_3), 1.27 (3 H, s, CH_3), 2.52-2.61 (2 H, m) and 2.69-2.92 (3 H, m) (2,2,4,5,5-H_5), 3.34 (3 H, s, OMe), 4.30 (1 H, qn, *J* = 6.2 Hz, 3-H), 5.23 (1 H, d, *J* = 5.2 Hz, OH), 7.61 (1 H, br s, NH); ^{13}C NMR [100 MHz, $(CD_3)_2SO$] (HMQC, HMBC) δ 25.3 (CH_2), 27.0 (CH_3), 27.1 (CH_3), 27.2 (CH_3), 29.9 (C_q), 30.7 (CH_2), 31.6 (CH_3), 32.1 (CH_2), 36.4 (CH_2), 47.9 (CH), 50.7 (CH_2), 51.4 (C_q), 54.3 (CH), 74.5 (CH), 76.2 (CH), 87.5 (C_q), 168.1 (C_q), 170.9 (C_q), 207.4 (C_q); HRMS (EI+) (data for **165**) *m/z* 188.0701 (M + H) ($^{12}C_8H_{14}NO_2S$ requires 188.0745), 187.0672 (M) ($^{12}C_8H_{13}NO_2S$ requires 187.0667), 172 (M – CH_3).

(±)-*Trans*-N-Benzyl-3-benzyloxytetrahydrothiophene-4-carboxamide (169) and (±)-*Trans*-3-benzyloxytetrahydrothiophene-4-carboxamide (170)

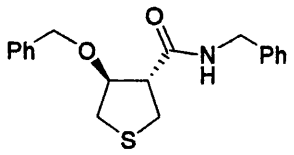

(169)

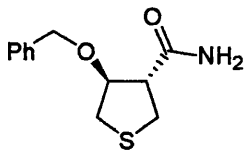

(170)

NaH (60% in mineral oil, 13.6 mg, 0.34 mmol, pre-washed in dry pentane) was stirred in dry DMF (0.5 ml) under N_2 for 30 min. Compound **164** (50 mg, 0.34 mmol) in dry DMF (0.4 mL) was added and the mixture was stirred for a further 30 min. Benzyl bromide (58.2 mg, 0.34 mmol) was added and the mixture was stirred overnight. Ice-water (10 mL) was added and the organic layer was extracted with Et_2O (x 3) and dried. Evaporation and chromatography (EtOAc / hexane, 7:3) afforded **169** (20 mg, 18%) as a white solid: TLC R_f = 0.8 (EtOAc / hexane, 7:3); mp 73-74°C; IR ν_{max} (KBr) 734, 1524 (NH), 1665 (C=O), 3437 (NH) cm^{-1}; ^1H NMR (400 MHz, $CDCl_3$) δ 2.81 (1 H, m, 2-H), 2.91-3.03 (2 H, m, 4,5-H_2), 3.16 (2 H, m, 2,5-H_2), 4.27 (1 H, dt, *J* = 6.3, 8.3 Hz, 3-H), 4.35 (1 H, dd, *J* = 14.6, 5.4 Hz, NCH), 4.45 (1 H, d, *J* = 11.7 Hz, PhCH), 4.47 (1 H, dd, *J* = 14.6, 6.3 Hz, NCH), 4.51 (1 H, d, *J* = 11.7 Hz, PhCH), 6.51 (1 H, br, NH), 7.15-7.32 (10 H, m, 2 × Ph-H_5); ^{13}C NMR (100 MHz, $CDCl_3$) (HMQC) δ 28.5 (5-CH_2), 34.2 (2-CH_2), 43.6 (NCH_2), 53.1 (4-CH), 72.6 ($PhCH_2$), 83.9 (3-CH), 127.5 (CH), 127.8 (2 x CH), 128.0 (2 x CH), 128.1 (CH), 128.6 (2 x CH), 128.7 (2 x CH), 137.1 (C_q), 138.0 (C_q), 170.8 (C=O); MS (FAB+) *m/z* 328 (M + H), 220 (M – $NHCH_2Ph$); Anal. Calcd. for $C_{19}H_{21}NO_2S$: C, 69.69; H, 6.46; N, 4.28. Found: C, 69.52; H, 6.41; N, 4.30.

Further elution afforded **170** (50 mg, 62%) as a white solid: TLC R_f = 0.4 (EtOAc / hexane, 7:3); mp 80-81°C; IR ν_{max} (KBr) 735, 1454, 1671, 2920, 3344 cm^{-1}; ^1H NMR (400 MHz, $CDCl_3$) δ 2.85 (1 H, dd, *J* = 10.6, 7.7 Hz, 2-H), 2.96-3.03 (2 H, m, 4,5-H_2), 3.10-3.16 (2 H, m, 2,5-H_2), 4.27 (1 H, dt, *J* = 9.2, 6.2 Hz, 3-H), 4.54 (1 H, d, *J* = 11.4 Hz, PhCH), 4.63 (1H, d, *J* = 11.4 Hz, PhCH), 5.6 (1 H, br s, NH), 6.2 (1 H, br s, NH), 7.28-7.37 (5 H, m, Ph-H_5); ^{13}C NMR (100 MHz, $CDCl_3$) (HMQC) δ 28.5 (5-CH_2), 34.3 (2-CH_2), 52.6 (4-CH), 72.5 ($PhCH_2$), 83.7 (3-CH), 127.9 (2 x CH), 128.2 (CH), 128.6 (2 x CH), 137.2 (C_q), 173.4 (C=O); MS (FAB+) *m/z* 238 (M + H); Anal. Calcd. for $C_{12}H_{15}NO_2S$: C, 60.73; H, 6.37; N, 5.90. Found: C, 60.88; H, 6.88; N, 5.08.

(±)-*Trans*-3-Benzyloxy-1-oxotetrahydrothiophene-4-carboxamide (171)

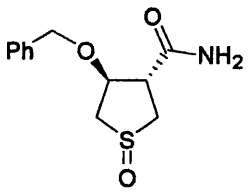

Compound **170** (100 mg, 0.42 mmol) was treated with *m*CPBA (73 mg, 0.42 mmol) in DCM (7 mL) at –40°C for 5 h. The mixture was diluted with DCM (10 mL) and washed with aq. NaOH (1 M) and water and dried. Evaporation and chromatography ($CHCl_3$ / MeOH, 4:1) afforded **171** (94 mg, 88%) as a pale yellow solid: TLC R_f = 0.2 ($CHCl_3$ / MeOH, 4:1); mp 78-80°C; ^1H NMR (270 MHz, $CDCl_3$) (data given for major diastereoisomer) δ 3.18 (1 H, dd, *J* = 14.1, 6.0 Hz, 2-H or 5-H), 3.26-3.46 (4 H, m, 2,4,5-H_3 + 5-H or 2-H), 4.54 (1 H, d, *J* = 11.7 Hz, PhCH), 4.65 (1 H, d, *J* = 11.7 Hz, PhCH), 4.96 (1 H, dt, *J* = 4.0, 5.9 Hz, 3-H); HRMS (FAB+) *m/z* 254.0811 (M + H) ($^{12}C_{12}H_{16}NO_3S$ requires 254.0851), 253.0780 (M) ($^{12}C_{12}H_{15}NO_3S$ requires 253.0073), 210 (M + H – $CONH_2$), 147 (M – OBn).

(±)-*Trans*-N-[(3-Benzyloxytetrahydrothiophen-4-yl)methyl]benzamide (174)

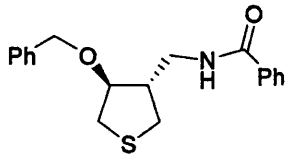

To a solution of **170** (238 mg, 1 mmol) in dry THF (2 mL) was added $LiAlH_4$ (2.0 M in THF, 10 mmol, 5 mL) under N_2 and the mixture was boiled under reflux overnight. It was then cooled to 0°C and water (2 mL) was added dropwise. After stirring for 1 h, it was poured into hot MeOH (10 mL), filtered (Celite®) and evaporated. The evaporation residue was dissolved in boiling $CHCl_3$ and dried. Evaporation gave the crude primary amine (**173**, 200 mg, 0.90 mmol), which was immediately treated with triethylamine (273 mg, 2.7 mmol) in dry DCM (5 mL) for 10 minutes. Benzoyl chloride (190 mg, 1.35 mmol) was added and the mixture was stirred overnight. The evaporation residue, in DCM, was washed with 5% citric acid and aq. $NaHCO_3$ (1 M) and dried. Evaporation and chromatography (hexane / Et_2O, 5:1) gave **174** (130 mg, 40% overall yield) as a white solid: TLC R_f = 0.2 [pet. ether (40-60°C) / Et_2O, 1:1]; mp 83-86°C; IR ν_{max} (film)

1536, 1640, 3401 cm^{-1}; ^1H NMR (400 MHz, $CDCl_3$) δ 2.51 (1 H, m, 4-H), 2.63 (1 H, dd, *J* = 10.6, 9.0 Hz, 5-H), 2.89 (1 H, dd, *J* = 10.4, 7.5 Hz, 2-H), 2.98 (1 H, dd, *J* = 10.8, 7.3 Hz, 5-H), 3.18 (1 H, dd, *J* = 10.4, 5.8 Hz, 2-H), 3.32 (1 H, ddd, *J* = 12.4, 8.7, 3.7 Hz, NCH), 3.81 (1 H, ddd, *J* = 11.7, 6.9, 4.8 Hz, NCH), 4.01 (1 H, dt, *J* = 5.8, 8.0 Hz, 3-H), 4.49 (1 H, d, *J* = 11.1 Hz, PhCH), 4.67 (1 H, d, *J* = 10.9 Hz, PhCH), 6.92 (1 H, br, NH), 7.25-7.30 (2 H, m, Ph' 3,5-H_2), 7.31-7.53 (5 H, m, Ph-H_5), 7.41-7.45 (1 H, m, Ph' 4-H), 7.50-7.53 (2 H, m, Ph' 2,6-H_2); ^{13}C NMR (100 MHz, $CDCl_3$) (HMQC) δ 29.8 (5-CH_2), 33.9 (2-CH_2), 42.0 (NCH_2), 46.5 (4-CH), 72.3 ($PhCH_2$), 85.6 (3-CH), 126.8 (2 x CH), 128.2 (2 x CH), 128.4 (2 x CH), 128.7 (2 x CH), 134.0 (C_q), 137.4 (C_q), 167.1 (C=O); Anal. Calcd. for $C_{19}H_{21}NO_2S$: C, 69.69; H, 6.46; N, 4.28. Found: C, 69.63; H, 6.56; N, 4.06.

References

1. Westwell, A. D.; Stevens, M. F. G. Hitting the chemotherapy jackpot: Strategy, productivity and chemistry. *Drug Discov. Today* **2004**, *9*, 625-627.

2. Baselga, J. Targeting tyrosine kinases in cancer: The second wave. *Science* **2006**, *312*, 1175-1178.

3. Pandya, N. M.; Dhalla, N. S.; Santani, D. D. Angiogenesis - a new target for future therapy. *Vascular Pharmacol.* **2006**, *44*, 265-274.

4. Fan, T. P.; Yeh, J. C.; Leung, K. W.; Yue, P. Y. K.; Wong, R. N. S. Angiogenesis: From plants to blood vessels. *Trends Pharmacol. Sci.* **2006**, *27*, 297-309.

5. Sharma, R. A.; Harris, A. L.; Dalgleish, A. G.; Steward, W. P.; O'Bryne, K. J. Angiogenesis as a biomarker and target in cancer chemoprevention. *Lancet Oncol.* **2001**, *2*, 726-732.

6. Fox, S. B.; Gasparini, G.; Harris, A. L. Angiogenesis: Pathological, prognostic, and growth-factor pathways and their link to trial design and anticancer drugs. *Lancet Oncol.* **2001**, *2*, 278-289.

7. Longo, R.; Sarmiento, R.; Fanelli, M.; Capaccetti, B.; Gattuso, D.; Gasparini, G. Anti-angiogenic therapy: Rationale, challenges and clinical studies. *Angiogenesis* **2002**, *5*, 237-256.

8. Gasparini, G. Clinical significance of determination of surrogate markers of angiogenesis in breast cancer. *Crit. Rev. Oncol. Hematol.* **2001**, *37*, 97-114.

9. Claesson-Welsh, L.; Welsh, M.; Ito, N.; Anand-Apte, B.; Soker, S.; Zetter, B.; O'Reilly, M.; Folkman, J. Angiostatin induces endothelial cell apoptosis and activation of focal adhesion kinase independently of the integrin-binding motif RGD. *Proc. Natl. Acad. Sci. U.S.A.* **1998**, *95*, 5579-5583.

10. Okada, F.; Rak, J. W.; St Croix, B.; Lieubeau, B.; Kaya, M.; Roncari, L.; Shirasawa, S.; Sasazuki, T.; Kerbel, R. S. Impact of oncogenes in tumor angiogenesis: Mutant K-ras up-regulation of vascular endothelial growth factor vascular permeability factor is necessary, but not sufficient for tumorigenicity of human colorectal carcinoma cells. *Proc. Natl. Acad. Sci. U.S.A.* **1998**, *95*, 3609-3614.

11. Vanmeir, E. G.; Polverini, P. J.; Chazin, V. R.; Huang, H. J. S.; Detribolet, N.; Cavenee, W. K. Release of an inhibitor of angiogenesis upon induction of wild-type p53 expression in glioblastoma cells. *Nature Genet.* **1994**, *8*, 171-176.

12. Brown, N. S.; Bicknell, R. Thymidine phosphorylase, 2-deoxy-*D*-ribose and angiogenesis. *Biochem. J.* **1998**, *334*, 1-8.

13. Friedkin, M.; Roberts, D. The enzymatic synthesis of nucleosides. I. Thymidine phosphorylase in mammalian tissue. *J. Biol. Chem.* **1954**, *207*, 245-256.

14. Toi, M.; Rahman, M. A.; Bando, H.; Chow, L. W. C. Thymidine phosphorylase (platelet-derived endothelial-cell growth factor) in cancer biology and treatment. *Lancet Oncol.* **2005**, *6*, 158-166.

15. Miyadera, K.; Dohmae, N.; Takio, K.; Sumizawa, T.; Haraguchi, M.; Furukawa, T.; Yamada, Y.; Akiyama, S. I. Structural characterization of thymidine phosphorylase purified from human placenta. *Biochem. Biophys. Res. Commun.* **1995**, *212*, 1040-1045.

16. Cole, C.; Foster, A. J.; Freeman, S.; Jaffar, M.; Murray, P. E.; Stratford, I. J. The role of thymidine phosphorylase/PD-ECGF in cancer chemotherapy: A chemical perspective. *Anti-Cancer Drug Des.* **1999**, *14*, 383-392.

17. Cole, C.; Marks, D. S.; Jaffar, M.; Stratford, I. J.; Douglas, K. T.; Freeman, S. A similarity model for the human angiogenic factor, thymidine phosphorylase/platelet derived-endothelial cell growth factor. *Anti-Cancer Drug Des.* **1999**, *14*, 411-420.

18. McNally, V. A.; Gbaj, A.; Douglas, K. T.; Stratford, I. J.; Jaffar, M.; Freeman, S.; Bryce, R. A. Identification of a novel class of inhibitor of human and *Escherichia coli* thymidine phosphorylase by *in silico* screening. *Bioorg. Med. Chem. Lett.* **2003**, *13*, 3705-3709.

19. Ackland, S. P.; Peters, G. J. Thymidine phosphorylase: Its role in sensitivity and resistance to anticancer drugs. *Drug Resist. Updates* **1999**, *2*, 205-214.

20. Matsushita, S.; Nitanda, T.; Furukawa, T.; Sumizawa, T.; Tani, A.; Nishimoto, K.; Akiba, S.; Miyadera, K.; Fukushima, M.; Yamada, Y.; Yoshida, H.; Kanzaki, T.; Akiyama, S. The effect of a thymidine phosphorylase inhibitor on angiogenesis and apoptosis in tumors. *Cancer Res.* **1999**, *59*, 1911-1916.

21. Moghaddam, A.; Zhang, H. T.; Fan, T. P. D.; Hu, D. E.; Lees, V. C.; Turley, H.; Fox, S. B.; Gatter, K. C.; Harris, A. L.; Bicknell, R. Thymidine phosphorylase is angiogenic and promotes tumor-growth. *Proc. Natl. Acad. Sci. U.S.A.* **1995**, *92*, 998-1002.

22. Sengupta, S.; Sellers, L. A.; Matheson, H. B.; Fan, T. P. D. Thymidine phosphorylase induces angiogenesis *in vivo* and *in vitro*: An evaluation of possible mechanisms. *Br. J. Pharmacol.* **2003**, *139*, 219-231.

23. Kitazono, M.; Takebayashi, Y.; Ishitsuka, K.; Takao, S.; Tani, A.; Furukawa, T.; Miyadera, K.; Yamada, Y.; Aikou, T.; Akiyama, S. Prevention of hypoxia-induced apoptosis by the angiogenic factor thymidine phosphorylase. *Biochem. Biophys. Res. Commun.* **1998**, *253*, 797-803.

24. Ikeda, R.; Furukawa, T.; Kitazono, M.; Ishitsuka, K.; Okumura, H.; Tani, A.; Sumizawa, T.; Haraguchi, M.; Komatsu, M.; Uchimiya, H.; Ren, X. Q.; Motoya, T.; Yamada, K.; Akiyama, S. Molecular basis for the inhibition of hypoxia-induced apoptosis by 2-deoxy-*D*-ribose. *Biochem. Biophys. Res. Commun.* **2002**, *291*, 806-812.

25. Akiyama, S.; Furukawa, T.; Sumizawa, T.; Takebayashi, Y.; Nakajima, Y.; Shimaoka, S.; Haraguchi, M. The role of thymidine phosphorylase, an angiogenic enzyme, in tumor progression. *Cancer Sci.* **2004**, *95*, 851-857.

26. Brown, N. S.; Jones, A.; Fujiyama, C.; Harris, A. L.; Bicknell, R. Thymidine phosphorylase induces carcinoma cell oxidative stress and promotes secretion of angiogenic factors. *Cancer Res.* **2000**, *60*, 6298-6302.

27. Uchimiya, H.; Furukawa, T.; Okamoto, M.; Nakajima, Y.; Matsushita, S.; Ikeda, R.; Gotanda, T.; Haraguchi, M.; Sumizawa, T.; Ono, M.; Kuwano, M.; Kanzaki, T.; Akiyama, S. Suppression of thymidine phosphorylase-mediated angiogenesis and tumor growth by 2-deoxy-*L*-ribose. *Cancer Res.* **2002**, *62*, 2834-2839.

28. Nakajima, Y.; Gotanda, T.; Uchimiya, H.; Furukawa, T.; Haraguchi, M.; Ikeda, R.; Sumizawa, T.; Yoshida, H.; Akiyama, S. Inhibition of metastasis of tumor cells overexpressing thymidine phosphorylase by 2-deoxy-*L*-ribose. *Cancer Res.* **2004**, *64*, 1794-1801.

29. Takao, S.; Akiyama, S.; Nakajo, A.; Yoh, H.; Kitazono, M.; Natsugoe, S.; Miyadera, K.; Fukushima, M.; Yamada, Y.; Aikou, T. Suppression of metastasis by thymidine phosphorylase inhibitor. *Cancer Res.* **2000**, *60*, 5345-5348.

30. Fukushima, M.; Suzuki, N.; Emura, T.; Yano, S.; Kazuno, H.; Tada, Y.; Yamada, Y.; Asao, T. Structure and activity of specific inhibitors of thymidine phosphorylase to potentiate the function of antitumor 2'-deoxyribonucleosides. *Biochem. Pharmacol.* **2000**, *59*, 1227-1236.

31. Norman, R. A.; Barry, S. T.; Bate, M.; Breed, J.; Colls, J. G.; Emill, R. J.; Luke, R. W. A.; Minshull, C. A.; McAlister, M. S. B.; McCall, E. J.; McMiken, H. H. J.; Paterson, D. S.; Timms, D.; Tucker, J. A.; Pauptit, R. A. Crystal structure of human thymidine phosphorylase in complex with a small molecule inhibitor. *Structure* **2004**, *12*, 75-84.

32. Focher, F.; Spadari, S. Thymidine phosphorylase: A two-face Janus in anti-cancer chemotherapy. *Curr. Cancer Drug Targets* **2001**, *1*, 141-153.

33. Hatse, S.; De Clercq, E.; Balzarini, J. Role of antimetabolites of purine and pyrimidine nucleotide metabolism in tumor cell differentiation. *Biochem. Pharmacol.* **1999**, *58*, 539-555.

34. Stryer, L., *Biochemistry.* Fourth ed.; ISBN 0-7167-2009-4; W. H. Freeman and Company: New York, 1995.

35. Watterson, S. H.; Liu, C. J.; Dhar, T. G. M.; Gu, H. H.; Pitts, W. J.; Barrish, J. C.; Fleener, C. A.; Rouleau, K.; Sherbina, N. Z.; Hollenbaugh, D. L.; Iwanowicz, E. J. Novel amide-based inhibitors of inosine 5'-monophosphate dehydrogenase. *Bioorg. Med. Chem. Lett.* **2002**, *12*, 2879-2882.

36. Sintchak, M. D.; Nimmesgern, E. The structure of inosine 5'-monophosphate dehydrogenase and the design of novel inhibitors. *Immunopharmacol.* **2000**, *47*, 163-184.

37. Allison, A. C.; Eugui, E. M. Mycophenolate mofetil and its mechanisms of action. *Immunopharmacol.* **2000**, *47*, 85-118.

38. Jain, J.; Almquist, S. J.; Ford, P. J.; Shlyakhter, D.; Wang, Y. P.; Nimmesgern, E.; Germann, U. A. Regulation of inosine monophosphate dehydrogenase type I and type II isoforms in human lymphocytes. *Biochem. Pharmacol.* **2004**, *67*, 767-776.

39. Konno, Y.; Natsumeda, Y.; Nagai, M.; Yamaji, Y.; Ohno, S.; Suzuki, K.; Weber, G. Expression of human IMP dehydrogenase types I and II in *Escherichia coli* and distribution in human normal lymphocytes and leukemic cell lines. *J. Biol. Chem.* **1991**, *266*, 506-509.

40. Natsumeda, Y.; Ohno, S.; Kawasaki, H.; Konno, Y.; Weber, G.; Suzuki, K. Two distinct cDNAs for human IMP dehydrogenase. *J. Biol. Chem.* **1990**, *265*, 5292-5295.

41. Colby, T. D.; Vanderveen, K.; Strickler, M. D.; Markham, G. D.; Goldstein, B. M. Crystal structure of human type II inosine monophosphate dehydrogenase: Implications for ligand binding and drug design. *Proc. Natl. Acad. Sci. U.S.A.* **1999**, *96*, 3531-3536.

42. Pankiewicz, K. W. Novel nicotinamide adenine dinucleotide analogues as potential anticancer agents: Quest for specific inhibition of inosine monophosphate dehydrogenase. *Pharmacol. Ther.* **1997**, *76*, 89-100.

43. Popsavin, M.; Torovic, L.; Kojic, V.; Bogdanovic, G.; Popsavin, V. Synthesis and biological evaluation of two novel 2'-substituted tiazofurin analogues. *Tetrahedron Lett.* **2004**, *45*, 7125-7128.

44. Srivastava, P. C.; Robins, R. K. Synthesis and anti-tumour activity of 2-β-*D*-ribofuranosylselenazole-4-carboxamide and related derivatives. *J. Med. Chem.* **1983**, *26*, 445-448.

45. Goldstein, B. M.; Bell, J. E.; Marquez, V. E. Dehydrogenase binding by tiazofurin anabolites. *J. Med. Chem.* **1990**, *33*, 1123-1127.

46. Makara, G. M.; Keseru, G. M. On the conformation of tiazofurin analogues. *J. Med. Chem.* **1997**, *40*, 4154-4159.

47. Franchetti, P.; Cappellacci, L.; Perlini, P.; Jayaram, H. N.; Butler, A.; Schneider, B. P.; Collart, F. R.; Huberman, E.; Grifantini, M. Isosteric analogues of nicotinamide adenine dinucleotide derived from furanfurin, thiophenfurin, and selenophenfurin as mammalian inosine monophosphate dehydrogenase (type I and II) inhibitors. *J. Med. Chem.* **1998**, *41*, 1702-1707.

48. Franchetti, P.; Marchetti, S.; Cappellacci, L.; Jayaram, H. N.; Yalowitz, J. A.; Goldstein, B. M.; Barascut, J. L.; Dukhan, D.; Imbach, J. L.; Grifantini, M. Synthesis, conformational analysis, and biological activity of C-thioribonucleosides related to tiazofurin. *J. Med. Chem.* **2000**, *43*, 1264-1270.

49. Schalk-Hihi, C.; Zhang, Y. Z.; Markham, G. D. The conformation of NADH bound to inosine 5'-monophosphate dehydrogenase determined by transferred nuclear Overhauser effect spectroscopy. *Biochemistry* **1998**, *37*, 7608-7616.

50. Zatorski, A.; Watanabe, K. A.; Carr, S. F.; Goldstein, B. M.; Pankiewicz, K. W. Chemical synthesis of benzamide adenine dinucleotide: Inhibition of inosine monophosphate dehydrogenase (types I and II). *J. Med. Chem.* **1996**, *39*, 2422-2426.

51. Salamon, A.; Hagenauer, B.; Thalhammer, T.; Szekeres, T.; Krohn, K.; Jayaram, H. N.; Jager, W. Metabolism and disposition of the novel antileukaemic drug, benzamide riboside, in the isolated perfused rat liver. *Life Sci.* **2001**, *69*, 2489-2502.

52. Pankiewicz, K. W.; Watanabe, K. A.; Lesiak-Watanabe, K.; Goldstein, B. M.; Jayaram, H. N. The chemistry of nicotinamide adenine dinucleotide (NAD) analogues containing C-nucleosides related to nicotinamide riboside. *Curr. Med. Chem.* **2002**, *9*, 733-741.

53. Dhar, T. G. M.; Shen, Z. Q.; Guo, J. Q.; Liu, C. J.; Watterson, S. H.; Gu, H. H.; Pitts, W. J.; Fleener, C. A.; Rouleau, K. A.; Sherbina, N. Z.; McIntyre, K. W.; Witmer, M. R.; Tredup, J. A.; Chen, B. C.; Zhao, R. L.; Bednarz, M. S.; Cheney, D. L.; MacMaster, J. F.; Miller, L. M.; Berry, K. K.; Harper, T. W.; Barrish, J. C.; Hollenbaugh, D. L.; Iwanowicz, E. J. Discovery of N-[2-[2-[[3-methoxy-4-(5-oxazolyl)phenyl]amino]-5-oxazolyl]phenyl]-N-methyl-4-morpholineacetamide as a novel and potent inhibitor of inosine monophosphate dehydrogenase with excellent *in vivo* activity. *J. Med. Chem.* **2002**, *45*, 2127-2130.

54. Carr, S. F.; Papp, E.; Wu, J. C.; Natsumeda, Y. Characterization of human type I and type II IMP dehydrogenases. *J. Biol. Chem.* **1993**, *268*, 27286-27290.

55. Sintchak, M. D.; Fleming, M. A.; Futer, O.; Raybuck, S. A.; Chambers, S. P.; Caron, P. R.; Murcko, M. A.; Wilson, K. P. Structure and mechanism of inosine monophosphate dehydrogenase in complex with the immunosuppressant mycophenolic acid. *Cell* **1996**, *85*, 921-930.

56. Plummer, E. R. Inhibition of poly(ADP-ribose) polymerase in cancer. *Curr. Opin. Pharmacol.* **2006**, *6*, 364-368.

57. Wang, Z. DNA damage-induced mutagenesis: A novel target for cancer prevention. *Mol. Interv.* **2001**, *1*, 269-281.

58. Madhusudan, S.; Middleton, M. R. The emerging role of DNA repair proteins as predictive, prognostic and therapeutic targets in cancer. *Cancer Treat. Rev.* **2005**, *31*, 603-617.

59. Tong, W. M.; Cortes, U.; Wang, Z. Q. Poly(ADP-ribose) polymerase: A guardian angel protecting the genome and suppressing tumorigenesis. *Biochim. Biophys. Acta - Rev. on Cancer* **2001**, *1552*, 27-37.

60. Herceg, Z.; Wang, Z. Q. Functions of poly(ADP-ribose) polymerase (PARP) in DNA repair, genomic integrity and cell death. *Mutation Res.* **2001**, *477*, 97-110.

61. Schreiber, V.; Dantzer, F.; Ame, J. C.; de Murcia, G. Poly(ADP-ribose): Novel functions for an old molecule. *Nature Rev. Mol. Cell Biol.* **2006**, *7*, 517-528.

62. Ame, J. C.; Spenlehauer, C.; de Murcia, G. The PARP superfamily. *BioEssays* **2004**, *26*, 882-893.

63. Diefenbach, J.; Burkle, A. Introduction to poly(ADP-ribose) metabolism. *Cell. Mol. Life Sci.* **2005**, *62*, 721-730.

64. Bürkle, A. Poly(ADP-ribose) - the most elaborate metabolite of NAD^+. *FEBS J.* **2005**, *272*, 4576-4589.

65. Smith, S. The world according to PARP. *Trends Biochem. Sci.* **2001**, *26*, 174-179.

66. Griffin, R. J.; Curtin, N. J.; Newell, D. R.; Golding, B. T.; Durkacz, B. W.; Calvert, A. H. The role of inhibitors of poly(ADP-ribose) polymerase as resistance-modifying agents in cancer therapy. *Biochimie* **1995**, *77*, 408-422.

67. D'Amours, D.; Desnoyers, S.; D'Silva, I.; Poirier, G. G. Poly(ADP-ribosyl)ation reactions in the regulation of nuclear functions. *Biochem. J.* **1999**, *342*, 249-268.

68. Pleschke, J. M.; Kleczkowska, H. E.; Strohm, M.; Althaus, F. R. Poly(ADP-ribose) binds to specific domains in DNA damage checkpoint proteins. *J. Biol. Chem.* **2000**, *275*, 40974-40980.

69. Kim, M. Y.; Zhang, T.; Kraus, W. L. Poly(ADP-ribosyl)ation by PARP-1: 'PARP-laying' NAD^+ into a nuclear signal. *Genes Dev.* **2005**, *19*, 1951-1967.

70. Davidovic, L.; Vodenicharov, M.; Affar, E. B.; Poirier, G. G. Importance of poly(ADP-ribose) glycohydrolase in the control of poly(ADP-ribose) metabolism. *Exp. Cell. Res.* **2001**, *268*, 7-13.

71. Oka, J.; Ueda, K.; Hayaishi, O.; Komura, H.; Nakanishi, K. ADP-ribosyl protein lyase - purification, properties, and identification of the product. *J. Biol. Chem.* **1984**, *259*, 986-995.

72. Bouchard, W. J.; Rouleau, M.; Poirier, G. G. PARP-1, a determinant of cell survival in response to DNA damage. *Exp. Hematol.* **2003**, *31*, 446-454.

73. Nguewa, P. A.; Fuertes, M. A.; Valladares, B.; Alonso, C.; Perez, J. M. Poly(ADP-ribose) polymerases: Homology, structural domains and functions. Novel therapeutical applications. *Prog. Biophys. Mol. Biol.* **2005**, *88*, 143-172.

74. Koh, D. W.; Dawson, T. M.; Dawson, V. L. Mediation of cell death by poly(ADP-ribose) polymerase-1. *Pharmacol. Res.* **2005**, *52*, 5-14.

75. Chiarugi, A.; Moskowitz, M. A. Cell biology: PARP-1 - a perpetrator of apoptotic cell death? *Science* **2002**, *297*, 200-201.

76. Scovassi, A. I.; Diederich, M. Modulation of poly(ADP-ribosylation) in apoptotic cells. *Biochem. Pharmacol.* **2004**, *68*, 1041-1047.

77. Erdelyi, K.; Bakondi, E.; Gergely, P.; Szabó, C.; Virag, L. Pathophysiologic role of oxidative stress-induced poly(ADP-ribose) polymerase-1 activation: Focus on cell death and transcriptional regulation. *Cell. Mol. Life Sci.* **2005**, *62*, 751-759.

78. Chiarugi, A. Poly(ADP-ribose) polymerase: Killer or conspirator? The 'suicide hypothesis' revisited. *Trends Pharmacol. Sci.* **2002**, *23*, 122-129.

79. Watson, C. Y.; Whish, W. J. D.; Threadgill, M. D. Synthesis of 3-substituted benzamides and 5-substituted isoquinolin-1(2*H*)-ones and preliminary evaluation as inhibitors of poly(ADP-ribose) polymerase (PARP). *Bioorg. Med. Chem.* **1998**, *6*, 721-734.

80. Jagtap, P.; Szabó, C. Poly(ADP-ribose) polymerase and the therapeutic effects of its inhibitors. *Nature Rev. Drug Discovery* **2005**, *4*, 421-440.

81. McDonald, M. C.; Mota-Filipe, H.; Wright, J. A.; Abdelrahman, M.; Threadgill, M. D.; Thompson, A. S.; Thiemermann, C. Effects of 5-aminoisoquinolinone, a water-soluble, potent inhibitor of the activity of poly(ADP-ribose) polymerase on the organ injury and dysfunction caused by haemorrhagic shock. *Br. J. Pharmacol.* **2000**, *130*, 843-850.

82. White, A. W.; Almassy, R.; Calvert, A. H.; Curtin, N. J.; Griffin, R. J.; Hostomsky, Z.; Maegley, K.; Newell, D. R.; Srinivasan, S.; Golding, B. T. Resistance-modifying agents. 9. Synthesis and biological properties of benzimidazole inhibitors of the DNA repair enzyme poly(ADP-ribose) polymerase. *J. Med. Chem.* **2000**, *43*, 4084-4097.

83. Skalitzky, D. J.; Marakovits, J. T.; Maegley, K. A.; Ekker, A.; Yu, X. H.; Hostomsky, Z.; Webber, S. E.; Eastman, B. W.; Almassy, R.; Li, J. K.; Curtin, N. J.; Newell, D. R.; Calvert, A. H.; Griffin, R. J.; Golding, B. T. Tricyclic benzimidazoles as potent poly(ADP-ribose) polymerase-1 inhibitors. *J. Med. Chem.* **2003**, *46*, 210-213.

84. Southan, G. J.; Szabó, C. Poly(ADP-ribose) polymerase inhibitors. *Curr. Med. Chem.* **2003**, *10*, 321-340.

85. Virag, L.; Szabó, C. The therapeutic potential of poly(ADP-ribose) polymerase inhibitors. *Pharmacol. Rev.* **2002**, *54*, 375-429.

86. Haince, J. F.; Rouleau, M.; Hendzel, M. J.; Masson, J. Y.; Poirier, G. G. Targeting poly(ADP-ribosyl)ation: A promising approach in cancer therapy. *Trends Mol. Med.* **2005**, *11*, 456-463.

87. Tentori, L.; Portarena, I.; Graziani, G. Potential clinical applications of poly(ADP-ribose) polymerase (PARP) inhibitors. *Pharmacol. Res.* **2002**, *45*, 73-85.

88. Graziani, G.; Szabó, C. Clinical perspectives of PARP inhibitors. *Pharmacol. Res.* **2005**, *52*, 109-118.

89. Tentori, L.; Graziani, G. Chemopotentiation by PARP inhibitors in cancer therapy. *Pharmacol. Res.* **2005**, *52*, 25-33.

90. Yung, T. M. C.; Sato, S.; Satoh, M. S. Poly(ADP-ribosyl)ation as a DNA damage-induced post-translational modification regulating poly(ADP-ribose) polymerase-1-topoisomerase II interaction. *J. Biol. Chem.* **2004**, *279*, 39686-39696.

91. Chiarugi, A. Poly (ADP-ribosyl)ation and stroke. *Pharmacol. Res.* **2005**, *52*, 15-24.

92. Szabó, C. Cardioprotective effects of poly (ADP-ribose) polymerase inhibition. *Pharmacol. Res.* **2005**, *52*, 34-43.

93. Szabó, C. Roles of poly(ADP-ribose) polymerase activation in the pathogenesis of diabetes mellitus and its complications. *Pharmacol. Res.* **2005**, *52*, 60-71.

94. Cuzzocrea, S. Shock, inflammation and PARP. *Pharmacol. Res.* **2005**, *52*, 72-82.

95. Devalaraja-Narashimha, K.; Singaravelu, K.; Padanilam, B. J. Poly(ADP-ribose) polymerase-mediated cell injury in acute renal failure. *Pharmacol. Res.* **2005**, *52*, 44-59.

96. Virag, L. Poly(ADP-ribosyl)ation in asthma and other lung diseases. *Pharmacol. Res.* **2005**, *52*, 83-92.

97. Bentley, R. Role of sulfur chirality in the chemical processes of biology. *Chem. Soc. Rev.* **2005**, *34*, 609-624.

98. Reggelin, M.; Zur, C. Sulfoximines: Structures, properties and synthetic applications. *Synthesis* **2000**, 1-64.

99. Ronzio, R. A.; Meister, A. Phosphorylation of methionine sulfoximine by glutamine synthetase. *Biochemistry* **1968**, *59*, 164-170.

100. Ronzio, R. A.; Rowe, W. B.; Meister, A. Studies on the mechanism of inhibition of glutamine synthetase by methionine sulfoximine. *Biochemistry* **1969**, *8*, 1066-1075.

101. Rowe, W. B.; Ronzio, R. A.; Meister, A. Inhibition of glutamine synthetase by methionine sulfoximine. Studies on methionine sulfoximine phosphate. *Biochemistry* **1969**, *8*, 2674-2680.

102. Manning, J. M.; Moore, S.; Rowe, W. B.; Meister, A. Identification of *L*-methionine *S*-sulfoximine as the diastereoisomer of *L*-methionine *R*-sulfoximine that inhibits glutamine synthetase. *Biochemistry* **1969**, *8*, 2681-2685.

103. Rowe, W. B.; Meister, A. Identification of *L*-methionine-*S*-sulfoximine as convulsant isomer of methionine sulfoximine. *Proc. Natl. Acad. Sci. U.S.A.* **1970**, *66*, 500-506.

104. Richman, P. G.; Orlowski, M.; Meister, A. Inhibition of γ-glutamylcysteine synthetase by *L*-methionine-*S*-sulfoximine. *J. Biol. Chem.* **1973**, *248*, 6684-6690.

105. Griffith, O. W.; Meister, A. Differential inhibition of glutamine and γ-glutamyl-cysteine synthetases by α-alkyl analogs of methionine sulfoximine that induce convulsions. *J. Biol. Chem.* **1978**, *253*, 2333-2338.

106. Griffith, O. W.; Anderson, M. E.; Meister, A. Inhibition of glutathione biosynthesis by prothionine sulfoximine (S-n-propyl homocysteine sulfoximine), a selective inhibitor of γ-glutamylcysteine synthetase. *J. Biol. Chem.* **1979**, *254*, 1205-1210.

107. Griffith, O. W.; Meister, A. Potent and specific-inhibition of glutathione synthesis by buthionine sulfoximine (S-n-butyl homocysteine sulfoximine). *J. Biol. Chem.* **1979**, *254*, 7558-7560.

108. Griffith, O. W. Mechanism of action, metabolism, and toxicity of buthionine sulfoximine and its higher homologs, potent inhibitors of glutathione synthesis. *J. Biol. Chem.* **1982**, *257*, 3704-3712.

109. Tokutake, N.; Hiratake, J.; Katoh, M.; Irie, T.; Kato, H.; Oda, J. Design, synthesis and evaluation of transition-state analogue inhibitors of *Escherichia coli* γ–glutamylcysteine synthetase. *Bioorg. Med. Chem.* **1998**, *6*, 1935-1953.

110. Curi, R.; Lagranha, C. J.; Doi, S. Q.; Sellitti, D. F.; Procopio, J.; Pithon-Curi, T. C.; Corless, M.; Newsholme, P. Molecular mechanisms of glutamine action. *J. Cell Physiol.* **2005**, *204*, 392-401.

111. Roth, E.; Oehler, R.; Manhart, N.; Exner, R.; Wessner, B.; Strasser, E.; Spittler, A. Regulative potential of glutamine - relation to glutathione metabolism. *Nutrition* **2002**, *18*, 217-221.

112. Llorca, O.; Betti, M.; Gonzalez, J. M.; Valencia, A.; Marquez, A. J.; Valpuesta, J. M. The three-dimensional structure of an eukaryotic glutamine synthetase: Functional implications of its oligomeric structure. *J. Struct. Biol.* **2006**, *156*, 469-479.

113. Meister, A. Glutathione metabolism and its selective modification. *J. Biol. Chem.* **1988**, *263*, 17205-17208.

114. Filomeni, G.; Rotilio, G.; Ciriolo, M. R. Cell signalling and the glutathione redox system. *Biochem. Pharmacol.* **2002**, *64*, 1057-1064.

115. Anderson, M. E. Glutathione: An overview of biosynthesis and modulation. *Chem.-Biol. Interact.* **1998**, *112*, 1-14.

116. Calvert, P.; Yao, K. S.; Hamilton, T. C.; O'Dwyer, P. J. Clinical studies of reversal of drug resistance based on glutathione. *Chem.-Biol. Interact.* **1998**, *112*, 213-224.

117. Rudin, C. M.; Yang, Z. J.; Schumaker, L. M.; VanderWeele, D. J.; Newkirk, K.; Egorin, M. J.; Zuhowski, E. G.; Cullen, K. J. Inhibition of glutathione synthesis reverses Bcl-2-mediated cisplatin resistance. *Cancer Res.* **2003**, *63*, 312-318.

118. Anderson, C. P.; Reynolds, C. P. Synergistic cytotoxicity of buthionine sulfoximine (BSO) and intensive melphalan (L-PAM) for neuroblastoma cell lines established at relapse after myeloablative therapy. *Bone Marrow Transplant.* **2002**, *30*, 135-140.

119. Bailey, H. H. L-*S*,*R*-buthionine sulfoximine: Historical development and clinical issues. *Chem.-Biol. Interact.* **1998**, *112*, 239-254.

120. Yang, B.; Keshelava, N.; Anderson, C. P.; Reynolds, C. P. Antagonism of buthionine sulfoximine cytotoxicity for human neuroblastoma cell lines by hypoxia is reversed by the bioreductive agent tirapazamine. *Cancer Res.* **2003**, *63*, 1520-1526.

121. Lee, C. S.; Park, S. Y.; Ko, H. H.; Han, E. S. Effect of change in cellular GSH levels on mitochondrial damage and cell viability loss due to mitomycin C in small cell lung cancer cells. *Biochem. Pharmacol.* **2004**, *68*, 1857-1867.

122. Wolf, M. B.; Baynes, J. W. The anti-cancer drug, doxorubicin, causes oxidant stress-induced endothelial dysfunction. *Biochim. Biophys. Acta* **2006**, *1760*, 267-271.

123. Chew, E. H.; Matthews, C. S.; Zhang, J. H.; McCarroll, A. J.; Hagen, T.; Stevens, M. F. G.; Westwell, A. D.; Bradshaw, T. D. Antitumor quinols: Role of glutathione in modulating quinol-induced apoptosis and identification of putative cellular protein targets. *Biochem. Biophys. Res. Commun.* **2006**, *346*, 242-251.

124. Berlicki, L.; Obojska, A.; Forlani, G.; Kafarski, P. Design, synthesis, and activity of analogues of phosphinothricin as inhibitors of glutamine synthetase. *J. Med. Chem.* **2005**, *48*, 6340-6349.

125. Hiratake, J.; Irie, T.; Tokutake, N.; Oka, J. Recognition of a cysteine substrate by *E. coli* γ-glutamylcysteine synthetase probed by sulfoximine-based transition-state analogue inhibitors. *Biosci. Biotechnol. Biochem.* **2002**, *66*, 1500-1514.

126. Bolm, C.; Kahmann, J. D.; Moll, G. Sulfoximines in pseudopeptides. *Tetrahedron Lett.* **1997**, *38*, 1169-1172.

127. Bolm, C.; Moll, G.; Kahmann, J. D. Synthesis of pseudopeptides with sulfoximines as chiral backbone modifying elements. *Chem. Eur. J.* **2001**, *7*, 1118-1128.

128. Bolm, C.; Muller, D.; Dalhoff, C.; Hackenberger, C. P. R.; Weinhold, E. The stability of pseudopeptides bearing sulfoximines as chiral backbone modifying element towards proteinase K. *Bioorg. Med. Chem. Lett.* **2003**, *13*, 3207-3211.

129. Mock, W. L.; Tsay, J. T. Sulfoximine and sulfodiimine transition-state analog inhibitors for carboxypeptidase A. *J. Am. Chem. Soc.* **1989**, *111*, 4467-4472.

130. Mock, W. L.; Zhang, J. Z. Mechanistically significant diastereoselection in the sulfoximine inhibition of carboxypeptidase A. *J. Biol. Chem.* **1991**, *266*, 6393-6400.

131. Levenson, C. H.; Meyer, R. B. Design and synthesis of tetrahedral intermediate analogs as potential dihydroorotase inhibitors. *J. Med. Chem.* **1984**, *27*, 228-232.

132. Olbe, L.; Carlsson, E.; Lindberg, P. A proton-pump inhibitor expedition: The case histories of omeprazole and esomeprazole. *Nature Rev. Drug Discovery* **2003**, *2*, 132-139.

133. Pitchen, P.; Dunach, E.; Deshmukh, M. N.; Kagan, H. B. An efficient asymmetric oxidation of sulfides to sulfoxides. *J. Am. Chem. Soc.* **1984**, *106*, 8188-8193.

134. Brandt, J.; Gais, H. J. An efficient resolution of (±)-S-methyl-S-phenylsulfoximine with (+)-10-camphorsulfonic acid by the method of half-quantities. *Tetrahedron-Asymm.* **1997**, *8*, 909-912.

135. Okamura, H.; Bolm, C. Sulfoximines: Synthesis and catalytic applications. *Chem. Lett.* **2004**, *33*, 482-487.

136. Huang, S. L.; Swern, D. Oxidation of N-acylsulfilimines, N-sulfonylsulfilimines, and N-arylsulfilimines to sulfoximines by *meta*-chloroperoxybenzoate anion. *J. Org. Chem.* **1979**, *44*, 2510-2513.

137. Kinahan, T. C.; Tye, H. Synthesis of (*S*)-N-(diphenylphosphinyl)-S-methyl-S-phenyl sulfoximide: A new ligand for asymmetric catalysis. *Tetrahedron-Asymm.* **2001**, *12*, 1255-1257.

138. Xu, W. L.; Li, Y. Z.; Zhang, Q. S.; Zhu, H. S. A selective, convenient, and efficient conversion of sulfides to sulfoxides. *Synthesis* **2004**, 227-232.

139. Misani, F.; Fair, T. W.; Reiner, L. The reaction of hydrazoic acid with thioether-sulfoxides: Synthesis of sulfoximines. *J. Am. Chem. Soc.* **1951**, *73*, 459-461.

140. Tamura, Y.; Minamikawa, J.; Ikeda, M. O-mesitylenesulfonylhydroxylamine and related compounds - powerful aminating reagents. *Synthesis* **1977**, 1-17.

141. Johnson, C. R.; Kirchhof, R. A.; Corkins, H. G. Synthesis of optically active sulfoximines from optically active sulfoxides. *J. Org. Chem.* **1974**, *39*, 2458-2459.

142. Carpino, L. A. *O*-acylhydroxylamines. II. *O*-mesitylenesulfonyl-, *O*-*p*-toluenesulfonyl- and *O*-mesitoylhydroxylamine. *J. Am. Chem. Soc.* **1960**, *82*, 3133-3135.

143. Knight, F. I.; Brown, J. M.; Lazzari, D.; Ricci, A.; Blacker, A. J. Electrophilic amination of catecholboronate esters formed in the asymmetric hydroboration of vinylarenes. *Tetrahedron* **1997**, *53*, 11411-11424.

144. Siu, T.; Yudin, A. K. Electrochemical imination of sulfoxides using N-aminophthalimide. *Org. Lett.* **2002**, *4*, 1839-1842.

145. Krasnova, L. B.; Hili, R. M.; Chemoloz, O. V.; Yudin, A. K. Phenyliodine(III) diacetate as a mild oxidant for aziridination of olefins and imination of sulfoxides with N-aminophthalimide. *Arkivoc* **2005**, 26-38.

146. Muller, J. F. K.; Vogt, P. Cu(I)-catalyzed sulfoximination. *Tetrahedron Lett.* **1998**, *39*, 4805-4806.

147. Cren, S.; Kinahan, T. C.; Skinner, C. L.; Tye, H. A study of the functional group compatibility of sulfoximination methods. *Tetrahedron Lett.* **2002**, *43*, 2749-2751.

148. Lacôte, E.; Amatore, M.; Fensterbank, L.; Malacria, M. Catalytic synthesis of sulfoximines using copper(II) salts. *Synlett* **2002**, 116-118.

149. Cho, G. Y.; Bolm, C. Silver-catalyzed imination of sulfoxides and sulfides. *Org. Lett.* **2005**, *7*, 4983-4985.

150. Mancheno, O. G.; Bolm, C. Iron-catalyzed imination of sulfoxides and sulfides. *Org. Lett.* **2006**, *8*, 2349-2352.

151. Okamura, H.; Bolm, C. Rhodium-catalyzed imination of sulfoxides and sulfides: Efficient preparation of N-unsubstituted sulfoximines and sulfilimines. *Org. Lett.* **2004**, *6*, 1305-1307.

152. Bach, T.; Korber, C. Iron(II)-mediated nitrene transfer from *t*-butyloxycarbonyl azide ($BocN_3$) to sulfoxides, sulfides, and ketene acetals. *Tetrahedron Lett.* **1998**, *39*, 5015-5016.

153. Bach, T.; Korber, C. The preparation of N-*tert*-butyloxycarbonyl-(Boc) protected sulfoximines and sulfimines by an iron(II)-mediated nitrene transfer from $BocN_3$ to sulfoxides and sulfides. *Eur. J. Org. Chem.* **1999**, 1033-1039.

154. Dauban, P.; Dodd, R. H. Iminoiodanes and C–N bond formation in organic synthesis. *Synlett* **2003**, 1571-1586.

155. Cho, G. Y.; Bolm, C. Metal-free imination of sulfoxides and sulfides. *Tetrahedron Lett.* **2005**, *46*, 8007-8008.

156. Carpino, L. A.; Carpino, B. A.; Crowley, P. J.; Giza, C. A.; Terry, P. H. *t*-Butyl azidoformate. *Org. Synth. Coll. Vol 5.* **1973**, 157-159.

157. Bach, T.; Schlummer, B.; Harms, K. Intramolecular iron(II)-catalyzed nitrogen transfer reactions of unsaturated alkoxycarbonyl azides: A facile and stereoselective route to 4,5-disubstituted oxazolidinones. *Chem. Eur. J.* **2001**, *7*, 2581-2594.

158. Hwang, K. J.; Logusch, E. W.; Brannigan, L. H.; Thompson, M. R. Diastereoselective 1,2-addition of lithiated N-(trialkylsilyl)methylphenyl-sulfoximines to aldehydes - preparation of 1,4,3-oxathiazin-2(6H)-one 4-oxides as novel cyclic sulfoximines. *J. Org. Chem.* **1987**, *52*, 3435-3441.

159. Hainz, R.; Gais, H. J.; Raabe, G. Stereoselective hydroxyalkylation of titanated allyl sulfoximines at the α- as well as the γ-position through variation of the titanation reagent. *Tetrahedron-Asymm.* **1996**, *7*, 2505-2508.

160. Hwang, K. J. N-(trimethylsilyl)methylphenylsulfoximine - a convenient intermediate for the preparation of functionalized sulfoximines. *J. Org. Chem.* **1986**, *51*, 99-101.

161. Carpino, L. A.; Han, G. Y. 9-Fluorenylmethoxycarbonyl amino-protecting group. *J. Org. Chem.* **1972**, *37*, 3404-3408.

162. Espino, C. G.; Du Bois, J. A Rh-catalyzed C-H insertion reaction for the oxidative conversion of carbamates to oxazolidinones. *Angew. Chem. Int. Ed. Engl.* **2001**, *40*, 598-600.

163. Huang, J. M.; Xu, K. C.; Loh, T. P. Indium-mediated allylation reaction in aqueous media: Synthetic studies towards the total synthesis of dysiherbaine. *Synthesis* **2003**, 755-764.

164. Ornstein, P. L.; Bleisch, T. J.; Arnold, M. B.; Kennedy, J. H.; Wright, R. A.; Johnson, B. G.; Tizzano, J. P.; Helton, D. R.; Kallman, M. J.; Schoepp, D. D.; Herin, M. 2-Substituted (2*SR*)-2-amino-2-((1*SR*,2*SR*)-2-carboxycyclo-prop-1-yl)glycines as potent and selective antagonists of group II metabotropic glutamate receptors. 2. Effects of aromatic substitution, pharmacological characterization, and bioavailability. *J. Med. Chem.* **1998**, *41*, 358-378.

165. Beletskaya, I. P.; Sigeev, A. S.; Peregudov, A. S.; Petrovskii, P. V. Catalytic Sandmeyer cyanation as a synthetic pathway to aryl nitriles. *J. Organomet. Chem.* **2004**, *689*, 3810-3812.

166. Creary, X.; Sky, A. F.; Phillips, G.; Alonso, D. E. Reaction of arylhalodiazirines with thiophenoxide - a redox process. *J. Am. Chem. Soc.* **1993**, *115*, 7584-7592.

167. Procházka, M.; Široký, M. Preparation of unsaturated nitriles. *Coll. Czech. Chem. Commun.* **1983**, *48*, 1765-1773.

168. Sundermeier, M.; Zapf, A.; Beller, M. Palladium-catalyzed cyanation of aryl halides: Recent developments and perspectives. *Eur. J. Inorg. Chem.* **2003**, 3513-3526.

169. Yang, C. H.; Williams, J. M. Palladium-catalyzed cyanation of aryl bromides promoted by low-level organotin compounds. *Org. Lett.* **2004**, *6*, 2837-2840.

170. Weissman, S. A.; Zewge, D.; Chen, C. Ligand-free palladium-catalyzed cyanation of aryl halides. *J. Org. Chem.* **2005**, *70*, 1508-1510.

171. Tatsumi, R.; Fujio, M.; Satoh, H.; Katayama, J.; Takanashi, S.; Hashimoto, K.; Tanaka, H. Discovery of the α-7 nicotinic acetylcholine receptor agonists. (*R*)-3'-(5-Chlorothiophen-2-yl)spiro-1-azabicyclo[2.2.2]octane-3,5'-[1',3']-oxazolidin-2'-one as a novel, potent, selective, and orally bioavailable ligand. *J. Med. Chem.* **2005**, *48*, 2678-2686.

172. Fernández, I.; Khiar, N. Recent developments in the synthesis and utilization of chiral sulfoxides. *Chem. Rev.* **2003**, *103*, 3651-3705.

173. Legros, J.; Bolm, C. Highly enantioselective iron-catalyzed sulfide oxidation with aqueous hydrogen peroxide under simple reaction conditions. *Angew. Chem. Int. Ed. Engl.* **2004**, *43*, 4225-4228.

174. Legros, J.; Dehli, J. R.; Bolm, C. Applications of catalytic asymmetric sulfide oxidations to the syntheses of biologically active sulfoxides. *Adv. Synth. Cat.* **2005**, *347*, 19-31.

175. Capozzi, M. A. M.; Cardellicchio, C.; Naso, F.; Tortorella, P. Substituted benzene anions as leaving groups in the reaction of sulfinyl derivatives with Grignard reagents: A new and convenient route to dialkyl sulfoxides in high enantiomeric purity. *J. Org. Chem.* **2000**, *65*, 2843-2846.

176. Horváth, A.; Benner, J.; Bäckvall, J.-E. Enantiocontrolled synthesis of 3-pyrrolines from α-amino allenes. *Eur. J. Org. Chem.* **2004**, 3240-3243.

177. Feit, P. W. 1,4-Bismethanesulfonates of the stereoisomeric butanetetraols and related compounds. *J. Med. Chem.* **1964**, *7*, 14-17.

178. Batty, D.; Crich, D. Acyl radical cyclizations in synthesis. 4. Tandem processes - the 7-endo/5-exo serial cyclization approach to enantiomerically pure bicyclo[5.3.0]decan-2-ones. *J. Chem. Soc., Perkin Trans. 1* **1992**, 3193-3204.

179. Pak, C. S.; Lee, E.; Lee, G. H. Reductive cleavage reaction of γ-functionalized α,β-unsaturated esters and halomethyls mediated with magnesium in methanol. *J. Org. Chem.* **1993**, *58*, 1523-1530.

180. Mitsunobu, O. The use of diethyl azodicarboxylate and triphenylphosphine in synthesis and transformation of natural products. *Synthesis* **1981**, 1-28.

181. Falck, J. R.; Lai, J. Y.; Cho, S. D.; Yu, J. R. Alkylthioether synthesis *via* imidazole mediated Mitsunobu condensation. *Tetrahedron Lett.* **1999**, *40*, 2903-2906.

182. Kürti, L.; Czakó, B., *Strategic applications of named reactions in organic synthesis*. ISBN 0-12-429785-4. Elsevier Academic Press: 2005.

183. Falconer, R. A.; Jablonkai, I.; Toth, I. Efficient synthesis of thioglycosides *via* a Mitsunobu condensation. *Tetrahedron Lett.* **1999**, *40*, 8663-8666.

184. O'Neil, I. A.; Thompson, S.; Murray, C. L.; Kalindjian, S. B. DPPE: A convenient replacement for triphenylphosphine in the Staudinger and Mitsunobu reactions. *Tetrahedron Lett.* **1998**, *39*, 7787-7790.

185. Dembinski, R. Recent advances in the Mitsunobu reaction: Modified reagents and the quest for chromatography-free separation. *Eur. J. Org. Chem.* **2004**, 2763-2772.

186. Knutsen, L. J. S.; Lau, J.; Petersen, H.; Thomsen, C.; Weis, J. U.; Shalmi, M.; Judge, M. E.; Hansen, A. J.; Sheardown, M. J. N-Substituted adenosines as novel neuroprotective A_1 agonists with diminished hypotensive effects. *J. Med. Chem.* **1999**, *42*, 3463-3477.

187. Ko, S. Y.; Lee, A. W. M.; Masamune, S.; Reed, L. A.; Sharpless, K. B.; Walker, F. J. Total synthesis of the *L*-hexoses. *Tetrahedron* **1990**, *46*, 245-264.

188. Kumar, P. S.; Bharatam, P. V. Theoretical studies on the S-N interactions in sulfoximine. *Tetrahedron* **2005**, *61*, 5633-5639.

189. Garofalo, A.; Campiani, G.; Fiorini, I.; Nacci, V. Polycondensed heterocycles. X. A new method for the preparation of pyrrolo[2,1-*C*][1,4]benzothiazepines by intramolecular Mitsunobu cyclisation. *Tetrahedron* **1999**, *55*, 1479-1490.

190. Johansson, R.; Samuelsson, B. Regioselective reductive ring-opening of 4-methoxybenzylidene acetals of hexopyranosides - access to a novel protecting-group strategy. 1. *J. Chem. Soc., Perkin Trans. 1* **1984**, 2371-2374.

191. Riley, A. M.; Jenkins, D. J.; Marwood, R. D.; Potter, B. V. L. Synthesis of glucopyranoside-based ligands for *D*-myo-inositol 1,4,5-trisphosphate receptors. *Carbohydr. Res.* **2002**, *337*, 1067-1082.

192. De, S. Y. K.; Gibbs, R. A. Ruthenium(III) chloride-catalyzed chemoselective synthesis of acetals from aldehydes. *Tetrahedron Lett.* **2004**, *45*, 8141-8144.

193. Zheng, T. C.; Burkart, M.; Richardson, D. E. A general and mild synthesis of thioesters and thiols from halides. *Tetrahedron Lett.* **1999**, *40*, 603-606.

194. Bolm, C.; Hildebrand, J. P. Palladium-catalyzed carbon-nitrogen bond formation: A novel, catalytic approach towards N-arylated sulfoximines. *Tetrahedron Lett.* **1998**, *39*, 5731-5734.

195. Bolm, C.; Hildebrand, J. P. Palladium-catalyzed N-arylation of sulfoximines with aryl bromides and aryl iodides. *J. Org. Chem.* **2000**, *65*, 169-175.

196. Harmata, M.; Hong, X. C.; Ghosh, S. K. Microwave-assisted N-arylation of a sulfoximine with aryl chlorides. *Tetrahedron Lett.* **2004**, *45*, 5233-5236.

197. Cho, G. Y.; Remy, P.; Jansson, J.; Moessner, C.; Bolm, C. Copper-mediated cross-coupling reactions of N-unsubstituted sulfoximines and aryl halides. *Org. Lett.* **2004**, *6*, 3293-3296.

198. Moessner, C.; Bolm, C. $Cu(OAc)_2$-catalyzed N-arylations of sulfoximines with aryl boronic acids. *Org. Lett.* **2005**, *7*, 2667-2669.

199. Karlsson, S.; Hogberg, H. E. Pheromones of pine sawflies: Synthesis of a pure (2*S*,3*R*)-3-methylalkan-2-ol stereoisomer *via* an asymmetric 1,3-dipolar cycloaddition; preparation of a pheromone component *Macrodiprion nemoralis*. *Synthesis* **2000**, 1863-1867.

200. Karlsson, S. A.; Hogberg, H. E. Enantiomerically pure *trans*-3,4-disubstituted tetrahydrothiophenes from diastereoselective thiocarbonyl ylide addition to chiral α,β-unsaturated amides. *Org. Lett.* **1999**, *1*, 1667-1669.

201. Karlsson, S.; Hogberg, H. E. Synthesis of enantiomerically pure 4-substituted pyrrolidin-3-ols *via* asymmetric 1,3-dipolar cycloaddition. *Tetrahedron-Asymm.* **2001**, *12*, 1977-1982.

202. Lu, X. Y.; Zhang, C. M.; Xu, Z. R. Reactions of electron-deficient alkynes and allenes under phosphine catalysis. *Acc. Chem. Res.* **2001**, *34*, 535-544.

203. Inanaga, J.; Baba, Y.; Hanamoto, T. Organic synthesis with trialkylphosphine catalysts - Conjugate addition of alcohols to α,β-unsaturated alkynic acid esters. *Chem. Lett.* **1993**, 241-244.

204. Hudlicky, T.; Radesca, L.; Rigby, H. L. Menthyl 2-bromocrotonate and menthyl 4-bromocrotonate - reagents for chiral vinylogous Darzens and Reformatsky reactions. *J. Org. Chem.* **1987**, *52*, 4397-4399.

205. Harada, N.; Watanabe, M.; Kuwahara, S.; Sugio, A.; Kasai, Y.; Ichikawa, A. 2-Methoxy-2-(1-naphthyl)propionic acid, a powerful chiral auxiliary for enantio-resolution of alcohols and determination of their absolute configurations by the ^{1}H NMR anisotropy method. *Tetrahedron-Asymm.* **2000**, *11*, 1249-1253.

206. Hosomi, A.; Matsuyama, Y.; Sakurai, H. Chloromethyl trimethylsilylmethyl sulfide as a parent thiocarbonyl ylide synthon - a simple synthesis of dihydrothiophenes and tetrahydrothiophenes. *J. Chem. Soc., Chem. Commun.* **1986**, 1073-1074.

207. Block, E.; Laffitte, J. A.; Eswarakrishnan, V. Synthesis and reactions of 3-mercaptocyclobutanol and derivatives - preparation of a 2,4-dithiabicyclo-[3.1.1]heptane. *J. Org. Chem.* **1986**, *51*, 3428-3435.

208. Evans, D. A.; Mathre, D. J.; Scott, W. L. Asymmetric synthesis of the enkephalinase inhibitor thiorphan. *J. Org. Chem.* **1985**, *50*, 1830-1835.

209. Ren, X. F.; Turos, E.; Lake, C. H.; Churchill, M. R. Regiochemical and stereochemical studies on halocyclization reactions of unsaturated sulfides. *J. Org. Chem.* **1995**, *60*, 6468-6483.

210. Ren, X. F.; Turos, E. Regiochemical studies on halocyclization reactions of unsaturated sulfides. *Tetrahedron Lett.* **1993**, *34*, 1575-1578.

211. Shinkwin, A. E.; Whish, W. J. D.; Threadgill, M. D. Synthesis of thiophenecarboxamides, thieno[3,4-c]pyridin-4(5H)-ones and thieno[3,4-d] pyrimidin-4(3H)-ones and preliminary evaluation as inhibitors of poly(ADP-ribose) polymerase (PARP). *Bioorg. Med. Chem.* **1999**, *7*, 297-308.

212. Woodward, R. B.; Eastman, R. H. Tetrahydrothiophene ("Thiophane") derivatives. *J. Am. Chem. Soc.* **1946**, *68*, 2229-2235.

213. Baraldi, P. G.; Pollini, G. P.; Zanirato, V.; Barco, A.; Benetti, S. A new simple synthesis of α-substituted acrylonitriles. *Synthesis* **1985**, 969-971.

214. Hoffmann, R. W.; Weidmann, U. Stereoselective synthesis of alcohols. 19. The sense of asymmetric induction on addition to α-chiral aldehydes. *Chem. Ber. Recueil* **1985**, *118*, 3966-3979.

215. Baraldi, P. G.; Barco, A.; Benetti, S.; Manfredini, S.; Pollini, G. P.; Simoni, D.; Zanirato, V. Synthesis and reactivity of a stable precursor of 2-cyano-1,3-butadiene. *Tetrahedron* **1988**, *44*, 6451-6454.

216. Payne, G. B.; Williams, P. H. Reactions of hydrogen peroxide. VI. Alkaline epoxidation of acrylonitrile. *J. Org. Chem.* **1961**, *26*, 651-659.

217. Dehli, J. R.; Gotor, V. Dynamic kinetic resolution of 2-oxocyclo-alkane-carbonitriles: Chemoenzymatic syntheses of optically active cyclic β- and γ-amino alcohols. *J. Org. Chem.* **2002**, *67*, 6816-6819.

218. Naka, T.; Nishizono, N.; Minakawa, N.; Matsuda, A. Nucleosides and nucleotides. 189. Investigation of the stereoselective coupling of thymine with *meso*-thiolane-3,4-diol-1-oxide derivatives *via* the Pummerer reaction. *Tetrahedron Lett.* **1999**, *40*, 6297-6300.

219. Euerby, M. R.; Waigh, R. D. The synthesis of isoquinolines using methylthio activating groups. *J. Chem. Res. Miniprint* **1987**, *2*, 527-553.

220. Cooper, G. D. Organosilicon mercaptans. *J. Am. Chem. Soc.* **1954**, *76*, 2500.

Appendices

Appendix 1. X-ray crystallography data for compound S-(*S*)-104

Identification code	Compound **S-(*S*)-104**
Empirical formula	$C_{20}H_{25}NO_4S$
Formula weight	375.47
Temperature	150(2) K
Wavelength	0.71073 Å
Crystal system	Orthorhombic
Space group	$P2_12_12_1$
Unit cell dimensions	a = 5.5540(1)Å α = 90°
	b = 18.4970(3)Å β = 90°
	c = 19.2410(4)Å γ = 90°
Volume	1976.67(6) $Å^3$
Z	4
Density (calculated)	1.262 Mg/m^3
Absorption coefficient	0.188 mm^{-1}
F(000)	800
Crystal size	0.20 x 0.20 x 0.10 mm
Theta range for data collection	3.93 to 27.46°
Index ranges	-7<=h<=7; -24<=k<=24; -24<=l<=24
Reflections collected	31757
Independent reflections	4490 [R(int) = 0.0497]
Reflections observed (>2σ)	3837
Data Completeness	0.995
Absorption correction	Semi-empirical from equivalents
Max. and min. transmission	0.98 and 0.94
Refinement method	Full-matrix least-squares on F^2
Data / restraints / parameters	4490 / 104 / 304
Goodness-of-fit on F^2	1.036
Final R indices [I>2σ(I)]	R^1 = 0.0358 wR_2 = 0.0772
R indices (all data)	R^1 = 0.0479 wR_2 = 0.0824
Absolute structure parameter	-0.05(6)
Largest diff. peak and hole	0.191 and -0.307 $eÅ^{-3}$

Table A. Crystal data and structure refinement for **S-(*S*)-104**.

Atom	x	y	z	U(eq)
S(1)	940(1)	1574(1)	9277(1)	29(1)
O(1)	-1619(2)	1747(1)	9233(1)	36(1)
O(2)	1342(2)	2741(1)	8016(1)	43(1)
O(3)	3119(2)	3841(1)	7998(1)	46(1)
O(4)	3829(2)	4794(1)	9204(1)	41(1)
N(1)	2046(3)	1253(1)	9929(1)	38(1)
C(1)	1580(3)	1038(1)	8530(1)	31(1)
C(2)	3706(3)	646(1)	8510(1)	45(1)
C(3)	4167(4)	205(1)	7942(1)	54(1)
C(4)	2536(4)	155(1)	7411(1)	58(1)
C(5)	445(4)	552(1)	7429(1)	63(1)
C(6)	-40(3)	1000(1)	7990(1)	46(1)
C(7)	2631(3)	2382(1)	9188(1)	31(1)
C(8)	1511(3)	2953(1)	8725(1)	33(1)
C(9)	3078(3)	3641(1)	8714(1)	33(1)
C(10)	2053(3)	4239(1)	9145(1)	38(1)
C(11)	2878(4)	3197(1)	7608(1)	46(1)
C(12)	1592(4)	3390(1)	6941(1)	62(1)
C(13)	5264(4)	2824(2)	7499(1)	79(1)
C(14)	3120(30)	5352(10)	9679(8)	49(3)
C(15)	5050(40)	5882(12)	9673(7)	48(4)
C(16)	6234(18)	6090(4)	10279(5)	67(2)
C(17)	8133(19)	6571(5)	10300(6)	74(3)
C(18)	8860(18)	6882(6)	9683(6)	71(3)
C(19)	7832(14)	6672(4)	9062(4)	77(2)
C(20)	5902(18)	6199(5)	9069(4)	58(2)
C(14A)	2870(30)	5420(10)	9543(8)	61(4)
C(15A)	5060(40)	5887(12)	9777(7)	40(3)
C(16A)	5924(15)	5832(4)	10436(4)	49(2)
C(17A)	7874(11)	6224(4)	10631(3)	65(1)
C(18A)	8907(18)	6717(6)	10174(6)	71(3)
C(19A)	8060(20)	6765(5)	9515(6)	84(3)
C(20A)	6129(19)	6348(5)	9314(4)	73(3)

Table B. Atomic coordinates (x 10^4) and equivalent isotropic displacement parameters ($Å^2$ x 10^3) for **S-(*S*)-104**.

S(1)-O(1)	1.4588(11)	S(1)-N(1)	1.5173(15)
S(1)-C(7)	1.7735(15)	S(1)-C(1)	1.7830(16)
O(2)-C(8)	1.422(2)	O(2)-C(11)	1.433(2)
O(3)-C(11)	1.413(2)	O(3)-C(9)	1.4271(19)
O(4)-C(14A)	1.431(17)	O(4)-C(10)	1.429(2)
O(4)-C(14)	1.434(16)	C(1)-C(6)	1.377(2)
C(1)-C(2)	1.386(2)	C(2)-C(3)	1.387(3)
C(3)-C(4)	1.368(3)	C(4)-C(5)	1.374(3)
C(5)-C(6)	1.388(3)	C(7)-C(8)	1.516(2)
C(8)-C(9)	1.541(2)	C(9)-C(10)	1.494(2)
C(11)-C(13)	1.509(3)	C(11)-C(12)	1.511(3)
C(14)-C(15)	1.45(2)	C(15)-C(16)	1.394(10)
C(15)-C(20)	1.385(10)	C(16)-C(17)	1.380(10)
C(17)-C(18)	1.379(12)	C(18)-C(19)	1.381(10)
C(19)-C(20)	1.383(10)	C(14A)-C(15A)	1.56(2)
C(15A)-C(16A)	1.359(11)	C(15A)-C(20A)	1.369(10)
C(16A)-C(17A)	1.357(9)	C(17A)-C(18A)	1.391(9)
C(18A)-C(19A)	1.356(12)	C(19A)-C(20A)	1.376(10)
O(1)-S(1)-N(1)	121.90(8)	O(1)-S(1)-C(7)	109.01(7)
N(1)-S(1)-C(7)	101.28(8)	O(1)-S(1)-C(1)	105.64(7)
N(1)-S(1)-C(1)	111.55(8)	C(7)-S(1)-C(1)	106.55(7)
C(8)-O(2)-C(11)	108.87(12)	C(11)-O(3)-C(9)	107.01(13)
C(14A)-O(4)-C(10)	111.2(8)	C(14A)-O(4)-C(14)	12.9(12)
C(10)-O(4)-C(14)	112.3(7)	C(6)-C(1)-C(2)	120.57(16)
C(6)-C(1)-S(1)	120.44(13)	C(2)-C(1)-S(1)	118.97(13)
C(1)-C(2)-C(3)	119.16(18)	C(4)-C(3)-C(2)	120.36(19)
C(3)-C(4)-C(5)	120.30(18)	C(4)-C(5)-C(6)	120.2(2)
C(1)-C(6)-C(5)	119.41(18)	C(8)-C(7)-S(1)	115.27(11)
O(2)-C(8)-C(7)	113.48(13)	O(2)-C(8)-C(9)	104.63(12)
C(7)-C(8)-C(9)	110.55(13)	O(3)-C(9)-C(10)	110.46(14)
O(3)-C(9)-C(8)	103.60(12)	C(10)-C(9)-C(8)	112.87(13)
O(4)-C(10)-C(9)	108.29(13)	O(3)-C(11)-O(2)	105.16(14)
O(3)-C(11)-C(13)	112.09(17)	O(2)-C(11)-C(13)	109.27(18)
O(3)-C(11)-C(12)	107.21(17)	O(2)-C(11)-C(12)	108.80(16)
C(13)-C(11)-C(12)	113.90(18)	O(4)-C(14)-C(15)	106.1(14)
C(16)-C(15)-C(20)	115.1(8)	C(16)-C(15)-C(14)	121.8(10)
C(20)-C(15)-C(14)	123.1(11)	C(17)-C(16)-C(15)	124.2(8)
C(16)-C(17)-C(18)	117.9(7)	C(17)-C(18)-C(19)	120.4(8)
C(20)-C(19)-C(18)	119.3(7)	C(19)-C(20)-C(15)	122.8(8)
O(4)-C(14A)-C(15A)	106.9(15)	C(16A)-C(15A)-C(20A)	119.9(7)
C(16A)-C(15A)-C(14A)	120.3(9)	C(20A)-C(15A)-C(14A)	119.8(10)
C(17A)-C(16A)-C(15A)	120.1(7)	C(16A)-C(17A)-C(18A)	120.3(7)
C(19A)-C(18A)-C(17A)	119.4(8)	C(18A)-C(19A)-C(20A)	119.7(7)
C(19A)-C(20A)-C(15A)	120.4(8)		

Table C. Bond lengths [Å] and angles [°] for **S-(*S*)-104**.

Atom	U11	U22	U33	U23	U13	U12
S(1)	26(1)	30(1)	32(1)	-4(1)	2(1)	-1(1)
O(1)	25(1)	40(1)	42(1)	-8(1)	3(1)	-1(1)
O(2)	46(1)	44(1)	38(1)	-1(1)	-11(1)	-10(1)
O(3)	55(1)	49(1)	33(1)	3(1)	1(1)	-18(1)
O(4)	47(1)	28(1)	47(1)	-5(1)	4(1)	-3(1)
N(1)	40(1)	39(1)	35(1)	1(1)	-1(1)	-4(1)
C(1)	30(1)	28(1)	36(1)	-3(1)	4(1)	-3(1)
C(2)	36(1)	46(1)	52(1)	-12(1)	-3(1)	6(1)
C(3)	43(1)	51(1)	68(1)	-20(1)	9(1)	9(1)
C(4)	55(1)	59(1)	60(1)	-29(1)	6(1)	0(1)
C(5)	57(1)	82(2)	49(1)	-29(1)	-9(1)	10(1)
C(6)	40(1)	54(1)	45(1)	-14(1)	-5(1)	7(1)
C(7)	26(1)	31(1)	37(1)	-6(1)	-1(1)	-4(1)
C(8)	29(1)	33(1)	37(1)	-1(1)	0(1)	-1(1)
C(9)	31(1)	36(1)	33(1)	1(1)	0(1)	-3(1)
C(10)	36(1)	31(1)	47(1)	1(1)	0(1)	0(1)
C(11)	42(1)	60(1)	36(1)	-7(1)	1(1)	-9(1)
C(12)	65(1)	82(2)	38(1)	1(1)	-7(1)	-17(1)
C(13)	53(1)	120(2)	63(1)	-31(2)	3(1)	8(1)
C(14)	53(6)	43(4)	52(4)	-11(3)	8(5)	12(4)
C(15)	65(7)	33(6)	45(5)	-2(4)	-14(4)	15(5)
C(16)	85(5)	71(6)	44(4)	-1(4)	4(4)	17(4)
C(17)	78(7)	56(6)	88(7)	-22(4)	-24(5)	-16(5)
C(18)	54(4)	38(4)	121(7)	-16(4)	-24(5)	5(3)
C(19)	86(4)	43(3)	102(5)	2(4)	-5(5)	-21(3)
C(20)	70(3)	46(3)	57(4)	9(3)	-21(4)	-13(3)
C(14A)	56(4)	43(5)	83(8)	-26(5)	-27(4)	10(4)
C(15A)	47(6)	26(5)	46(5)	-16(4)	0(4)	2(4)
C(16A)	55(3)	60(4)	33(3)	-1(2)	2(2)	-1(3)
C(17A)	58(3)	75(4)	62(4)	-29(3)	2(3)	-6(3)
C(18A)	58(5)	35(4)	119(7)	-25(4)	11(5)	-14(3)
C(19A)	95(9)	39(5)	117(9)	14(6)	30(7)	-5(5)
C(20A)	105(7)	66(6)	48(4)	10(4)	-19(4)	23(5)

Table D. Anisotropic displacement parameters ($Å^2 \times 10^3$) for **S-(*S*)-104**.

Atom	x	y	z	U(eq)
H(2)	4832	678	8880	54
H(3)	5623	-64	7921	64
H(4)	2852	-155	7028	69
H(5)	-671	519	7056	75
H(6)	-1478	1278	8001	55
H(7A)	2878	2593	9655	37
H(7B)	4237	2257	8999	37
H(8)	-130	3076	8903	39
H(9)	4745	3524	8875	40
H(10A)	583	4433	8921	46
H(10B)	1615	4056	9611	46
H(12A)	136	3667	7050	93
H(12B)	1148	2946	6694	93
H(12C)	2659	3681	6648	93
H(13A)	6278	3119	7194	118
H(13B)	4994	2350	7285	118
H(13C)	6068	2759	7948	118
H(14C)	2903	5152	10152	59
H(14D)	1586	5576	9529	59
H(16)	5699	5888	10706	80
H(17)	8916	6683	10725	89
H(18)	10074	7244	9686	85
H(19)	8445	6849	8634	92
H(20)	5130	6088	8642	69
H(14A)	1895	5276	9951	73
H(14B)	1838	5697	9219	73
H(16A)	5162	5519	10759	59
H(17A)	8536	6162	11082	78
H(18A)	10195	7018	10323	85
H(19A)	8797	7085	9192	100
H(20A)	5535	6381	8852	88
H(1)	1410(30)	830(5)	10030(10)	50(6)

Table E. Hydrogen coordinates (x 10^4) and isotropic displacement parameters ($Å^2$ x 10^3) for **S-(*S*)-104**.

Appendix 2. X-ray crystallography data for compound S-(*S*)-91

Identification code	Compound **S-(*S*)-91**
Empirical formula	C_{20} H_{24} Br N O_4 S
Formula weight	454.37
Temperature	150(2) K
Wavelength	0.71073 Å
Crystal system	Monoclinic
Space group	P21
Unit cell dimensions	a = 12.3520(2)Å α = 90°
	b = 5.5440(1)Å β = 103.459(1)°
	c = 15.7540(3)Å γ = 90°
Volume	1049.20(3) $Å^3$
Z	2
Density (calculated)	1.438 Mg/m^3
Absorption coefficient	2.083 mm^{-1}
F(000)	468
Crystal size	0.35 x 0.30 x 0.30 mm
Theta range for data collection	3.79 to 29.97°
Index ranges	-17<=h<=16; -7<=k<=7; -20<=l<=22
Reflections collected	15898
Independent reflections	5447 [R(int) = 0.0506]
Reflections observed (>2σ)	4752
Data Completeness	0.939
Absorption correction	Semi-empirical from equivalents
Max. and min. transmission	0.55 and 0.40
Refinement method	Full-matrix least-squares on F^2
Data / restraints / parameters	5447 / 2 / 248
Goodness-of-fit on F^2	1.032
Final R indices [I>2σ(I)]	R^1 = 0.0347 wR_2 = 0.0731
R indices (all data)	R^1 = 0.0454 wR_2 = 0.0780
Absolute structure parameter	-0.010(6)
Largest diff. peak and hole	0.479 and -0.498 $eÅ^{-3}$

Table A. Crystal data and structure refinement for **S-(*S*)-91**.

Atom	x	y	z	U(eq)
Br(1)	9339(1)	1118(1)	4107(1)	49(1)
S(2)	5641(1)	3026(1)	1400(1)	21(1)
O(1)	5839(1)	459(3)	1296(1)	26(1)
O(2)	8156(1)	3911(3)	1157(1)	31(1)
O(3)	8751(1)	5205(3)	-20(1)	32(1)
O(4)	7261(1)	5741(3)	-1835(1)	30(1)
N(1)	4483(2)	4054(4)	1289(1)	28(1)
C(1)	8084(2)	3068(5)	3598(2)	33(1)
C(2)	7426(2)	2368(4)	2798(2)	26(1)
C(3)	6526(2)	3822(4)	2436(1)	23(1)
C(4)	6284(2)	5910(5)	2845(1)	32(1)
C(5)	6959(2)	6506(5)	3654(2)	42(1)
C(6)	7860(2)	5090(5)	4032(2)	40(1)
C(7)	6162(2)	4702(4)	621(1)	23(1)
C(8)	7224(2)	3715(4)	429(1)	24(1)
C(9)	7568(2)	5166(4)	-298(1)	25(1)
C(10)	8998(2)	5364(4)	906(2)	29(1)
C(11)	8924(3)	7928(6)	1204(2)	59(1)
C(12)	10124(2)	4260(5)	1262(2)	39(1)
C(13)	7190(2)	4007(5)	-1181(1)	28(1)
C(14)	6964(3)	4714(5)	-2685(2)	43(1)
C(15)	6884(2)	6732(5)	-3329(2)	35(1)
C(16)	5866(2)	7784(6)	-3703(2)	42(1)
C(17)	5798(3)	9730(6)	-4271(2)	47(1)
C(18)	6742(3)	10640(6)	-4463(2)	50(1)
C(19)	7763(3)	9605(6)	-4098(2)	52(1)
C(20)	7829(3)	7650(6)	-3538(2)	46(1)

Table B. Atomic coordinates (x 10^4) and equivalent isotropic displacement parameters ($Å^2$ x 10^3) for **S-(*S*)-91**.

Br(1)-C(1)	1.906(3)	S(2)-O(1)	1.4599(16)
S(2)-N(1)	1.512(2)	S(2)-C(7)	1.775(2)
S(2)-C(3)	1.795(2)	O(2)-C(8)	1.427(3)
O(2)-C(10)	1.442(3)	O(3)-C(10)	1.421(3)
O(3)-C(9)	1.425(3)	O(4)-C(14)	1.422(3)
O(4)-C(13)	1.426(3)	C(1)-C(6)	1.374(4)
C(1)-C(2)	1.388(3)	C(2)-C(3)	1.384(3)
C(3)-C(4)	1.391(4)	C(4)-C(5)	1.390(3)
C(5)-C(6)	1.378(4)	C(7)-C(8)	1.516(3)
C(8)-C(9)	1.537(3)	C(9)-C(13)	1.506(3)
C(10)-C(12)	1.504(3)	C(10)-C(11)	1.507(4)
C(14)-C(15)	1.499(4)	C(15)-C(20)	1.382(4)
C(15)-C(16)	1.387(4)	C(16)-C(17)	1.392(4)
C(17)-C(18)	1.368(5)	C(18)-C(19)	1.383(5)
C(19)-C(20)	1.387(5)		
O(1)-S(2)-N(1)	122.22(11)	O(1)-S(2)-C(7)	109.61(10)
N(1)-S(2)-C(7)	102.01(10)	O(1)-S(2)-C(3)	105.03(10)
N(1)-S(2)-C(3)	111.85(11)	C(7)-S(2)-C(3)	104.96(10)
C(8)-O(2)-C(10)	108.70(17)	C(10)-O(3)-C(9)	106.00(17)
C(14)-O(4)-C(13)	111.3(2)	C(6)-C(1)-C(2)	122.5(2)
C(6)-C(1)-Br(1)	119.46(18)	C(2)-C(1)-Br(1)	118.1(2)
C(3)-C(2)-C(1)	117.1(2)	C(2)-C(3)-C(4)	122.2(2)
C(2)-C(3)-S(2)	119.45(18)	C(4)-C(3)-S(2)	118.33(17)
C(5)-C(4)-C(3)	118.3(2)	C(6)-C(5)-C(4)	120.8(3)
C(1)-C(6)-C(5)	119.0(2)	C(8)-C(7)-S(2)	114.78(15)
O(2)-C(8)-C(7)	112.66(18)	O(2)-C(8)-C(9)	104.34(18)
C(7)-C(8)-C(9)	111.19(18)	O(3)-C(9)-C(13)	111.42(19)
O(3)-C(9)-C(8)	102.72(17)	C(13)-C(9)-C(8)	112.65(19)
O(3)-C(10)-O(2)	104.51(18)	O(3)-C(10)-C(12)	108.5(2)
O(2)-C(10)-C(12)	109.51(19)	O(3)-C(10)-C(11)	111.4(2)
O(2)-C(10)-C(11)	110.0(2)	C(12)-C(10)-C(11)	112.6(2)
O(4)-C(13)-C(9)	108.76(19)	O(4)-C(14)-C(15)	107.5(2)
C(20)-C(15)-C(16)	118.5(3)	C(20)-C(15)-C(14)	120.7(3)
C(16)-C(15)-C(14)	120.8(3)	C(15)-C(16)-C(17)	120.8(3)
C(18)-C(17)-C(16)	120.1(3)	C(17)-C(18)-C(19)	119.8(3)
C(18)-C(19)-C(20)	120.1(3)	C(19)-C(20)-C(15)	120.7(3)

Table C. Bond lengths [Å] and angles [°] for **S-(*S*)-91**.

Atom	U11	U22	U33	U23	U13	U12
Br(1)	29(1)	68(1)	40(1)	13(1)	-10(1)	-1(1)
S(2)	21(1)	21(1)	19(1)	0(1)	1(1)	-1(1)
O(1)	31(1)	21(1)	24(1)	-1(1)	-1(1)	0(1)
O(2)	21(1)	44(1)	27(1)	11(1)	1(1)	4(1)
O(3)	26(1)	39(1)	29(1)	5(1)	5(1)	-5(1)
O(4)	36(1)	35(1)	20(1)	-2(1)	8(1)	-2(1)
N(1)	23(1)	31(1)	29(1)	4(1)	4(1)	-1(1)
C(1)	25(1)	45(1)	24(1)	9(1)	-2(1)	-6(1)
C(2)	25(1)	31(1)	21(1)	3(1)	2(1)	-3(1)
C(3)	25(1)	24(1)	20(1)	0(1)	4(1)	-5(1)
C(4)	39(1)	28(1)	28(1)	-3(1)	4(1)	-3(1)
C(5)	56(2)	36(2)	31(1)	-11(1)	6(1)	-9(1)
C(6)	47(2)	48(2)	23(1)	-4(1)	0(1)	-16(1)
C(7)	24(1)	23(1)	20(1)	2(1)	1(1)	3(1)
C(8)	27(1)	23(1)	23(1)	1(1)	5(1)	3(1)
C(9)	25(1)	24(1)	25(1)	3(1)	6(1)	0(1)
C(10)	31(1)	26(1)	30(1)	4(1)	4(1)	-3(1)
C(11)	84(2)	32(1)	47(2)	-6(1)	-10(2)	4(2)
C(12)	24(1)	44(2)	46(2)	2(1)	1(1)	-3(1)
C(13)	28(1)	30(1)	25(1)	0(1)	7(1)	0(1)
C(14)	60(2)	43(2)	26(1)	-8(1)	7(1)	-1(1)
C(15)	45(1)	41(2)	20(1)	-7(1)	7(1)	0(1)
C(16)	42(2)	53(2)	31(1)	-2(1)	11(1)	-2(1)
C(17)	59(2)	51(2)	29(1)	-4(1)	7(1)	3(1)
C(18)	86(2)	42(2)	26(1)	-1(1)	19(1)	-5(2)
C(19)	62(2)	62(2)	38(2)	-10(2)	24(2)	-19(2)
C(20)	42(2)	63(2)	33(1)	-8(1)	11(1)	0(1)

Table D. Anisotropic displacement parameters ($Å^2 \times 10^3$) for **S-(*S*)-91**.

Atom	x	y	z	U(eq)
H(2)	7586	951	2510	31
H(4)	5672	6904	2579	38
H(5)	6798	7907	3949	50
H(6)	8318	5505	4585	49
H(7A)	5582	4756	70	27
H(7B)	6300	6379	835	27
H(8)	7112	1986	248	29
H(9)	7268	6845	-313	30
H(11A)	9477	8919	1009	88
H(11B)	9070	7971	1843	88
H(11C)	8177	8563	955	88
H(12A)	10147	2645	1014	59
H(12B)	10260	4143	1899	59
H(12C)	10698	5274	1106	59
H(13A)	7668	2601	-1227	33
H(13B)	6413	3435	-1264	33
H(14A)	6241	3869	-2771	52
H(14B)	7535	3535	-2762	52
H(16)	5207	7170	-3569	50
H(17)	5095	10426	-4527	56
H(18)	6697	11979	-4846	60
H(19)	8420	10233	-4231	62
H(20)	8532	6936	-3296	55
H(1)	4151	3051	1534	58(10)

Table E. Hydrogen coordinates (x 10^4) and isotropic displacement parameters ($Å^2$ x 10^3) for **S-(*S*)-91**.

Appendix 3. X-ray crystallography data for compound (±)-164

Identification code	Compound **(±)-164**
Empirical formula	C5 H9 N O2 S
Formula weight	147.19
Temperature	150(2) K
Wavelength	0.71073 Å
Crystal system	Monoclinic
Space group	$P2_1/a$
Unit cell dimensions	a = 8.0940(2)Å α = 90°
	b = 9.5710(3)Å β = 107.961(1)°
	c = 8.9660(3)Å γ = 90°
Volume	660.73(3) $Å^3$
Z	4
Density (calculated)	1.480 Mg/m^3
Absorption coefficient	0.411 mm^{-1}
F(000)	312
Crystal size	0.25 x 0.20 x 0.15 mm
Theta range for data collection	4.26 to 27.47 °.
Index ranges	-10<=h<=10; -12<=k<=12; -11<=l<=11
Reflections collected	9540
Independent reflections	1505 [R(int) = 0.0363]
Reflections observed (>2σ)	1307
Data Completeness	0.996
Absorption correction	Multiscan
Max. and min. transmission	0.942, 0.893
Refinement method	Full-matrix least-squares on F^2
Data / restraints / parameters	1505 / 0 / 86
Goodness-of-fit on F^2	1.064
Final R indices [I>2σ(I)]	R^1 = 0.0325 wR_2 = 0.0804
R indices (all data)	R^1 = 0.0389 wR_2 = 0.0833
Largest diff. peak and hole	0.212 and -0.333 $eÅ^{-3}$

Table A. Crystal data and structure refinement for **(±)-164**. Notes: The lattice contains a racemate. Gross structure dominated by hydrogen-bonding.

Atom	x	y	z	U(eq)
S(1)	3463(1)	1935(1)	9122(1)	36(1)
O(2)	-943(1)	-961(1)	7170(1)	26(1)
O(3)	2740(1)	-492(1)	5415(1)	26(1)
N(1)	763(2)	-2712(1)	6818(1)	26(1)
C(2)	3797(2)	1400(2)	7297(2)	31(1)
C(3)	2349(2)	364(1)	6559(2)	24(1)
C(4)	2142(2)	-546(1)	7905(2)	22(1)
C(5)	2053(2)	459(2)	9196(2)	28(1)
C(41)	529(2)	-1441(2)	7286(2)	22(1)

Table B. Atomic coordinates (x 10^4) and equivalent isotropic displacement parameters ($Å^2$ x 10^3) for **(±)-164**.

S(1)-C(2)	1.8127(16)	S(1)-C(5)	1.8306(15)
O(2)-C(41)	1.2506(16)	O(3)-C(3)	1.4229(16)
N(1)-C(41)	1.3198(18)	C(2)-C(3)	1.522(2)
C(3)-C(4)	1.5386(18)	C(4)-C(41)	1.5163(18)
C(4)-C(5)	1.5238(19)		
C(2)-S(1)-C(5)	94.73(7)	C(3)-C(2)-S(1)	105.52(9)
O(3)-C(3)-C(2)	112.08(11)	O(3)-C(3)-C(4)	109.96(11)
C(2)-C(3)-C(4)	106.45(11)	C(41)-C(4)-C(5)	113.42(11)
C(41)-C(4)-C(3)	108.82(11)	C(5)-C(4)-C(3)	106.29(11)
C(4)-C(5)-S(1)	106.48(9)	O(2)-C(41)-N(1)	122.59(12)
O(2)-C(41)-C(4)	120.90(12)	N(1)-C(41)-C(4)	116.44(11)

Table C. Bond lengths [Å] and angles [°] for **(±)-164**.

Atom	U11	U22	U33	U23	U13	U12
S(1)	45(1)	27(1)	35(1)	-8(1)	13(1)	-11(1)
O(2)	22(1)	28(1)	28(1)	3(1)	7(1)	3(1)
O(3)	30(1)	27(1)	23(1)	3(1)	9(1)	6(1)
N(1)	21(1)	25(1)	33(1)	-5(1)	8(1)	-3(1)
C(2)	34(1)	27(1)	32(1)	2(1)	10(1)	-6(1)
C(3)	26(1)	22(1)	24(1)	2(1)	9(1)	1(1)
C(4)	22(1)	21(1)	23(1)	1(1)	6(1)	0(1)
C(5)	32(1)	25(1)	27(1)	-3(1)	10(1)	-4(1)
C(41)	22(1)	24(1)	18(1)	3(1)	6(1)	0(1)

Table D. Anisotropic displacement parameters ($Å^2$ x 10^3) for **(±)-164**.

Atom	x	y	z	U(eq)
H(3)	2268	-157	4518	40(5)
H(1A)	-137	-3258	6405	33(4)
H(1B)	1819	-3013	6918	39(5)
H(2B)	3728	2214	6600	37
H(2A)	4948	953	7497	37
H(3A)	1244	884	6062	28
H(4)	3182	-1163	8304	26
H(5A)	2461	-5	10232	33
H(5B)	845	782	9016	33

Table E. Hydrogen coordinates (x 10^4) and isotropic displacement parameters ($Å^2$ x 10^3) for **(±)-164**.

Publications

Kwong, J. S. W.; Lloyd, M. D.; Threadgill, M. D. Synthesis of cyclic sulfoximine mimics of 2-deoxyribosides as enzyme inhibitors in cancer. *J. Pharm. Pharmacol.* **2006**, 58 (S1), 58.

Abstract presented at the American Chemical Society (ACS) 232nd National Meeting, San Francisco, U.S.A., 10 – 14 September 2006.

Design, synthetic approaches and characterisation of a novel cyclic sulfoximine NAD^+ (nicotinamide adenine dinucleotide) analogue

Joey S. W. Kwong, Matthew D. Lloyd and Michael D. Threadgill, Department of Pharmacy and Pharmacology, University of Bath, Claverton Down, Bath, BA2 7AY, United Kingdom, Fax: +44(0)1225386114, J.S.W.Kwong@bath.ac.uk

Nicotinamide adenine dinucleotide (NAD^+, **1**) is the substrate for both poly(ADP-ribose) polymerase-1 (PARP-1) and inosine-5'-monophosphate dehydrogenase (IMPDH), important enzymes implicated in cancer development. We herein describe an innovative approach to the synthesis of a cyclic sulfoximine 2-deoxyriboside mimic, where the anomeric carbon has been replaced by the sulfoximine group. Sulfoximines possess extremely versatile chemistry and their use in the design of ribose mimics has not been reported previously. A key step in our ongoing studies towards the target **2** involves a thio-Mitsunobu reaction of a sulfur nucleophile **3** and a homochiral dioxolane compound **4**. The two diastereoisomers of an important, novel intermediate **5** have been separated and the stereochemistry at the sulfur centre established by X-ray crystallography. Development of synthetic routes from this intermediate to the target cyclic sulfoximine will be reported.

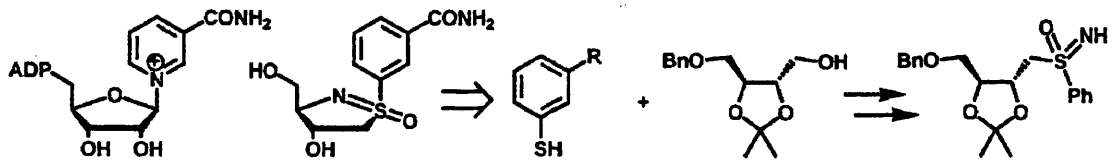

Abstract presented at the Conférences Européenes du Groupement Des Pharmacochimistes de L'Arc Atlantique (GP2A) Meeting, Bath, U.K., 7 – 8 September, 2006 and the 2nd National Cancer Research Institute (NCRI) Cancer Conference, Birmingham, U.K., 8 – 11 October 2006.

Design and synthesis of a novel transition-state mimic for poly(ADP-ribose) polymerase 1 (PARP-1) inhibition

Joey S. W. Kwong*, Matthew D. Lloyd and Michael D. Threadgill

Department of Pharmacy and Pharmacology, University of Bath, Claverton Down, Bath, BA2 7AY, United Kingdom. E-mail J.S.W.Kwong@bath.ac.uk

Nicotinamide adenine dinucleotide (NAD^+, **1**) is the substrate for poly(ADP-ribose) polymerase-1 (PARP-1). PARP-1 is responsible for cellular DNA repair and high levels in tumours confer resistance to DNA-damaging chemotherapy and hence lead to treatment failure.[1] Inhibition of PARP-1 is therefore of great clinical interest in cancer therapy. Here we report on the synthesis of a cyclic sulfoximine NAD^+ transition-state analogue **2** where the anomeric carbon of the ribosyl ring has been replaced by a sulfoximine group. The sulfoximine functional group is configurationally and chemically stable; it is tetrahedral and, when the two carbon substituents attached to the sulfur atom are different, is chiral. The imino nitrogen is weakly basic.[2] Sulfoximines possess versatile chemistry and their application in the design of ribose mimics has not been reported previously.

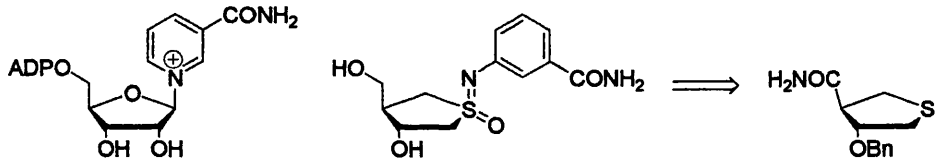

NAD^+, **1** PARP-1 transition state analogue, **2** **3**

The important, novel lead compound, (±)-3-benzyloxytetrahydrothiophene-4-carboxamide (**3**) was obtained with moderate yield. Dieckmann cyclisation of acrylonitrile and methyl mercaptoacetate with sodium and anhydrous methanol gave (±)-3-oxotetrahydrothiophene-4-carbonitrile.[3] Subsequent reduction of the ketone afforded the corresponding hydroxyl compound. Separation of the diastereoisomers was achieved by column chromatography and the stereochemistry was determined by X-ray crystallography of the amide compound, synthesised by acid-hydrolysis of the nitrile. *O*-benzylation gave rise to the target lead compound. Development of synthetic routes from this intermediate to the target cyclic sulfoximine will be reported. In conclusion, we have herein described a highly novel and efficient reaction sequence towards the synthesis of a cyclic sulfoximine NAD^+ transition-state mimic, the enzyme inhibitory profile of which will be investigated by biological assay.